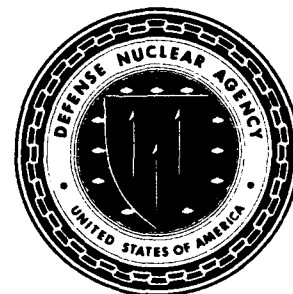


D-A242 981



Defense Nuclear Agency
Alexandria, VA 22310-3398



DTIC
ELECTE
DEC 5 1991
S C D

DNA-TR-90-157

Biological Effects of Protracted Exposure to Ionizing Radiation: Review, Analysis, and Model Development

George H. Anno, et al.
Pacific-Sierra Research Corporation
12340 Santa Monica Boulevard
Los Angeles, CA 90025-2587

November 1991

Technical Report

CONTRACT Nos. DNA 001-86-C-0307
and DNA 001-87-C-0104

Approved for public release;
distribution is unlimited.

91-17031



91 12 4 027

Destroy this report when it is no longer needed. Do not return to sender.

PLEASE NOTIFY THE DEFENSE NUCLEAR AGENCY,
ATTN: CSTI, 6801 TELEGRAPH ROAD, ALEXANDRIA, VA
22310-3398, IF YOUR ADDRESS IS INCORRECT, IF YOU
WISH IT DELETED FROM THE DISTRIBUTION LIST, OR
IF THE ADDRESSEE IS NO LONGER EMPLOYED BY YOUR
ORGANIZATION.



DISTRIBUTION LIST UPDATE

This mailer is provided to enable DNA to maintain current distribution lists for reports. We would appreciate your providing the requested information.

- ☐ Add the individual listed to your distribution list.
- ☐ Delete the cited organization/individual.
- ☐ Change of address.

NOTE:

Please return the mailing label from the document so that any additions, changes, corrections or deletions can be made more easily.

NAME: _____

ORGANIZATION: _____

OLD ADDRESS

CURRENT ADDRESS

TELEPHONE NUMBER: () _____

SUBJECT AREA(s) OF INTEREST:

DNA OR OTHER GOVERNMENT CONTRACT NUMBER: _____

CERTIFICATION OF NEED-TO-KNOW BY GOVERNMENT SPONSOR (if other than DNA):

SPONSORING ORGANIZATION: _____

CONTRACTING OFFICER OR REPRESENTATIVE: _____

SIGNATURE: _____

CUT HERE AND RETURN



Director
Defense Nuclear Agency
ATTN: TITL
Washington, DC 20305-1000

Director
Defense Nuclear Agency
ATTN: TITL
Washington, DC 20305-1000

REPORT DOCUMENTATION PAGE			Form Approved OMB No. 0704-0188	
Public reporting burden for this collection of information is estimated to average 1 hour per response, including the time for reviewing instructions, searching existing data sources, gathering and maintaining the data needed, and completing and reviewing the collection of information. Send comments regarding this burden estimate or any other aspect of this collection of information, including suggestions for reducing this burden, to Washington Headquarters Services, Directorate for Information Operations and Reports, 1215 Jefferson Davis Highway, Suite 1204, Arlington, VA 22202-4302, and to the Office of Management and Budget, Paperwork Reduction Project (0704-0188), Washington, DC 20503.				
1. AGENCY USE ONLY (Leave blank)	2. REPORT DATE 911101	3. REPORT TYPE AND DATES COVERED Technical 860915--900720		
4. TITLE AND SUBTITLE Biological Effects of Protracted Exposure to Ionizing Radiation: Review, Analysis, and Model Development		5. FUNDING NUMBERS C - DNA001-86-C-0307 C - DNA001-87-C-0104 PE - 62715H PR - RM TA - RH WU - DH008899		
6. AUTHOR(S) George H. Anno, Gene E. McClellan, Michael A. Dore, Siegmund J. Baum				
7. PERFORMING ORGANIZATION NAME(S) AND ADDRESS(ES) Pacific-Sierra Research Corporation 12340 Santa Monica Boulevard Los Angeles, California 90025-2587		8. PERFORMING ORGANIZATION REPORT NUMBER PSR Report 2040		
9. SPONSORING/MONITORING AGENCY NAME(S) AND ADDRESS(ES) Defense Nuclear Agency 6801 Telegraph Road Alexandria, Virginia 22310-3398 RARP/Young		10. SPONSORING/MONITORING AGENCY REPORT NUMBER DNA-TR-90-157		
11. SUPPLEMENTARY NOTES This work was sponsored by the Defense Nuclear Agency under RDT&E RMC Code B3500864662 RM RH 00016 25904D.				
12a. DISTRIBUTION/AVAILABILITY STATEMENT Approved for public release; distribution is unlimited.			12b. DISTRIBUTION CODE	
13. ABSTRACT (Maximum 200 words) Two basic approaches are developed to mathematically model biological responses to ionizing radiation exposure, including upper gastrointestinal (UG) distress (nausea, vomiting), lower gastrointestinal (LG) distress (diarrhea, fluid loss), and GI-syndrome lethality. Models are constructed to accommodate arbitrary histories of protracted exposure. Sets of coupled differential equations are employed to simulate dynamics of the biological processes involved. The modeling approaches are guided by a comprehensive review and analysis of relevant literature, including radiation-induced symptomatology, response dynamics, physiological changes, morphological changes, cell/tissue damage and recovery mechanisms, and existing radiobiological injury and recovery models. The upper gastrointestinal distress model (UGIDM) is a two-compartment toxicokinetic model to simulate radiation-induced production and clearing of humoral substances involved in triggering UG distress. Calculated model results for constant dose rate exposures				
14. SUBJECT TERMS Ionizing Radiation Human Effects Fluid Loss Protracted Dose Animal Effects Emesis Dose Fractionation Mathematical Modeling Nausea			15. NUMBER OF PAGES 278	
			16. PRICE CODE	
17. SECURITY CLASSIFICATION OF REPORT UNCLASSIFIED	18. SECURITY CLASSIFICATION OF THIS PAGE UNCLASSIFIED	19. SECURITY CLASSIFICATION OF ABSTRACT UNCLASSIFIED	20. LIMITATION OF ABSTRACT SAR	

CLASSIFIED BY:

N/A since Unclassified

DECLASSIFY ON:

N/A since Unclassified

ABSTRACT (continued)

compare reasonably well with human data. Suggested modeling improvements are discussed involving further model validation with additional protracted exposure data in humans and the ferret.

The gut injury model (GIM) is a three-compartment hierarchical-type tissue model to simulate radiation-induced changes in the intestinal epithelium responsible for LG distress and GI syndrome lethality. Target cell (crypt clonogen) survival is simulated by explicitly modeling radiation-induced chromosome damage (lesion production), mitotic delay, chromosome lesion repair/misrepair, and cell proliferation. Clonogen proliferation and migration dynamics of intestinal epithelial cells are determined by cell cycle parameters and homeostatic feedback based on time-dependent crypt transit and villus cell levels. Modeling parameters are determined from measured dose rate dependent clonogen survival data and empirical data for the anatomical structure of the jejunal crypt and villus of the mouse.

Comparisons of model calculations with empirical data for protracted radiation exposure (constant dose rate and fractionated exposure) provide good qualitative agreement for cell dynamics. Calculations for dose rate dependent LD_{50/5} in mice provide an independent measure of model validity when compared with experiment. Calculations of the symptomatology response for diarrhea (ED₅₀) and fluid loss are consistent with limited data extrapolated from rats. Similar calculations are made for human response based on model parameter adjustments. Suggested modeling improvements are pointed out in areas of cell cycle sensitivity and statistical treatment, physiological processes for symptomatology response, and vascular damage effects.

Review of radiation-induced fatigability and weakness and possible causal mechanisms suggests approaches for modeling this response to protracted radiation exposure. Two mechanistic modeling approaches are discussed based on observed response dynamics and physiological considerations of capillary damage following irradiation.

SUBJECT TERMS (continued)

Radiobiological Effects	Prodromal Symptoms	Diarrhea
Gastrointestinal Symptoms	Dose Rate	Cell Survival
Intestinal Injury	Fatigability	Cell Damage
Cell Repair	Cell Proliferation	

PREFACE

This document was prepared by PSR investigators as the final report for the Defense Nuclear Agency (DNA) under contract DNA001-86-C-0307 and in partial fulfillment of contract DNA001-87-C-0104. It represents a research effort in support of the DNA's continuing Human Response Program (HRP) in the investigation of the biological effects of ionizing radiation in humans. Mathematical approaches are developed and demonstrated for modeling the upper and lower gastrointestinal symptomatological response to protracted radiation exposure.

The authors would like to acknowledge Dr. Robert W. Young of DNA/RARP who supported this effort; Dr. Rodney W. Withers, Kathy A. Mason, and Dr. Jeremy M. G. Taylor of the UCLA Medical Center, Department of Radiation Oncology, for providing valuable assistance and mouse intestinal cell data; Dr. Gregory L. King of the Armed Forces Radiobiological Research Institute for providing support and data on radiation-induced emesis; and last but not least, Jean Eggen of PSR, who patiently typed and prepared this document.



Accession For	
NTIS GRA&I	<input checked="" type="checkbox"/>
DTIC TAB	<input type="checkbox"/>
Unannounced	<input type="checkbox"/>
Justification	
By _____	
Distribution/	
Availability Codes	
Dist	Avail and/or Special
A-1	

TABLE OF CONTENTS

Section	Page
PREFACE	iii
LIST OF ILLUSTRATIONS	vi
LIST OF TABLES	xiii
1 INTRODUCTION	1
2 LITERATURE REVIEW	4
2.1 Protracted exposure annotated bibliography	4
2.1.1 Description of bibliographic entries	5
2.1.2 Description of codes	7
2.2 Prodromal signs and symptoms	16
2.2.1 Nausea and vomiting	16
2.2.2 Fatigability and weakness	35
2.3 Hematopoietic effects	50
2.3.1 Blood cell levels	51
2.3.2 Damage to lymphoid tissue	59
2.3.3 Blood cell modeling	62
2.4 Radiation lethality	65
2.4.1 Bone marrow damage	67
2.4.2 Gastrointestinal damage	73
2.5 Radiation injury and recovery	84
2.5.1 Constant dose rate models	99
2.5.2 Operational equivalent dose as injury accumulation	104
3 PROTRACTED DOSE MODELING CONSIDERATIONS	107
3.1 Physiological changes and modeling	108
3.2 Target cell hypothesis	110
3.3 Residual injury or effective residual dose	116
3.4 Equivalent prompt dose	117
3.5 Comparison of effective residual dose and equivalent prompt dose	118
3.6 ERD modeling with a recovery function	119
3.7 Single step and multistep modeling	124
3.8 Selected modeling approach	127
4 UPPER GASTROINTESTINAL DISTRESS MODEL (UGIDM)	129
4.1 Basis for modeling	129
4.2 Model description and equations	132
4.3 Protracted dose response	144
4.3.1 Continuous exposure	144
4.3.2 Fractionated exposure	146
4.3.3 Fallout field exposure	147

Table of Contents (continued)

Section	Page
4.4 The ferret--an experimental model	154
4.4.1 UG severity scale	155
4.4.2 UG severity curves for acute dose	158
4.4.3 UGIDM for ferrets	160
4.4.4 Fractionated and continuous exposures predictions	161
4.4.5 Suggested ferret experiments	164
5 GUT INJURY MODEL (GIM)	168
5.1 Symptomatology of LG distress	168
5.2 Causes of LG distress and lethality	169
5.3 Model description	172
5.3.1 Anatomical and physiological modeling basis .	172
5.3.2 Modeling arrangement of the GIM	175
5.3.3 Compartmental structure	176
5.3.4 Symptomatology and lethality	177
5.4 Validation of the GIM	178
5.4.1 Decline of mucosa	178
5.4.2 Crypt recovery	179
5.4.3 Clonogen response to exposure at constant dose rate	181
5.4.4 Dose rate dependence of LD _{50/5} for mice	182
5.4.5 LG distress symptomatology in mice and rats .	185
5.5 Lethality and diarrhea estimates for humans	188
5.6 Future developments	191
6 CONCLUSIONS	193
6.1 Literature Review	194
6.2 UGIDM	197
6.3 GIM	198
6.4 Fatigability and Weakness	202
7 BIBLIOGRAPHY	204
Appendix	
A SPECIAL SOLUTIONS OF THE UGIDM EQUATIONS	233
B INCIDENCE OF NAUSEA AND VOMITING WITHIN 24 HOURS IN NUCLEAR ACCIDENT EXPOSURES	239
C EQUATIONS OF THE GUT INJURY MODEL	251

LIST OF ILLUSTRATIONS

Figure	Page
1 Incidence of vomiting (within 2 days of dose) as function of dose assuming lognormal distribution of quantal response	17
2 Incidence of nausea and vomiting within 2 days post-exposure for accidental and clinical exposures	18
3 Vomiting time versus dose rate	20
4 Vomiting time versus dose	20
5 Onset of prodromal symptoms related to dose	21
6 ED ₅₀ for vomiting versus dose rate	28
7 Gastrointestinal signs and symptoms in the early stage	30
8 Cumulative whole body gamma fallout dose for 23 Japanese fishermen during the first day	31
9 ED ₅₀ for nausea versus dose rate	32
10 Fatigability/weakness severity levels for dose ranges	38
11 Fatigue, headache, and fever	38
12 Incidence of fatigability and weakness (FW)	39
13 Pulmonary impedance from therapy patients	41
14 Relationship between workload (cardiac rate) and pulmonary impedance (average variance)	42
15 Time course study of exercise tolerance for an accidental exposure	43
16 Experimental design of exposure time for specific dose rates and times of radioactive tracer ⁵⁹ Fe injection ...	52
17 Effects of variable dose rates on iron incorporation into newly formed erythrocytes--total dose 214 cGy	52

LIST OF ILLUSTRATIONS (continued)

Figure		Page
18	B-lymphocyte antibody formation as function of radiation exposure rate (625 cGy ^{60}Co gamma)	53
19	Mean leukocyte values of Duroc swine following whole-body exposure to 256 cGy ^{60}Co gamma radiation	53
20	Conglomerate model ("template") of human dose: hematological response	55
21	Single and protracted radiation exposures; hematological response level based upon white blood cells	55
22	Blood count levels following single acute radiation exposures	57
23	Standard curves showing the changes of the neutrophil and platelet counts after various doses (number on the curves indicate the dose in Gy) in the case of relatively uniform whole body gamma irradiation of human subjects	58
24	Lymphocyte count after single acute gamma radiation	62
25	LD ₅₀ versus dose rate--three parameter model	68
26	LD ₅₀ versus dose rate--two parameter model	68
27	LD ₅₀ versus dose rate--three parameter model for mouse	69
28	LD ₅₀ versus dose rate--two parameter model for mouse ...	69
29	LD ₅₀ versus dose rate--two parameter model for mouse, from Thompson and Tourtellote (1953) only	70
30	LD ₅₀ versus dose rate--three parameter model for sheep	70
31	LD ₅₀ versus dose rate--two parameter model for sheep ...	71
32	Effect of dose rate on gastrointestinal LD _{50/5} in mice	74
33	Acute single LD _{50/5} dose equivalent to a 10 Gy protracted dose for constant dose rate and fractioned exposures	76

LIST OF ILLUSTRATIONS (continued)

Figure	Page
34 Recovery comparison of LD _{50/5} and cell survival endpoints; the origin of both scales refer to 1060 rads acute single exposure	78
35 Cell counts of mouse ileum after a sterilizing dose of 3000 R	79
36 Survival time of untreated, GI-decontaminated, and Pseudomonas-infected animals after exposure to various doses of Cs-137 gamma rays and cyclotron neutrons	81
37 Theoretical injury recovery curve with fraction of injury assumed unrecoverable	86
38 Maximum Fe ⁵⁹ incorporation for male and female rats exposed periodically to 300 r of X-rays and for female rats irradiated with 400 r	87
39 Residual injury of erythropoietic system in irradiated rats	87
40 Hamster--acute exposure	88
41 Rhesus monkey--acute exposure	88
42 Sheep--acute exposure	89
43 Residual injury of erythrocyte stem cells in irradiated rats--17-day observation period	90
44 Erythropoiesis in normal and in polycythemic dogs exposed to 150 rads mixed gamma-neutron radiation	90
45 Dog--acute exposure	92
46 Swine--acute exposure	92
47 Swine--injury and recovery versus exposure time at fixed dose rate	93
48 Species comparison for acute exposure	96
49 Sheep--acute and protracted dose (0.63 and 0.32 cGy/h)	96

LIST OF ILLUSTRATIONS (continued)

Figure	Page
50 Sheep--acute and protracted dose over 3.7 days (1.1 cGy/h)	97
51 Sheep--acute and protracted dose over 1.8 days (2.4 cGy/h)	97
52 Sheep--acute and protracted dose over 3.2 days (2.4 cGy/h)	98
53 Sheep--acute and protracted dose comparisons	98
54 LD ₅₀ versus dose rate	100
55 LD ₅₀ dose rate models	101
56 OED (injury) for constant daily exposure rate	104
57 Residual injury--comparison between formula and data derived from experiments with sheep	106
58 Protracted dose modeling considerations	107
59 Isosurvival relationship of mice and jejunal crypt cells	113
60 Upper gastrointestinal distress model (UGIDM)	133
61 UG severity levels for prompt dose ranges midline tissue (MLT)	140
62 The severity level of upper gastrointestinal (UG) distress in humans	142
63 Accumulated dose versus dose rate: UGIDM-predicted severity levels and data from humans	145
64 UGIDM prediction of severity level for upper gastro- intestinal (UG) distress/fractionated doses	147
65 UGIDM prediction of severity level for upper gastro- intestinal (UG) distress/fractionated doses--non-depleting reservoir	148
66 Protracted exposure in a fallout field ($t^{-1.2}$ radio- active decay) UG distress--equivalent prompt dose for RES 2 (emesis ED ₁₀): 150 cGy (FIA)	149

LIST OF ILLUSTRATIONS (continued)

Figure		Page
67	Protracted exposure in a fallout field ($t^{-1.2}$ radioactive decay) UG distress--equivalent prompt dose for RES 2 (emesis ED ₁₀): 150 cGy (FIA)	149
68	Protracted exposure in a fallout field ($t^{-1.2}$ radioactive decay) UG distress--equivalent prompt dose for emesis: ED ₅₀ = 255 cGy (FIA)	151
69	Protracted exposure in a fallout field ($t^{-1.2}$ radioactive decay) UG distress--equivalent prompt dose for emesis: ED ₅₀ = 255 cGy (FIA)	151
70	Fallout exposure scenarios (A and B) ($t^{-1.2}$ radiodecay)	152
71	UGIDM prediction of upper gastrointestinal distress (UG) severity level for scenario A	153
72	UGIDM prediction of upper gastrointestinal distress (UG) severity level for scenario B	153
73	Ferret upper gastrointestinal (UG) distress--post-exposure severity levels	158
74	UGIDM acute dose severity levels for ferret--upper gastrointestinal (UG) distress	160
75	UGIDM prediction of severity level for upper gastrointestinal (UG) distress in the ferret--fractionated dose	162
76	UGIDM calculations of isoseverity dose versus dose rate for UG distress levels (2, 3, and 4) in the ferret	163
77	UGIDM calculations of isoseverity dose versus dose rate for UG distress levels in ferrets and humans	165
78	Lower gastrointestinal (LG) severity levels for acute dose ranges cGy (free-in-air)	169
79	The villus/crypt structure of the intestinal epithelium	173
80	A nested arrangement of models provides the overall description of the response of the intestinal epithelium to protracted radiation exposure	176

LIST OF ILLUSTRATIONS (continued)

Figure		Page
81	Schematic diagram of the cell compartments comprising the gut injury model (solid arrows represent cell movements; dashed arrows represent control signals)	176
82	Crypt and villus cell counts of mouse ileum after sterilizing dose: 33.5 Gy @ 26.8 Gy/h, 250 kVp X-rays	179
83	Cell survival ratio for recovery of jejunal crypt cells after 660 cGy acute dose, conventional mice, 200 kVp X-rays	180
84	Crypt cell survival in mouse jejunum for varying dose rates, ⁶⁰ Co radiation	182
85	Relative villus cell population for conventional mice, 30 Gy/h, ⁶⁰ Co radiation	183
86	LD _{50/5} ratio related to constant dose rate exposure for mice	184
87	Diarrhea and fluid loss in rats and mice	185
88	Estimated fluid loss in mice	186
89	Normalized compartment population response to a 9 Gy dose	187
90	Predicted ED ₅₀ for diarrhea (conventional mice; isoeffect = 27% villi level)	188
91	Estimated protracted radiation exposure effects for GI tract injury in humans	191
92	Incidence of nausea and vomiting within 24 hours (data set I, lognormal model)	247
93	Incidence of nausea and vomiting within 24 hours (data set I, lognormal model)	248
94	ED ₅₀ for emesis versus neutron RBE (basis: data set I; lognormal model)	249
95	Cell radiation response based on the lethal, potentially lethal (LPL) cell lesions model	252

LIST OF ILLUSTRATIONS (continued)

Figure		Page
96	Clonogen homeostatis factor, H	258
97	Cell fluxes between compartments in the GIM model; note that ϕ is subscripted, but θ is not in the equations	259

LIST OF TABLES

Table		Page
1	The structure of the prototypical bibliographic entry	6
2	Information content of the bibliographic data fields for the four publication types	7
3	Description of codes for the publication type field ...	8
4	Description of codes for the publication name field ...	9
5	Description of codes for the species field	12
6	Description of codes for the effects field	12
7	Description of codes for the data source field	13
8	Description of codes for the radiation type field	13
9	Description of codes for the exposure geometry field	14
10	Description of codes for the exposure history field ...	14
11	Description of codes for the keyword fields	15
12	Accident cases--vomiting onset and duration	23
13	Therapy (and some accident) cases--vomiting onset and duration	24
14	Dog studies--vomiting onset and duration	27
15	Fatigability and weakness	36
16	Fatigability and weakness--accident victims	37
17	Work capacity--Chernobyl accident victims	46
18	Energy expenditure by a 150-pound person in various activities	47
19	Parameters for LD ₅₀ versus dose rate	72
20	LD _{50/5} day of pseudomonas-infected GI, conventional, and GI-decontaminated rats	82

LIST OF TABLES (continued)

Table		Page
21	Mortality of Chernobyl accident victims with skin and intestinal injuries	83
22	Gastrointestinal syndrome lethality in man	83
23	Protracted dose irradiation studies--sheep	94
24	Remaining injury and maximum over-recovery in sheep subjected to radiation at different rates	99
25	Split dose irradiation studies	122
26	Protracted dose--experimental/model comparison	123
27	Severity levels of upper gastrointestinal (UG) distress in humans	134
28	Severity levels of upper gastrointestinal (UG) distress in ferrets	156
29	GIM calculated LD _{50/5} versus dose rate for conventional mice	184
30	GIM parameters	189
31	Nuclear accident cases--nausea and vomiting within 24 hours	241
32	Regression models and parameters	243
33	Effective doses (ED) and 95% confidence intervals for 10, 50, and 90 percent nausea and vomiting probabilities within 24 hours postexposure; basis: data set I (N = 40, v = 38 dgf.)	245
34	Effective doses (ED) and 95% confidence intervals for 10, 50, and 90 percent nausea and vomiting probabilities within 24 hours postexposure; basis: data set II (N = 40, v = 38 dgf.)	246

SECTION 1

INTRODUCTION

This report describes the research and progress made by PSR on modeling the biological response to protracted doses of ionizing radiation. It is based on an investigation of the repair and recovery in biological systems following tissue damage and functional changes caused by the disruptive effects of ionizing radiation. Biological repair and recovery take place following either acute (i.e., prompt) or protracted radiation exposure.

From the standpoint of performance level and personnel casualties, protracted doses from both repeated and continuous, low dose rate exposures enter into important operational situations in a nuclear combat environment. Planning for these situations requires the appropriate exposure criteria to evaluate mission completion reliability and to assess casualty risk. Because comprehensive protracted dose models or algorithms do not exist for predicting the severity of radiation sickness, current military guidance makes no distinction between acute or protracted radiation exposure with regard to effects in humans. This lack of distinction between acute and protracted exposures in a combat setting has been a concern for some time and was brought into focus by the Defense Nuclear Agency's (DNA) Intermediate Dose Program (IDP) effort that dealt with acute exposure effects.

The research effort described in this report addresses that concern based on a thorough literature review and evaluation culminating in the development of two models, the UGIDM (upper gastrointestinal distress model) and the GIM (gut injury model). These two models are based on fundamentally different mechanisms and provide the basis for modeling the symptomatology of acute radiation sickness originating from two kinds of effects that radiation has on bodily tissues.

The literature review (Section 2) covers a variety of empirical experience and radiobiological modeling relevant to protracted dose response. Biological repair and recovery are illustrated by cellular and organism responses involving animal experiments, human accidents, and clinical radiation therapy. Various degrees of the repair and recovery are seen in biological systems ranging from intracellular repair that takes place within about one-half hour to proliferative tissue recovery that takes place from days to months depending upon the tissue type. Our literature sources have been incorporated into a computer data base in the form of an annotated bibliography [Baum et al., 1990]. References cited in this report are included in the bibliographic list in Section 7.

Section 3 presents the key considerations for developing our protracted modeling approach. The discussion is based on the objectives of this effort and the literature review and evaluation performed in Section 2. A primary consideration that shaped our modeling approach is that protracted exposure can be comprised of any number of exposure histories requiring differential equations to properly develop response relationships.

Section 4 describes the development of the UGIDM for gastrointestinal distress. We refer to this model as a *toxicokinetic* type of model since it is based on the release and bioclearing of toxins or humoral agents that cause the upper gastrointestinal (UG) sign/symptom responses such as nausea and vomiting. The model is based upon our review of the basic physiology involved in the emetic process. Modeling parameters are developed from the DNA/IDP data for acute response. Example calculations for protracted doses are performed to illustrate model applications.

To explore a possible means of model verification, the UGIDM was also applied to data from ferret experiments involving the UG distress response to acute radiation exposure. Because the UG distress response in ferrets is similar to that in man, some possible experiments are suggested for verification of the UGIDM involving fractionated and low dose rate exposure.

Section 5 describes the development of the GIM for gut injury based on the target-cell hypothesis for a hierarchical(H)-tissue system. There are basically three nested models involved including the LPL (lethal, potentially lethal) model, PAIR (proliferation and intracellular repair) model, and GIM (gut injury model). The LPL model accounts for intracellular lesion production and repair on chromosomal DNA, the PAIR model combines the LPL model with mitotic delay and cell proliferation, and the GIM combines the PAIR model with the homeostatic control relationship for gut epithelial cell loss and replenishment. Gastrointestinal syndrome lethality and symptomatology are related to depletion of the intestinal epithelium. Modeling parameters were developed from gut (jejunal) crypt cell survival and morphological data for mice. Calculated LD_{50/5} values are compared with experiment to evaluate the validity of the GIM for protracted exposures. Example calculations are made for LD₅₀, diarrhea, and fluid loss to illustrate the model.

Section 6 of this report provides a brief summary and conclusions based on this research effort.

SECTION 2

LITERATURE REVIEW

We carried out an extensive review of the literature on the ionizing radiation effects relevant to protracted exposure. Literature sources covered animal experimentation, human radiation accidents, clinical radiotherapy, and protracted dose modeling. The literature reviewed has been cataloged in the form of an annotated bibliography described in the following subsection.

Aside from gathering and cataloging research papers and documents, we also performed an analysis and evaluation of the material contained in them. Relevant technical material extracted for this effort is discussed below and is divided into four areas, including: (1) prodromal signs and symptoms, (2) hematopoietic effects, (3) radiation lethality, and (4) radiation and recovery.

2.1 PROTRACTED EXPOSURE ANNOTATED BIBLIOGRAPHY.

The Protracted Exposure Annotated Bibliography (PEAB) is a catalog of experimental results and other research papers dealing with the biological response to protracted exposure to ionizing radiation. It has been implemented in software form as described below. Although not a database in the numerical sense, the PEAB is meant to provide a guide for finding data regarding protracted exposure. This guide is in the form of coded information in the bibliography which briefly describes the type of data contained in each original research paper. These codes are the annotation of the bibliography. The software also has a provision for adding abstracts for each bibliographic entry. This feature remains to be utilized in the future.

The database files for the annotated bibliography have been prepared in dBASE III Plus* format for use on IBM-compatible personal computers. The software, database files, and a report [Baum, McClel-

*dBASE III Plus is a registered trademark of Ashton-Tate, Torrance, California.

lan, and Anno, 1990] describing the bibliography in detail are available from Pacific-Sierra Research Corporation. The software will do tailored searches of the bibliography, display the selected entries, and print either the selected entries or the whole bibliography. The bibliography of this report (Sec. 7) consists of a complete printout of the present version of the PEAB which contains all the references cited.

The computer record for an entry in the bibliography consists of a number of fields each containing specified information about the entry. There are fields for bibliographic (publication) data, such as author and title; and there are fields for technical information, such as the type of ionizing radiation considered in the report. To reduce the storage space for the bibliography, short (two or three character) codes have been devised for many of the fields. The following paragraphs describe the bibliographic entries of the annotated bibliography, the field structure, and the definitions of codes.

2.1.1 Description of Bibliographic Entries.

The prototype entry in the PEAB is an article from a scientific journal reporting data on the response of a certain animal species to a protracted dose of ionizing radiation. Entries are structured to provide four types of information for the article: bibliographic data, a brief description of the scientific data being reported, a keyword list, and an abstract. The initial version (1.0) of the bibliography contains only the first three types of information.

Table 1 shows the field structure of the prototype entry. The fields for an entry are shown in the same order as they appear in a record of the PUBLICAT.DBF database file. In addition to the four types of information listed above, each entry in the bibliography has an accession number and may have an archive number. The archive number refers to an indexed collection of papers [Baum, McClellan, and Anno, 1990].

In addition to articles from refereed journals, the annotated bibliography contains three other types of entries. In descending order of frequency, they are technical reports, proceedings of con-

Table 1. The structure of the prototypical bibliographic entry.

Type of information	Number of fields	Content of fields
Bibliographic Data	1	Entry (Accession) Number
	1	Archive Number
	6	Author(s)
	1	Title
	1	Subtitle
	1	Publication Type
	1	Publication Name
	1	Publication Volume
	1	Page Number(s)
	1	Publication Date
Data	4	Species
Descriptor	4	Effects Categories
Fields	2	Data Source
	3	Radiation Type or Source
	3	Exposure Geometry
	3	Exposure History
Keywords	6	Keyword(s)
Abstract	1	Abstract

ferences or symposia, and books. Technical reports from government agencies, contractors, and universities are a rich source of data but have generally not undergone the formal peer review process typical of journals. Proceedings sometimes contain original data that the authors did not publish elsewhere. Less frequently, books will contain original results from the authors or the book will be an edited collection of research articles.

The bibliographic (publication) data varies from one type of entry to another. Rather than create a new field structure for each type of entry, we have chosen to adapt the contents of the fields named in Table 1 to accommodate each type. Table 2 lists the information that is contained in each field for the four different entry types. Codes JA, RE, PR, and BK in the publication type field have the obvious correspondence to the above mentioned types.

Table 2. Information content of the bibliographic data fields for the four publication types.

Journal Article	Book	Technical Report	Proceedings
Author(s)	Author(s) of book or chapter	Author(s)	Author(s) of paper
Title	Title of book or chapter	Title	Title of paper
Subtitle	(Blank) or book title and editors	Subtitle and report number	Conference identification
Publication type (JA)	BK	RE	PR
Publication Name	Publisher	Agency, contractor, or university	Sponsor or publisher
Volume no.	(Blank)	(Blank)	(Blank)
Page nos.	Page Nos.	(Blank)	Page Nos.
Date of publication	Date of publication	Date of report	Date of publication

2.1.2 Description of Codes.

Codes are used for recurrent data, such as journal names and keywords, in the PEAB. These two- and three-character codes reduce storage space requirements by at least a factor of 10.

Each table in this subsection defines codes for one of the fields specified in Table 1. For each of these tables, there is a corresponding database file in the software that contains the same information. These database files are used by the software to interpret the codes contained in the main bibliographic file.

Table 3 shows the codes for publication type. These codes were discussed previously. Table 4 lists the numerical codes for the field referred to as publication name.

Table 3. Description of codes for the publication type field.

Code	Description
BK	Book
JA	Journal article (refereed)
PR	Proceedings of conference or symposium
RE	Agency, contractor, or university report

Note that the actual meaning of the field varies from one type of publication to another as discussed in the previous subsection.

The next six tables (Tables 5 through 10) show the codes for the data descriptor fields. These fields provide a brief description of the kind of scientific data that is contained in the referenced publication. Generally, if these fields have information in them, then the publication contains original data, or at least an analysis of original data, relating to the response of animals or humans to protracted exposure to ionizing radiation. If these fields are blank, then the publication probably reports theoretical work, analytical work, review material, speculation, applications, or some other subject related to protracted exposure or biological response. In this case, the keyword fields provide a guide to the subject of the publication.

The codes for species, effects category, and data source are shown in Tables 5, 6, and 7, respectively. For species, as well as for other codes, a three-letter code indicates a subset of the set corresponding to the first two letters taken alone. A search for a two-letter code will ignore the third letter and select all entries that have the correct two letters or a three-letter code whose first two letters match. On the other hand, a search for a three-letter code will require that all three letters be present.

The code for the effects category tells which biological effect or endpoint is being reported for the indicated species. The code for data source indicates whether the data was from an experiment or an accident, etc. and should not be confused with the type of ionizing radiation source that is shown in Table 8.

Table 4. Description of codes for the publication name field.

Code	Description
84	Academic Press, New York, NY
12	Acta Radiologica Oncology
78	Acta Radiologica Supplement
38	Akademie-Verlag, Berlin
83	American College of Surgeons 1987 Surgical Forum
95	American Institute of Physics, Inc.
71	American Journal of Medical Science
6	American Journal of Physiology
7	American Journal of Roentgenology
117	American Journal of Roentgenology, Radium Therapy, and Nuclear Medicine
18	American Journal of Veterinary Research
70	Anatomical Record
99	Annals of Internal Medicine
8	Annals of The New York Academy of Sciences
118	Annual Review of Nuclear Science
91	Annual Reviews of Medicine
32	Archives of Pathology
101	Army Institute of Pathology
59	Biophysics Journal
126	Biophysik
55	Blood
10	British Journal Haematology
26	British Journal of Cancer
5	British Journal of Radiology
119	British Medical Journal
34	Bulletin Ac. Polish Sci. Ser. Sci. Biol.
116	Butterworths, London, Boston
48	Cancer
54	Cancer Research
53	Cell and Tissue Kinetics
124	Churchill Livingstone, Edinburgh
87	Clinical Radiology
121	Comision Nacional de Seguridad Nuclear Y Salvaguardias
20	CRC Press, Inc., Boca Raton, Florida
94	Defence Research Establishment, Ottawa, Canada
31	Defense Nuclear Agency, Washington, DC
104	Defense Technical Information Center, Alexandria, VA
37	Elsevier North Holland, Inc., New York
24	European Journal Cancer
30	Excerpta Medica Amsterdam
49	Frontiers of Radiation Therapy and Oncology
103	Gosudarstvennoe Izdatel'stvo Meditsinskoy Literatury, Moskva
76	Grune & Stratton, New York, NY
97	Harper & Row, Hagerstown, MD
27	Health Physics
51	Home Office, Great Britain

Table 4. Description of codes for the publication name field. (continued)

Code	Description
36	Igaku Shoin Ltd., Tokyo, Japan
62	Industrial Medicine
44	Inhalation Toxicology Research Institute
77	Institute for Defense Analyses, Washington, DC
74	Institute for Defense Analysis, Arlington, VA
3	Int. J. of Radiation Biology
14	Int. J. of Radiation Oncology, Biology, and Physics
45	International Atomic Energy Agency, Vienna
42	J.W. Press, Salt Lake City
86	John Wiley and Sons, New York, NY
85	Journal of Clinical Pharmacology
2	Journal of Immunology
61	Journal of Mathematical Biology
79	Journal of Occupational Medicine
127	Journal of Radiation Research
90	Journal of The Canadian Association of Radiologists
13	Journal of The Faculty of Radiology
50	Journal of The National Cancer Institute
25	Laucet
35	Martinus Nighoff Publishers, Dordrecht, The Netherlands
89	Masson Publishing USA Inc., New York, NY
52	Mathematical Biosciences
47	McGraw-Hill, New York, NY
81	Medical and Health Sciences Division, Oak Ridge Associated Universities, Oak Ridge, TN
115	Military Medicine
73	Ministry of Health of The U.S.S.R.
16	Molecular Aspects of Medicine
29	Mutation Research
23	National Academy of Sciences/National Research Council, Washington, DC
105	National Aeronautics and Space Administration, Washington, DC
41	National Council on Radiation Protection and Measurement, Bethesda, MD
100	National Technical Information Service, Springfield, VA
22	Nature
17	Naval Radiological Defense Lab, San Francisco, CA
102	New England Journal of Medicine
120	Pacific-Sierra Research Corporation, Los Angeles, CA.
21	Pathologie Biologie
82	Pergamon Press, New York, NY
98	Pharmacology and Therapeutics
43	Plenum Press, New York & London
68	Prentice Hall, Inc., Englewood Cliffs, NJ
56	Radiation Environmental Biophysics
28	Radiation Oncology

Table 4. Description of codes for the publication name field. (continued)

Code	Description
1	Radiation Research
75	Radiation Research Supplement
64	Radiobiologia Radiotherapia
33	Radiobiologiia
57	Radiology
11	Radiotherapy and Oncology
58	Raven Press, New York
113	S. Karger, Basel
60	Science
15	Scientia Sinica
63	Scientific American
88	Springer-Verlag, Berlin, Heidelberg
19	Stanford Research Institute, Project PYU-8150
110	Strahlentherapie und Onkologie
39	Taylor & Francis Ltd., London-New York-Philadelphia
69	The Johns Hopkins Press, Baltimore, MD
4	Transplantation
80	Trends in Pharmacological Science
92	U.S. Armed Forces Medical Journal
65	U.S. Atomic Energy Comm., Technical Information Service Extension, Oak Ridge, TN
9	U.S. Atomic Energy Commission, Division of Technical Information
66	U.S. Atomic Energy Commission, Washington, DC
46	U.S. Department of Defense, Atomic Energy Commission
93	U.S. Departments of Defense and Energy, Washington, DC
108	U.S. Departments of The Army, Navy, and Air Force, Washington, DC
112	U.S. Dept. of Energy Technical Infor. Center, Oak Ridge, TN
109	U.S. Public Health Service
72	U.S.A.F. School of Aerospace Medicine, Brooks AFB, TX
114	UCLA Medical Center, Los Angeles, CA
123	United Nations Scientific Committee on The Effects of Atomic Radiation (UNSCEAR)
125	University of Cincinnati Medical School, Cincinnati, OH
67	University of Rochester, Rochester, NY
111	University of Tennessee
122	University of Ulm, D-7500 Ulm, FRG
107	Verlag Karl Thieme, Munich
96	W. B. Saunders Co., Philadelphia, PA
106	Williams & Wilkins, Baltimore, MD
40	Zastosowania Matematyki (Applicationes Mathematicae)

Table 5. Description of codes for the species field.

Code	Description
BI	Birds
CL	Cell lines (<i>in vitro</i>)
DO	Dogs
HU	Human
MO	Monkeys
OM	Other mammals
RO	Rodents
ROH	Hamster
ROM	Mouse
ROO	Other rodents
ROR	Rat
SC	Single-celled organisms
SH	Sheep
SW	Swine

The kind of radiation exposure involved in the data is indicated by Tables 8, 9 and 10 which describe the codes for radiation type, exposure geometry, and exposure history, respectively. The exposure geometry determines the spatial distribution of ionizing radiation impinging on the subject, and the exposure history refers to the time dependence of the dose rate on the subject.

Table 6. Description of codes for the effects field.

Code	Description
CE	Cells
CED	Dicentrics, chromosome aberrations
FW	Fatigability and weakness
GI	Gastrointestinal syndrome
HE	Hematopoietic syndrome
LU	Lung damage
MA	Mathematical modeling and analysis
MO	Mortality
PD	Performance decrement
PE	Prodromal effects
SK	Skin damage

Table 7. Description of codes for the data source field.

Code	Description
AC	Accident
EX	Experiment
JD	Japanese data
TH	Therapy

Table 11 presents the final code description showing the keyword list accumulated for the bibliography.

The foregoing subsections have described the structure of the Protracted Exposure Annotated Bibliography and the guidelines for the information contained in that structure. The bibliography contains references to an extensive set of data on the biological response to protracted exposure to ionizing radiation. Although the bibliography does not represent the complete set of available radiobiological data, it should contain the bulk of the data having direct bearing on the Defense Nuclear Agency's Human Response Program. The rest of this section is devoted to a review and discussion of that data.

Table 8. Description of codes for the radiation type field.

Code	Description
AP	Alpha particles
BR	Beta rays
EL	Electrons, accelerator
GR	Gamma rays
IO	Ions
LA	Linear accelerator, unspecified
NE	Neutrons
NO	No exposure
PH	Photons (unspecified)
PHB	Bremsstrahlung
PN	Protons
XR	X-rays

Table 9. Description of codes for the exposure geometry field.

Code	Description
NU	Nonuniform
NUH	Half body
NUP	Partial body
NUU	Unilateral
UN	Uniform
UNB	Bilateral
UNO	Omnidirectional
UNR	Rotational
UNT	Total body (TBI)

Table 10. Description of codes for the exposure history field.

Code	Description
CR	Constant dose rate
DF	Dose fractionation--roughly equal doses
PR	Prompt (or acute) single dose
SP	Split-dose
VR	Varying dose rate or dose protraction

Table 11. Description of codes for the keyword fields.

Code	Description
AB	Alpha/beta ratio (LQ cell survival model)
AN	Anorexia
AS	Acute symptoms
BL	Bleeding
BM	Bone marrow
BR	Biological recovery
CC	Cell cycle redistribution
CH	Chromosome aberrations
CI	Continuous irradiation
CK	Cell kinetics
CP	Cell proliferation (repopulation)
CR	Cell repair
CS	Cell survival
CT	Crypt
CY	Chlamydomonas reinhardi (algae)
DI	Diarrhea
DL	Duration of life
DQ	Desquamation
DR	Dose rate
ER	Erythema
HY	Hypoxia
IA	Injury accumulation
IE	Iso effects
IK	Injury kinetics
IM	Immune response
IN	Infection
IV	In vivo cells
IVT	In vitro cells
LD	Lethal dose
LS	Life shortening
LYB	B-Lymphocytes
LYT	T Cell lymphocytes
MD	Mitotic delay
MG	Marrow graft
MM	Mathematical modeling
NA	Nausea
PN	Pneumonitis
RB	Relative biological effectiveness
RM	Radiation mortality
SD	Sublethal radiation
SDU	Symptom duration
SI	Symptom incidence
SO	Symptom onset
SS	Symptom severity
ST	Survival time
SU	Survival
TA	Targets
TK	Tissue (cell population) kinetics
TU	Tumor
VM	Vomiting
WR	Wasted radiation

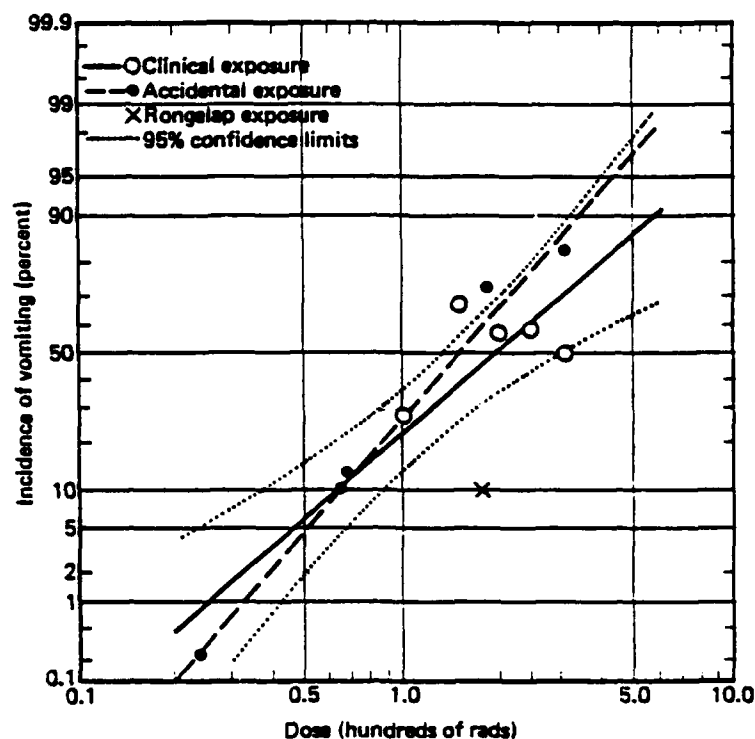
2.2 PRODROMAL SIGNS AND SYMPTOMS.

Nausea, vomiting, fatigability, and weakness have been identified as the principle signs and symptoms of acute radiation sickness associated with human performance degradation [Anno, Wilson, and Dore, 1984]. Consistent with the *Intermediate Dose Program (IDP) of the DNA* [Young, Auton, and Levin, in press], nausea and vomiting fall under the designation of uppergastrointestinal distress (UG), and fatigability and weakness are referred to as FW. Furthermore, the initial sequelae for both UG and FW are well known and quite similar following a brief exposure to radiation adequate to produce the responses. However, comparatively less is quantitatively known regarding these responses and their effect upon human performance when radiation exposure is protracted. Below we present a review of UG and FW sign/symptom categories that include protracted radiation exposures from some selected literature sources compiled in order to guide our modeling effort.

2.2.1 Nausea and Vomiting.

More frequently than not, literature sources do not distinguish between nausea and vomiting, although nausea is normally taken to be the milder component of the UG category and may occur at lower doses, not followed by emesis; also, based on some instances, emesis may not be preceded by nausea (this has been referred to as "projectile vomiting"). However, most will agree that both most commonly occur together; our review below distinguishes between the two responses where data permit.

Figure 1, developed by the Space Radiation Panel [Langham, 1967], demonstrates the incidence of vomiting within 48 h postirradiation. The incidence of vomiting is presented as a function of dose, assuming lognormal distribution of quantal response based on probit analysis. The incidence of vomiting in patients is shown by the solid line; accident victims are represented by the dashed line. The dotted lines are the 95 percent confidence limits. The data points for accidental exposures of primarily very high dose rates fall within the confidence limits determined from clinical data where the dose rate was about 30



Source: Langham [1987].

Figure 1. Incidence of vomiting (within 2 days of dose) as function of dose assuming lognormal distribution of quantal response.

to 60 cGy/h (MLT). Therefore, it is possible that the two groups respond similarly to protracted radiation with regard to incidence, although the estimated ED₅₀ values are significantly different--about 140 cGy for the accident group and 200 cGy for the clinical group.

The isolated point marked "X" in Fig. 1 indicates the incidence of vomiting in 64 Marshallese (Rongelap) accidentally exposed to an estimated dose of 175 cGy of fallout radiation from a nuclear weapon test [Cronkite, Bond, and Dunham, 1956]. Dose rates probably ranged from 5.5 cGy/h at the beginning to about 1.6 cGy/h at the end of exposure. The estimated range of the average dose rate over 51 h was about 3 to 3.5 cGy/h. This dose rate is much lower than that received by the patients. The incidence of vomiting was 10 percent in the Marshallese. Figure 1 indicates that patients who received their dose at a much higher rate of 30 to 60 cGy/h would have a similar incidence of vomiting at only about 65 cGy. The difference in dose at the

10 percent incidence level was probably caused by a modifying effect due to the much lower dose rate; this is one of a few of the low dose rate effects that have been directly observed in humans.

Figure 2 provides some additional insight into the difference in UG between acute and protracted exposures for the incidence of nausea and vomiting. Plots of incidence for clinical exposures are based on nausea and vomiting data given by Lushbaugh et al. [1968], Lushbaugh [1969], and Langham [1967] that reflect dose rates in the range of about 30 to 60 cGy/h. The accidental exposures are based on log likelihood probit analysis of 40 different cases of accidental acute exposure of humans to nuclear radiation [Anno and Dore, 1988]. The two isolated points indicate the incidence of nausea, "+" symbol [Gerstner, 1958], and vomiting, "x" symbol (as in Fig. 1), in the 64 Marshallese (Rongelap) accidentally exposed to fallout radiation (discussed above in regard to Fig. 1). With the exception of vomiting

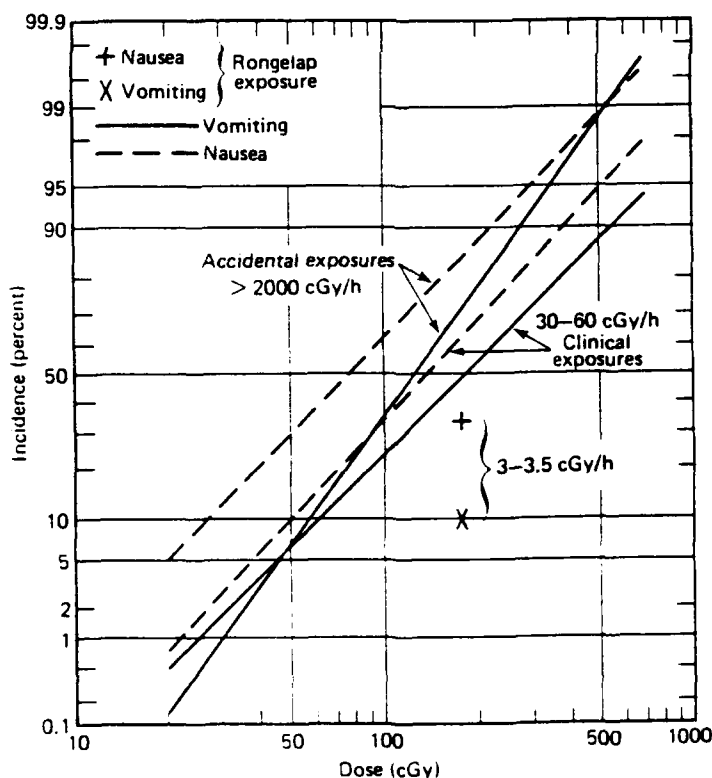
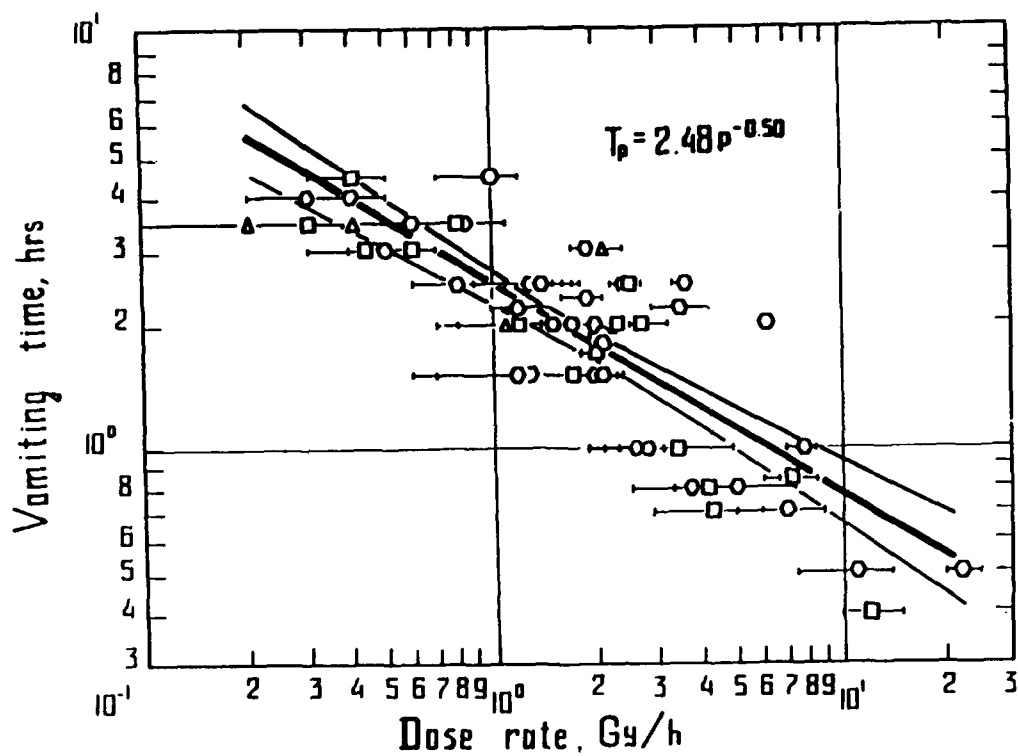


Figure 2. Incidence of nausea and vomiting within 2 days postexposure for accidental and clinical exposures.

for accidents at doses lower than 50 cGy, larger doses are required to effect an equivalent response for clinical exposure than that for accidental exposure. Moreover, the steeper slope for the accident vomiting curve reflects less variation in response as would be expected for normal men compared to patients with malignant disease. The steeper slope is not apparent for nausea; however, this may be due to the data which included some questionable points for nausea at low doses (23 and 61 cGy).

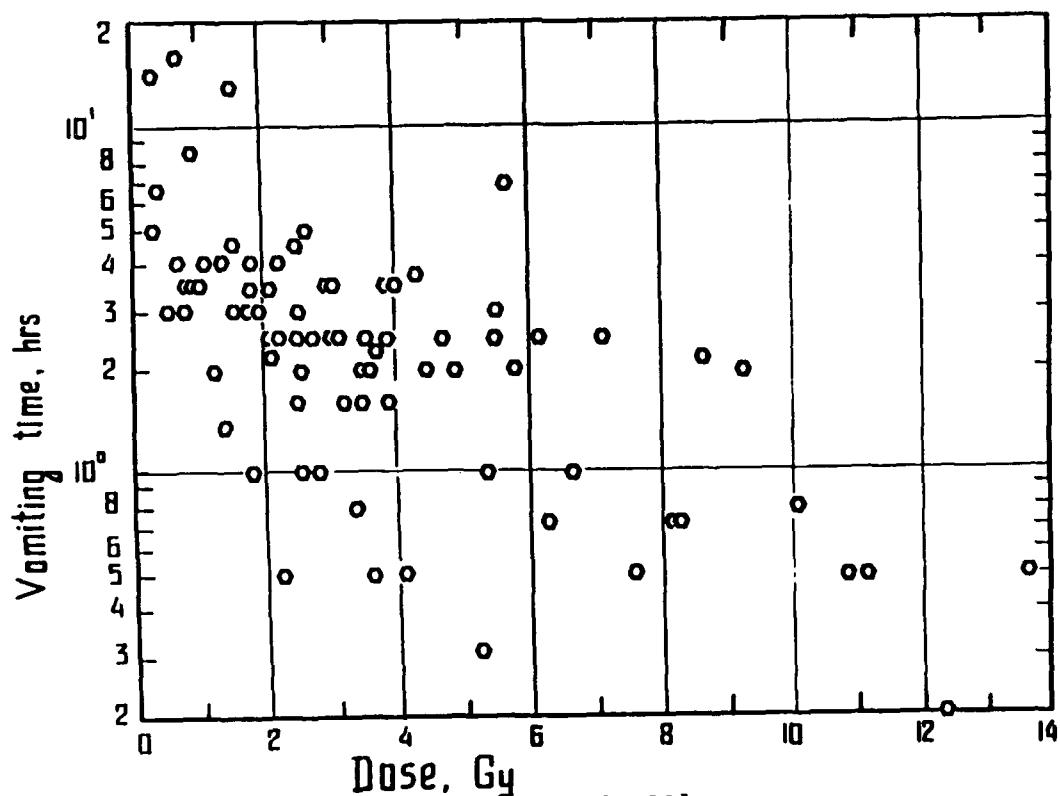
Based on Chernobyl accident exposures, Baranov and Guskova [1988] present data indicating a correlation of the time of vomiting with dose rate (Fig. 3). Dose rates range between 0.2 Gy/h and 20 Gy/h, and the time of vomiting between approximately 20 minutes and several hours. They also present data indicating the lack of correlation for the time of vomiting with dose (Fig. 4) ranging from approximately 0.3 to 13.6 Gy. However, two aspects of this data remain unclear regarding the vomiting time reference and cumulated dose. At high dose rates (and especially for low doses), whether or not vomiting time is referenced from the beginning or end of exposure may not matter much. However, at low dose rates (and especially for high doses), the reference time can be important. An example which follows serves to illustrate.

In Fig. 4, for 2.2 Gy, two extreme points for vomiting time (onset) can be found at 0.5 and 4 h. First, for the 0.5 h time point in Fig. 3, there are two corresponding dose rate points at 11 and 22 Gy/h. Assuming a cumulative dose of 2.2 Gy, results in exposure times of $(2.2/11) = 0.2$ h (12 min) and $(2.2/22) = 0.1$ h (6 min). Vomiting time referenced from the start of exposure would mean vomiting onset at $(0.5 - 0.2) = 0.3$ h (18 min) and $(0.5 - 0.1) = 0.4$ h (24 min) following the end of exposure. For acute or high rate (≥ 10 Gy/h) 18 and 24 min are significantly shorter than what would be expected for 2.2 Gy as indicated in Fig. 5 from Anno et al. [1989]. The curves given in Fig. 5 are based on a best-fit linear regression of accident, therapy, and combined (pooled accident and therapy) data. Therapeutic dose rates are all considerably in excess of



Source: Baranov and Guskova [1988].

Figure 3. Vomiting time versus dose rate.



Source: Baranov and Guskova [1988].

Figure 4. Vomiting time versus dose.

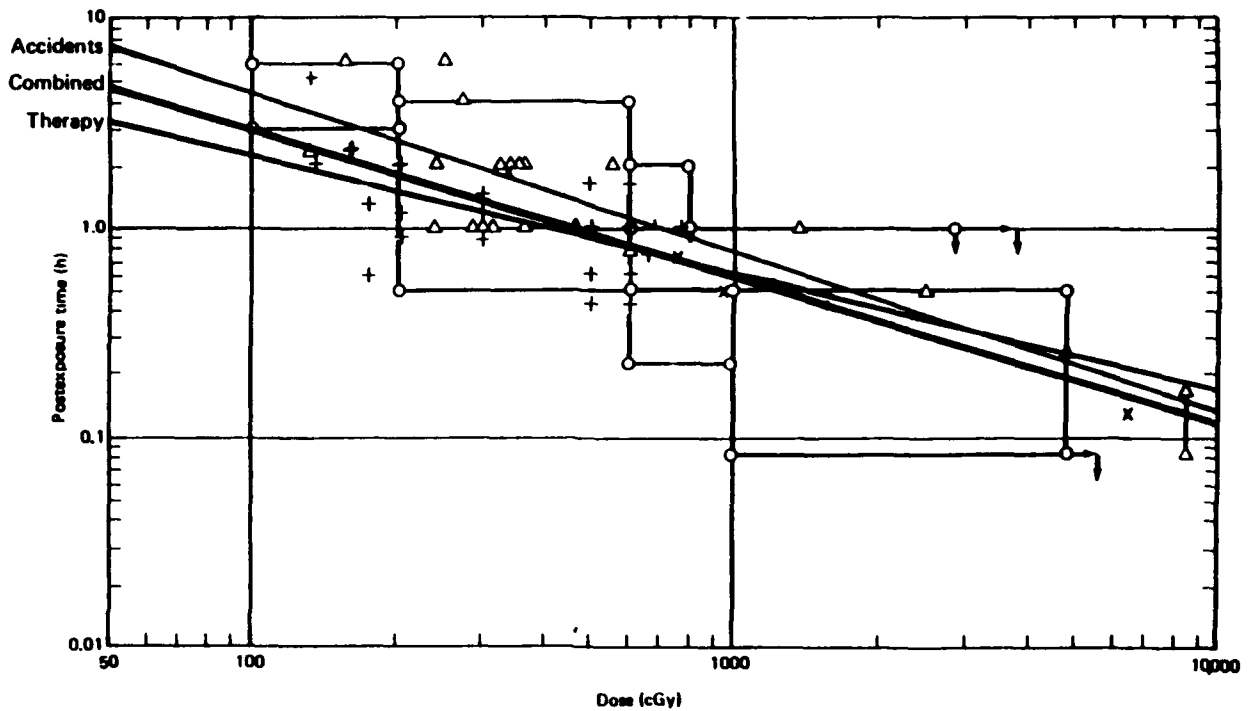


Figure 5. Onset of prodromal symptoms related to dose.*

*

△ Accident	Brucer 1959; Cronkite et al. 1956; Fanger and Lushbaugh 1967; Hübner and Fry 1980; Karas and Stanbury 1965; Laumets 1965; Lushbaugh 1973; Thoma and Wald 1959; Wald and Thoma 1961.
+ Therapy	Court Brown 1953; Miller et al. 1958; Rider and Hasselback 1968; Salazar et al. 1978.
○ Composite	Gerstner 1958; Gerstner 1970; Glasstone and Dolan 1977; Laumets 1965; Lushbaugh 1973; NATO 1973; Warren and Grahn 1973; Zellmer 1961.
X Expert Opinion	Anno 1983; Fanger and Lushbaugh 1967; Gerstner 1958; Glasstone and Dolan 1977; Saenger 1963; Thoma and Wald 1959; Wald and Thoma 1961.

100 cGy/h. Vomiting onset time (h), referenced from the end of exposure, was found to be related to dose (cGy) given by,

$$T = 10^{\alpha} \cdot D^{\beta}$$

where

Data Category	α	β
Accidents (23 pts.)	2.1830	-0.77260
Therapy (25 pts.)	1.4611	-0.56271
Combined (52 pts.)	1.8641	-0.69022

The second vomiting time point of 4 h, which corresponds to 2.2 Gy in Fig. 4, matches the dose rate points of 0.3 and 0.4 Gy/h in Fig. 3. Then exposure times to cumulate 2.2 Gy would be $(2.2/0.3) = 7.3$ h and $(2.2/0.4) = 5.5$ h, respectively. These time periods both exceed the 4 h vomiting time. Accordingly, for vomiting time referenced from the beginning of radiation exposure, it must be presumed that vomiting occurred during the exposure period at the time that doses of $(0.3 \times 4) = 1.2$ Gy and $(0.4 \times 4) = 1.6$ Gy were accumulated, both less than 2.2 Gy. It is obvious that difficulties arise in properly interpreting the data in Figs. 3 and 4 without more definitive data regarding the vomiting time reference and actual dose and associated dose rate. It appears that this data could be quite useful for protracted radiation response if it were more definitive.

Both onset and the duration of vomiting are time parameters that are relevant for modeling dynamic response to radiation. Table 12 summarizes onset and duration for some accident cases for acute or high dose rate (≥ 1000 cGy/h) exposures. These data indicate that acute doses must be at least 1200 cGy in order for vomiting to onset well under an hour postexposure; these data are reflected in Fig. 5. Table 13 summarizes vomiting onset and duration information extracted from primarily clinical radiation therapy experience; some investigators also drew from accident experience.

In addition to the illness condition of the radiation therapy patients that affect response, other difficulties arise in published therapeutic data for response modeling purposes. These are mainly nonuniform clinical treatment conditions involving various drugs (chemotherapeutic cytotoxins, antiemetics, analgesics, sedatives, etc.) and different irradiation conditions (doses, dose rates, and uniformity of body exposure). Moreover, the UG toxicity effects often receive only scant attention or are given as responses aggregated over the parameters of interest unless they are the specific focus of clinical interest. Also, most of the therapeutic exposure rates are at least several hundred cGy/h where the vomiting response becomes less sensitive to dose rate. This is reflected in Table 13, where only a few sources of information are associated with dose rates less

Table 12. Accident cases--vomiting onset and duration.

Case ^a	Dosimetry		Onset	Duration	Comments	Reference ^d
	γ/n ratio	Internal Dose (cGy) ^b				
A1	0.01	156	6 h	1 h		T
UT/CARL	0	165 ^c	2.25 h	24 h		H
LA4	6.4	192	6 h	1 h		T,H
NJ(2)	0	200	2 h	1.5 h		H
Y5(H)	0.26	226	~1 h	~2 d		L,T,H
OR5(E)	0.36	236	2nd d	6 h	(Nausea and vomiting 2nd day)	A,T,H
OR4(B)	0.36	270	4 h	2 d		A,T,H
Y4(G)	0.28	290	~1 h	~2 d		L,T,H
Y2(D)	0.28	293	~1 h	~2 d		L,T,H
Y3(M)	0.27	298	~1 h	~2 d		L,T,H
R2	?	300	1 h	4 h		T
P(B)	0	300	~1 h	~1-2 d		H
Y1(V)	0.26	305	~1 h	~2 d		L,T,H
LA1	0.55	310	1.5 h	1 d		T,H
OR3(D)	0.36	327	2 h	1 d		A,T,H
OR2(C)	0.36	339	2nd d	30 min	(Nausea and vomiting 2nd day)	A,T,H
OR1(A)	0.36	365	2 h	2 d		A,T,H
NJ(1)	0	410	1 h	?	(Vomited several times; nausea 18 h)	H
R1	?	450	1 h	3 d		T
B	0.1	550	2 h	few h	(Antiemetics given effective)	H
P(C)	0.0	670	45 min	brief		H
LA(3)	8.8	1114	1 h	~12 h		T,H
I	0	1200	30 min	few h		H
LA11(K)	0.25	4500	15 min	35 h		F
RI(P)	0.313	8800	5-10 min	~3.5 h		F

^aCase nomenclature relates to that reported in the literature; numbers and/or letters that may be parenthetical following the geographical location keys given below, designate specific individuals.

LA: Los Alamos A: Argonne RI: Rhode Island P: Pittsburgh OR: Oak Ridge I: Italy
 NJ: New Jersey R: Russia UT: U. of Tennessee Y: Yugoslavia B: Belgium

^bMidline body or mean bone marrow dose neutron (RBE = 1).

^cAverage dose to stomach and intestines.

^dA = Andrews, et al. (1959) L = Lushbaugh (1969) T = Thoma and Wald (1959)
 H = Hubner and Frye (1980) F = Fanger and Lushbaugh (1967)

than 200 cGy/h. In general, onset for the low dose rate exposure is later than that for high dose rate as indicated by Baranov and Guskova [1988] in Fig. 3. There may not be much difference in duration, although it may be difficult to immediately discern this from Tables 12 and 13.

It has been suggested that the dog is in some regards a reasonable laboratory study model for radiation-induced emesis in man due to similar behavior. In terms of emesis onset, this appears to be somewhat the case from Tables 12, 13, and 14. However, in terms of duration of vomiting, man seems to exist in a state of intermittent vomiting over a substantially longer period.

Table 13. Therapy (and some accident) cases--vomiting onset and duration^a.

Reference	Basis or Case(s)	Dose (cGy) ^b and Dose rate (cGy/h) ^b in parentheses	Onset	Duration	Comments
Thomas, et al. (1971)	7	1000 (190-220)	≤5 h	during irradiation (6/7); 0-24 h (3/7); 24-48 (3/7)	premedication antiemetics
Gerstner (1958)	Mixed review: 101 accidents & 75 TBI	50-400 (150)	≤2 h	5-8 h climax; rapid decline in 1 d; occasional in 2 d	64 Marshallese, 175 cGy at 3-3.5 cGy h; 1/3 nausea and 1/10 vomiting
Levin, et al. (1959)	11	100-134 (300-320)	2-4 h	5-8 h climax; intense 4-10 h; subside 2nd or 3rd day	
Gerstner (1960)	Consensus: TBI and accidents	≥134-800 rad (300-320)	2-4 h	5-8 h climax; subside by 2nd d	
Rubin & Casarett (1968)	Typical TBI	330-660 (~300)	≤2 h	8 h climax; subside by 2nd d	
Lushbaugh (1969)	Review based on accidents	few 1000 rad	5-15 min	Might persist up to several days, usually less than 48 h	
Lushbaugh, et al. (1967)	84 TBI	30-2-- rad (30-64)	≤6 h	≤2 d, scoring time	
Cassady, et al. (1976)	8	1000 (300)	≥3.5 h	1-5 d	Antiemetics
Deeg (1983)	Review of TBI (Seattle experience)	1000 (300-480)	2-3 h	1-2 d	Antiemetics not too effective, chemo- therapy may contrib- ute to toxicity
Miller, et al. (1958)	30	130 (150)	~2 h	1st 24 h 12/17 2nd 24 h 7/17 3rd 24 h 3/17	17/30 (57%) vomited ≤72 h; 15/30 vomited ≤24 h; some anti- emetic treatment
Rider and Hasselback (1968)	20	300 (1200)	45 to 60 min	7-8 h	

Table 13. Therapy (and some accident) cases--vomiting onset and duration^a (continued)

Reference	Basis or Case(s)	Dose (cGy) ^b and Dose rate (cGy/h) ^b in parentheses	Onset	Duration	Comments
Millburn, et al. (1968)	6	300 (600-900)	1 h	≤36 h	Antiemetics
Grant, et al. (1979)	271	3 subgroups ≤600 ~800 ≥1000	30 min-2 h 50 min (mean)	1-9 h 2.5 h (mean)	Half-body irradiation
	137	600-1000 (2700) 800	≤3.4 h 0.83 h (avg.)	≤9.0 h 2.5 h (avg.)	UHBI
Danjoux, et al. (1979)	189	300-1000 (900-1000)	80 min	6 h (mean)	Half-body irradiation
Warren & Grahn (1973)	Review	100-200 200-550 550-750 1000	<5 h <5 h, mean: 2 h <4 h <1-2 h	~1 d ~1 d ~1 d ~1 d	
Fitzpatrick & Rider (1976)	82	500, 600, 800 1000 (1000-6000)	~1 h	Mostly few h; few >24 h	All half-body, UHBI moderate to severe, LHBI none to mild
Fitzpatrick & Rider (1975)	139	500, 600, 800 1000 (1000-6000)	45 min-3.5 h	4-5 h (80%); >24 h (few)	All half body; vomiting: 80% UHBI, 33% LHBI; antiemetics in 1/2
Salazar et al. (1978)	40	800 (1800-2400)	~0.5 h	8-10 h	55% UHBI; 17% LHBI
Epstein (1979)	10	800 (1600)	>0.5 h	≤24 h	Half-body irradiation, antiemetics
Court Brown (1953)	50	100-150 (≥1000)	2.25 h	2-3 h	Partial body irradiation

Table 13. Therapy (and some accident) cases--vomiting onset and duration^a (continued).

Reference	Basis or Case(s)	Dose (cGy) ^b and Dose rate (cGy/h) ^b in parentheses	Onset	Duration	Comments
Saenger, et al. (1973)	88	100-200 TBI 100-300 UHB or LHB (180-360)	≤3 h	≤24 h	44% no nausea and vomiting
Barrett (1982)	15 TBI centers, 23 patients	750-1050 (150-2760)	30 min to 2.3 h	Not given	Premedication: sedatives, tranquilizers, steroids, antiemetics
Westbrook, et al. (1987)	178	950-1050 (120-240)	~3-3.5 h	≤12 h	Low dose rates, 120 to 240 rad/h; most vomit after 2 to 4 Gy accum. Premedication: sedatives, tranquilizers, steroids, antiemetics

^aAbbreviations: TBI = Total-body irradiation
UHB = Upper-half-body irradiation
LHB = Lower-half-body irradiation
^bAbsorbed midline tissue dose

Table 14. Dog studies--vomiting onset and duration.

Reference	Basis or case(s)	Dose (cGy) (dose rate)	Onset	Duration	Comments
Mattson, et al. (1984)	202	206-250	3.4 h	48 min	Controls:
		303-368	2.1 h	66 min	6/15, 2.2 times
		446	2.7 h	7 min	5/7, 5.2 times
		170-658 (3600 cGy/h)	1.5-3 h	3.5 h few, ≥ 6 h	1/1, 2.0 times
Gralla, et al. (1979)	13	800 rad abdominal area (3000 r/h)	46 min	~2 h	Average for all in- cluding controls and antiemetic drug drug trials
Carpenter, et al. (1986)	24	~800 (1200-2400 cGy/h)	1.7 h	1.6 h	Controls 13/13, 6-7 times
					Controls 5/5, 7-8 times

In Fig. 6, we have summarized some data on vomiting, plotting estimates of the 50-percentile dose response, ED₅₀, for constant dose rate exposure. Although relevant, not all the data represented in Fig. 6 reflect an ED₅₀ due to lack of samples, inadequate definitive breakdown of information, or substantial uncertainty. However, we include these data in Fig. 6 and the discussion below to illustrate their relevance to modeling emesis for protracted dose exposure particularly in view that they represent some of the only data available for humans.

The data indicated by (A), (B), (C), and (D) are reasonably reliable estimates of ED₅₀. The data given by (A) are based on a log-likelihood probit regression analysis of 40 different accident cases for the emetic response within two days following very short exposures of dose rates exceeding ~20 Gy/h [Anno and Dore, 1988]. The data for (B), (C), and (D) are based on total body irradiation (TBI) exposure of patients with malignant diseases. The uncertainty is indicated by the error bars (standard error) for (B) and (C) as well as the rectangular representation given for (D). The data given by (E) and (G), also based on TBI clinical data are quite uncertain as indicated. The data for (E) was constructed from an ED₅₀ estimate of about 490 rad

protracted over a period of from 2 to 8 days. The data at (G) carries even more uncertainty; it is based on a questionable ED₅₀ estimate of about 590 rad protracted over a period of greater than 8 days, where a dose rate of at least 0.6 to 0.8 rad/h is thought to be the apparent threshold to cause vomiting within 30 days or more (open-ended dose indicated by arrows pointing upward).

The data indicated at (F) is based on an extrapolation of the data for the Marshallese (Rongelap) accidentally exposed to fallout irradiation from nuclear weapon testing in the Pacific, that corresponds to the "x" data point in Fig. 1 (and 2) at the 10 percent incidence level. The basis for our extrapolation assumes a shallower slope for the probit relationship in terms of the logarithm of dose. That is in Fig. 2, a shallower slope of the incidence curve is shown for clinical than for accidental exposures, where the dose rate corresponds to about 30 to 60 rad/h compared to acute exposures for

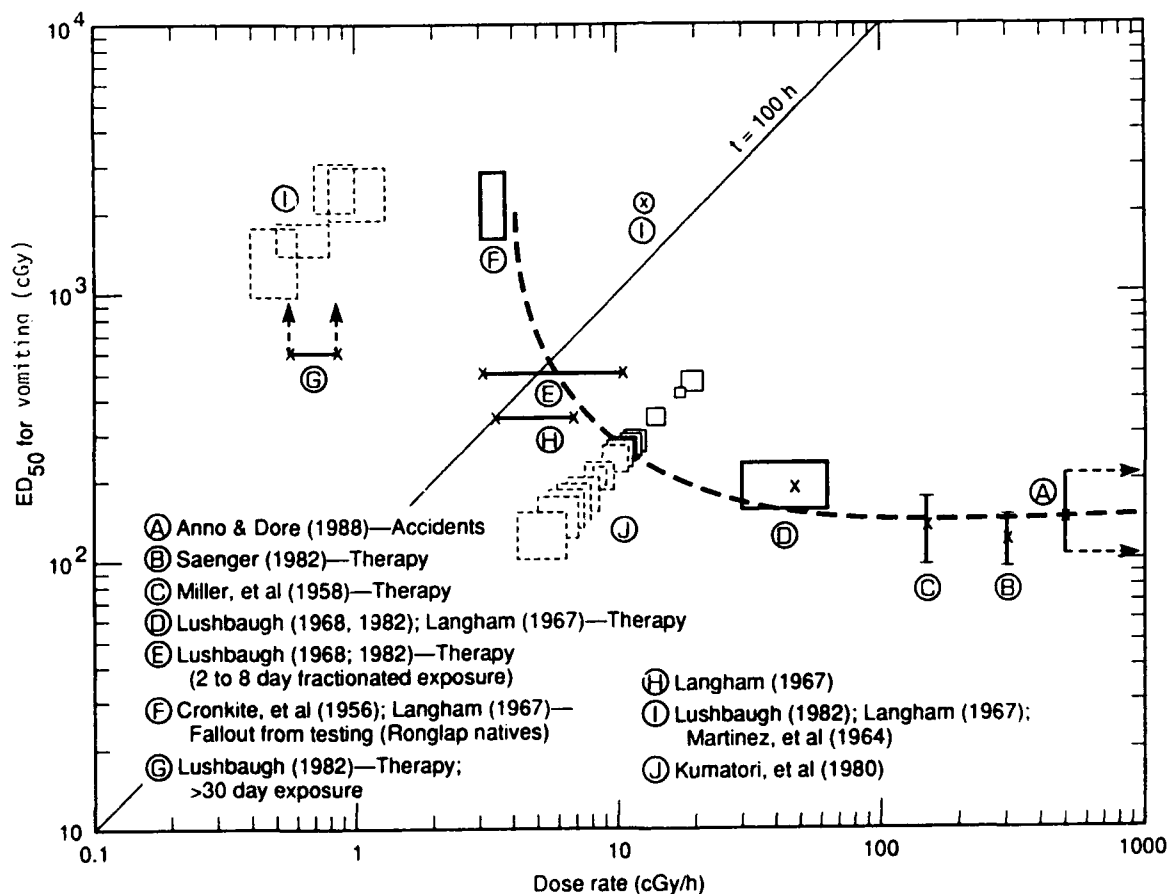


Figure 6. ED₅₀ for vomiting versus dose rate.

accidents. The dose rates estimated for the Marshallese fallout accident were only about 3 to 3.5 rad/h. We arbitrarily chose to assume probit slopes of 0.4 to 0.5 of that for the clinical probit relationships which enabled estimates to be made for the constants in probit relationships for the lower dose rate response when the curves pass through the "x" point. The lower dose level of (F) corresponds to 0.5 slope and the higher to a 0.4 slope. This means of extrapolation from only a single data point does not engender a great amount of confidence. In fact, because of the lack of any additional data, the actual uncertainty must be assumed to be significantly greater than represented.

The data given by (H) are based on a suggested prescription by the space radiation study panel to take dose protraction into account for prodromal symptoms (or signs), e.g., nausea or vomiting, when radiation exposure extends to a period of two to four days compared to two to four hours [Langham, 1967]. Here it is suggested that the effective dose to cause a given dose response level is a factor of 2.5 times higher when protracted over the longer period.

The data designated by (I) do not apply to ED₅₀, rather they are based on the 1962 Mexican accident in which five family members were exposed to ⁶⁰Co radiation over a period of about 100 days [Martinez et al., 1964]. The four dashed rectangles represent family members who were exposed to average dose rates less than about 1 cGy/h; only one survived (father, lower left rectangle). The dose and dose rates are estimated ranges; none of these individuals were reported to have vomited over the course of exposure. However, the family member (son) indicated by the circled x-point had vomiting after being exposed for the first seven days at an average dose rate of about 12.5 rad/h after cumulating a dose of about 2100 rads (this individual also died after subsequently accumulating an additional dose, but at a lower dose rate). This data serves to illustrate the lack of vomiting for dose rates less than about 1 cGy/h and its occurrence at least as low as 12.5 cGy/h.

The series of rectangles designated (J) also do not directly apply to ED₅₀ for vomiting, but are also relevant to the response for protracted radiation. Following a nuclear test device explosion in the Pacific in March 1954, twenty-three Japanese fishermen were continuously exposed to radiation over a period of about two weeks from lingering radioactive fallout that contaminated their fishing vessel, the 5th Fukuryumaru (the Luck Dragon). Kumatori et al. [1980], indicate the frequency of vomiting as a function of time in Fig. 7; on the first day, vomiting is indicated for eight of the fishermen. Kumatori et al. also give whole body gamma radiation dose estimates (ranges) for each exposed fisherman for the first day and the total accumulated dose over the two-week exposure period. We assumed that the eight fishermen who vomited on the first day also had the highest doses in the first day. The dashed line in the cumulative dose plot of Fig. 8 suggests that the eight who vomited had doses of at least 220-270 cGy which corresponds to average dose rates over 24 h of at least 9 to 11 cGy/h. The solid rectangles in Fig. 6 indicate those who vomited on the first day based on the assumption given above; the dashed rectangles presumably correspond to those who did not vomit.

Even though our review and analysis of the data shown in Fig. 6 was burdened by an appreciable measure of uncertainty, particularly at low dose rates, the data are quite relevant. Dose rates less than perhaps a few cGy/h are probably not high enough to cause significant

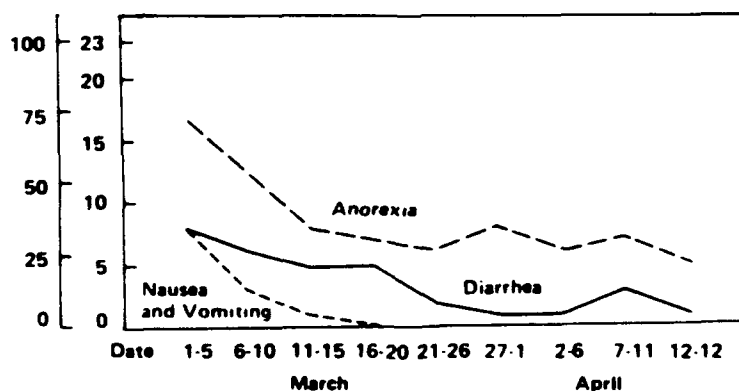


Figure 7. Gastrointestinal signs and symptoms in the early stage.

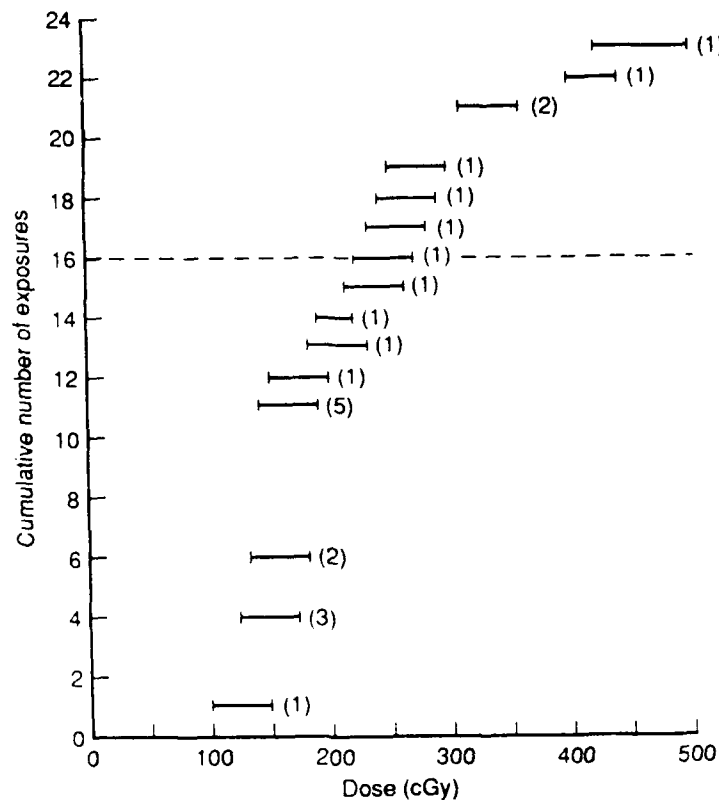


Figure 8. Cumulative whole body gamma fallout dose for 23 Japanese fishermen during the first day.
Data source: Kumatori et al., 1980.

vomiting in humans exposed to radiation protracted continuously over a period of one to two weeks. However, continuous dose rates of around 10 cGy/h are probably enough to cause significant vomiting within a period of a few days. Therefore, between a few cGy/h to around 10 cGy/h, there exists a considerable amount of uncertainty of the human response to continuous exposure of radiation. The dashed curve drawn through some of the data is simply an "eye fit" of what the ED₅₀ might look like based on our interpretation of the available data.

Fig. 9 contains a summary of some ED₅₀ data for nausea for continuous constant dose rate exposure. Some of the data sources are common to some of those in Fig. 6. Therefore, much of the discussion pertaining to Fig. 6 regarding uncertainty, etc., applies to Fig. 9. The data given by (A) are from a log-likelihood probit regression analysis of the 40 different accident cases for nausea occurring within two days following acute exposure [Anno and Dore, 1988]. The

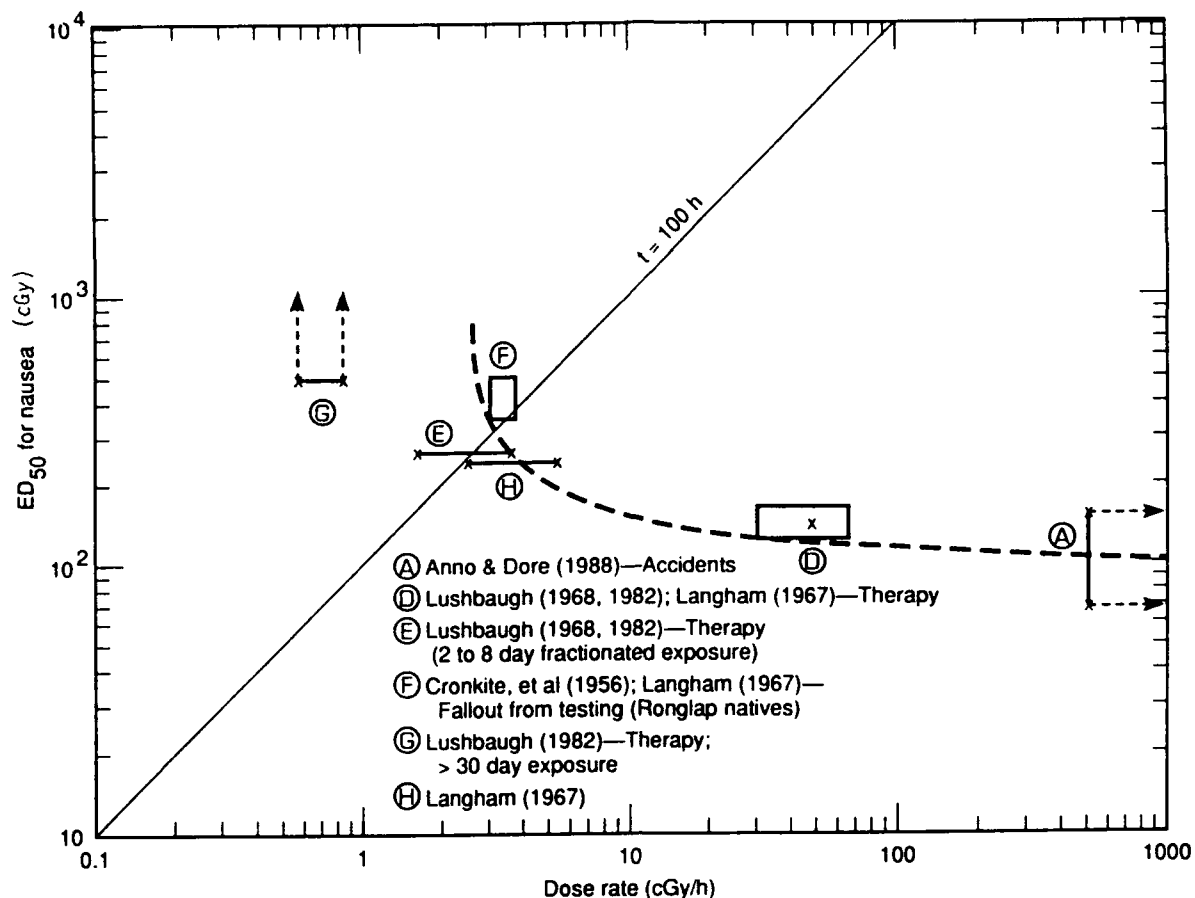


Figure 9. ED₅₀ for nausea versus dose rate.

data at (D) are based on TBI patients with malignant diseases. The dose and dose (standard error) rate uncertainty (standard error is expressed by the rectangular boundaries). The data at (E) and (G) are quite uncertain as indicated. The data at (E) was constructed from an ED₅₀ estimate of 262 rad protracted over a period of 2 to 8 days. The data at (G) are even more uncertain; it is based on a questionable ED₅₀ estimate of about 500 rad protracted over a period exceeding 8 days where, like for vomiting, a dose rate of at least 0.6 to 0.8 rad/h is thought to be required to also cause nausea within 30 days or more (open-ended dose indicated by arrows pointing upward).

The data at (F) is based on the Marshallese fallout radiation exposures, except that nausea occurred in one-third of those exposed to 175 cGy (compared to one-tenth for vomiting), as indicated in Fig. 2 by the cross (+) symbol. Extrapolation of that data to that given at (F) in Fig. 9 was carried out in the same manner as that

described for the (F) vomiting data in Fig. 6. The data at (H) are also based on the same prescription as was suggested for vomiting by the Space Radiation Study Panel [Langham, 1967].

Compared to the emesis data in Fig. 6, the data for nausea shown in Fig. 9 are even less definitive with at least as much uncertainty for low dose rates. However, since nausea and vomiting generally occur together, responses with regard to protracted dose rates, thresholds, etc., are probably similar in magnitude. Although generally because of the relative sensitivity suggested by Lushbaugh et al. [1968], the ED₅₀ curve for nausea would generally fall below the ED₅₀ curve for vomiting (Fig. 6) and also be shifted toward lower dose rates. The dashed curve drawn along some of the data is also simply an "eye-fit" of what the ED₅₀ might look like based on the available information.

The 1984 Juarez accident [Comision Nacional de Seguridad Nuclear Y Salvaguandias, 1984] provides some additional low dose rate information based on estimates of accumulated dose and human activities. The accident involved multipersonnel exposure to gamma radiation from a mishandled teletherapy unit that was mistakenly disassembled and used in the manufacture of scrap iron materials. During the course of handling and processing the unit, workers at Yónke Fenix (scrap metal processing facility) were estimated to have received the highest levels of radiation exposure.

Working Area #4 at Yónke Fenix was the area with the highest dose rate environment of 10 r/h with an occupancy factor of 25 percent. Based on work schedules for that time at the facility, exposure times were estimated to be 8 h per day for 28 days and 5 h per day for 6 days. This results in 254 work hours for Area #4 and an estimated accumulated reference dose of 420 cGy. During occupancy at Area #4, the midline tissue (MLT) dose rate would be about 6.6 cGy/h (assuming a 0.66 cGy/r conversion factor).

Based on chromosome observation analysis, the three highest doses calculated for Yónke Fenix workers were 355, 390, and 550 cGy. When these doses are normalized to the estimated reference dose of 420 cGy for Area #4 occupancy, the daily doses that correspond to these three

highest doses average between about 10 to 16 cGy/day; during actual occupancy, dose rates would range from 5.6 to 8.7 cGy/h. None of the workers declared that they had nausea, vomiting, or fatigue. Assuming this was indeed the case, intermittent periods of gamma radiation exposure at the above dose rate levels for many days apparently are not enough to produce upper GI symptoms (as well as fatigue). However, since the time intervals of constant dose rate exposures were interpreted by longer periods devoid of irradiation, it would be difficult to generalize the effect of dose rate alone on vomiting or nausea from this experience.

No qualitative human data could be identified in our review that illustrates the habituation effect of increasing exposure fraction upon the UG response in terms of either onset time, incidence, or severity. However, anecdotal accounts from radiation therapy experience suggest a diminishing response with repetitive periods of fractionated exposure over the duration of treatment. Based on 6 TBI fractions of 200 cGy given at high dose rate (1200 cGy/h) over a three-day treatment period, Tichelli et al. [1987] indicated that most patients (83 percent) experience nausea and emesis, but usually just after the first or second session of TBI. Also based on a therapy protocol of 6 TBI fractions of 170 cGy each administered at a high dose rate (1500 cGy/h) over a three-day treatment period, ward nurses indicate that patients become nauseated and vomit 0.5 to 1.0 h after the first fraction; following the second fraction, signs and symptoms may become more severe than after the first, but they become increasingly less frequent and severe after the third and subsequent fractions [Anno, 1983].

The effect diminishing emetic response for a second radiation given 24 h following the first one was demonstrated in cats by Borison et al. [1988]. Using ^{60}Co radiation, cats were exposed to two equal doses ranging from 7.5 to 60 Gy (at a high dose rate of 1.0 Gy/min). Emesis was recorded within two time periods, 12 h and 24 h. As expected, emesis incidence increased monotonically with dose for the single exposure. However, in sharp contrast with the initial radiation exposure, the emetic results of the second radiation showed a

reversal of pattern as compared to the first exposure, where the incidence is monotonically decreased with dose with an apparent cross-over at about 15 Gy. Also significant was an increase in the mean emetic latency time from approximately 2 to 16 h. Within 12 h following the second exposure at 30, 45, and 60 Gy, emesis did not occur; at 24 h following the second exposure, it still did not occur at the 45 and 60 Gy dose level. These results lend credence to the idea of a diminished emetic response with increasing secondary periods of exposure. Also, in regard to modeling UG response, it is important to note that there may be a finite "mechanistic capacity" to consider that limits emesis.

2.2.2 Fatigability and Weakness.

It is common knowledge that both therapy patients and nuclear radiation accident victims experience postirradiation episodes of easy fatigability. However, with few exceptions, this "easy fatigability" is a qualitative assessment, and subjective descriptions of severity and duration may vary considerably even for common levels of radiation dosage. Table 15 is a summary of radiation-induced fatigability and weakness (FW) described by various investigations. Table 16 lists FW onset and duration data compiled by Thoma and Wald [1959] based on some nuclear accident victims. Much of the information in these tables refers to either acute or high-dose rate exposures, and because of the lack of low-dose rate data, it is difficult to contrast differences in response due to protracted radiation exposure. Although for acute radiation exposure, typically the FW response is believed to correlate temporally with the UG response [Baum et al., 1984; Anno, Wilson, and Baum, 1985].

Using the kind of information exemplified in Tables 15 and 16, the DNA/IDP developed an interpretation of the FW response to acute and high-dose rate radiation exposure based on an arbitrary 5-point ordinal scale to grade severity (Fig. 10). These dose response profiles are an attempt to incorporate the qualitative description of FW into a plausible time-frame which is a first step necessary to (1) assess correlation with more objective data and (2) provide a

Table 15. Fatigability and weakness.

Lushbaugh, 1969	Median lethal doses (300 ± 100 rad?) principal prodromal reaction symptoms: anorexia, nausea, vomiting, and <u>easy fatigability</u> .
Lushbaugh, 1973	Demonstrated <u>exercise intolerance</u> and decreased performance capability in patients (physiologic monitoring and bicycle ergometry) irradiated at tolerance levels (up to 150 rads).
Ricks et al., 1972	<u>Decreased performance capability</u> after single prompt exposures of less than 200 r (~132 rad).
Gerstner, 1958	"Typical" acute initial period radiation syndrome: upset stomach, anorexia, nausea, malaise, listlessness, drowsiness, and <u>fatigue</u> within 2 h--rapid deterioration of condition leading to profuse vomiting, <u>extreme weakness</u> , or even <u>prostration</u> culminating in 8 h and lasting 2 to 3 days.
Messerschmidt, 1979	≥ 600 rad, repeated <u>fatiguing vomiting</u> , nausea, and dizziness follow in a matter of minutes--drowsiness, <u>severe exhaustion</u> , and circulatory symptoms to the point of collapse are evident within a few hours; 200-600 rad, nausea, vomiting, and exhaustion are milder.
Rubin & Casarett, 1968	<u>Muscle fatigue</u> a common complaint in radiation therapy patients--severest degree of creatinuria observed in patients with severe fatigue--no direct effect of ionizing irradiation or muscle clinically recognizable.
Hall, 1978	At LD _{50/60} , principal prodromal reaction symptoms are anorexia, nausea, vomiting, and <u>easy fatigability</u> .
Miller et al., 1958	At 200 r (~132 rad), 3.8 r/min (~2.5 rad/min), 27/30 (90%) patients reported <u>fatigue</u> , decreased energy, drowsiness, or malaise within a few hours post irradiation, peaking 6 to 8 h, subsiding 24 hours later.
Bond, 1965	In all (accident) cases (150 to 450 rads), a definite sense of <u>fatigue</u> was reported--coincidental with nausea and vomiting--persisted in all cases for months.
Court Brown, 1953	Halfbody irradiation, 3-4 megagram-r, mean time to symptoms 2.7 hours--sudden bouts of nausea or <u>feeling of severe fatigue</u> ; outstanding complaints of fatigue by some--nausea, mild and transitory, fatigue without nausea, rare.
Vodopick and Andrews. (Hübner and Fry, 1980)	127 rad co ⁶⁰ accident-- <u>excessive fatigue</u> with least amount of exertion (endurance tested with bicycle exercise monitored by ergometer--accompanying CPK level rise in serum monitored) continuing for months.

Table 16. Fatigability and weakness--accident victims.
Source: Thoma and Wald, 1959

Case	Dose (Rad)	<u>Prodromal Period</u>		<u>Manifest Period</u>	
		Onset	Duration	Onset	Duration
OR8	22.8	2 h	1 d		
Y6	145	1 d	>120 d		
LA4	192	1 d	70 d		
Y5	226	1 d	>120 d		
Y4	290	1 d	>120 d		
Y2	293	1 d	>120 d		
Y3	298	1 d	>120 d		
R2	300	1 h	4 d	24 d	20 d
Y1	305	1 d	31 d		
LA1	310	1 h	24 d		
R1	450	1 h	4 d	19 d	22 d
LA3	1114	1 h	1 d	1 d	9 d
LA11	4500	5 min	35 h		

basis for the dynamic behavior required for modeling the response to protracted radiation exposure. These profiles suggest a biphasic behavior below certain dose levels which has invited considerable phenomenological speculation such as tissue/organ damage and recovery involving toxic substance accumulation, disrupted enzymatic processes, inhibited oxygen transport capability, etc. Furthermore, there may be at least two primary mechanisms that dominate behavior over different time periods following exposure. However, no single casual mechanism has, or a comprehensive set of mechanisms have been clearly identified to serve as a reliable basis for mechanistically modeling the FW response.

Data that relate FW succinctly to dose rate are very rare. Figure 11 shows the incidence of fatigue for the accidental fallout radiation exposures of Japanese fishermen discussed previously above [Kumatori et al., 1980]. Figure 11 indicates that nearly all, 21 to 22 individuals, had fatigue the first day of exposure. Assuming those who had fatigue also sustained the highest doses, Fig. 8 would suggest that perhaps 1 to 2 individuals out of 5 vomited who received doses between 100 to 170 cGy on the first day. This would correspond to an emetic incidence of 20 to 40 percent for a fallout dose rate between 4

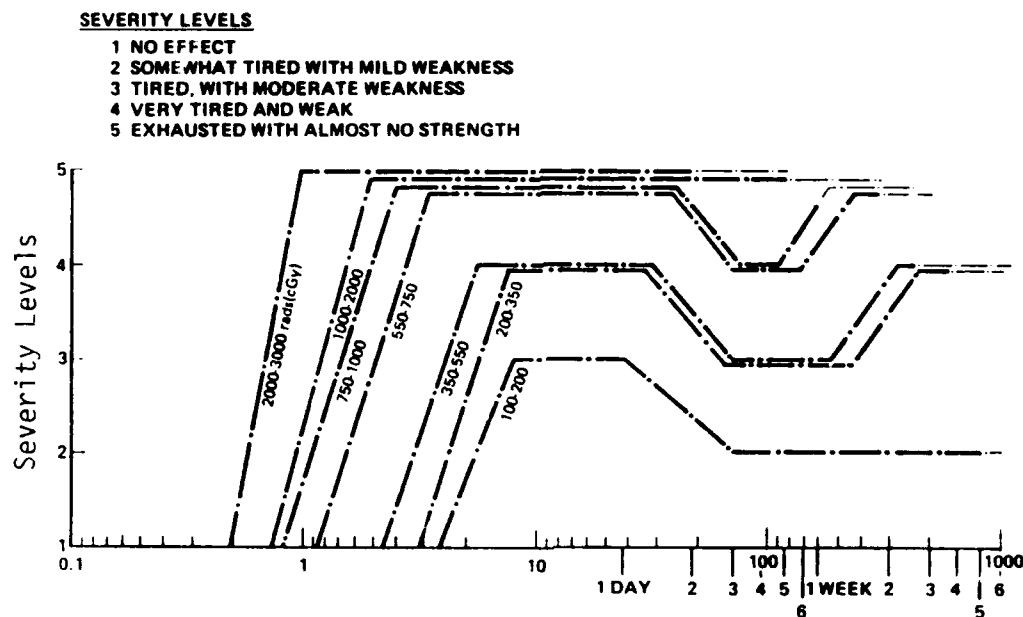


Figure 10. Fatigability/weakness severity levels for dose ranges (Dose (FIA) = 1.5 dose (MLT)).

to 7 cGy/h based on Japanese fishermen exposed during the first day, as indicated in Fig. 12. The straight-line curve is a log-normal fit based on probit regression analysis of therapy patient data [Langham, 1967] where dose rates were about 30 to 60 cGy/h. The "X"-point is based on therapy from Miller et al. [1958] where the dose rate was 150 cGy/h.

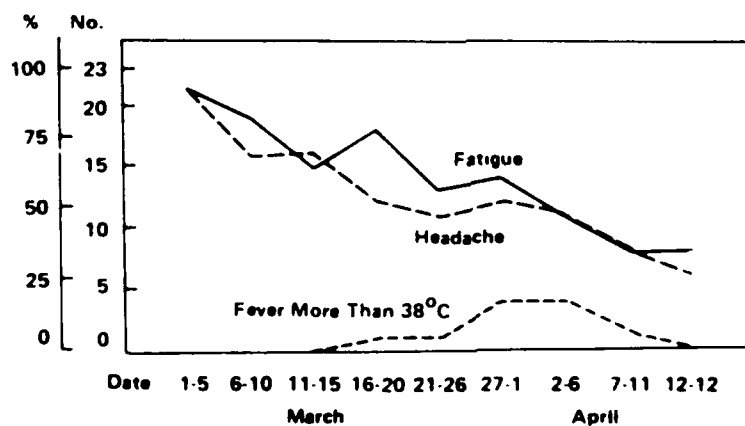


Figure 11. Fatigue, headache, and fever.
Source: Kumatori et al., 1980.

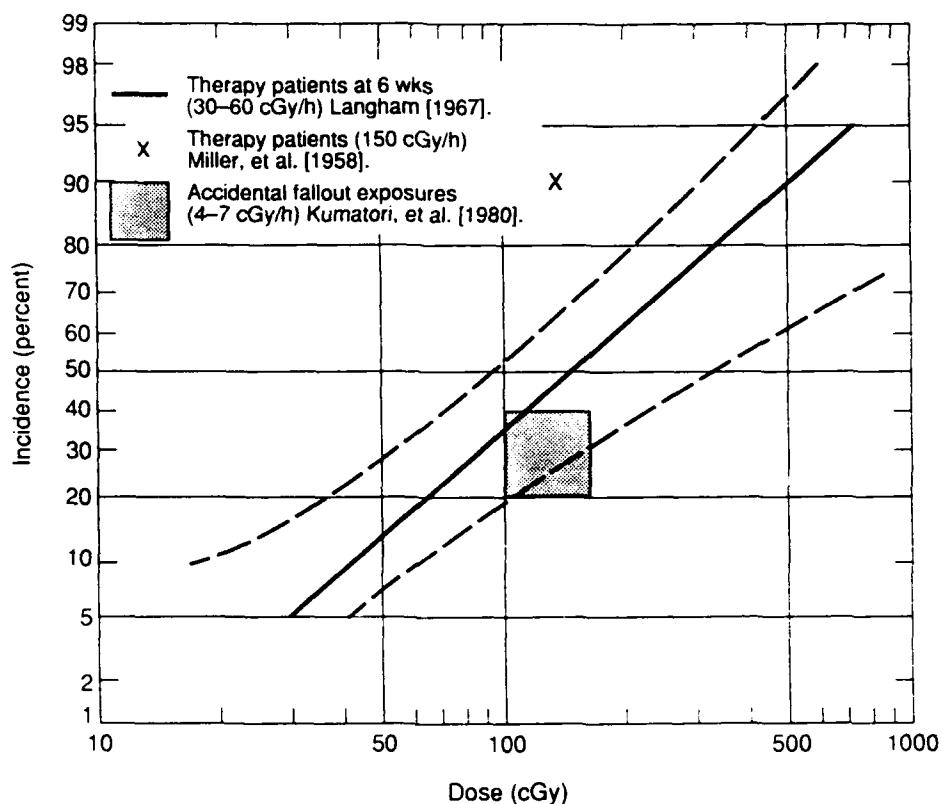


Figure 12. Incidence of fatigability and weakness (FW) (95 percent confidence limits are dashed curves).

The limited data in Fig. 12 suggest a marked difference in FW incidence according to dose rate. Whether or not the difference is as pronounced as indicated cannot be corroborated without additional data.

Also, there is considerable uncertainty in those associated with the data. For example, in addition to the wide 95 percent confidence bounds, FW was assessed six weeks postexposure, but it was probably present (maybe even at a high incidence) much earlier [Lushbaugh, 1989]. The point that represents the accidental fallout radiation involving the Japanese fishermen is not based on a one-to-one incidence and dose relationship but rather assumptions regarding cumulative doses and incidence outlined above. Furthermore, as pointed out, the dose rates range considerably.

Some objective measurements have been described to measure physical work and exercise capacity of individuals exposed to radiation accidentally or for malignant disease therapy. A clinical protocol

was described by Ricks et al. [1972] in an attempt to measure radiation-induced fatigue in radiation therapy patients based on changes in pulmonary impedance waveform. Fourier analysis was applied to perform power spectral analysis of respiration cycle (waveform) data gathered from normal and irradiated individuals exercising (bicycle ergometry) under controlled conditions. The computed average pulmonary impedance variance was a measure of the breathing demand under workload or stress conditions. The comparative ability of nonirradiated and irradiated individuals to adapt to exercise or workload was indicated by the average pulmonary impedance variance measurements. They found an amplified increase in respiratory demand for two patients after radiation exposure of only 82 rads and 126 rads indicating fatigability increased (performance decreased) on the third day postirradiation and appeared to subside within 10 days to two weeks.

Periods of increased respiratory effort (amplified impedance) were defined as diminished exercise capacity (DEC). A comparison of pulmonary impedance data from therapy patients who participated in controlled exercise stress testing (and demonstrated DEC) with normal, control volunteers is shown in Fig. 13. When the response to exercise (variance during exercise stress) was normalized to pretreatment values, therapy patients began to adapt to submaximal stress loads, as did controls, but this adaptation was interrupted by exposure accumulation apparently in a dose rate dependent manner. Not all exercise-stressed therapy patients experienced DEC. Of 11 participating in controlled ergometry, 8 responded with DEC; generally these were men as opposed to women, even though workloads were comparable.

The hypothesis that DEC is indicated by amplified pulmonary impedance variance (due to increased respiratory effort to perform at non-varying workloads) is supported by studies that demonstrate a direct relationship between work and impedance. That is, as workload on the ergometer is increased, respiratory effort increases and therefore pulmonary impedance. Furthermore, there appears to be a linear relationship between workload (up to subject's maximal efforts) and pulmonary impedance as illustrated in Fig. 14. These typical data,

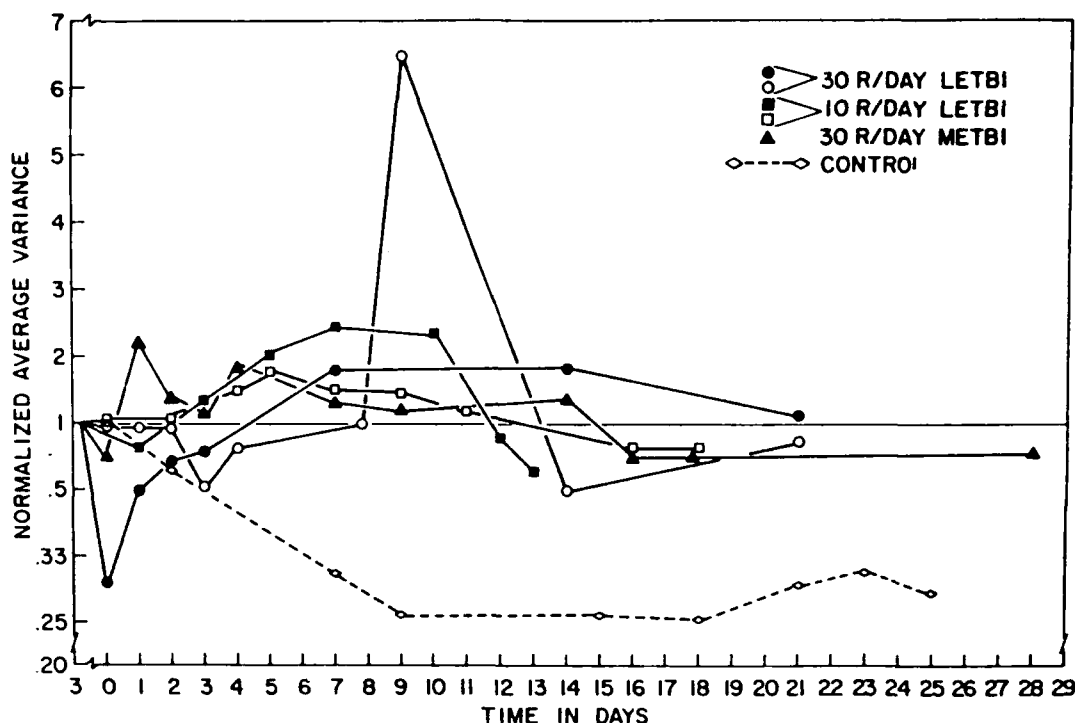


Figure 13. Pulmonary impedance from therapy patients.
Source: Ricks et al., 1972.

generated by alternate 2 min work/rest cycles, also illustrate cardiac rate changes. In light of the response of radiation therapy patients to controlled exercise stress, it is therefore possible that amplified pulmonary impedance during and after irradiation reflects a physiological deconditioning (DEC) to a non-varying workload.

A similar time-course study of radiation-induced performance decrement was made using this method after the accidental TBI of a man to 260 rem of ^{60}Co gamma rays for approximately 40 sec at 350 rad/min. The estimated bone marrow depth dose, based on thermoluminescent dosimetry, was 115-155 rads. Pulmonary-impedance measurements during controlled exercise were obtained commencing three days postexposure and on a regular basis for a total of 60 days. Initially, the individual exercised to his subjective tolerance against a workload of 50 watts. There was one minute of exercise on the third day, but tolerance progressively increased to 30 min until on the 7th day postexposure, the workload was doubled to 100 watts. At this exercise level, exercise tolerance time remained relatively constant

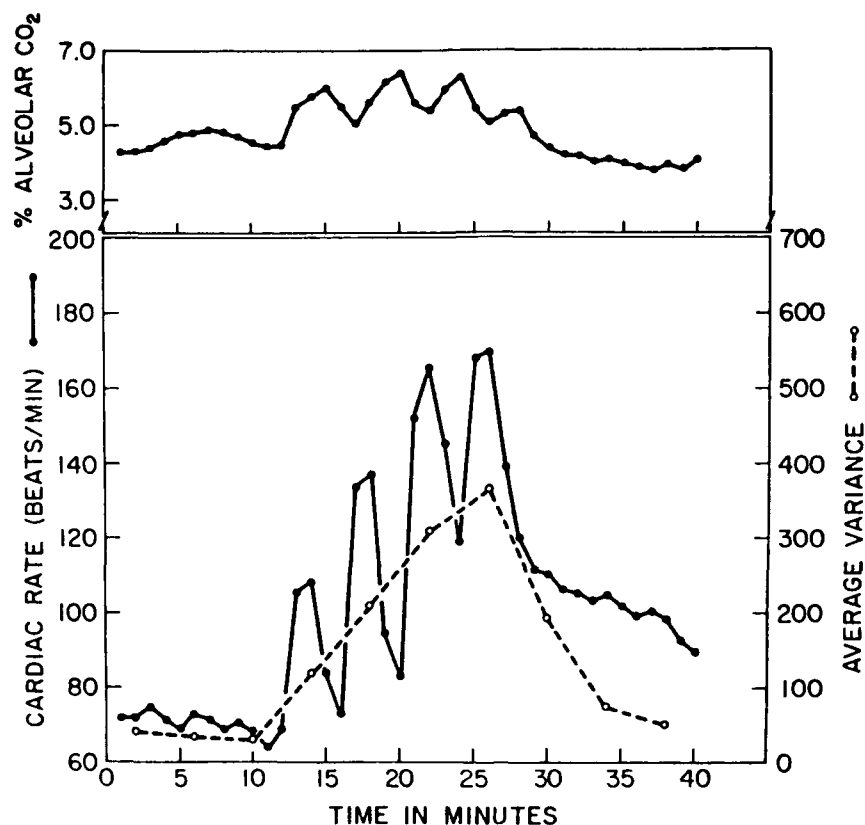


Figure 14. Relationship between workload (cardiac rate) and pulmonary impedance (average variance).
Source: Ricks et al., 1972.

at ~6 min. The zenith of variance in pulmonary impedance was reached within the first 6-8 min of each exercise test period. The results are summarized in Fig. 15. Decrement in performance occurred at days 7 through 13 and then at unpredictable times thereafter. Surprisingly, during the first week after exposure, no significant changes in the respiratory variance could be demonstrated even though the individual said he was exercising to tolerance.

Subjective symptoms of fatigue were apparently not respiratory as in the radiation-induced fatigue of the irradiated patients. This observation suggests that radiation-induced fatigue was not always directly related to shifts in the pulmonary-impedance power spectra and their variance. The investigators suggested that perhaps in persons in good physical condition, respiratory reserves were too large for their system of exercise stress to elicit signs of performance decrement even though respiratory or vascular changes had been

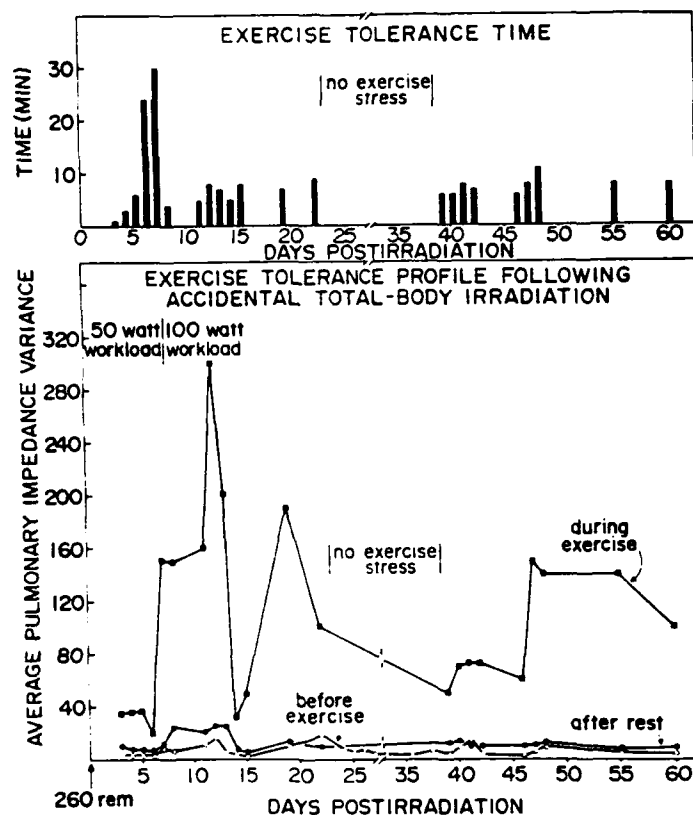


Figure 15. Time course study of exercise tolerance for an accidental exposure.
Source: Ricks et al., 1972.

induced by irradiation. This dichotomy in results may be explained on the basis of creatine phosphokinase studies in this accident victim. Following the first exercise period, the serum level of this muscle enzyme rose significantly and remained high for a few days. When creatine phosphokinase levels returned to normal, pulmonary impedance increased. It is unclear if creatine phosphokinase served as a "protective agent" against DEC.

Irradiation therapy in the absence of exercise stress failed to cause any significant shift in pulmonary impedance variance when measured before, during, or after exposure. In patients subjected to both radiation and exercise stress, there were some increases in basal resting pulmonary impedance during and shortly after therapy. Whether these basal changes were due to metabolic alterations, transient pulmonary edema or pulmonary vascular inflammation is not clear. However, these studies using pulmonary impedance waveform analysis

demonstrate that this noninvasive and remote monitoring technique can qualitatively recognize radiation-induced DEC and that the performance changes measured thereby are significant but reversible in man accumulating up to ~300 rads.

Based on the well-known association between (1) muscular weakness and creatinuria in muscle wasting disorders and (2) creatinuria and muscle fatigue observations in animals exposed to TBI, Kurohara et al. [1961] attempted to correlate the degree of creatinuria with fatigue in cancer patients undergoing radiation therapy. The preliminary evidence they gathered substantiated the hypothesis that radiation myasthenia may be due to an alteration in creatine metabolism.

Both male and female patients received fractionated pelvic, thoracic, and abdominal radiation over a period from approximately 30 to 45 days from ^{60}Co gamma and X-ray radiation. Total doses ranged from about 100 to 350 cGy. Creatine was measured and expressed as a creatine coefficient, which is the ratio creatine after therapy onset to that before. Fatigue symptoms were based on careful interviews of patients near the time curve collection. The fatigue symptoms were evaluated and graded subjectively on the following basis: 1+, mild; 2+, moderate; 3+, severe; 4+, extremely severe; \pm , equivocal; and 0, no symptomatology. Based on 35 patients, their summarized findings were:

- The degree of creatinuria appeared to be related to the severity of fatigue symptoms, tissue integral dose, the sex of the patient, and the anatomical site of irradiation.
- The greatest increases in the creatine coefficient values were found during the course of irradiation in female patients who received radiation therapy to the pelvis. This appeared to be related to the integral dose and the treatment time in which the radiation was absorbed.

- The male patients who received pelvic irradiation did not show any significant degree of creatinuria or fatigue symptoms.
- The patients who received relatively large volume doses to the thorax showed a significant degree of creatinuria and fatigue.
- The fatigue symptomatology and the degree of creatinuria appeared roughly to parallel each other. The most severe fatigue symptoms occurred at the height of creatinuria or just following it. The female patients who received radiation to the pelvis suffered more fatigue than the patients who received radiation to the abdomen, thorax, or head and neck region.
- The need for redefinition of clinical radiation sickness into two types of symptoms, (1) gastrointestinal and (2) muscular fatigue, is emphasized.

A brief investigation by Bigatello et al. [1987] demonstrated a depression of ATP in rats after 7.5 Gy irradiation. The ATP depression was determined in erythrocytes and muscle tissue as well as sugar and inorganic phosphate levels, which may impair resynthesis of high-energy compounds, thus compromising tissue function and integrity. It was also established that the effect was not due to anorexia or GI tract malfunction.

Studies of the physical work capacity of individuals exposed to radiation from the Chernobyl accident were briefly discussed by Guskova et al. [1989]. A summary of the discussion is tabulated in Table 17 for individuals with no signs or symptoms (S/S) and ARS Groups 1, 2, and 3. Details as to how the work capacity measurements were made were not given. However, for reference, Table 18 gives a list of various familiar physical activities, corresponding energy expenditure rates, and a scaling relationship for body weight.

Table 17. Work capacity--Chernobyl accident victims.
Source: Guskova et al., 1989.

Group	Dose (Gy)	Asthenia Incidence* Tested 4-6 Mos. Post-acc.	Work Capacity (Kcal/min)
Normal no S/S	---		4.9 (342 watts)** 67.28 watts/KCal min ⁻¹ 100%
ARS 1	1-2	1/3	4.3 (300 watts) (88%)
ARS 2,3	2-4	1/2	≤3.0-3.8 (201-265 watts) (61-78%)
ARS 3	4-6	3/4	Initial: 3.8 (265 watts) Early recovery phase: 3.5 (244 watts) (71%)

* Somatic basis for asthenia passed in 9-18 mos. (recovery in the function of main organs); definite improvement in 3/4 in 2nd year post-accident.

**Moderate activity: badminton, horseback riding (trotting), square dancing, volleyball, roller skating.

The subjective aspect of fatigability associated with irradiated individuals makes any quantitative assessment difficult. However, victims of the Goiania Brazilian accident may provide an opportunity for an objective approach based on a retrospective study. All 248 victims were treated at one facility where patient records are available. There are good estimates of dose for 100 or so patients. Part of the recovery process and therapy involved an exercise program involving the use of exercycles. Review of the medical records and the use of a questionnaire, together with dose information and estimates of exposure time, may provide information on postirradiation fatigability.

Research by Griem [1989] utilizing microscope video techniques and demonstrating *in vivo* changes after irradiation in the small blood vessels of rabbit ears suggests a possible mechanistic approach to interpreting postirradiation FW. Dynamic observation showed progressive changes in the vessel walls and blood flow pattern changes (i.e., clumping of blood cells and sluggish intermittent flow) in the

Table 18. Energy expenditure by a 150-pound person
in various activities.*

Activity	Gross Energy Cost (E) Cal. per hr.**
A. Rest and Light Activity	50-200
Lying down or sleeping	80
Sitting	100
Driving an automobile	120
Standing	140
Domestic work	180
B. Moderate Activity	200-350
Bicycling (5 1/2 mph)	210
Walking (2 1/2 mph)	210
Gardening	220
Canoeing (2 1/2 mph)	230
Golf	250
Lawn mowing (power mower)	250
Bowling	270
Lawn mowing (hand mower)	270
Fencing	300
Rowboating (2 1/2 mph)	300
Swimming (1/4 mph)	300
Walking (3 3/4 mph)	300
Badminton	350
Horseback riding (trotting)	350
Square dancing	350
Volleyball	350
Roller skating	350
C. Vigorous Activity	over 350
Table tennis	360
Ditch digging (hand shovel)	400
Ice skating (10 mph)	400
Wood chopping or sawing	400
Tennis	420
Water skiing	480
Hill climbing (100 ft. per h)	490
Skiing (10 mph)	600
Squash and handball	600
Cycling (13 mph)	660
Scull rowing (race)	840
Running (10 mph)	900

*Prepared by Robert E. Johnson, M.D., Ph.D., and
colleagues. Department of Physiology and
Biophysics, University of Illinois, August 1967.

**Body weight scaling: $E = E_{150} \left(\frac{W}{150} \right)^{0.6781}$;

E_{150} are table values in Kgm-cal/h and W is
body weight in lbs (multiply E-values by 1.163
to convert to watts).

small vessels (arterioles and capillaries). Gaps, observed to average about one per 250 μ of length, in the capillary endothelia (referred to as "potholes") were probably where single-layer cells were missing. The amount of damage is both dose and RBE (neutron) dependent.

This work indicates that vascular tissues of smaller blood vessels appear to be more sensitive than indicated in the literature. Early effects (increasing with dose) evidenced by vasodilation 1 to 15 days postirradiation were seen after doses as low as 0.4 to 5 Gy. After a 2 Gy dose, the mean diameter of surviving vessels doubles in size by 10 days, and returns to normal size in 15 days. These measurements were based on average vessel width versus dose and time after dose; this effect could be due to the disappearance of portions of the capillary network where the remaining observed vessels increase in diameter to accommodate the blood flow distribution.

Irradiation damage to the capillaries, arterioles, and small arteries generally follows a temporal pattern similar to postirradiation erythema (i.e., early, intermediate, and late effects) where signs and symptoms are also due to blood vessel damage in the dermal layers. In view that the body capillary network is the direct lifeline for all cells in the body, it seems plausible that the radiation damage and recovery effects from such large-scale exposure are related to fatigability and weakness. Furthermore, it is well known that the volume of bloodflow to the body's muscle tissue vastly increases during the demand brought about by exercise, and that an increased portion of the capillary network is utilized during these periods of accelerated physical activity; conversely much of the capillary network is minimally utilized when the body is physically inactive. A significant portion of the capillary network compromised by radiation damage would be consistent with the "fatigability" concept. That is, the damaged capillary networks would suffice for bodily needs during rest or sedentary activity, but would not be able to meet the needs during physical exertion. The temporal process of recovery also seems to be consistent with "fatigability" symptoms in that there is a long-term, local regulatory mechanism present that

readjusts the degree of vascularity over a period of weeks or months [Guyton, 1981]. Even though not a lot of work has been done on radiation damage to small blood vessels, there are certain interesting aspects of their behavior which parallel the observed fatigability response in humans:

- Damage to small blood vessels and fatigability in humans both develop at fairly low levels of radiation dose.
- Following radiation exposure, the expressed pattern of fatigability over time is similar for observed physiological changes in the small blood vessels.
- "Fatigability," as opposed to fatigue, is physiologically consistent with what would be expected under conditions of radiation damage to the small blood vessel network in the body.

Radiation-induced fatigability and weakness is observed to occur shortly after radiation exposure (comparable to the onset of nausea and vomiting). Toxin-producing mechanisms, an increase in capillary permeability, or separation of cell junctions might account for this initial response. Vascular damage due to necrosis or endothelial cell killing and damage to the basement membranes would apply to intermediate to long-term components of observed fatigability.

Assuming a biological toxin-producing mechanism, an approach similar to the prodromal response model of emesis could be taken to model radiation-induced fatigability. Response modeling fashioned after any other specific mechanism at this time lacks empirical guidance or verification. However, based on our review and assessment, possible mechanisms or modeling approaches and data sources for the radiation-induced fatigability weakness response include but are not limited to those given below:

Human Data Sources	Modeling/Mechanisms
<ul style="list-style-type: none"> ● Japanese fishermen ● Current clinical data ● Chernobyl accident victims ● Goiana accident victims ● ORAU/NASA studies ● Physiological research 	<ul style="list-style-type: none"> ● Vascular damage ● Multi-organ/tissue response ● Respiration and energy metabolism ● Cell membrane transport ● ATP depression ● Oxygen transport capability

2.3 HEMATOPOIETIC EFFECTS.

The effect of ionizing radiation exposure to the blood system is the most widely investigated in the field of radiobiology. With regard to dose protraction, lethality represents the endpoint that has received the most attention based on experimental investigation in animals and clinical observations of radiation therapy patients and accident victims. Lethality caused by radiation injury to the bone marrow is discussed below in the Radiation Lethality subsection, and some models of lethality for continuous exposure at a constant rate are reviewed below in the Radiation Injury And Recovery subsection.

Radiation-induced infection and bleeding form a sign/symptom complex known as IB in the DNA/IDP. However, in terms of IB severity level as an endpoint, infection and bleeding studies associated with protracted radiation exposure have not been as widely reported as lethality. Most of the literature on this subject is derived from clinical experience with leukemia patients who received radiation therapy under dose fractionation regimens. Because of the well-known hypersensitivity of the blood system in leukemia patients, application to healthy individuals is limited.

Some research investigations have been carried out to formulate models to describe the dynamics of circulating blood cells. However, most of them are empirically based descriptions of blood cell level response following single or brief high dose rate exposure. A limited number of the models attempt to accommodate or emulate the complicated dynamics necessary to make predictions of time-phased levels of the circulating blood components.

Because the IB-complex was not the main focus of this effort, we did not perform an extensive review of protracted irradiation-induced hypoplasia. Accordingly, the discussion below is limited to some selected topics.

2.3.1 Blood Cell Levels.

Because bone marrow suppression by radiation is one of the primary causes of lethality and infection/bleeding signs and symptoms, a review of some studies demonstrating the effect of dose rate on hematopoiesis was performed. In the first study, depicted in Figs. 16 and 17, four groups of rats were subjected to 214 cGy of gamma radiation at four dose rates--9, 27, 53, and 107 cGy/h [Baum and Kimeldorf, 1957].* Radioactive iron incorporation into newly formed red cells was used as the criterion for normal and postirradiation erythrocyte production. Since 214 cGy was a sublethal dose of radiation, all animals recovered. However, on day two, postirradiation recovery commenced in a dose rate related order. The rats subjected to the radiation dose at the lowest rate (9 cGy/h) recovered at a faster pace; the other groups followed in the order of increasing dose rate.

Figure 18 depicts antibody formation by B-lymphocytes as a function of radiation exposure rate [Gengozian, Carlson, and Gottlieb, 1968]. Mice received 625 cGy ^{60}Co gamma irradiation at dose rates ranging from 214 cGy/h to 5340 cGy/h. The graph indicates that antibody production decreased with increasing dose rate, most likely due to increased radiation induced damage to B-lymphocytes.

Figure 19 presents mean values of white cells in Duroc swine following TBI with 256 cGy ^{60}Co gamma irradiation at three dose rates: 1920, 380, and 38 cGy/h [Brown and Cragle, 1968]. Maximum depression of leukocytes occurs between postirradiation days 12 and 24 and increases with increasing dose rates.

*Note that a multiplicative factor of 0.89 is assumed for rats to convert free-in-air exposure in roentgens to midline absorbed tissue dose in centigray for ^{60}Co gamma irradiation.

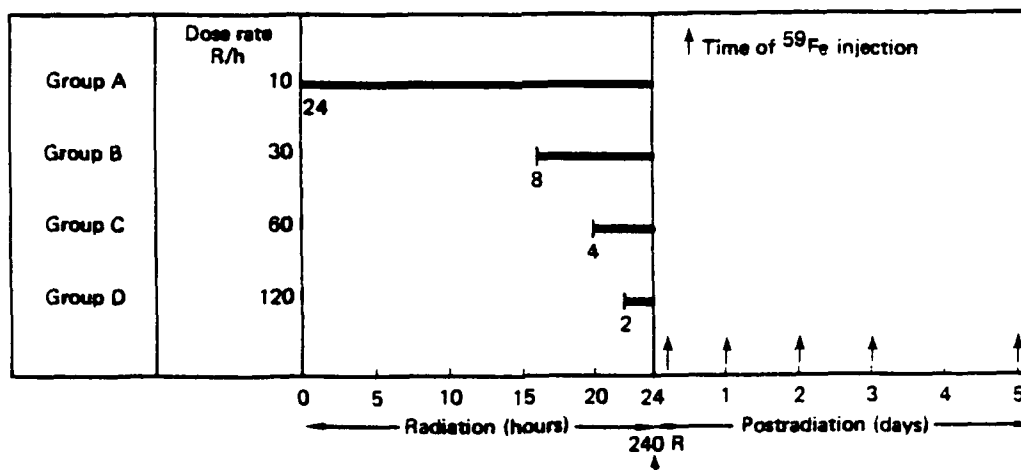


Figure 16. Experimental design of exposure time for specific dose rates and times of radioactive tracer ^{59}Fe injection.

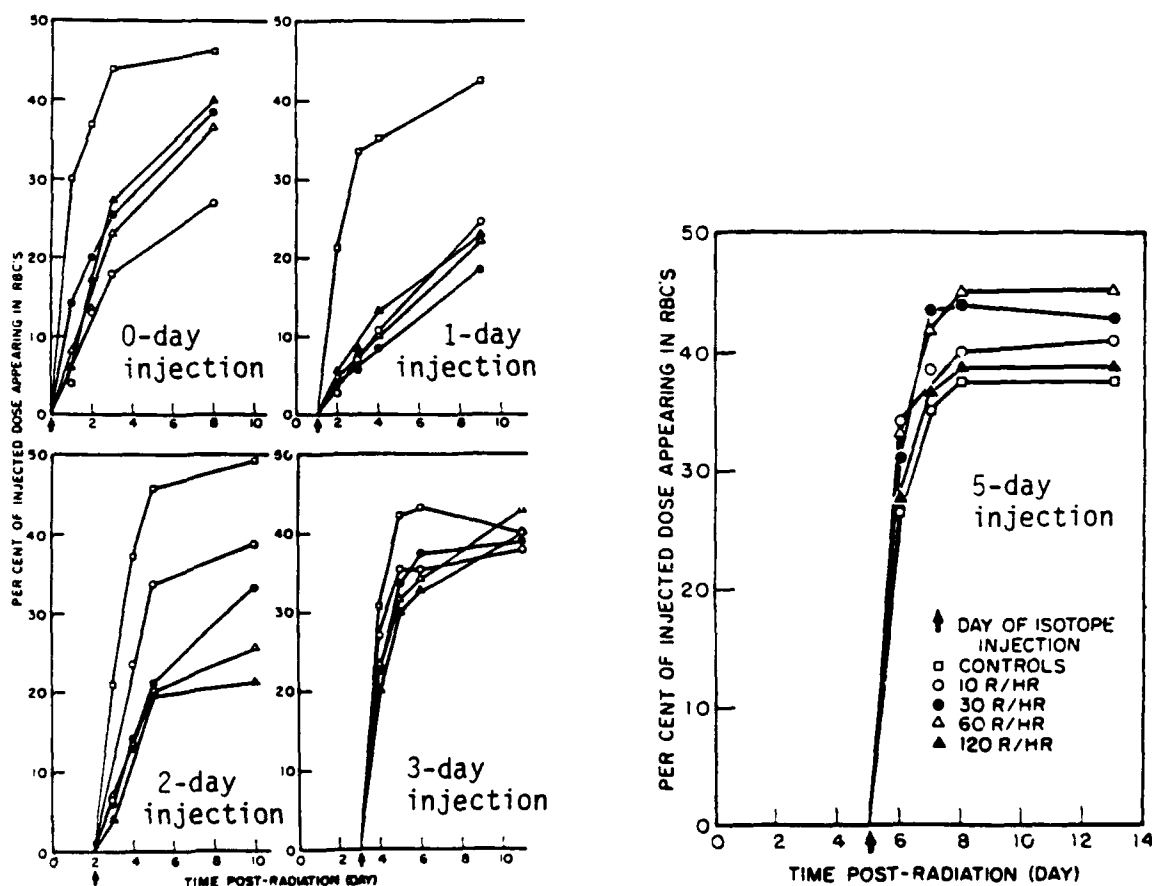
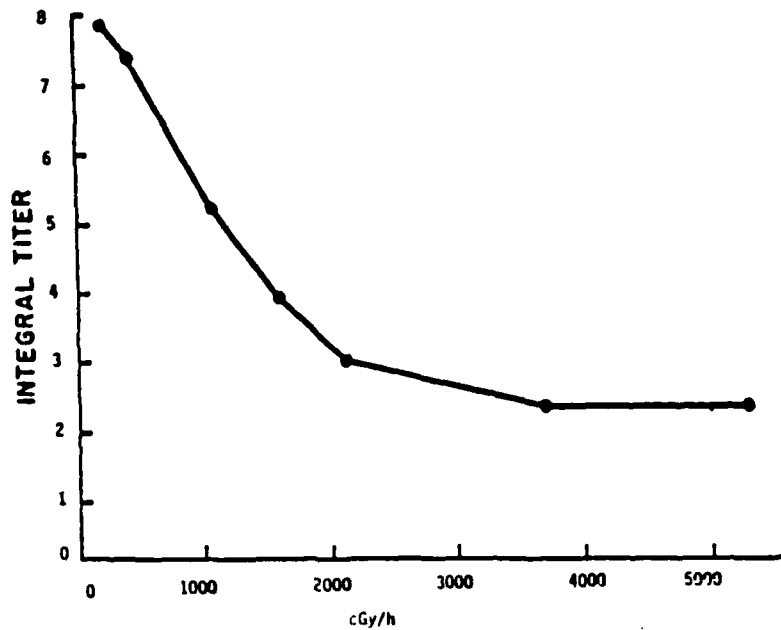
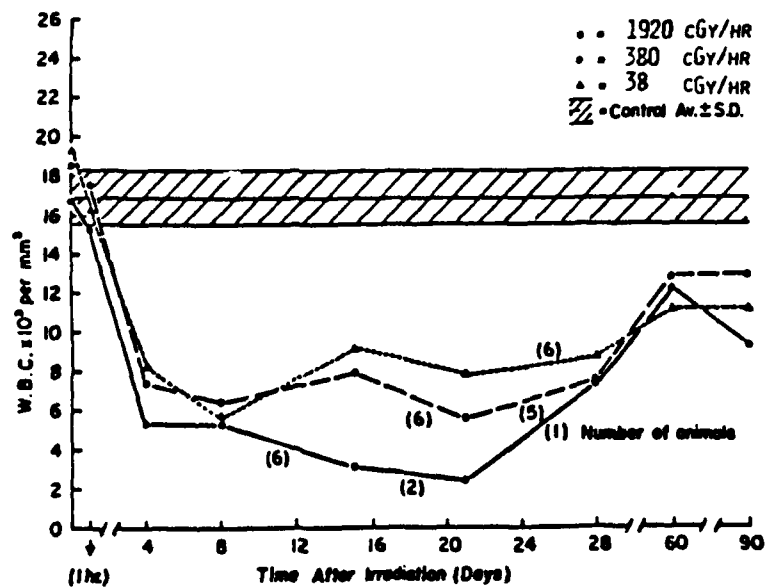


Figure 17. Effects of variable dose rates on iron incorporation into newly formed erythrocytes--total dose 214 cGy.



Source: Gengozian, Carlson, and Gottlieb [1968].

Figure 18. B-lymphocyte antibody formation as function of radiation exposure rate (625 cGy ^{60}Co gamma).



Source: Brown and Cragle [1968].

Figure 19. Mean leukocyte values of Duroc swine following whole-body exposure to 256 cGy ^{60}Co gamma radiation.

Lushbaugh et al. [1968] attempted to demonstrate the effect of protracted or prolonged radiation exposure on the blood system response in humans based on clinical observations of radiation therapy patients. They constructed and used a conglomerate model of white blood cell response expected in normal humans following various TBI dose levels (Fig. 20). Response levels were assigned to indicate severity according to dose used as a "template" for normal individuals which were compared with actual clinical values. In order to determine the response differences between radiation therapy patients with and without hematological disease (patients without hematological disease had chiefly renal disease), they also compared clinical data and found patients with hematological disease to be only slightly more sensitive than those without it.

Figure 21 is a plot of the hematological response level from clinical data (points) and that expected for normal individuals based on the conglomerate model (Fig. 20). The upper dashed line (single dose response) is directly from Fig. 20, and the lower dashed line (fractioned dose model) is constructed according to the conjecture of Space Radiation Study Panel [Langham, 1967] that suggests a factor of 2 less in dose effectiveness for hematological depression when the duration exposure is 3 to 4 weeks compared to 1 to 2 days or less. The solid lines follow the clinical data points. The "x" points are clinical response levels for single therapeutic exposures; the solid dots are for fractioned exposures within 8 days, and the points given by the concentric circles are for low constant dose rate exposure (1.5 r/h) protracted over a period of about 3 to 6 days (i.e., 100 to 200 r) in the low-exposure rate total-body irradiation (LETBI) facility at the Oak Ridge Associated Universities (ORAU) [Lushbaugh et al., 1968].

It is clear that the clinical levels very significantly differ from the expected (theoretical) response levels regardless of whether the exposures are protracted or not. Furthermore, even the differences in the clinical exposure response were judged to show an insignificant shift regardless of whether the exposure was single or protracted (up to 8 days). The clinical response levels for the first

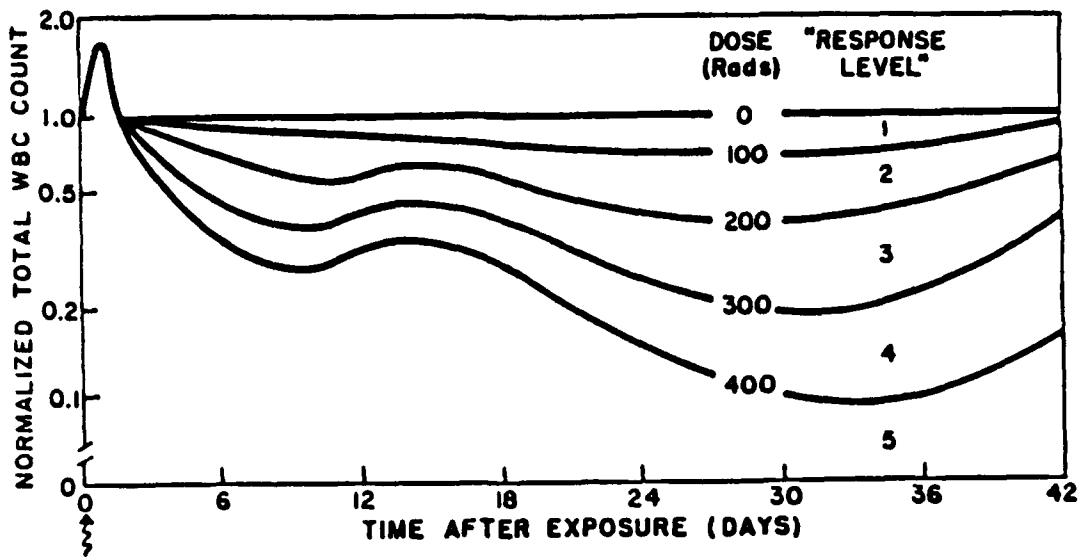


Figure 20. Conglomerate model ("template") of human dose: hematological response.
Source: Lushbaugh et al., 1968.

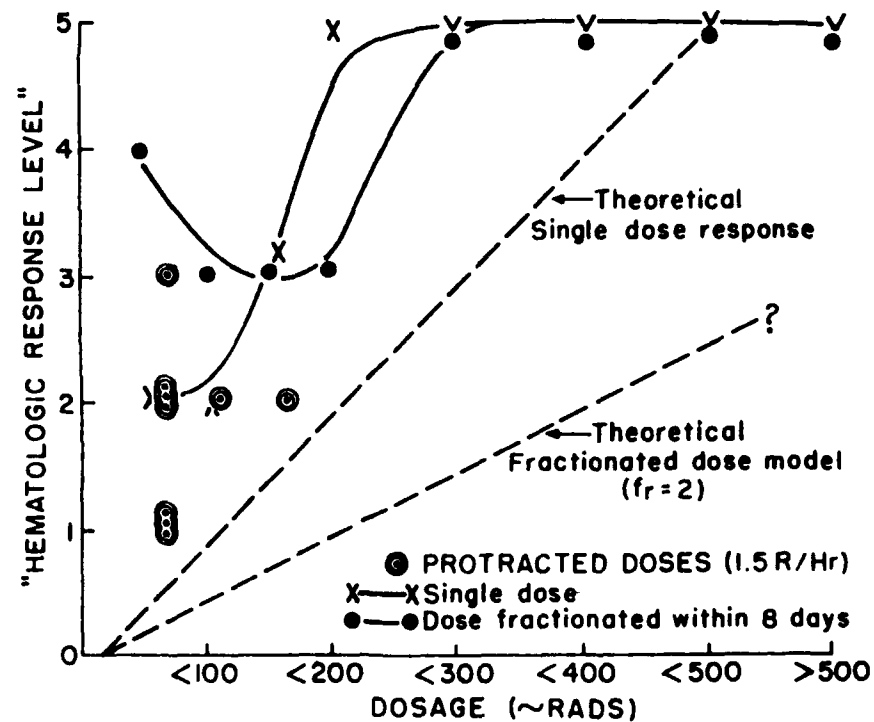


Figure 21. Single and protracted radiation exposures; hematological response level based upon white blood cells.
Source: Lushbaugh et al., 1968.

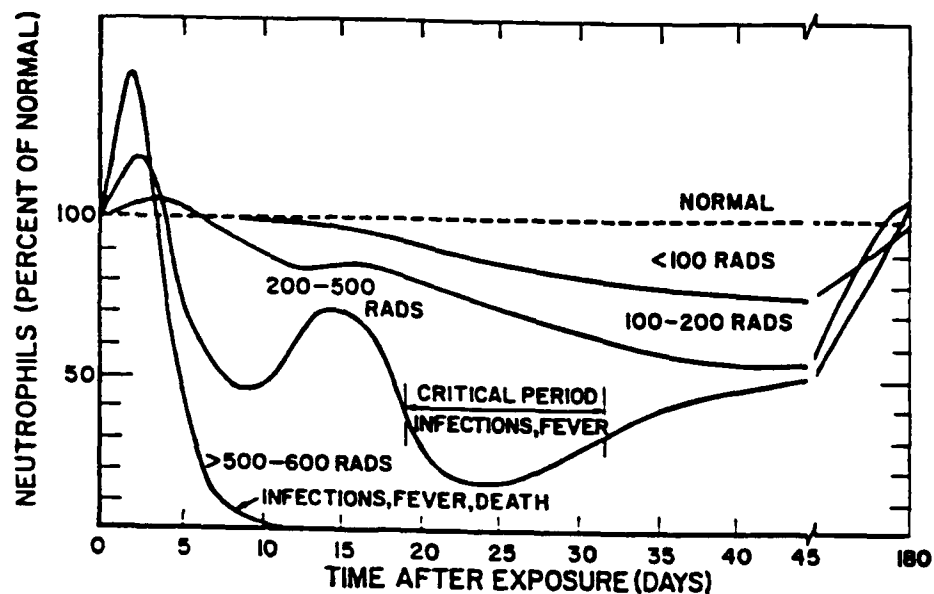
nine low-dose rate LETBI patients were also much in excess of those expected, although somewhat closer in agreement. This is somewhat puzzling when compared with the fractionated exposures of the same dose levels which may suggest some unknown resolved dynamics taking place at these relatively low exposure rates which could feasibly be associated with redistribution in cell cycling.

Lushbaugh et al. [1968] did not find a suggested factor of 2 less in dose effectiveness for the hematological response to protracted radiation suggested by the Space Radiation Study Panel [Langham, 1967]. However, the low-dose rate actually suggested by the panel was for an exposure duration of three to four weeks instead of only up to eight days. They conclude that their study seemed to indicate that during an exposure for one week, radiation damage to the (diseased) bone marrow is not repaired significantly enough to alter the course seen in man after a single exposure.

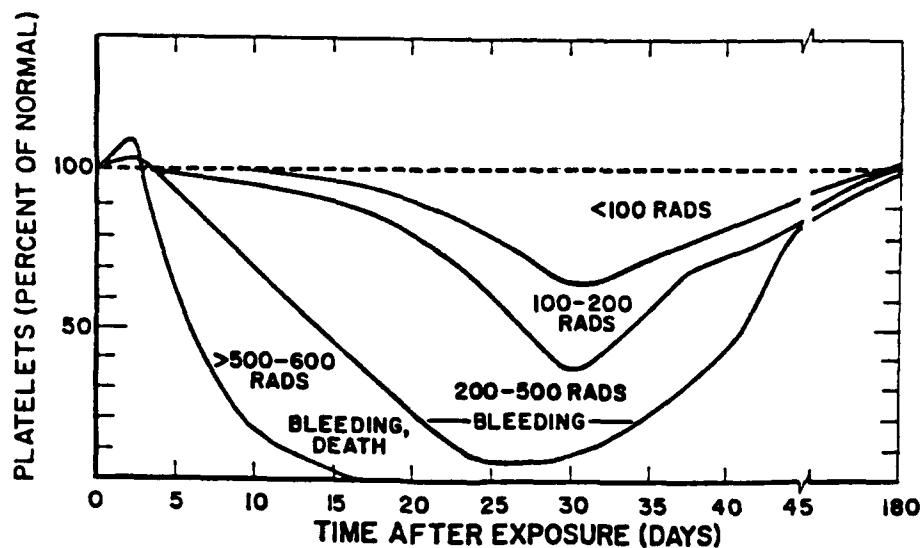
In principal, the severity of infection and bleeding can be related to the degree and duration of depressed WBC levels and platelets in the blood circulation. Accordingly, clinical data of dynamic response levels following protracted radiation exposure could provide useful insight for model construction. However, the appropriate data for protracted or low dose rate exposure in healthy individuals is fragmentary. Moreover, there appears to be appreciable uncertainty in IB/cell level relationships even for single acute exposure.

Figure 22 gives plots of neutrophil and platelet levels formulated by the Space Radiation Study Panel [Langham, 1967] following a single acute TBI exposure. Levels for infection and fever (critical period) are indicated for neutrophils and bleeding for platelets in terms of percent of normal level. Normal levels for neutrophils are about 4000 to 6000 per mm^3 and 300,000 per mm^3 for platelets. According to Fig. 22, the critical period for infection and fever is from about 18 to 32 days where the neutrophil level is at or below 40 percent of normal (or about 1800 mm^3) for the dose range of 200 to 500 cGy. For the same dose range, the platelet level associated with bleeding is at or below about 20 percent of normal (or $60,000 \text{ mm}^3$) extending over a period from 20 to 35 days following exposure.

Neutrophils



Platelets



Source: Langham (1967)

Figure 22. Blood count levels following single acute radiation exposures.

Soviet investigators [Guskova et al., 1988] have presented a similar idealized but more detailed dynamic profile of neutrophil and platelet counts following single acute TBI exposure shown in Fig. 23. Based on the same dose range (200 to 500 cGy) and neutrophil level (40 percent of normal), Fig. 23 would indicate a critical period from about 5 to 40 days. The significant difference (from Fig. 22) is due to a much earlier commencement time at the 500 cGy dose level. The "recovery" time following exposure is in somewhat better agreement which corresponds to the 200 cGy dose level in Fig. 23. The blood component profiles shown in Fig. 23 were utilized by the Soviets among other blood system indicators (lymphocytes, reticulocytes, and chromosome aberrations to estimate dose levels in Chernobyl accident victims. Subsequent clinical measurements made were generally in good agreement with the profiles.

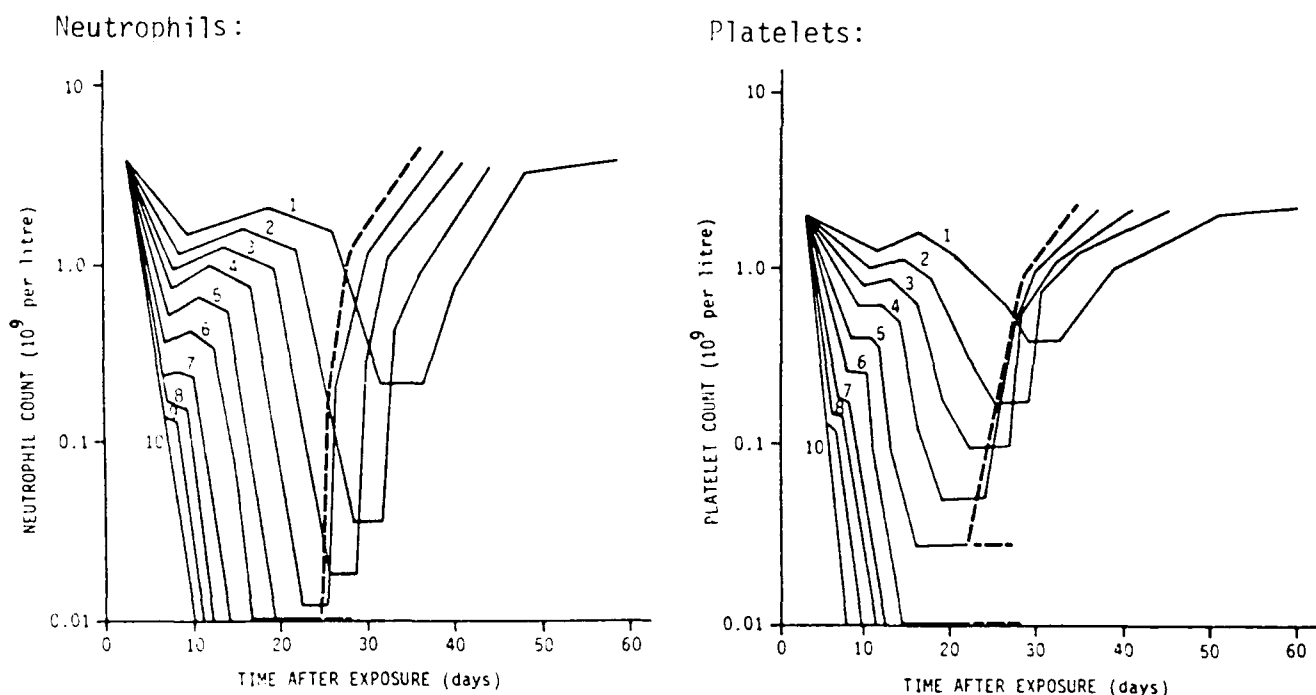


Figure 23. Standard curves showing the changes of the neutrophil and platelet counts after various doses (number on the curves indicate the dose in Gy) in the case of relatively uniform whole body gamma irradiation of human subjects. (Broken segments of curves at doses of 5-6 Gy indicate that recovery may not occur at these times in all patients.) Source: Guskova, et al., 1988.

Baranov and Guskova [1988] indicated a good correlation between agranulocytosis (when the neutrophil count is less than 0.5×10^9 per liter--about 10 percent of the normal level) and fever in the 1 to 5 Gy dose range. However, infections occurred in only about 27 of patients which were primarily bacterial and well controlled with antibacterial antibiotics. Beginning in the 5 to 6 Gy dose range, fever that occurred in those patients prior to agranulocytosis was not controlled by antibacterial antibiotics due to the rapid increase of viral infections with dose which required intensified systemic antibiotic treatment with antiviral drugs. Agranulocytotic bacterial and fungal infections rarely occurred in the high dose (>76 Gy) patient groups.

It is possible to speculate that viral infections may coincide with a depressed lymphocyte level of about 10 to 20 percent normal which roughly corresponds to the beginning of viral infections for the high-dose-range patient groups reported by Baranov and Guskova (1988). If such a relationship can be established between "high-dose-level" infections and lymphocytes, the overall "infection" response with regard to modeling should not only be based on neutrophils but would require consideration of the dynamics of the circulating lymphocyte component. It is interesting to note from Fig. 23, however, that agranulocytotic level (0.5×10^9 per liter) for the 200 to 500 cGy dose range corresponds to a period from 15 to 32 days following exposure; this is in good agreement with the critical period of 18 to 32 days indicated in Fig. 23, albeit the neutrophil levels are quite different (about 10 percent of normal for the former and 40 percent of normal for the latter).

2.3.2 Damage to Lymphoid Tissue.

A brief review was made of radiation damage to the lymphatic tissue as a possible contributory factor in the prodromal gastrointestinal reaction (i.e., nausea and vomiting) and the immunosuppression evidenced by viral infections that predominated in Chernobyl accident patients following high dose range exposures [Baranov and Guskova, 1988]. Young [1986] discusses mechanisms and treatment of radiation-

induced nausea and vomiting and points out that from current data it cannot be ascertained whether early postirradiation vomiting is mediated by blood-borne emetic factors acting on the area postrema (AP), by direct gastrointestinal afferent stimulation of the vomiting center, or by a combination of these inputs. This leaves open the possibility of various causal mechanisms. Here we discuss only a possible subset of those.

Gerstner [1970] provides a discussion of plausible mechanisms involving lymphatic tissue reaction to ionizing radiation exposure. Disintegration of lymphatic structures either parallels or slightly precedes the prodromal reaction; consequently, a cause-effect relationship appears entirely possible. The likelihood of such a causal connection is further strengthened by the surprisingly close agreement with respect to the time course of the two processes. Whole-body exposures in the several-hundred-rad range initiate surprisingly uniform processes in lymphatic nodules throughout the body, including the GI tract of various animal species. Within 15 to 60 min following irradiation, reduction of mitotic activity becomes noticeable, and evidence of necrotic change appears. Damage comprises the clumping of chromatin, lobation of nuclei, formation of giant cells, and complete destruction of lymphocytes into nuclear debris. As time passes, the amount of debris grows until a maximum is reached, sometime between 6 and 8 h postexposure. Simultaneously with the appearance of necrotic alterations, both fixed and free macrophages become active; they engulf dead cells and remove the debris from the nodules. Twenty-four hours after irradiation, most of the necrotic material has vanished, and the nodules have decreased correspondingly in size. Such a behavior of lymphatic tissue is demonstrable not only in lymph nodes themselves but also in the thymus, spleen, appendix, and Peyer's patches. Essentially identical histological observations have been made in studies on rabbits, rats, and guinea pigs [Rubin and Casarett, 1968; De Bruyn, 1948; Barnett, 1949]. This close agreement between species strongly suggests that the findings are applicable to man.

A possible sequence of physiological events is suggested by Edsall and Pemberton [1907]. Radiation initiates the destruction of certain sensitive cell types, and breakdown material suddenly floods the organism. Decomposition products (of nucleoproteins, especially) are more or less toxic, difficult to metabolize, and hard to excrete. When these compounds overtax the ability of the liver and the kidneys to detoxify and eliminate them, the concentration of these noxious substances rises, eventually causing the prodromal reactions.

Anatomical distribution of lymphoid tissue also explains quite well the probability that prodromal signs and symptoms will occur after irradiation of various body regions. Lymphatic formations are scattered abundantly throughout the entire abdomen; to a somewhat lesser degree, throughout the mediastinum and thymus of the thorax; and, in still smaller quantities, throughout extensive chains draining the neck and cranial base. In sharp contrast, the extremities contain minor amounts of such tissue.

As an initial step in investigating the possible connection between lymphoid tissue destruction and prodromal reactions, we plotted (Fig. 24) the human lymphocyte count as a function of time after radiation, based on the model parameters given by Guskova [1987]. That model, however, is given by a relationship of dose as a function of lymphocyte count of the form

$$D(y) = a - b \log_{10} y \quad ,$$

where D is the dose in grays; y is the lymphocyte count per liter; and the fixed constants (a and b) are for given times varying from 0 to 9 days postirradiation. The plots in Fig. 24 represent orthogonal relationships of the same data. Presumably then, the recession in lymphocyte count could provide a quantitative basis for the increase in decomposition products. In turn, the buildup of the decomposition products (up to a particular level before they are cleared by body elimination processes) may be related to the onset of prodromal reactions. The approach would be to assess such a relationship, if

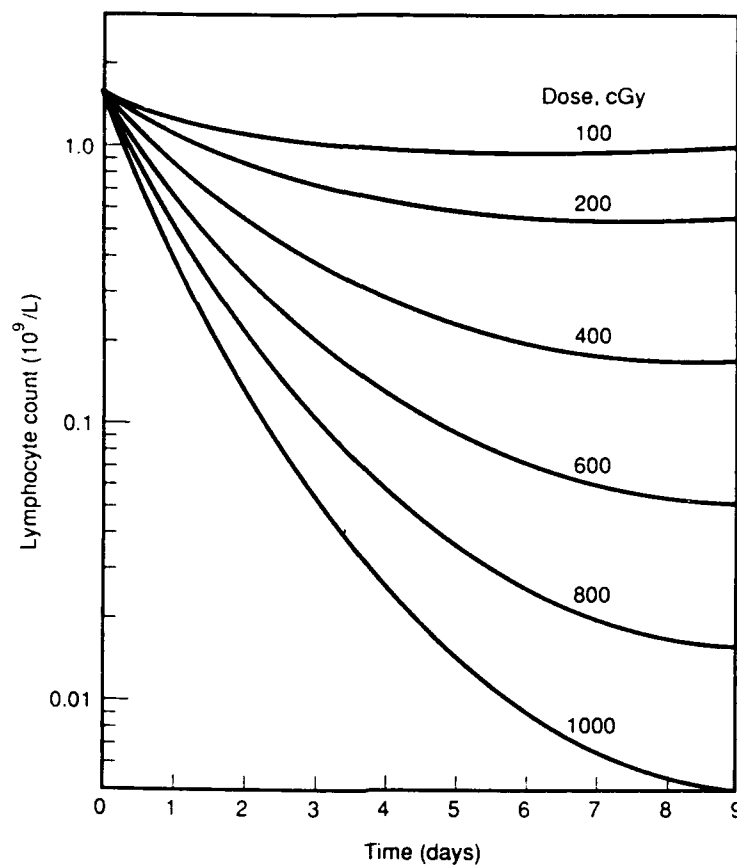


Figure 24. Lymphocyte count after single acute gamma radiation.
Based on Guskova et al., 1988.

any, based on kinetic modeling vis-a-vis data from human postirradiation experience.

With regard to the predominant viral infection described by Baranov and Guskova [1988] in Chernobyl accident patients exposed to high dose levels commencing in the 5 to 6 Gy range, plots such as those given in Fig. 24 can reveal dynamic response behavior which must be taken into consideration in formulating a response model for the IB complex.

2.3.3 Blood Cell Modeling.

Numerous dynamical mathematical models have been developed for hematopoiesis to simulate the response to various blood diseases, stimulating factors, and insults including chemicals, toxins, and radiation. However, few of them are directly relevant and comprehen-

sively applicable to modeling hematopoietic response to arbitrary irradiation histories. However, two models are discussed below that most comprehensively provide a means of predicting some of the blood level responses that consider most of the essential features.

Wichmann and Loeffler [1985] have developed a coupled dynamic standard model to simulate granulopoiesis and erythropoiesis that consist of six compartments including stem cells, granulopoietic progenitors and precursors; and erythropoietic progenitors (two compartments) and precursors. Mathematically, compartment dynamic activities are described by six first order differential equations linked by input/output cell flow rates. Feedback is simulated by a detailed set of functional forms of weighting factors and proliferation fractions that regulate cell activities. These include stem cell self removal probability and fraction of stem cells in active cycle. Cell generation times, transit times, and amplification factors for each compartment are also essential functional compartments of the model. Normal input values of regulating functions and fractions are achieved as homeostatic equilibrium is approached.

Based on some modifications of the standard model, Wichmann and Loeffler [1985] have simulated cell loss for acute and continuous radiation exposure. Their model does not attempt to simulate cellular radiation damage or account for DNA repair. Acute cell loss is simulated by a reduction of the initial conditions of the differential equations which must be gleaned from experimental cell survival curves. Continuous cell loss is simulated by including a constant loss rate term in the standard model compartment equations. Accordingly, the loss rates must be developed from experimental data or inferred by some other means. Also, since the model does not explicitly include radiation damage and Elkind-type repair, residual injury by irradiation cannot be interpreted within its framework. Accordingly, the model cannot be applied to an arbitrary irradiation exposure history. However, it has been compared with some experimental work in mice and appears to provide at least a reasonable simulation qualitatively.

Wichmann et al. [1979] have presented a mathematical model for thrombopoiesis in rats that has four compartments and associated differential equations for stem cells, megakaryocytes, thrombocytes, and thrombopoietin. A high thrombopoietin concentration influences bone marrow proliferation in three ways: (1) stem cell stimulation with a following slow increase in megakaryocyte number, (2) additional endomitoses in early megakaryocytes resulting in increased megakaryocyte volume, and (3) megakaryocyte maturation time is shortened. Model parameters are determined from experimental data. The model has been tested comparing simulated results of acute and chronic thrombocytopenia and thrombocytosis with experimental work although not involving irradiation exposure. The model and data agree within the limits of experimental error. Some of the thrombopoietic regulating mechanics still appear to be unknown and thrombopoiesis has not appeared to have been coupled with the granulopoiesis/enthropoiesis model of Wichmann and Loeffler [1985].

Steinbach et al. [1980] developed a mathematical model for canine granulopoiesis that was later modified to study the response of humans who were accidentally exposed to ionizing radiation [Fliedner, Steinbach, and Szepesi, 1988]. The model simulates granulopoiesis based on seven cellular compartments consisting of stem cells, two progenitor cell compartments, precursors, maturing cells, and functional cells circulating in the blood stream. The stem cells actually consist of two compartments which reflect "latently injured cells" and "intact cells"; the difference between these two stem cell populations is that the replicative potential of the former is restricted while the latter has a normal replicative potential which is essentially unlimited. The two progenitor compartments, which are in dynamic equilibrium with each other, assume one in the bone marrow and one in the peripheral blood. The stem cells, progenitors, and precursors are reduced by radiation exposure in accordance with the cell survival curve parameters, D_0 (100 cGy for acute exposure).

The two regulatory compartments control cellular generation and release. One compartment controls progenitor and precursor cell productivity to simulate humoral factor regulation, and the other

simulates stimulation triggering the release of granulocytes to the blood circulation from the reserve pool in the bone marrow. The chain of compartments is described by a system of coupled first order non-linear differential equations that include functional relationships and essential cellular parameters, including fraction in cycle, cycle time, and self-renewal probability for the stem cells, as well as transit time, generation time, and amplification factor for the other cellular components.

The model has been applied to predict and study the granulocytotic response in ten human accident cases involving acute exposure to ionizing radiation and eight cases involving protracted exposure. For the acute exposures, the initial conditions (cellular compartment capacities) are perturbed according to cell survival based on $D_0 = 100$ cGy. The model does not explicitly simulate Elkind-type repair; however, allowance is made in the two stem cell compartments to simulate intact and injured stem cells which are estimated input parameters. Accordingly, for protracted irradiation exposure, the model does not dynamically simulate cellular damage and repair. Cellular kill rates are estimated from the ratio of dose rate to the D_0 parameter estimated from cell survival data for constant dose rates. For the acute exposure cases analyzed, the model provides a reasonable dynamic profile of granulocyte cells following irradiation. However, simulation of the granulocyte levels for the protracted radiation exposure cases do not seem to be quite as impressive although expected trends are represented. The lack of data in some cases does not permit a comprehensive comparison to be made. In general, the model seems to provide the essential features of the granulocytotic response to irradiation. The suggested role that remaining injured stem cells play in transient recovery implies that explicit comprehensive modeling intracellular damage and recovery could make significant improvements for protracted radiation exposure.

2.4 RADIATION LETHALITY.

Acute lethality that culminates from severe forms of radiation-induced hematopoietic and gastrointestinal syndromes is the most well known. Animal research, some accidental human exposures, and clinical

trials involving TBI patients are bases of knowledge for hematopoietic death from protracted radiation exposure. Some animal research and a limited number of accidental human exposures are responsible for our understanding of gastrointestinal death, although to a much less extent. There are a number of reasons for this difference, some of which have to do with the relative difficulty in assay techniques and causality interpretation. The most familiar means to determine whether death is due to gastrointestinal or hematopoietic injury is the time of death following acute radiation exposure; in mice, for example, it is generally within five days for gastrointestinal death and generally within 30 days for hematopoietic death. However, for protracted dose exposures, the situation becomes somewhat more difficult and must be accompanied by assay techniques to determine the degree of intestinal injury such as developed by Withers and Elkind [1969, 1970]. Even so, under certain conditions, lethality may be the product of some combination of the two syndromes. This has been pointed out in a review of acute symptomatology in humans by Anno et al. [1989]. Also, based on a dose rate effect irradiation study in mice, Travis et al. [1985] point out that their data indicate that death after TBI is a result of multiple organ failure regardless of the primary tissue responsible for injury. Studies of mice by Mason et al. [1989] based on TBI or total-abdominal irradiation (TAI) indicate that damage to the hematopoietic/lymphopoietic system can result in animal lethality over the same ten-day period as the gastrointestinal syndrome even though damage to the gastrointestinal tract is usually designated as the predominate cause of death occurring within that period following acute radiation exposure. Furthermore, according to Hendry, Potten, and Roberts [1983], the two modes of lethality cannot be easily quantified in conventional animals (i.e., not germ-free) whose death is influenced by endogenous infection from the bowel which can be modified by antibiotic therapy.

2.4.1 Bone Marrow Damage.

Figures 25 through 31 give plots of LD₅₀ (the dose that is fatal to 50 percent of a test group) versus dose rate from bone marrow aplasia in various large animals (sheep, swine, goats, and dogs) and mice. The curves are least-square fits performed on animal data assuming a relationship of the form

$$LD_{50} = D_0 \left[1 + \left(\frac{R}{r} \right)^s \right] ,$$

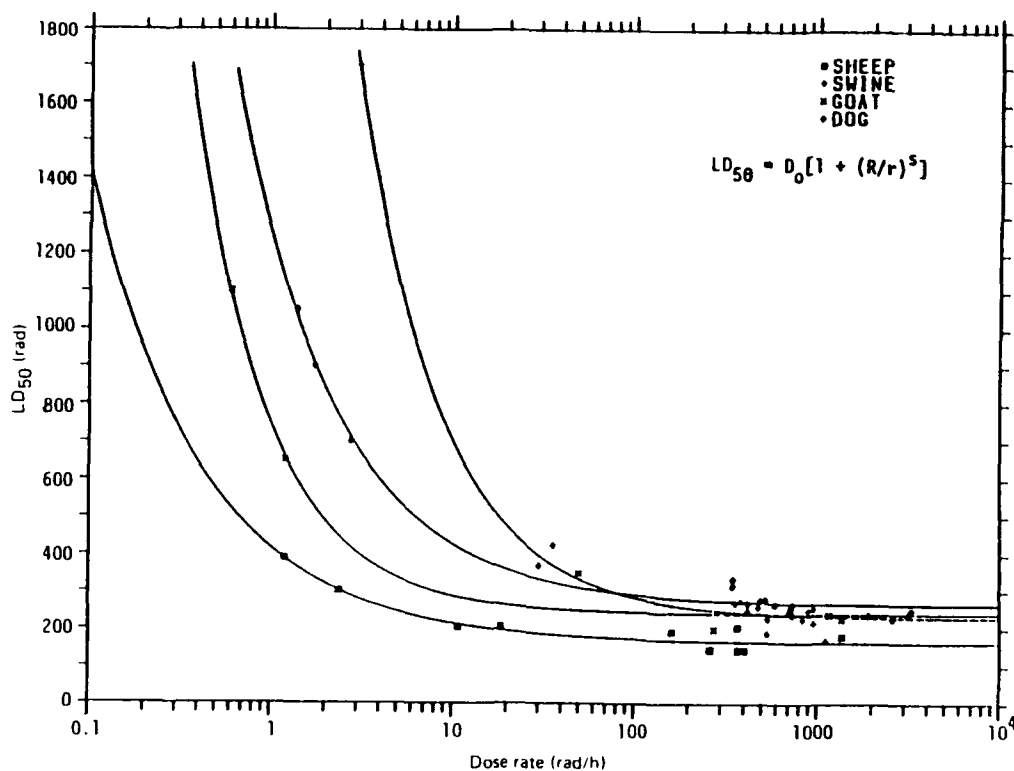
where D_0 = dose asymptote at high dose rate,

R = recovery parameter,

s = shape parameter ($s \neq 1$, or $s = 1$).

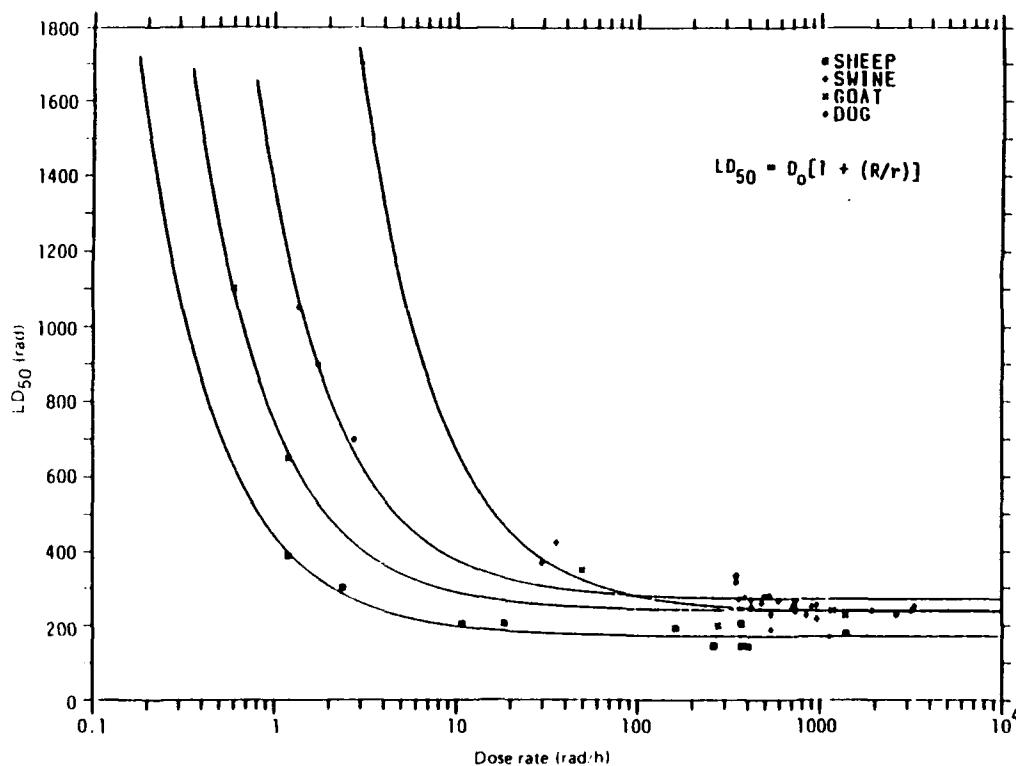
The data were fit in two ways to determine model accuracy between $s \neq 1$ (three parameter) and $s = 1$ (two parameter) as a choice of the shape parameter. Table 19 gives the calculated parameter results; the next to last column, " $(RMS/dgf)^{1/2}$," is a measure of the fit precision. It suggests that no significant advantage is gained from a three-parameter fit where $s \neq 1$. Therefore, the two-parameter model fits the data equally well and is also simpler.

The four large mammals--sheep, swine, goat, and dog--are of most interest. The curves for these animals are probably composed of two components. The high dose rate region of the curves flatten, beginning at approximately 10-20 cGy/h for the sheep, goat, and dog, and at 50 cGy/h for the swine; the curves bend upwards toward higher LD₅₀ values, and a clear dependency on dose rate is indicated. The flat part of the curves at the higher dose rates is the result of net injury to the bone marrow which increases with increasing dose. The LD₅₀ is not influenced by dose rate since the injury is great, inflicted rapidly, and recovery is absent during irradiation. The second component is the result of injury inflicted at a much slower rate, permitting recovery and repair concurrent with radiation exposure. Animals or humans therefore may absorb higher doses of radiation before reaching an LD₅₀ at the lower dose rates (≤ 10 cGy/h).



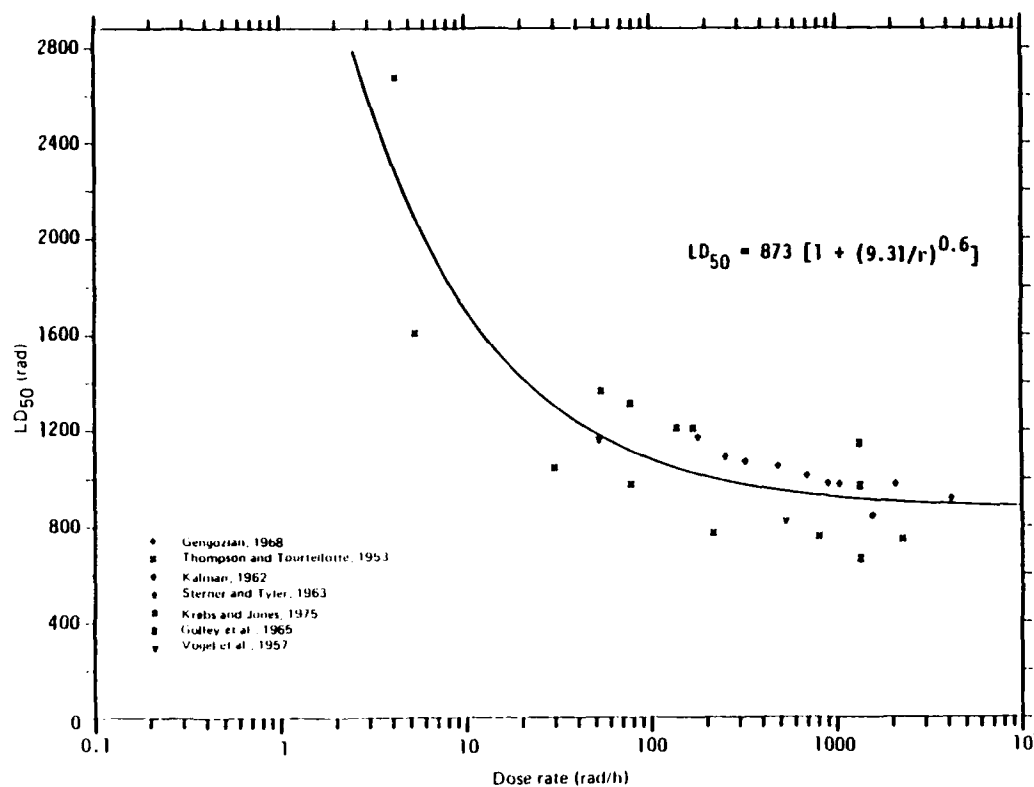
Source: Ainsworth and Leong [1966], Ainsworth et al. [1968], Hanks et al. [1966],
Nachtway, Ainsworth, and Leong [1967], Page [1968], Page et al. [1965]

Figure 25. LD₅₀ versus dose rate--three parameter model.



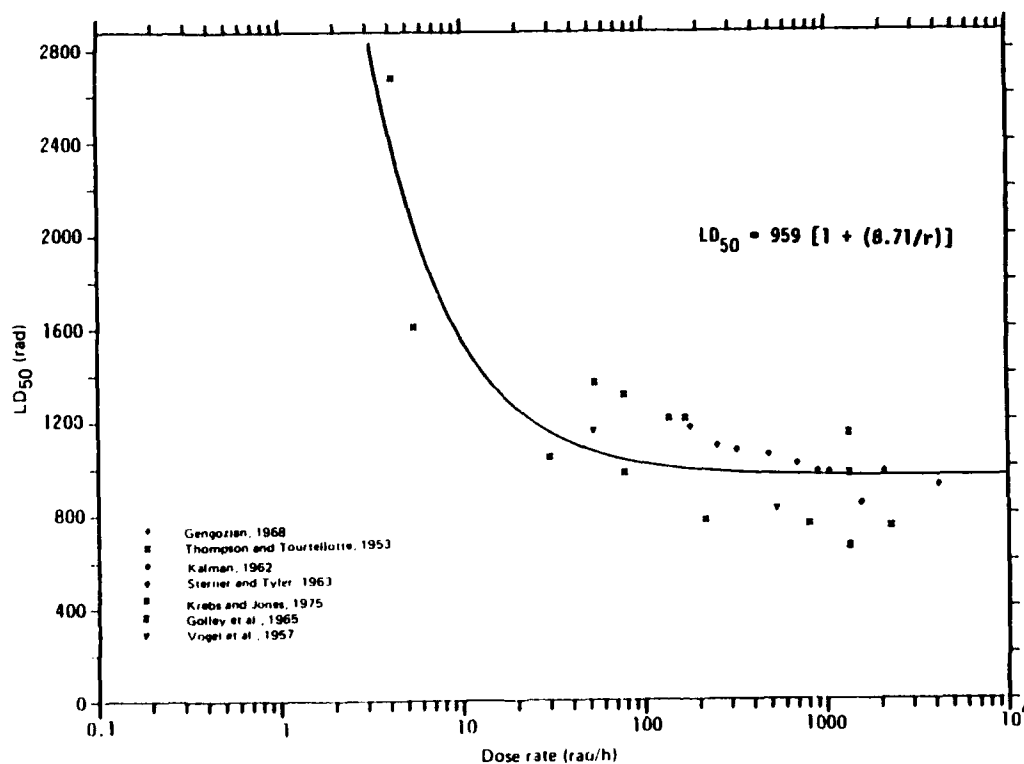
Source: Ainsworth and Leong [1966], Ainsworth et al. [1968], Hanks et al. [1966],
Nachtway, Ainsworth, and Leong [1967], Page [1968], Page et al. [1965]

Figure 26. LD₅₀ versus dose rate--two parameter model.



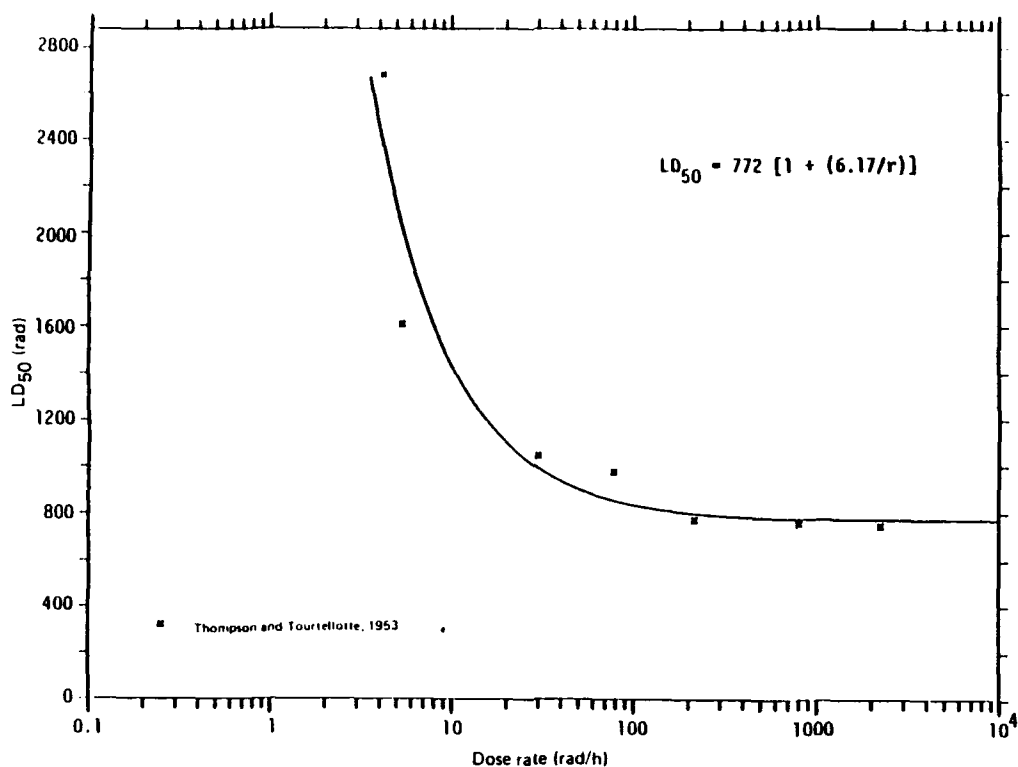
Source: Ainsworth and Leong (1966), Ainsworth et al. (1968), Hanks et al. (1966),
 Nachtway, Ainsworth, and Leong (1967), Page (1968), Page et al. (1965).

Figure 27. LD₅₀ versus dose rate--three parameter model for mouse.



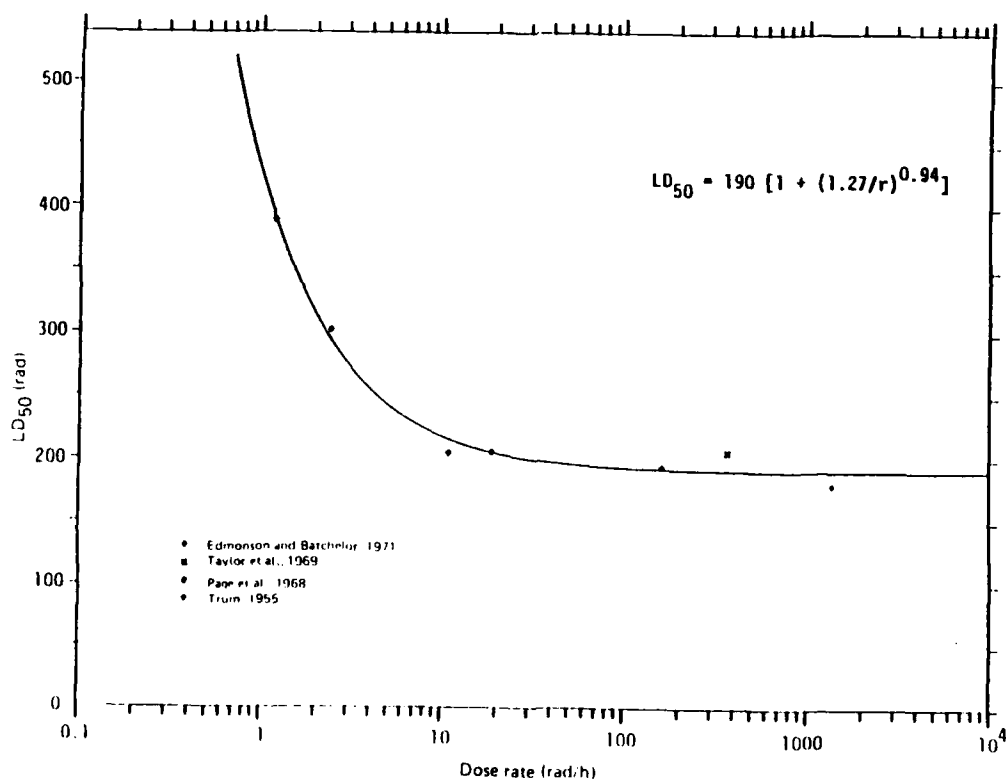
Source: Ainsworth and Leong (1966), Ainsworth et al. (1968), Hanks et al. (1966),
 Nachtway, Ainsworth, and Leong (1967), Page (1968), Page et al. (1965).

Figure 28. LD₅₀ versus dose rate--two parameter model for mouse.



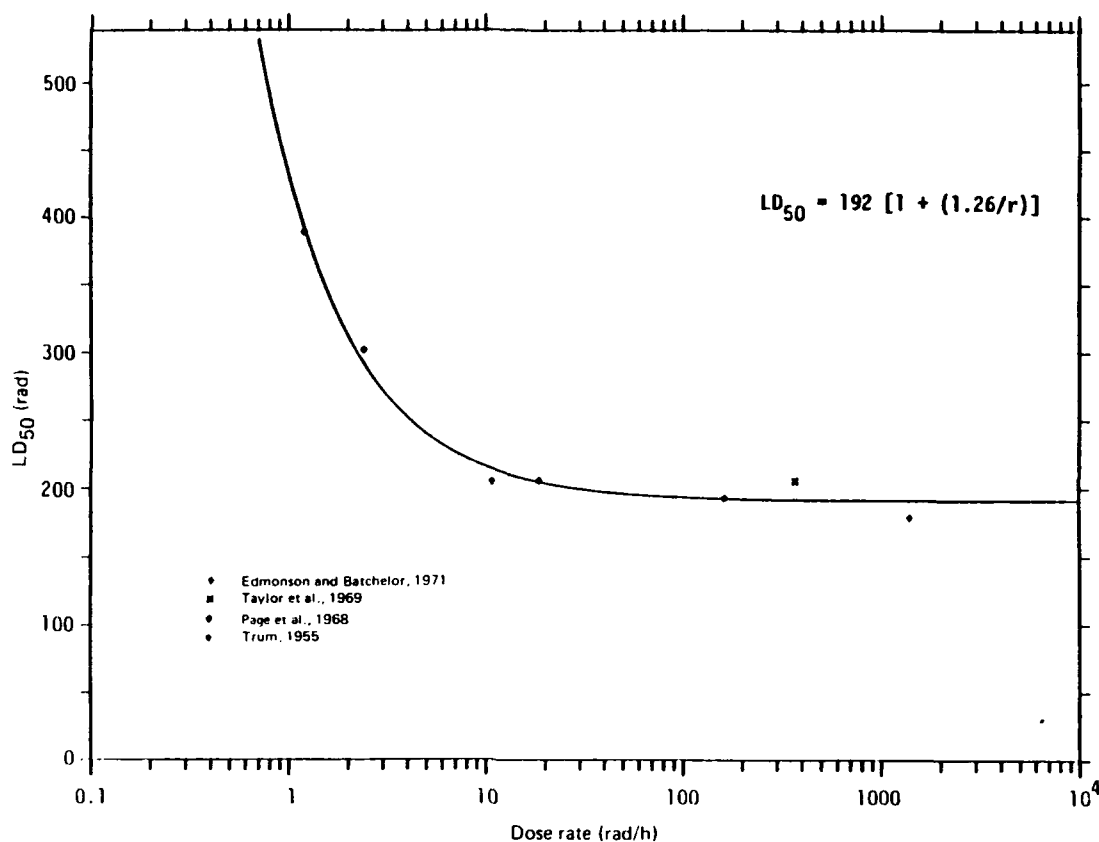
Source: Ainsworth and Leong [1966]; Ainsworth et al. [1968]; Hanks et al. [1966];
Nachtway, Ainsworth, and Leong [1967], Page [1968], Page et al. [1965].

Figure 29. LD₅₀ versus dose rate--two parameter model for mouse, from Thompson and Tourtellote (1953) only.



Source: Ainsworth and Leong [1966]; Ainsworth et al. [1968]; Hanks et al. [1966];
Nachtway, Ainsworth, and Leong [1967], Page [1968], Page et al. [1965].

Figure 30. LD₅₀ versus dose rate--three parameter model for sheep.



Source: Ainsworth and Leong [1966]; Ainsworth et al. [1968]; Hanks et al. [1966];
 Nachtway, Ainsworth, and Leong [1967]; Page [1968]; Page et al. [1965].

Figure 31. LD₅₀ versus dose rate--two parameter model for sheep.

An animal radiation study by Soviet researchers Grigorev, Gorlov, and Shafirkin [1978] was translated into English and reviewed. In that study, the effects on LD₅₀ of chronic (constant) dose rate exposure, ranging from 1 to 932 rads/day, was reported for a variety of animal species, including mice, rats, guinea pigs, rabbits, donkeys, sheep, goats, dogs, and monkeys. Empirical modeling was performed that included an extrapolation to man based on a polynomial relationship linking basal and water metabolism, animal weight, period of semirecovery from radiation damage, period of maximum white blood cell (WBC) depression, and lifetime of erythrocytes. Biological effectiveness was defined in terms of a dose-rate dependent coefficient that is the ratio of the effective dose D₀ (i.e., acute LD₅₀) to the accumulated dose, D, given as,

Table 19. Parameters for LD₅₀ versus dose rate.

Species	s	R	D ₀	dgf	(RMS/dgf) ^{1/2}	Figure No.
Swine	0.9394 ± 0.0321	21.74	229	14	32.51	9
Swine	1.0	18.77	235	15	32.32	10
Goat	1.0206 ± 0.2160	2.089	240	4	58.94	9
Goat	1.0	2.146	239	5	52.76	10
Dog	0.7805 ± 0.0913	5.482	263	14	31.78	9
Dog	1.0	4.074	270	15	33.12	10
Sheep	0.6887 ± 0.1931	1.960	162	8	23.33	9
Sheep	1.0	1.614	170	9	24.29	10
Sheep ^a	0.9423 ± 0.1472	1.272	190	4	11.21	14
Sheep ^a	1.0	1.258	192	5	10.21	15
Mice	0.5995 ± 0.0856	9.307	873	24	202.1	11
Mice	1.0	8.717	959	25	202.4	12
Mice ^b	1.0	6.173	772	4	236.0	13

^aSheep--without data from Hanks et al. [1966].

^bMice--data from Thompson and Tourtellotte [1953] only.

$$\frac{D}{D_0} = \left[1 - b \log_{10} \left(\frac{720}{r} \right) \right]^{-1},$$

where r is the dose rate in rads per hour; $b = 0.29$ for small animals (mice, rats, and guinea pigs); and $b = 0.22$ for large animals and humans. When the dose rate, r , is less than or equal to the approximate values listed below, D/D_0 can be expressed by the simple relationship,

$$D/D_0 = 1/ar,$$

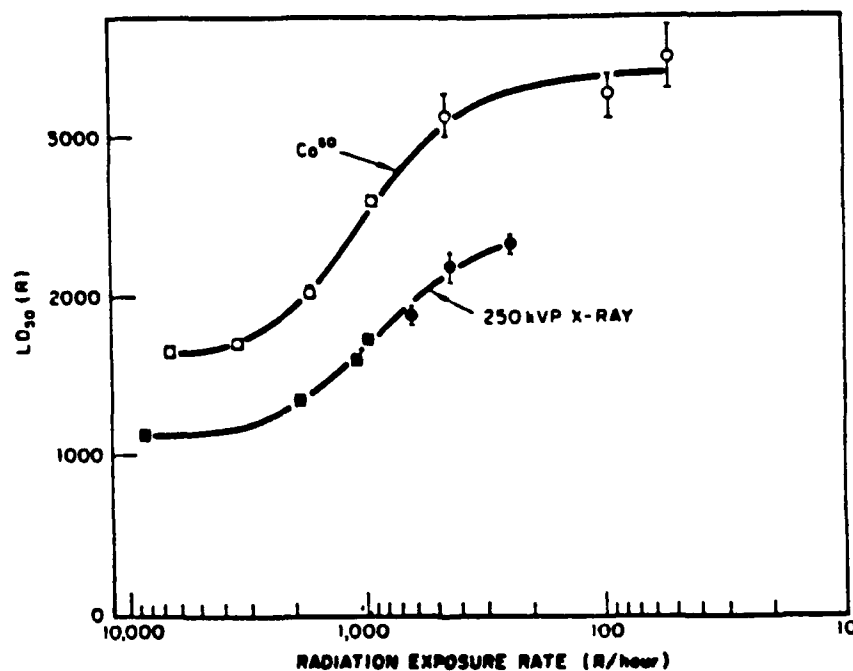
where:

	<u>a(h/rad)</u>	<u>r(rad/h)</u>
Mice	0.055	8.3
Rats	0.084	4.6
Large animals	0.168	2.5
Monkeys	0.36	1.3
Man	0.48	0.63

Although our review of the dose-rate dependent relationships above does not include comparisons with other empirical models, such as the form for LD₅₀ used to fit the animal data shown in Figs. 9 through 15, and those discussed below (Constant Dose Rate Models). Grigorev, Gorlov, and Shafirkin [1978] point out that D/D_0 does not depend on the dose rate beyond 720 rads/h, as can be seen in the first equation above.

2.4.2 Gastrointestinal Damage.

Using the split dose technique, Krebs and Leong [1970] performed a study with mice to determine the effect of constant exposure rates on the gastrointestinal LD_{50/5} for both ⁶⁰Co and 250 kVp X-ray irradiation. A plot of their results are given in Fig. 32 that indicates a factor of about two increase in LD_{50/5} when the dose rate decreases from about 8400 to 240 R/h for the 250 kVp X-rays and from about 6700 to 52 R/h for ⁶⁰Co gamma rays. The curves, based on probit regression fit of mortality, are separated by a factor of 1.48 which represents the effective RBE between the two types of photon radiation over the range of exposure rate. It should be mentioned that the two lowest dose rate points for ⁶⁰Co irradiation 52 and 93 R/h were developed from actual exposure periods of only 18 h plus a required "topping dose" given at a high dose rate (8400 R/h) to extend the radiation to lethality. Based on this data, however, the corresponding inferred exposure periods would be about 35 and 67 h. It is possible that the LD_{50/5} values would have been significantly higher at those two low dose rates had the exposure periods been allowed to full-term lethality. If so, the exposure periods would have been in excess of those estimated from their actual 18-h exposures.



Source: Krebs and Leong [1970].

Figure 32. Effect of dose rate on gastrointestinal LD_{50/5} in mice.

All actual exposure periods in the Krebs and Leong work were well short enough to avoid proliferation of the intestinal epithelium to ensure that the LD_{50/5} increase with decreasing dose rates only involved Elkind-type repair. Accordingly, an injury repair model was constructed on the basis of the measured recovery kinetics that assumed exponential repair. With the model, they were able to account for the LD_{50/5} behavior with increasing exposure time and estimate a recovery half-time of 23.4 min.

Krebs and Leong also estimated that some 40 to 50 percent of the injury is irreversible. That accounts for an apparent maximum finite limit of slightly more than twice the minimum value approached by the LD_{50/5} as the exposure rate becomes low in the absence of other repair mechanisms. However, this limit may be only transitory due to the onset of proliferation which might have been revealed for longer exposure periods. For example, as pointed out above, the lowest dose rate point (52 r/h) corresponds to an exposure period of 67 h (at least) or 2.8 days. In view that the fractionation studies of Withers and Elkind [1969] in mice provide clear evidence of proliferation

within that period, one would expect a correspondingly significant increase in the LD_{50/5} associated with that dose rate (i.e., 52 r/h). Moreover, Withers [1972] gives evidence of crypt cell proliferation for 50 and 60 cGy/h based on constant dose rate exposures.

Travis et al. [1985] exposed mice to TBI from ⁶⁰Co radiation to assess the effect on lethality of constant dose rate, ranging from 60 to 1500 cGy. Death was scored at ten days to determine the dose rate dependence of deaths from the gastrointestinal syndrome. The LD_{50/5} increased from about 1200 to 2050 cGy (about a factor of 1.7) for a decrease in dose rate from the high to the low ends of the range (1500 to 60 cGy/h). However, the LD_{50/5} values are significantly lower by a factor of about 1.5 than those given by Krebs and Leong [1970] over about the same dose range. The difference could partially be attributed to different strains of mice used, although deaths scored at ten days by Travis et al. rather than within five days compared to Krebs and Leong, may have also been affected by damage to the hematopoietic system; pathologic findings by Travis et al. indicated changes in the jejunum, ileum, and rectum were minimal, and when they occurred subjectively, they appeared as a loss of crypts in both the jejunum and ileum. Also, in addition to source-to-target distance, lead shielding was used to reduce the source radiation to the desired exposure rates. This can produce a lower photon energy spectrum from scattering, resulting in an increase in RBE that would contribute to lower LD_{50/5} values.

Dutreix et al. [1979] described studies of the effect on mice of constant dose rate exposures, ranging from 120 to 6000 cGy; they indicate a factor of 1.83 increase in LD_{50/5}, somewhat similar to that obtained by Krebs and Leong [1970] and Travis et al. [1985]. However, the actual LD_{50/5} values are again significantly lower than those of Krebs and Leong over a corresponding dose range--a factor of about 1.6 lower at the high dose rate end and 1.8 lower at the low dose rate end. Again, some of the difference may be attributable to a different strain of mice, particularly in view that the same strain (Balb/c mice) used by both Dutreix et al. and Travis et al. were in agreement in LD₅₀ values over corresponding dose rates and appeared to be well

within experimental error. Although not specifically indicated, presumably the LD₅₀ values given by Dutriex et al. involved ⁶⁰Co irradiation. Whether or not shielding material was employed to attenuate source radiation exposures, which would change the photon spectrum, was not indicated.

Dutreix et al. [1979] also provided data to demonstrate the reduced effectiveness of protracted radiation in terms of a single acute dose equivalent of 10 Gy. The data are plotted in Fig. 33 for both constant dose rates (connected by the dashed line) and fractionated exposures (connected by the solid line). The time axis includes a three-hour interval which separates dose fractions all given in 10 min or less (the three-hour intervals allow adequate time for intracellular repair to take place) It is interesting to note that over the same period, the continuous dose rate exposure provides more protection than fractionated exposures since the acute single dose equivalent is a measure of residual damage. Also, the single acute

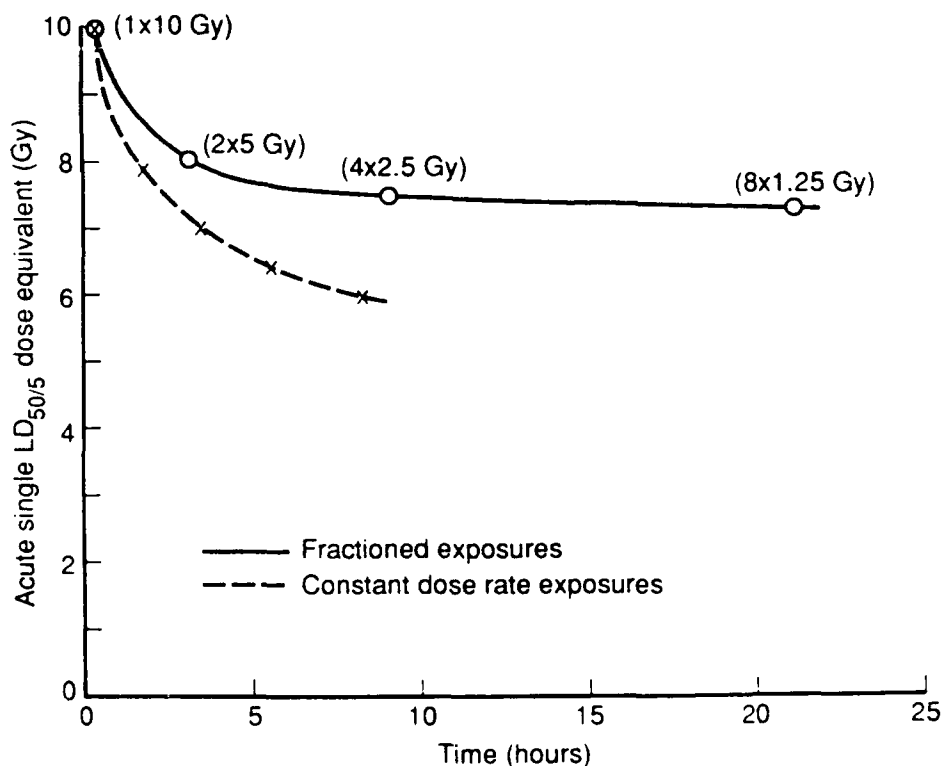
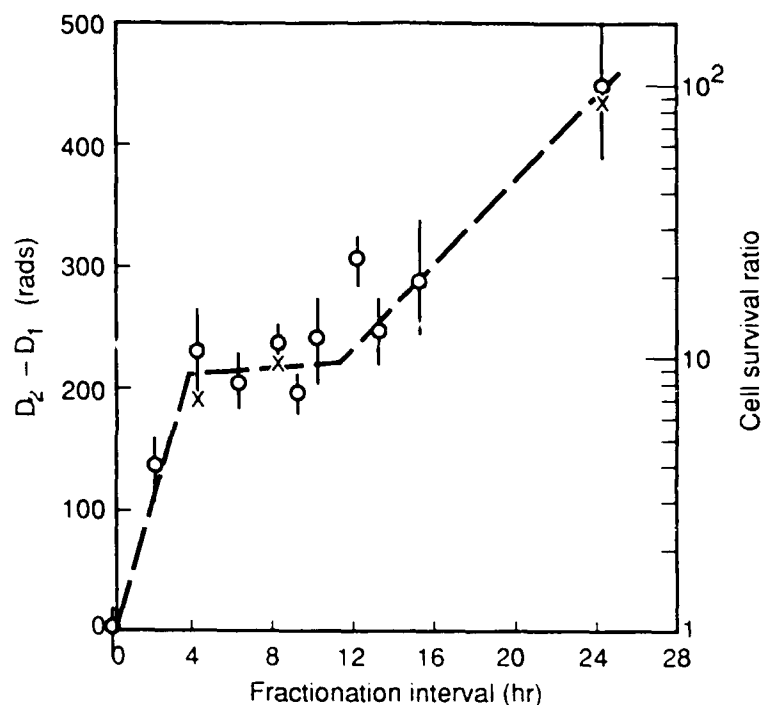


Figure 33. Acute single LD_{50/5} dose equivalent to a 10 Gy protracted dose for constant dose rate and fractionated exposures.

dose equivalent appears to tend to an asymptotic limit with time (increasing number of fractions) that would appear to be significantly higher than that for constant continuous radiation exposure. However, it would be difficult to assure this based on the limited data in Fig. 33. These data also point out that it would be inappropriate to infer the sparing effect of protracted radiation exposure based on dose-rate-averaging fractionated exposure. For example, 315 cGy/h would correspond to the dose rate obtained by averaging over the treatment time for the 2×5 Gy fractionated exposure where the acute single dose equivalent is larger than that for continuous exposure (i.e., 8 Gy compared to 7 Gy). Similarly, the dose rate averaged over the treatment time for the 4×2.5 Gy fractionated exposure is 109 cGy/h where the acute single dose equivalent is 7.5 Gy compared to only 6 Gy for continuous exposure.

Using 200 kVp X-rays, Withers and Elkind [1969] demonstrated intestinal radiosensitivity based on their milestone fractionated abdominal radiation studies in mice. They developed parallel data for the endpoints of lethality and jejunal crypt cell survival and determined that 50 percent animal survival within five days corresponds to a crypt cell survival fraction of around 0.002. Assuming a random crypt cell survival among the crypts, about 1/4 of the crypts will survive with proliferating cells. In normal mice, LD_{50/5} (50 percent lethality at five days) generally corresponds to about 1/3 of the crypts surviving where stem cell survival is 0.003 [Withers, 1989]. Potten and Hendry [1983] indicate a higher value of 0.4 (range 0.3 to 0.5) for fraction of surviving crypts at the LD_{50/5} for mice.

Fractionated radiation was given at a high dose rate (78 Gy/h) over two brief periods (5 to 11 minutes) separated by time intervals ranging from 2 h to 21 days. The first fraction was 660 rads followed by a second one of 1415 rads (total of 2075 rads) for *in vivo* cell colony counting. For lethality assessment, the second fraction was given to mice in graded amounts in order to calculate the LD_{50/5} from probit analyses of data that straddled the LD_{50/5}. The single dose LD_{50/5} was estimated to 1061 ± 24 rads, and for split doses, it was always higher, as shown in Fig. 34.



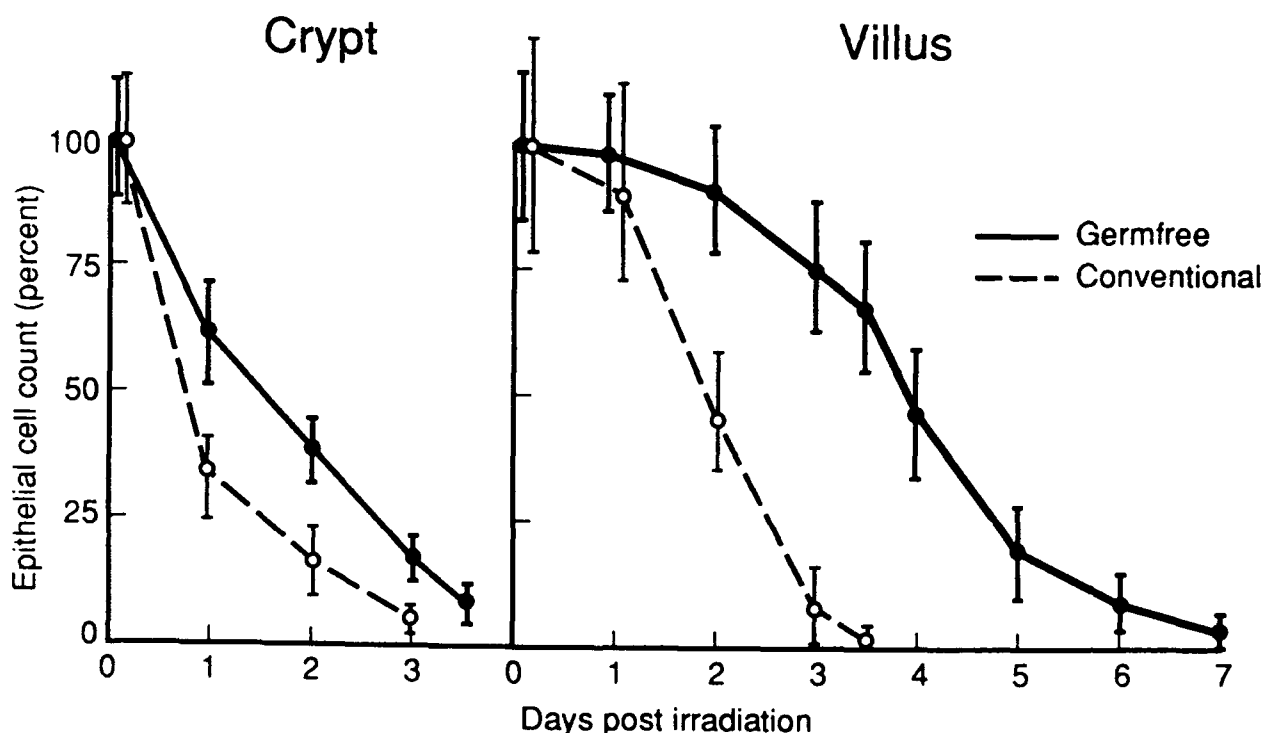
Source: Withers and Elkind [1969].

Figure 34. Recovery comparison of LD_{50/5} (open circles and dashed line) and cell survival (x-symbols at 4-, 8-, and 24-hours) endpoints; the origin of both scales refer to 1060 rads acute single exposure.

The data points in Fig. 34 (open squares with standard error bars) along the dashed "eye-fit" line are the LD_{50/5} data that correspond to the dose fractionation increment, $D_2 - D_1$. In terms of lethality, it represents the increment of total dose required with increasing fractionation interval in order to maintain 50 percent lethality in mice at five days. The zero-dose increment value at the origin corresponds to a single acute dose of 1060 rads. The X-symbols lying dose to the LD_{50/5} recovery curve at the 4-, 8-, and 24-h fractionation intervals are corresponding jejunal crypt cell survival ratios (right-hand ordinate) calculated at 1060 rads from expanded second-dose fraction cell survival data. The cell survival ratio of unity is at zero-dose increment that is normalized to the LD_{50/5} value of 1060 rads for a single acute exposure (cell survival fraction is about 0.002). In terms of cell survival, the dose fractionation intervals represent the increments of total dose required with increasing fractionation interval in order to maintain a survival ratio

of unity (or the cell survival fraction at about 0.002). The similarity of the recovery data for cell survival and the LD_{50/5} in Fig. 34 is evidence for a causal relationship between 5-day radiation death and lethal injury to stem cells of the intestinal mucosa.

Studies have been done using relatively high dose rates to characterize changes associated with intestinal radiation death or to determine possible causes. Matsuzawa and Wilson [1965] exposed mice to 3000 R of 250 kVp X-rays at a rate of about 40 R/min (~23 Gy/h) and determined a mean survival time of 3.5 days ranging from 2.9 to 3.8 days for conventional mice. For germfree mice, the mean survival was 7.3 days with a range of 6.4 to 7.7 days. Based on histological examination, they also obtained epithelial cell counts for the crypt and villi expressed as percentage versus post-irradiation time shown in Fig. 35. The curves show the progressive mucosal denudation with time that correlate well with lethality for both germfree and conventional mice. Based on the progress of thymidine -³H labeled cells,



Source: Matsuzawa and Wilson [1965].

Figure 35. Cell counts of mouse ileum after a sterilizing dose of 3000 R.

cell transit times were estimated for conventional and germfree mice, given below.

	Transit Time (days)	
	<u>Conventional Mice</u>	<u>Germfree Mice</u>
Crypt to villi junction	0.5	1.6
Villi junction to tip	0.75	3.55
Total (crypt to villi tip)	2.1	4.3

Cell movement from the base to the tip of the villi was found to be linear with time. Also, both in the conventional and germfree mice, the normal transit time (i.e., approximate lifetime of the intestinal mucosal cells) is about 60 percent of the mean survival time. According to Matsuzawa and Wilson, the difference between the life span of the cells and time required for denudation (approximately mean time to lethality) indicates a change in the life span of the cells effected by a decrease in cell population.

Jackson and Geraci [1986] performed irradiation studies using conventional, pseudomonas-contaminated and GI-decontaminated rats to investigate the pathophysiological causes of radiation-induced gastrointestinal death. They employed fission spectrum neutrons from a TRIGA reactor and approximately 8 MeV average energy neutrons from an accelerator. Gamma irradiation was also done with ^{137}Cs radiation and ^{60}Co radiation at dose rates of about 25 to 26 Gy/h. They concluded that the inability of the denuded mucosa to absorb fluid and electrolytes and consequent hypovolemic shock was the major mechanism involved in producing intestinal radiation death.

Figure 36 and Table 20 show some results for LD_{50/5} and median survival time, respectively, given by Jackson and Geraci. The RBE of cyclotron neutrons appears to be about two for gastrointestinal lethality regardless of treatment condition; for fission neutrons, the RBE is almost three (2.8). However, no significant difference was found in the median survival time for conventional rats regardless of the radiation source including gamma rays from either ^{137}Cs or ^{60}Co and neutrons from either the cyclotron or TRIGA. Also, the time of death is not explicitly dose dependent but given a sufficient amount of gastrointestinal damage (i.e., lethality threshold), the time of

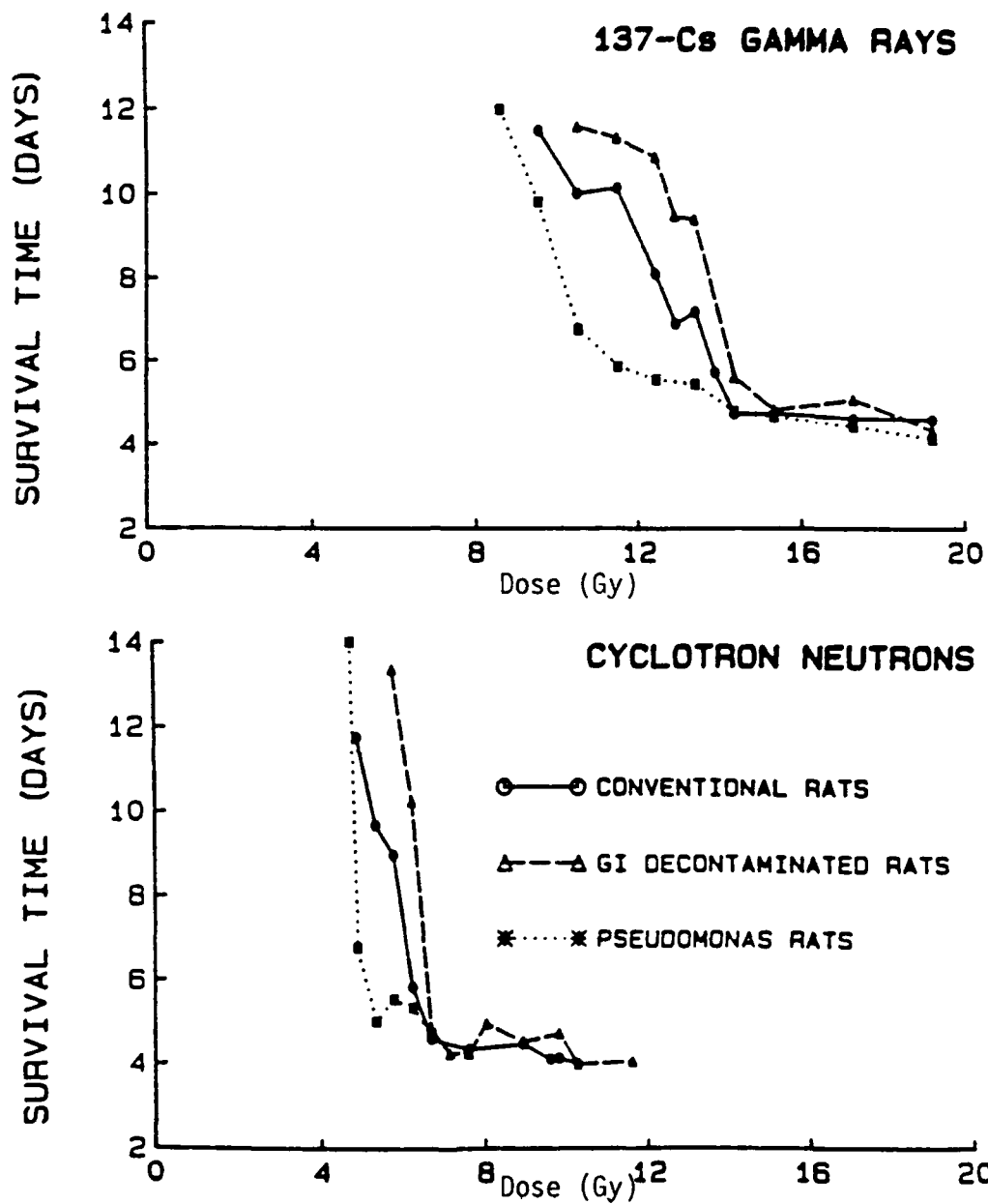


Figure 36. Survival time of untreated, GI-decontaminated, and Pseudomonas-infected animals after exposure to various doses of Cs-137 gamma rays and cyclotron neutrons (each point represents the median survival time of 8 to 40 rats). Source: Jackson and Geraci, 1986.

Table 20. LD_{50/5} day of pseudomonas-infected GI, conventional, and GI-decontaminated rats.
Source: Jackson and Geraci, 1986

Treatment	Radiation	LD _{50/5} day (Gy)
Pseudomonas	¹³⁷ Cs γ rays	13.7 (13.1-14.3) ^a
Pseudomonas	C-neutrons ^b	5.85 (5.11-6.69)
Conventional	¹³⁷ Cs γ rays	14.1 (13.4-14.7)
Conventional	C-neutrons	6.25 (6.10-6.40)
Conventional	F-neutrons ^c	5.0 (4.72-5.30)
Decontaminated	¹³⁷ Cs γ rays	15.0 (13.9-16.2)
Decontaminated	C-neutrons	7.40 (6.79-8.09)

^aValues in parentheses are 95 percent confidence limits.

^bC-neutrons = Cyclotron produced neutrons.

^cF-neutrons = TRIGA produced fission neutrons (1.2 MeV mean energy).

death proceeds according to degenerating physiological processes. When radiation exposure is protracted, the damage threshold is offset by recovery mechanisms which may either prevent or delay lethality.

Very little real data exist for lethality in humans that can be attributed purely to gastrointestinal injury. In fact, aside from being a predominate cause, it probably can never be expected to be the sole cause of lethality following TBI owing to other accompanying body injury. The most comprehensive set of lethality data for humans involving gastrointestinal injury is from the Chernobyl accident victims listed in Table 21 given by Guskova et al. [1988]. Dose estimates range from 10 to 12.5 Gy and the time of death from 10 to 20 days following the accident; the dose rates are indicated to be at a high level of at least 2 Gy/h or more [Baranov and Guskova, 1988]. Rather severe injury to the skin from beta radiation was a competing lethal effect as indicated in Table 21. The fact that some lethality extended up to 20 days might reflect the extensive medical care given.

Table 22 gives estimates of dose and time of gastrointestinal-syndrome-lethality for man based on some pre-Chernobyl experience (with the exception of that indicated by Guskova et al., 1987). The

Table 21. Mortality of Chernobyl accident victims with skin and intestinal injuries.

Case Number	Dose (Gy) (Marrow)	Treatment ^a	Day of Death
3	12.0	BMT	17
4	11.8	BMT	18
10	11.1	FLT	14
14	10.9	FLT	18
15	>10.0	FLT	14
17 ^b	10.0	BMT	18
20	12.4	FLT	17
23	13.7	FLT	15
26 ^b	12.5		20
2097 (Kiev)	10.2		10

^aBMT = bone marrow transplantation

FLT = fetal liver (cell) transplantation

^binvolved mycobacterial sepsis

accident cases given by Fanger and Lushbaugh [1967] are thought to be predominately due to gastrointestinal injury. Even though some of the dose ranges in Table 22 extend to 7000 cGy, Fanger and Lushbaugh [1967] give evidence for cardiovascular shock as the radiation

Table 22. Gastrointestinal syndrome lethality in man.

Dose (cGy)	Postexposure Time (days)	Source
1114, 1910	9, 10	Fanger and Lushbaugh (1967) ^a
1000-2000	8-16 ^b	Guskova et al. (1987)
≥1000	<14	Maisin et al. (1971) ^c
>1000	7-10	Fajardo (1982)
670-6700 ^d	7	Ingram (1969)
750-2000	7-14	Anno et al. (1989)
670-6700 ^d	6-10	Lushbaugh (1973)

^aTwo accident cases cited from Hemplemann et al. (1952) and Kurshakov (1962).

^bIntestinal changes most apparent, 8-12 days; total loss of epithelium, 10-16 days.

^cBased on histologic examinations from autopsies performed on eight Hiroshima and Nagasaki bombing victims (substantial dose uncertainty)

^dBased on a 0.67 internal-body-dose conversion factor for 1000-10,000 rads.

syndrome causing death based on pathologic changes in two accident victims who received doses of 4500 and 8800 cGy; furthermore, the times of death, 35 and 49 h, respectively, following exposure, are much too early for pure gastrointestinal injury to manifest in lethality.

We conclude that lethality solely from gastrointestinal injury in man exposed to TBI may exist in a limited range, perhaps ~8 to 12.5 Gy equivalent acute dose. Lethalities can be expected to occur within one to two weeks. However, GI injury may play an important part in lethality for doses on either side of that range. Also, when radiation exposure is protracted, the recovery potential of the intestinal mucosa can produce an increase in the total dose level required to effect lethality.

2.5 RADIATION INJURY AND RECOVERY.

Radiation injury and recovery research in mammalian species relevant to this effort is primarily based on the lethality endpoint from radiation-induced bone marrow cytopenia. The empirical techniques for the measurements required have been rather well established in a number of mammalian species. In other tissues, such as the intestines, *in vivo* injury and recovery assessment techniques with regard to the effect manifested in the whole organism have not been as well established. Accordingly, there exists a much larger body of literature with regard to demonstrating injury and recovery due to hematopoietic effects. However, compared to the hematopoietic system, the much earlier and more rapid rate of recovery of the intestines from radiation injury has been well established based on the work of many researchers including Quastler [1959], Quastler et al. [1959], Hornsey and Vatistas [1963], Leshner [1967], Withers and Elkind [1968, 1969, 1970], and Potten and Hendry [1975]. A more detailed discussion of intestinal injury and recovery accompanies the gut injury model we developed which is described in Section 5.

The postirradiation injury state, i.e., residual injury or injury that remains unrepaired, of an organism depends on the following considerations:

1. The extent to which the injury is dose dependent (i.e., radiosensitivity).
2. The physiological repair and recovery which can counteract the effects of injury.
3. Recovery must occur within a definite time or to a certain extent to effect survival.
4. Radiation exposure over a period of time induces fewer injuries per unit of time, permits repair processes to begin earlier, and enables proliferation to take place more rapidly.

Based upon lethality in mice from damage to the blood system, Blair [1952] developed a theory that radiation injury is repaired at a constant percentage per unit time of the net recoverable injury, and a small fraction of this injury is irreparable. This can be expressed in terms of net injury (acute single dose equivalent), D_e as

$$D_e = D_o [f + (1 - f)e^{-\beta t}]$$

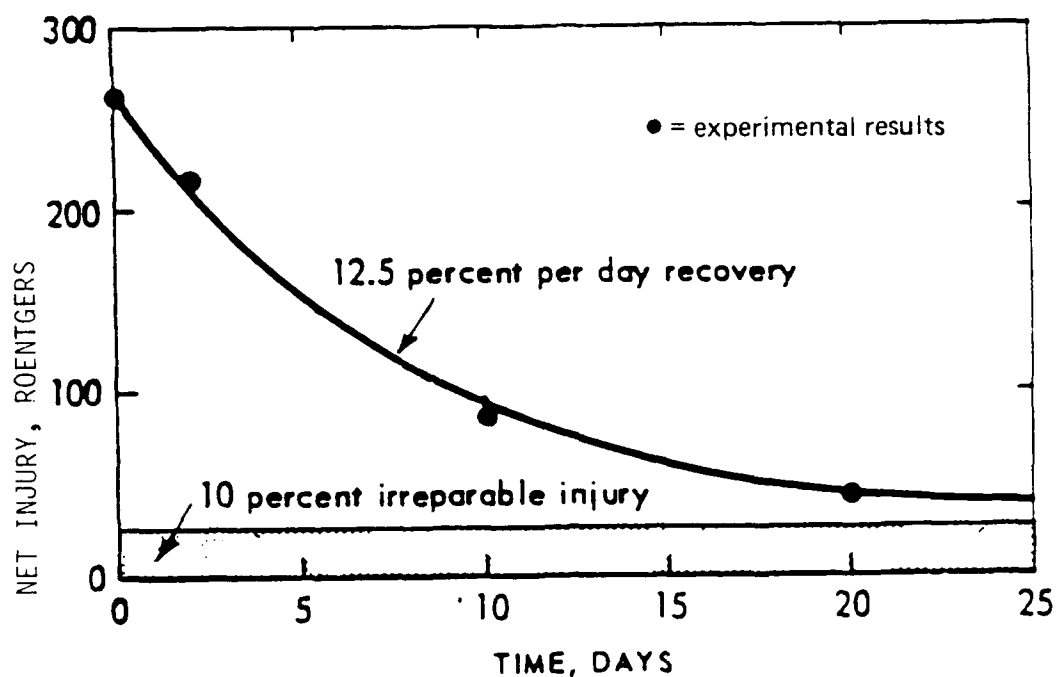
where f = irreparable fraction of injury,

β = recovery rate in percent per day,

t = number of days,

D_o = single acute dose.

Davidson [1957] applied this equation to the results of a split-dose recovery study in mice by Patterson, Gilbert, and Mathews [1947]. He then derived the graph depicted in Fig. 37 where net or residual injury is expressed in roentgens. Davidson estimated 10 percent irreparable injury, and determined that 2.5 percent recovery per day would yield a curve that would best fit the data of Patterson, Gilbert, and Mathews. He then proceeded to estimate WBC recovery half-life for several mammalian species and correlated these data with minimum white cell counts in response to an LD₅₀ exposure. He found an approximate linear correlation for the mouse, rat, dog,



Source: Davidson [1957].

Figure 37. Theoretical injury recovery curve with fraction of injury assumed unrecoverable.

and burro. Using human data available to him for WBC counts [Oughterson and Warren, 1956], Davidson estimated a recovery half-life for man of 690 h.

Subsequently, several investigators conducted a number of split-dose recovery and hematological studies to determine the validity of postirradiation exponential recovery and irreparable injury [Holloway et al., 1968; Ainsworth and Leong, 1966; Page et al., 1971; and Nachtway, Ainsworth, and Leong, 1967]. Irreparable or residual injury was confirmed; it appears to be dose, dose rate, and species dependent [Baum and Alpen, 1959; Baum, 1967]. Two examples of residual injury in the erythropoietic system are shown in Figs. 38 and 39. Rats were repeatedly irradiated with 300 or 400 R X-rays--five times at 90-day intervals. After each exposure, red cell production decreased during the recovery period. This decrease was significantly greater in rats subjected to 400 R X-radiation (Fig. 38). Figure 39 indicates that erythropoiesis significantly increases over the first five days following exposure.

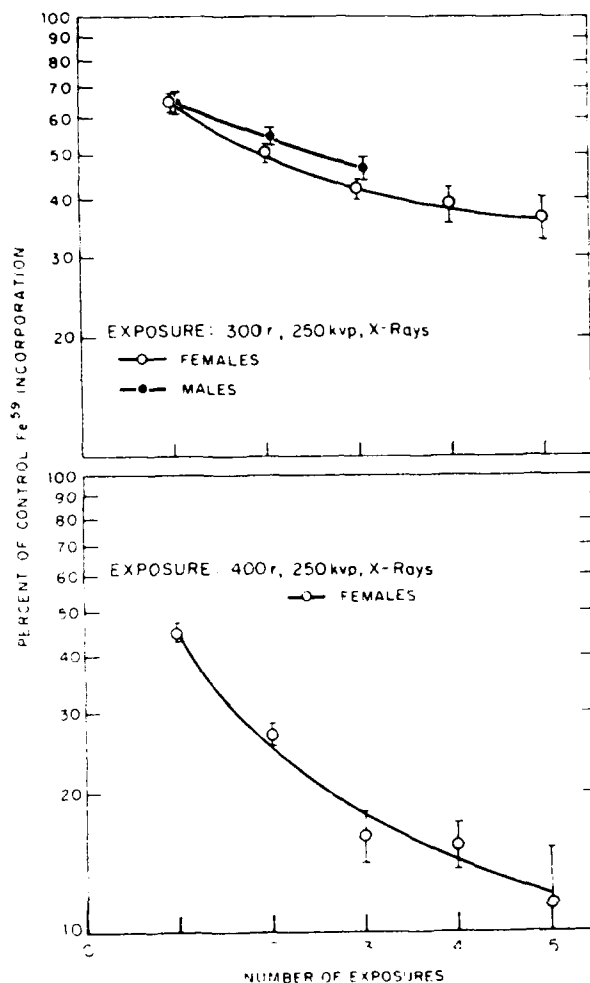


Figure 38. Maximum Fe^{59} incorporation for male and female rats exposed periodically to 300 r of X-rays and for female rats irradiated with 400 r (isotope was injected 5 days postirradiation, 3-month interval between exposures). Source: Baum and Alpen, 1959.

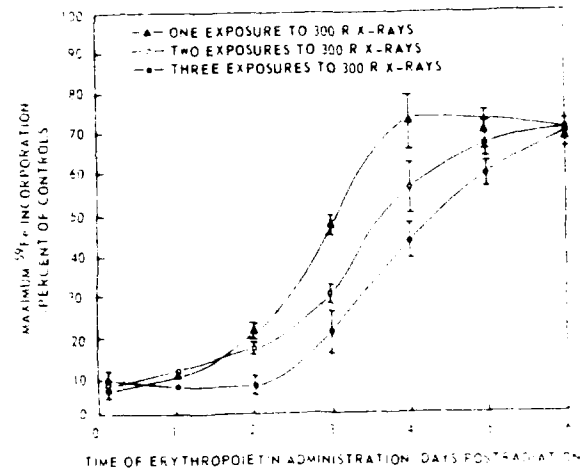


Figure 39. Residual injury of erythropoietic system in irradiated rats.

In Figs. 40, 41, and 42, data are plotted of split-dose recovery studies in hamsters and sheep performed at the Naval Radiological Defense Laboratory (NRDL) and rhesus monkeys at the Air Force School of Aerospace Medicine Laboratory [Holloway et al., 1968; Ainsworth and Leong, 1966; and Eltringham, 1967]. All these experiments show initial postirradiation recovery, over varying numbers of days, which is interrupted by a period of greater radiosensitivity (increased injury)

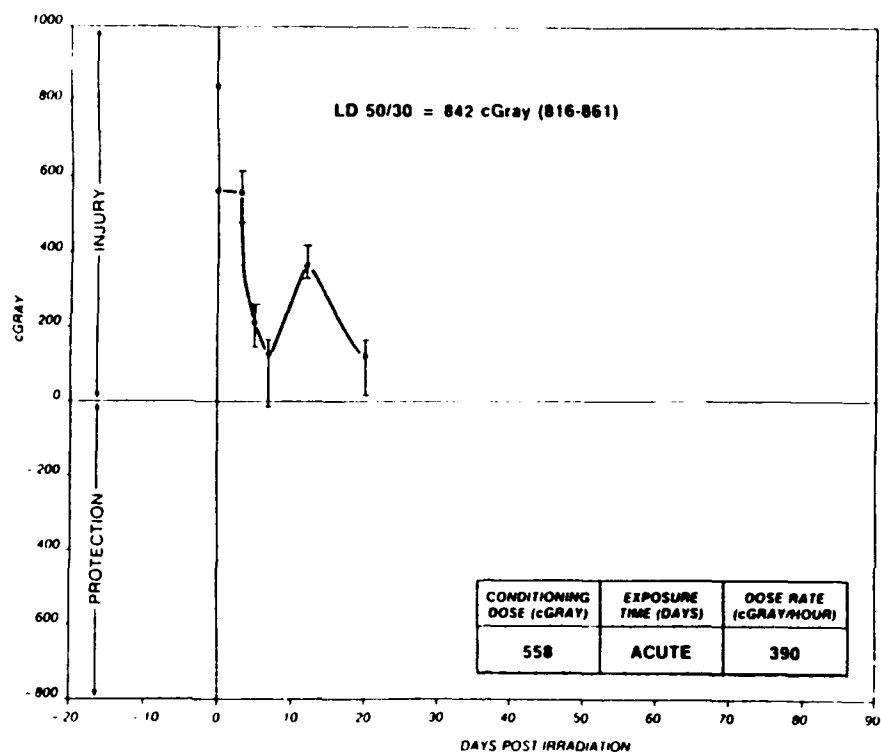


Figure 40. Hamster--acute exposure.

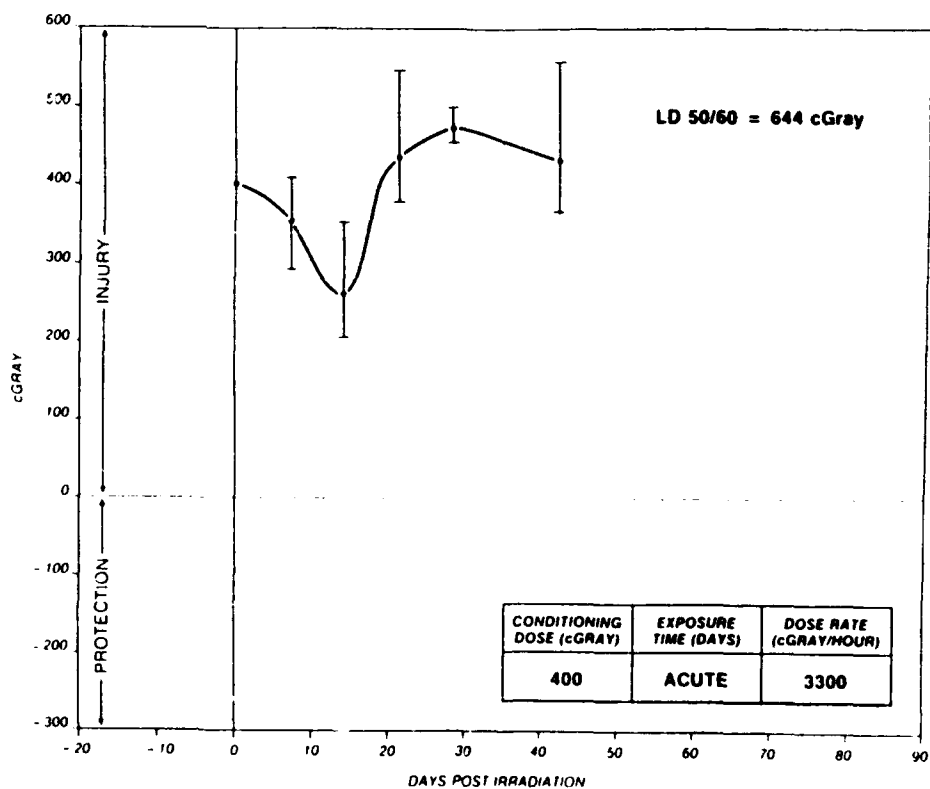


Figure 41. Rhesus monkey--acute exposure.

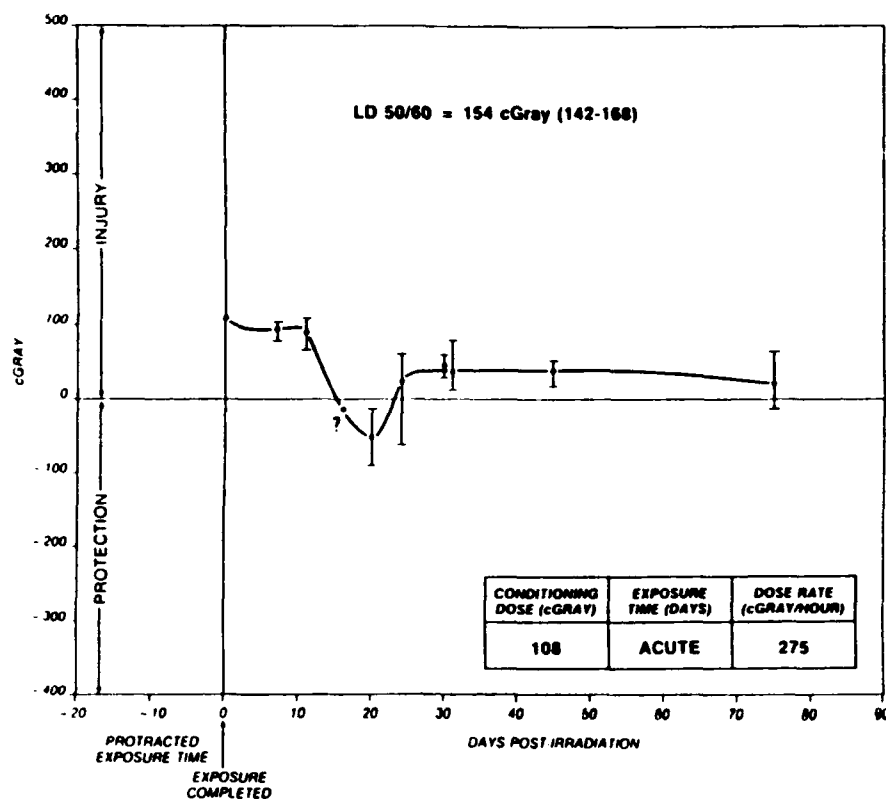
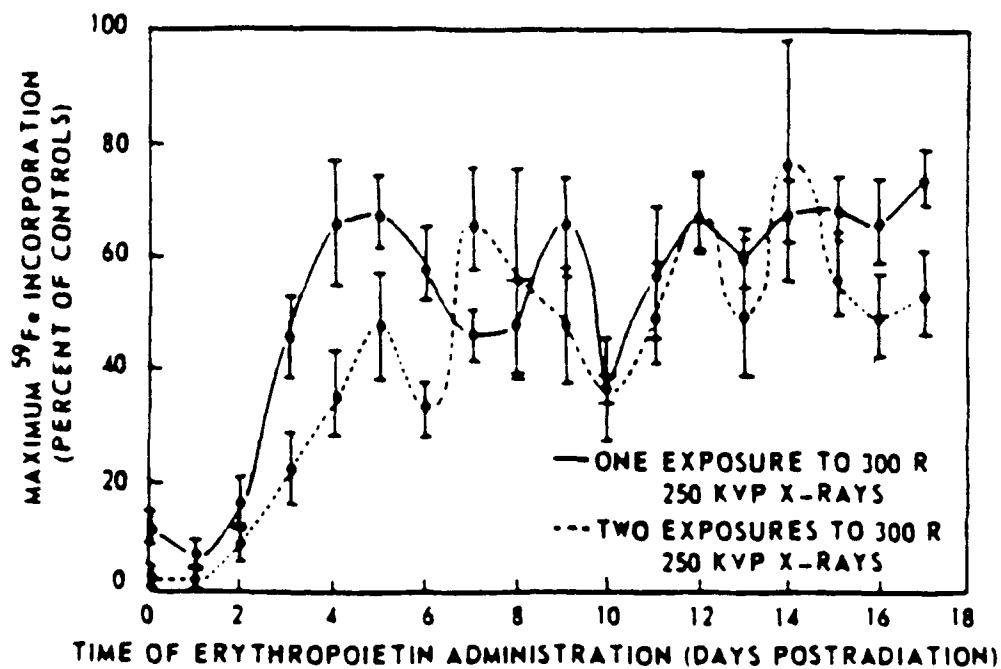


Figure 42. Sheep--acute exposure.

before final return to recovery occurs. None of these three species of animals appears to return completely to preirradiation levels. Similar reversals in recovery have been reported for the mouse and the rabbit [Leong, Wisecup, and Grisham, 1964].

Experiments designed to determine the pathophysiological responses of the blood-cell-forming system show postirradiation oscillatory recovery, which might be at least partly responsible for the return to hypersensitivity in the above-described split-dose recovery studies [Baum, 1967; Baum and Wyant, 1970; and Morley, King-Smith, and Stohlman, 1970]. Figures 43 (for the rat) and 44 (for the dog) demonstrate these oscillations for postirradiation red cell recovery. The finding that the above animals become radiosensitive after a period of substantial recovery suggests that a critical organ system (perhaps the bone marrow) has undergone some alterations such that little additional radiation is required to kill the animal. This, of course, questions the validity of Blair's theory of an exponential



Source: Baum [1967].

Figure 43. Residual injury of erythrocyte stem cells in irradiated rats--17-day observation period.

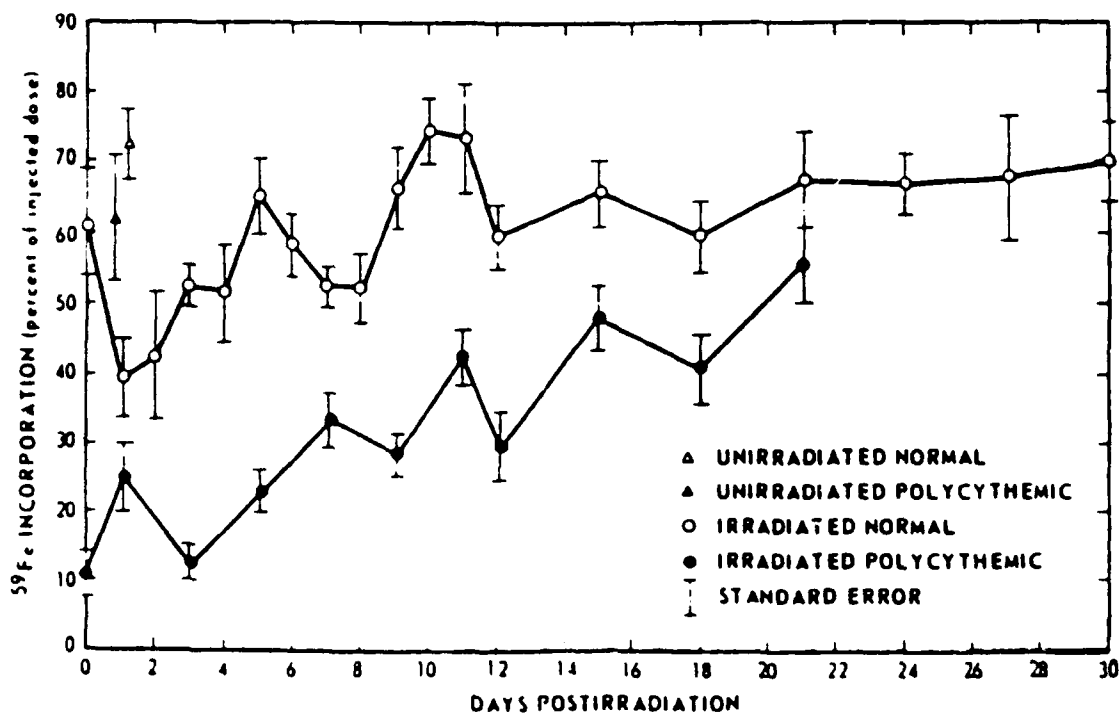


Figure 44. Erythropoiesis in normal and in polycythemic dogs exposed to 150 rads mixed gamma-neutron radiation. Source: Baum and Wyant, 1970.

recovery. Leong, Wisecup, and Grisham [1964] report a return to radiosensitivity for rabbits about three weeks after irradiation. Prior to that, continuous recovery of almost 60 percent was recorded. Since at the time of the reversed sensitivity, peripheral leukocytes were in the recovery phase and continued to recover, the authors questioned an involvement of the hematopoietic system with the return to radiation hypersensitivity. However, the postirradiation concentration of leukocytes in the circulatory blood system merely indicates that the perturbed bone marrow shunts newly formed leukocytes rapidly to the circulation for transportation to the tissues to protect against invading antigens. It does not necessarily mean that normal storage areas have been replenished and that sufficient numbers of white cells are available to counteract the deleterious effects of an additional dose of radiation.

In two other experiments (Figs. 45 and 46) conducted at NRDL using the dog and the swine, return to an increased injury condition is apparently not indicated. However, it must be emphasized that both studies were only carried out to day 20 postirradiation, and reversal of injury is seen in the sheep, another large mammal, between days 20 and 30.

For the swine, an experimental point is available for day 60 which could not be statistically evaluated. However, the swine may have a remarkable capability for recovery and be quite radio-resistant. Figure 47 shows that swine exposed to an acute dose of 155 cGy given in about 0.5 h have sustained injury at the conclusion of the exposure equivalent to 155 cGy [Ainsworth et al., 1968]. If the same dose is given in 61.5 h, the remaining injury is only 64 cGy. Doubling or tripling the dose increases the injury only slightly. One possible interpretation of this finding is that swine develop increased resistance to radiation while being irradiated. Another may well be that animals sustain the greater part of their injury during the early radiation period. Experiments with sheep by Still et al., [1969] and Jones and Krebs [1970] seem to give credence to the latter interpretation.

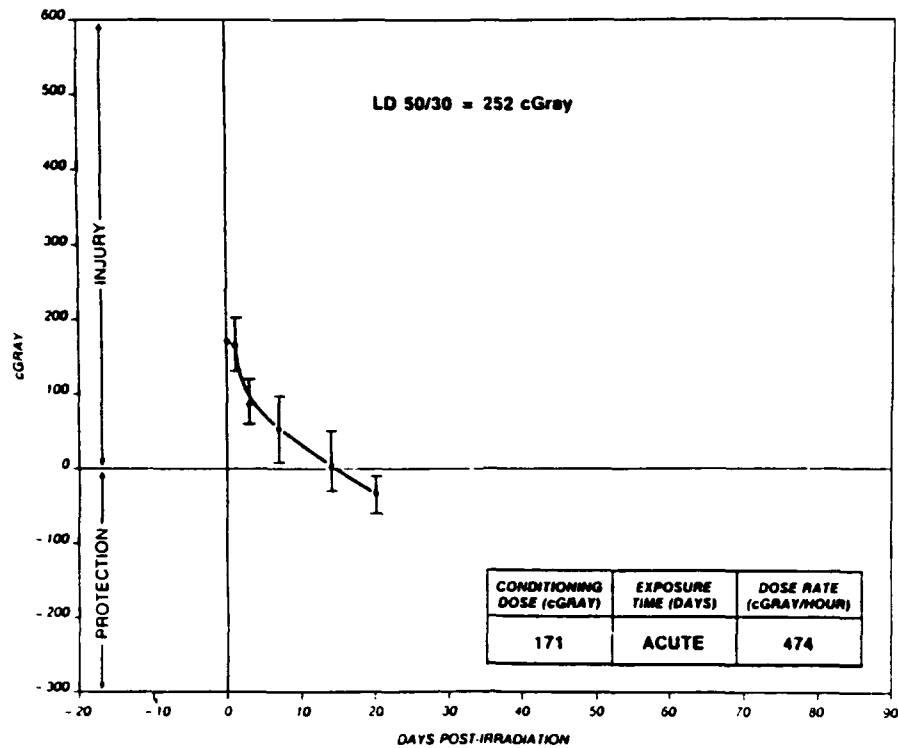


Figure 45. Dog--acute exposure.

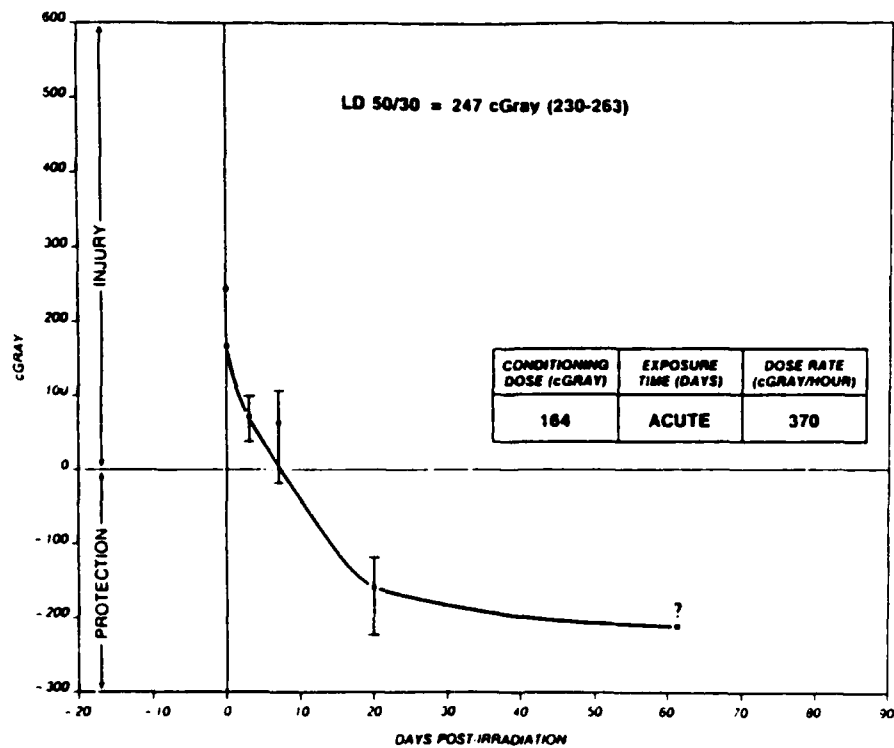


Figure 46. Swine--acute exposure.

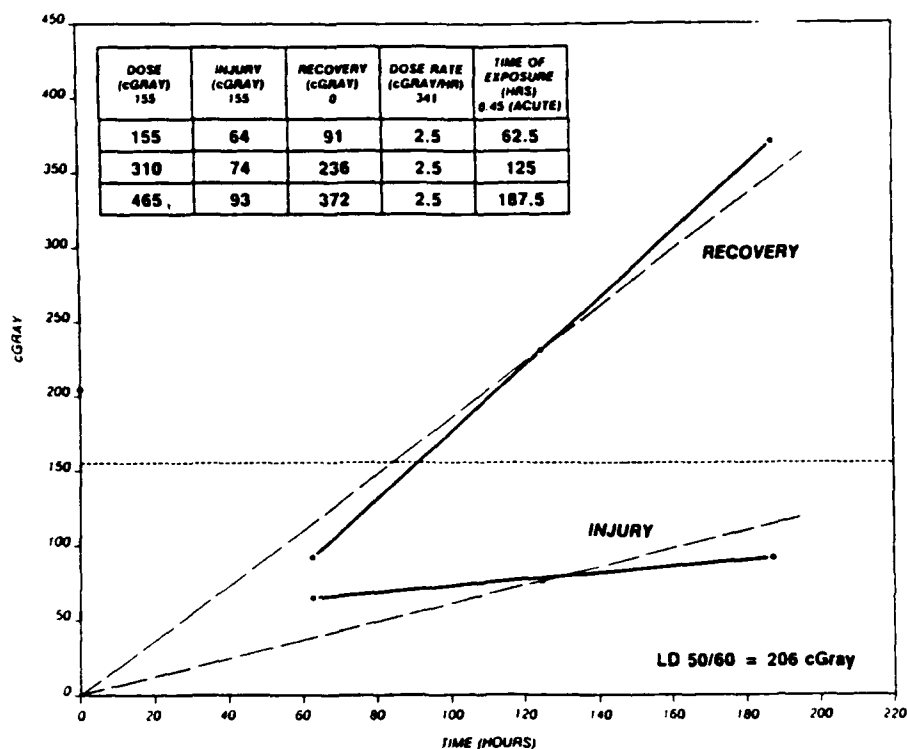


Figure 47. Swine--injury and recovery versus exposure time at fixed dose rate.

As indicated in Table 23, Still et al. [1969] gave animals 95 cGy at an acute dose rate of 311 cGy/h. Immediately after the completion of this conditioning (initial) dose, irradiation was continued at a reduced dose rate of 2.2 cGy/h until an LD₅₀ of 199 cGy was obtained; this value was not significantly different from the LD_{50/60} of 192 cGy observed when sheep received an acute dose rate at 275 cGy/h. However, 192 cGy did differ significantly from the LD_{50/60} of 302 cGy obtained with a protracted dose rate of 2.2 cGy/h [Ainsworth et al., 1968]. The bottom half of Table 6 shows similar results observed in studies by Jones and Krebs [1970].

Figure 48 shows postirradiation recovery of five large mammalian species. The dog, sheep, and swine show similar recovery patterns over the first 20 days postirradiation, but otherwise, these curves are quite dissimilar. It is difficult to extrapolate a recovery pattern for humans from these curves unless other response parameters measurable in humans exposed to ionizing radiation can be correlated

to them; reevaluation of postirradiation leukocyte responses in man might be helpful.

Sheep are the only large animals for which data are available to compare the radiation effects of various low dose rates with an acute one. Such studies were conducted at NRDL, and the results are depicted in Figs. 49 to 53. As may be seen from Table 24, the first five conditioning doses employed were similar. It appears that when sheep are exposed at below a dose rate of 1 cGy/h, no apparent injury remains at the end of irradiation. Above a dose rate of 1 cGy/h, injury can be determined at the end of the radiation exposure, which appears to increase with increasing dose rate. As the conditioning dose increases (186 cGy in Table 24), the remaining injury increases in direct proportion. When the conditioning dose is 101 cGy, injury accumulates at 0.63 cGy/cGy. However, when the total dose is increased to 186 cGy at the same dose rate, injury accumulates at only 0.5 cGy/cGy. Maximum over-recovery, given a similar size of conditioning dose, increases with dose rate and appears to be proportional to remaining injury, at least over the dose rate ranges indicated in Table 24. It appears that the severity of initial injury may be related to a humoral or hormonal release that stimulates increased cellular production in recovering bone marrow.

It has been established that recovery and repair are important factors that enable mammals to sustain increased radiation injuries with protracted exposures. Split dose experiments permit the measurement of recovery based on the increase in the radiation dose to satisfy a specific endpoint (e.g., 50 percent lethality). More complete measurements obtained from split-dose experiments could facilitate the development of relationships for dose protraction in animals and eventually extrapolations to humans. If physiological processes cause a deviation from a simple recovery process such as a return to hyper-radiosensitivity after a period of normal recovery (i.e., an undulating pattern), the underlying pathophysiology of the system which induces such changes must be considered. Cell cycling sensitivity to irradiation exposure, as demonstrated by Bedford et al. [1980], may also play a part, which should also be among the underly-

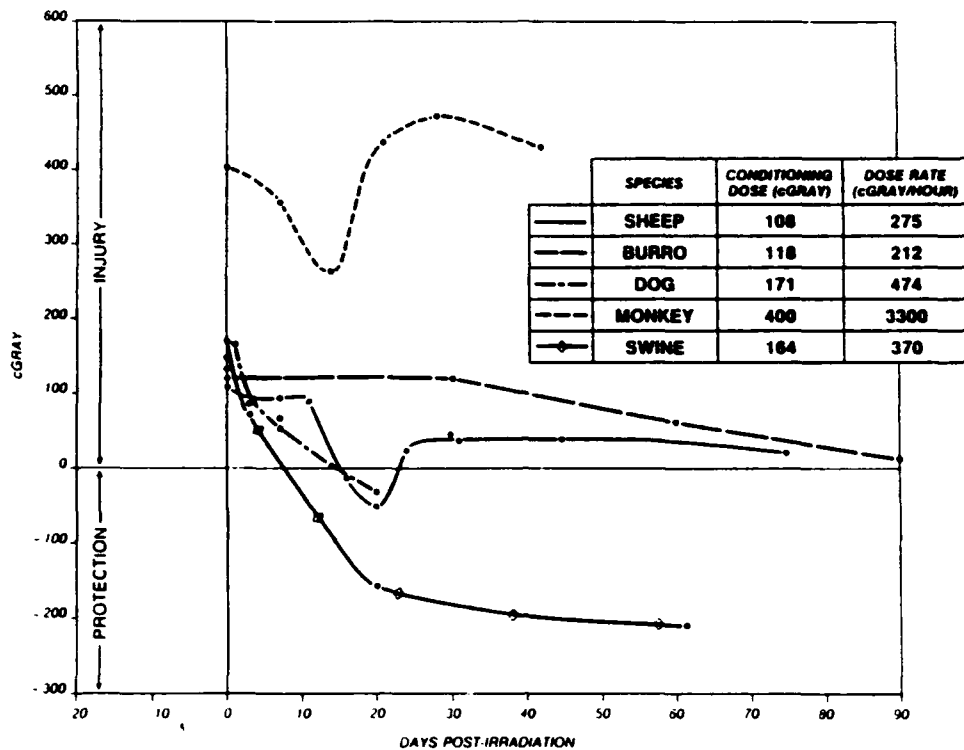


Figure 48. Species comparison for acute exposure.

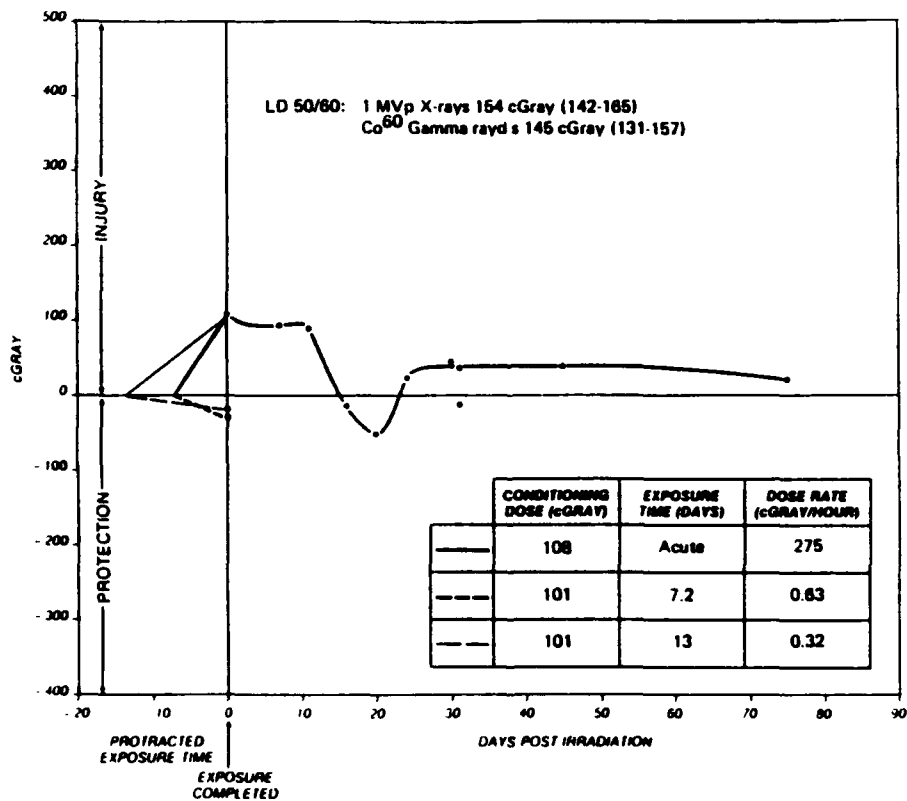


Figure 49. Sheep--acute and protracted dose (0.63 and 0.32 cGy/h).

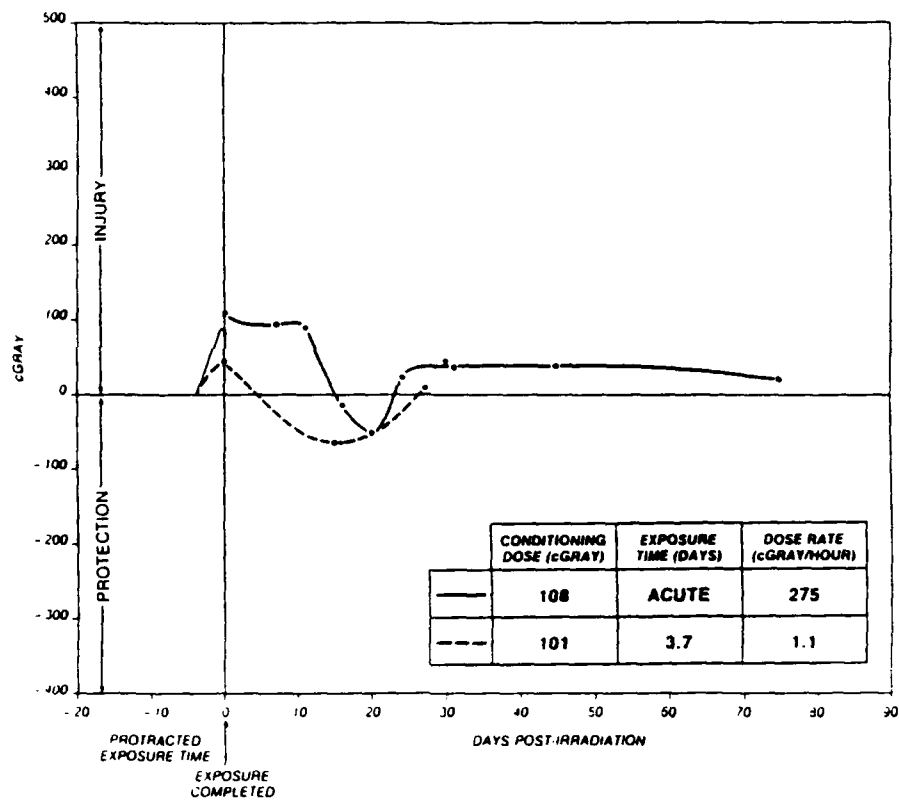


Figure 50. Sheep--acute and protracted dose over 3.7 days (1.1 cGy/h).

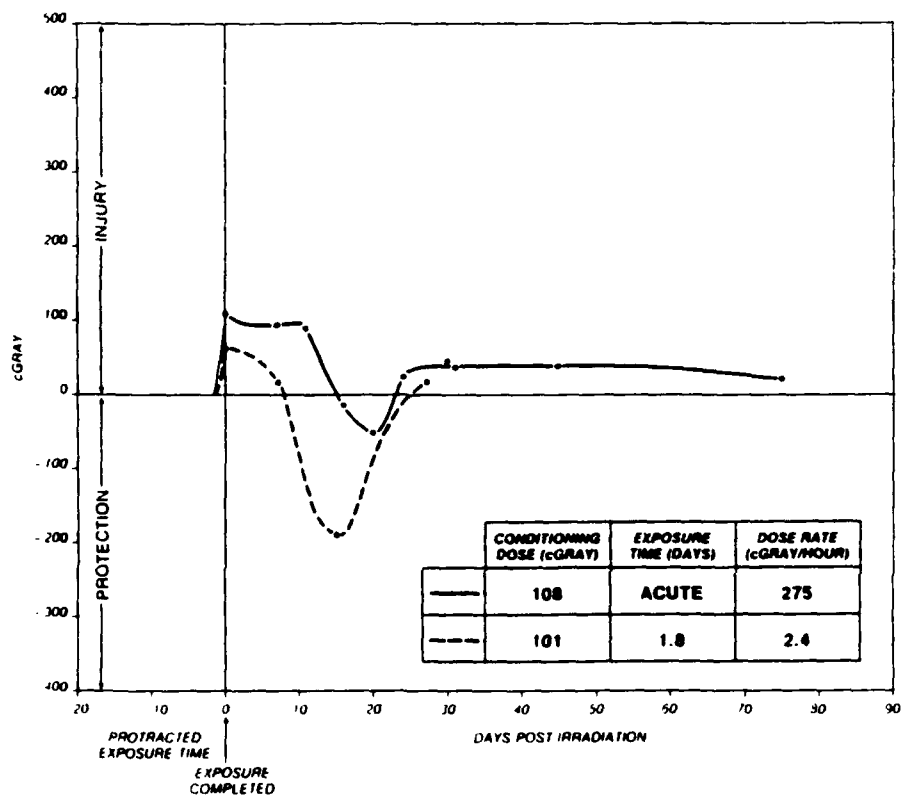


Figure 51. Sheep--acute and protracted dose over 1.8 days (2.4 cGy/h).

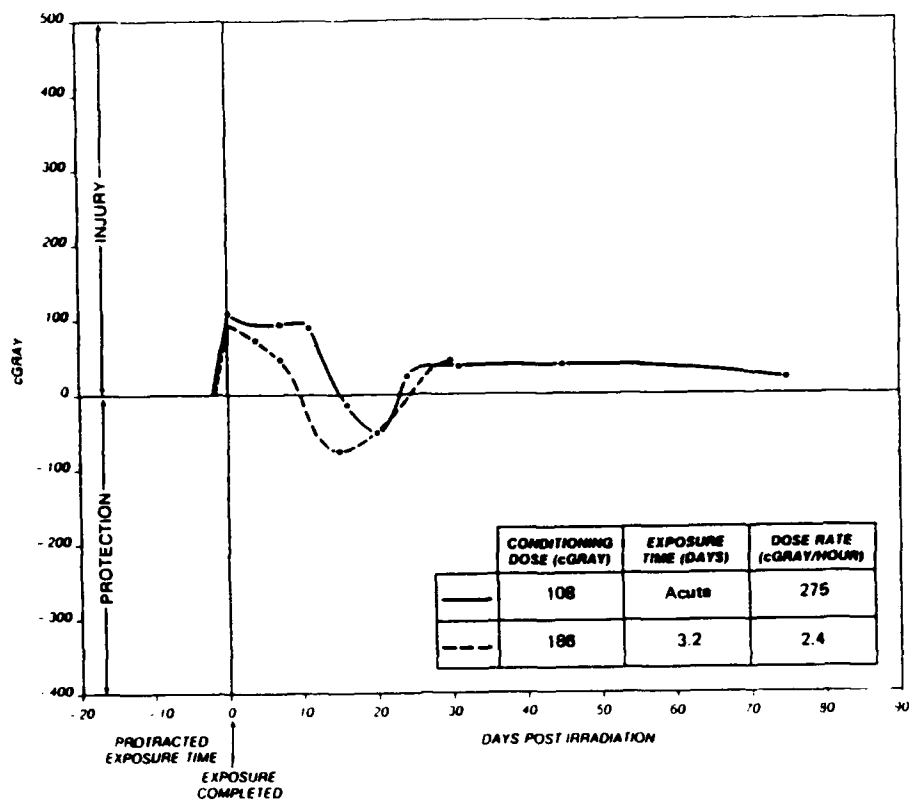


Figure 52. Sheep--acute and protracted dose over 3.2 days (2.4 cGy/h).

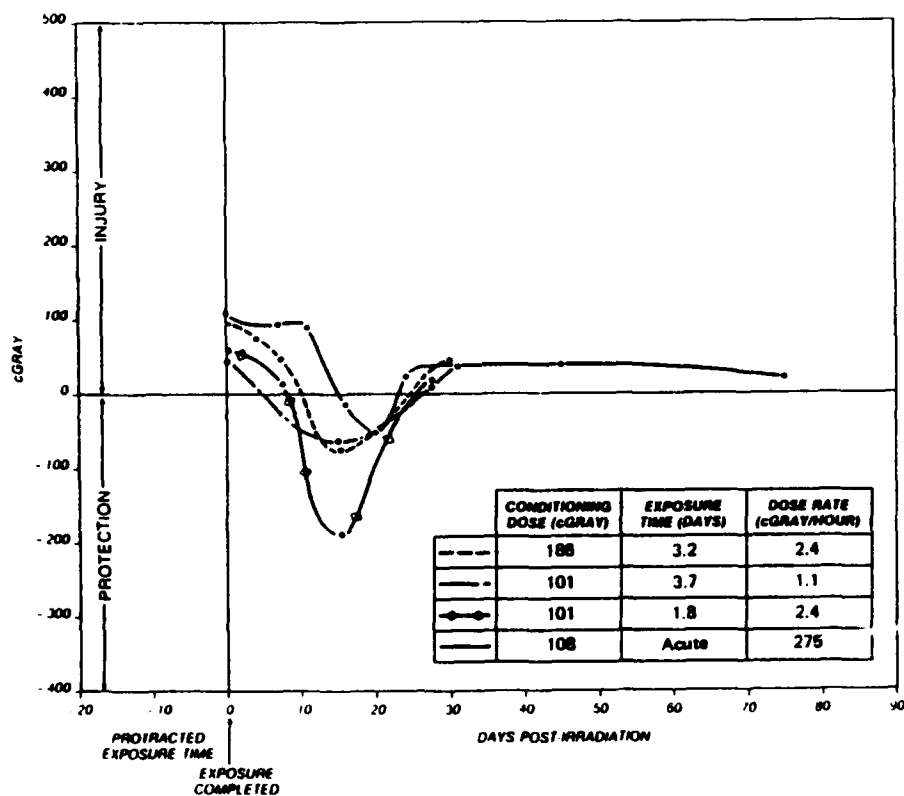


Figure 53. Sheep--acute and protracted dose comparisons.

Table 24. Remaining injury and maximum over-recovery in sheep subjected to radiation at different rates.

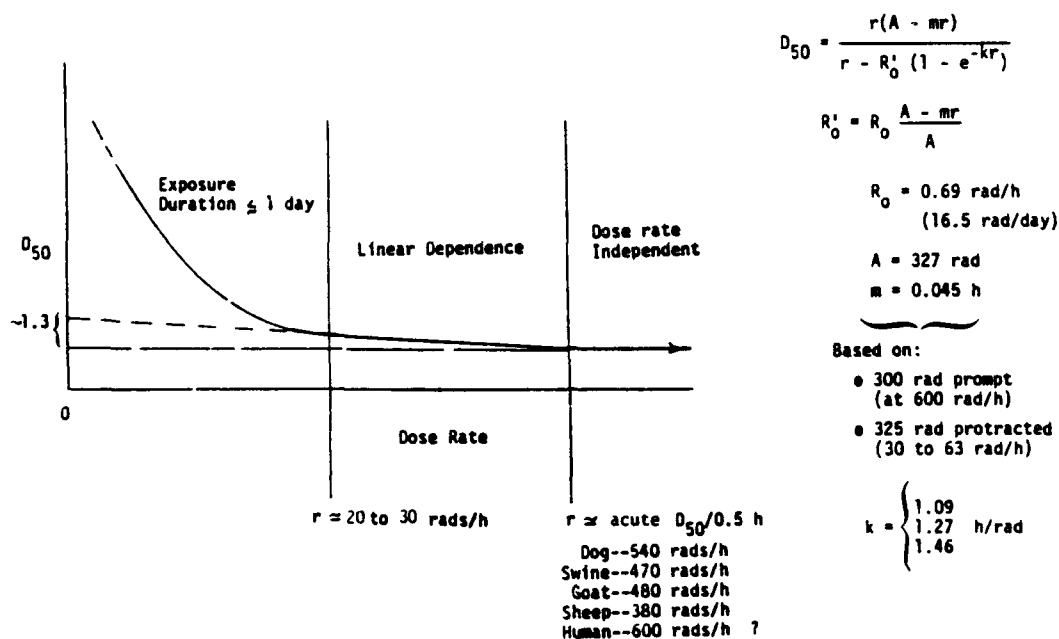
Conditioning Radiation Dose (cGy)	Dose Rate (cGy/h)	Exposure (h)	Time (days)	Remaining Injury (cGy)	Maximum Over-recovery (cGy)
108	275	0.4	--	108	-44
101	0.32	316	13	0	-19
101	0.60	168	7.2	0	-26
101	1.1	92	3.8	46	-64
101	2.4	42	1.8	64	-188
186	2.4	77.5	3.2	93	-75

ing casual factors considered.

2.5.1 Constant Dose Rate Models.

Accumulated injury models were reviewed by Anno and Baum [1986] in terms of LD₅₀ endpoint as a function of constant dose rate level such as depicted in Fig. 54. Figure 54 also summarizes some of the findings of Krebs and Jones [1975] from their review of animal data (sheep, dogs, swine, goat, and mice) and suggestions for modeling LD₅₀ response in animals, including extrapolation to humans. They developed a relationship LD₅₀ (D₅₀ in Fig. 54) as a function of dose rate r , which includes linear and exponential relationships, to model protracted radiation response. In their analysis of the animal data, Krebs and Jones found, in part, that

- lethal dose becomes dependent upon dose rate when the time required to deliver it is longer than about 30 min (otherwise, the LD₅₀-dose-rate relationship is flat where dose rates can be considered "acute"),



Source: Krebs and Jones [1975].

Figure 54. LD_{50} versus dose rate.

- the LD_{50} -dose-rate relationship is linear between about 20 to 30 rads/h and the acute dose rate level,
- between about 2.5 rads/h and 20 to 30 rads/h, there is a transition from a linear LD_{50} -dose-rate relationship to an exponential one,
- less than about 2.5 rads/h, the LD_{50} depends only on the average daily dose rate which can be averaged out over as much as two weeks.

Anno and Baum [1986] compared accumulated human injury models by plotting LD_{50} (rads) versus dose rate r (in rads per h). That comparison, shown in Fig. 55, required some algebraic adjustments to obtain the appropriate plotting forms that are given below along with the parameters.

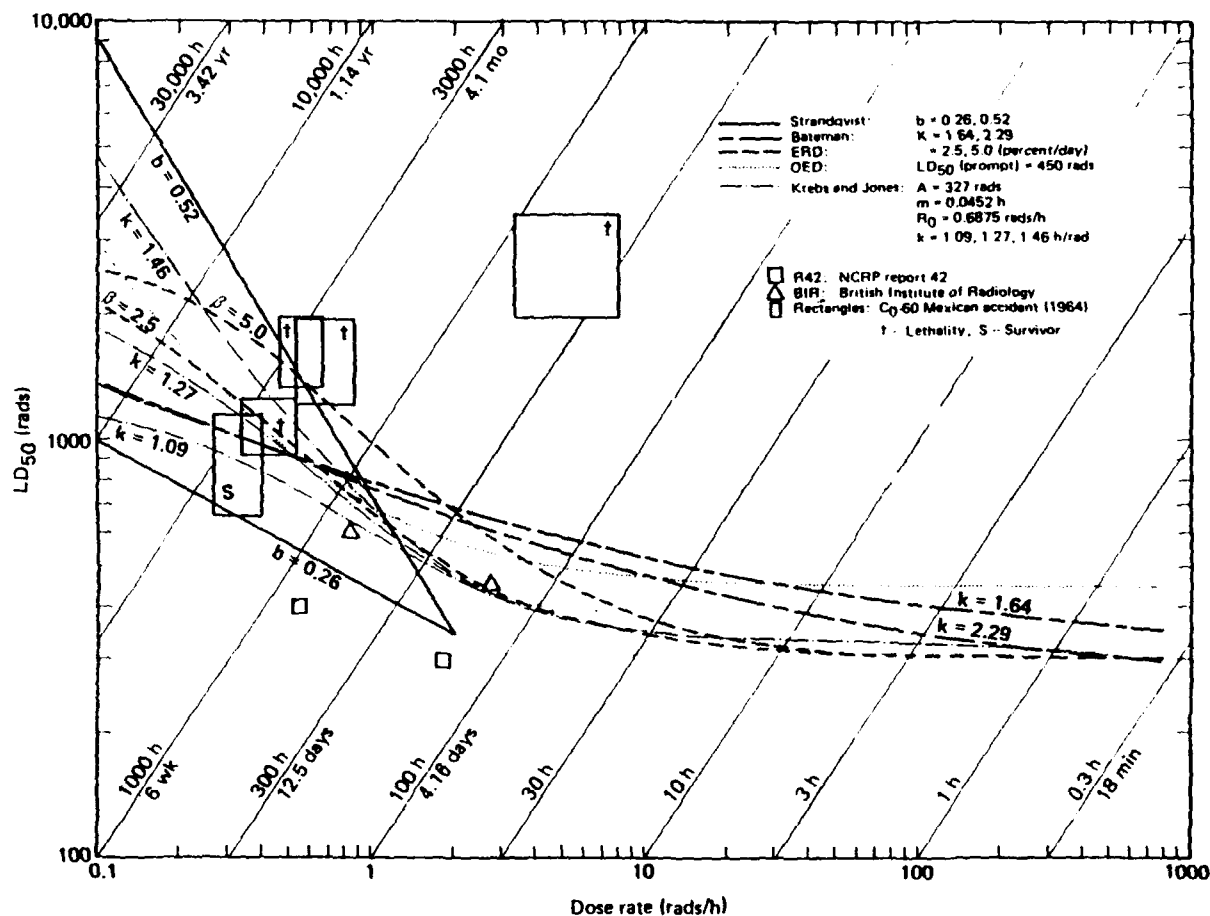


Figure 55. LD₅₀ dose rate models.

Strandqvist [1944].

$$D_{50} = D_0 [1/(1-b)] \cdot (168r)^{-[b/(1-b)]}$$

where $D_0 = 345$ rads (acute LD₅₀) and $b = 0.26, 0.52$.

Bateman [1968].

$$D_{50} = D_0 (1 + Kr^{-1/3})$$

where $D_0 = 300$ rads (fixed), $K = 1.64$ (rads/h)^{1/3} based on the 1964 Mexican accident [Martinez et al., 1964]; and $D_0 = 236$ rads, $K = 2.29$,

also based on the 1964 Mexican accident, but with the acute dose anchored at $D_0 = 300$ rads for $r = 600$ rads/h.

Equivalent Residual Dose [Blair, 1952; Davidson, 1957].

$$D_{50} = \frac{1}{f} \left\{ \text{ERD} - \frac{(1-f)}{\beta} \left[1 - \exp(-\beta D_{50}/r) \right] \right\} ,$$

where ERD (equivalent residual dose) = 300 rads, f (irreparable fraction) = 0.1, and the repair constant $\beta = 0.00104 \text{ h}^{-1}$ and 0.002083 h^{-1} ; (for $\beta = 2.5$ and 5.0 percent per day, respectively).

Operational Equivalent Dose, [Home Office Scientific Research and Development Branch, 1985].

$$D_{50} = \text{OED} + \frac{250}{r} ,$$

where OED (operational equivalent dose) = D_{50} (acute) = 450 rads.

Data from other sources are also individually plotted in Fig. 55. The two box-shaped "R42" values are based on the LD_{50} values given in the "Penalty Table" by the National Committee on Radiation Protection and Measurements [1974]. For one-week exposure, an LD_{50} of 300 rads (450 R) is given; that corresponds to an average dose rate of about 1.77 rads/h (2.68 R/h). For one-month exposure, an LD_{50} value of 400 rads (600 R) is given; that corresponds to an average dose rate of about 0.55 rads/h (0.82 R/h).

The two values marked "BIR" in Fig. 55 are based on information from the British Institute of Radiology (BIR) as quoted on p. 84 in the British Medical Association report of 1983.

The rectangles in Fig. 55 reflect dose and dose rate uncertainty and are based on the 1964 Mexican accident involving cobalt-60 γ -ray radiation exposure of five family members [Martinez et al., 1964] that resulted in four deaths (†) and one survivor (S). Accordingly, these are not LD_{50} data, but are shown for reference only.

Plots of the protracted radiation response models (Fig. 55) show a considerable variation in accumulated lethal exposure dose versus dose rate. However, with the exception of the Bateman model, those plotted suggest a marked increase in LD₅₀, commencing with dose rates less than about 3 to 10 rads/h; the even more rapid increase in LD₅₀ for dose rates from about 1 to 3 rads/h probably reflects cell proliferation. Anno and Baum [1986] provide a detailed discussion of the model plots.

A brief review of some suggested lethality-endpoint-based models of protracted radiation response illustrates the need for additional investigation. Lethality is only one of the endpoint responses of interest in casualty considerations; however, the models do predict various degrees of biological recovery. Any model selected should be better substantiated by more in-depth analysis of available data from animal studies and preferably human experience; for example, the Goiania, Brazil accident involving protracted exposure to cesium-137 γ -ray radiation from an abandoned teletherapy unit [International Atomic Energy Agency, 1988] could yield more clinical information. At present, data on arbitrary exposure periods and/or varying dose rates are scarce or limited in scope. Consequently, our comparisons of the protracted radiation exposure models are based on continuous and constant exposure rate levels. However, as Krebs and Jones [1975] imply, when average daily dose rates are less than about 2.6 rads/h (or about 62 rads/day), the exposure history for the 24-h period is largely irrelevant.

Our investigation of the kinds of models reviewed here indicates that they cannot be generally applied to other endpoints such as prodromal responses without possibly data-supported modifications--and then only for constant dose rate exposure. However, such models have been applied for prodromal symptomatology of protracted radiation involving fallout effects analysis [Knapp, 1965; and Schmidt, 1981]. Because the kind of biological recovery illustrated in this review may not adequately model other processes (such as a physiological clearing action and recovery), a different type of modeling approach is generally necessary to accommodate prodromal responses to protracted

radiation. For example, for dose rates in the therapy range of about 1 to 30 rads/min (60 to 1800 rads/h), there are indications that nausea and vomiting depend more on the total accumulated dose than on the dose rate [Baum et al., 1984]. Our assessment of the existing models of protracted radiation based on lethality as the endpoint reveals that additional study of available data is needed before proceeding to a systems analysis approach that is used in military operations and planning.

2.5.2 Operational Equivalent Dose as Injury Accumulation.

The residual injury accumulation based on the OED formula recommended for application in the UK [Home Office Scientific Research and Development Branch, 1985] is illustrated in Fig. 56. The OED formula is given by

$$\text{OED} = D - 150 - 10t \quad (\text{rads}) ,$$

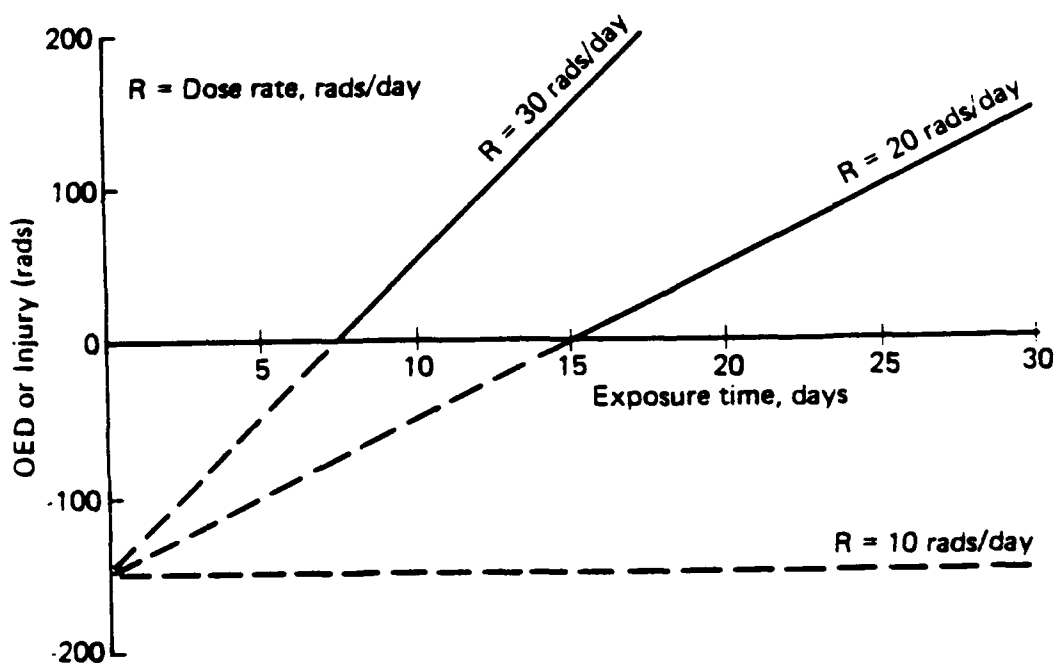


Figure 56. OED (injury, for constant daily exposure rate.

where D refers to the accumulated dose to the bone marrow, t is the exposure time in days, 150 (rads) is a rapid (Elkind) repair or recovery value that takes place within the first day following exposure, and 10 rads/day represents a daily recovery rate. Given a dose rate R, and letting $D = Rt$, the OED (or accumulated injury) can be expressed as

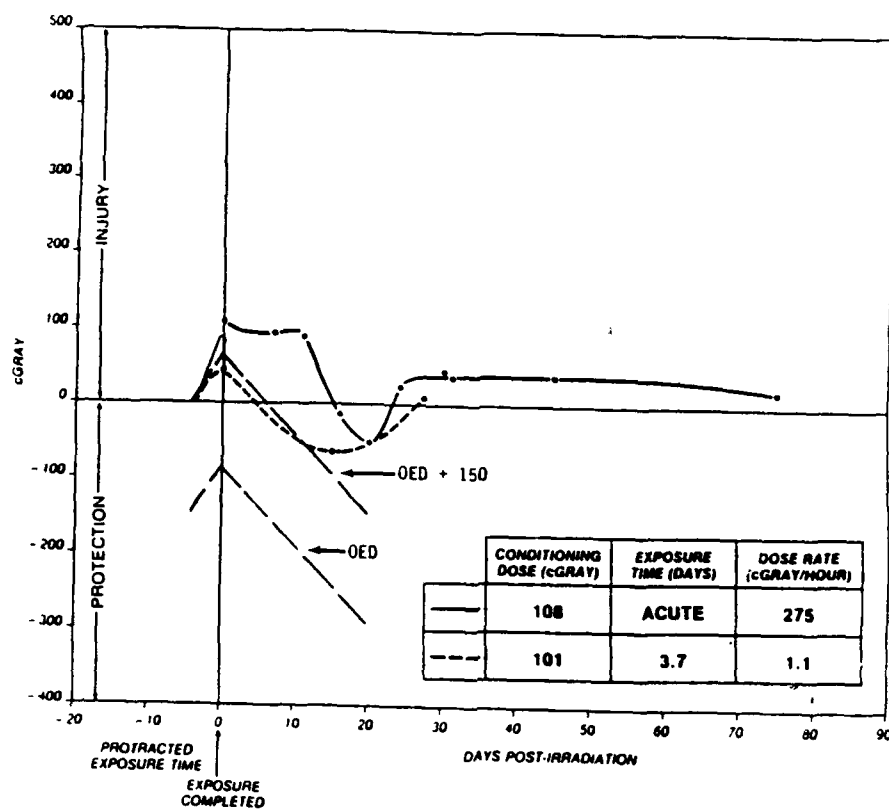
$$\text{OED} = (R - 10)t - 150 \quad (\text{rads}) .$$

Plots of the OED relationship above for dose rates, $R = 10, 20$, and 30 rads/day are shown in Fig. 56. Since negative values are ignored in applying the OED formula, the residual injury would remain at zero until it accumulates linearly after specific exposure times, depending on the dose rate, as shown.

The OED was also compared to data derived from experiments with sheep [Hanks et al., 1966]. Figure 57 illustrates the comparison for radiation exposure protracted over 3.7 days at the rate of 1.1 rads/h or 26.4 rads/day. The initial portion of the bottom curve (large dashes, marked OED) is a plot of the OED relationship given above over the period of exposure. For postirradiation times where $R = 0$, it is assumed that recovery continues at the rate of 10 rads/day.

It is clear from Fig. 57 that the OED considerably overestimates recovery from injury compared to the data drawn from experiments with sheep. The overestimate is primarily due to the 150 rads that purportedly accounts for "rapid recovery." When the 150 rads of repair recovery is ignored, given by the curve marked OED + 150, the agreement with the experimental data is vastly improved out to about 12 days postirradiation. This underscores the most significant problem with the OED formula, although the recovery rate of 10 rads/day appears to be within reason.

Our review and analysis of the literature provided us with a comprehensive assessment of radiobiological injury and recovery relevant to acute and protracted radiation exposure. In the section that follows, we discuss aspects of the review key to the development of modeling approaches for upper and lower gastrointestinal distress.



Source: Hanks, et al. [1966] for data on sheep.

Figure 57. Residual injury--comparison between formula and data derived from experiments with sheep.

SECTION 3

PROTRACTED DOSE MODELING CONSIDERATIONS

In this section, we discuss key considerations for developing models to assess the human response to protracted radiation. These modeling considerations are based on the objectives of this effort and the literature review described in Sec. 2. Figure 58 provides an overview of these considerations cast in the framework of the overall modeling process required for protracted dose response assessment.

The requirement that protracted dose response models be general enough to accommodate any arbitrary exposure history basically defines the core of the mathematical structure. Any one of a multitude of exposure histories can be defined that results in a unique symptomatology response profile as a function of dose and time, including incidence, severity, and duration. Moreover, tissue damage

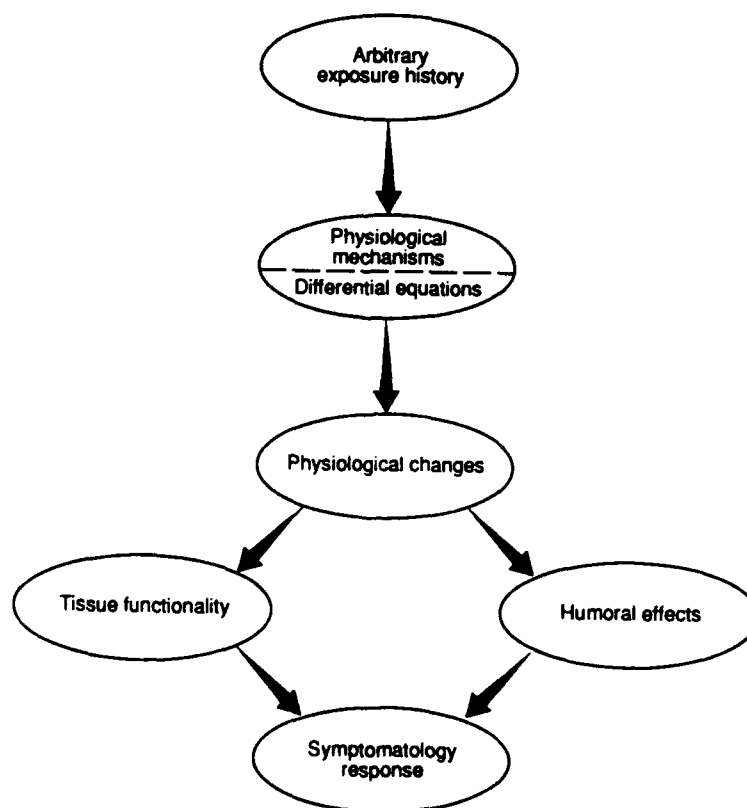


Figure 58. Protracted dose modeling considerations.

and recovery induced by radiation in a biological system is a transient phenomenon similar to that exhibited by an electromechanical system. Accordingly, the time response behavior is effectively modeled in terms of time rate processes comprising differential equations structured to simulate the appropriate measures of radiobiological damage and physiological recovery mechanisms, or biologically reasonable analogues thereof.

Physiological changes can be determined from solutions to the differential equations. The changes can be linked to a symptomatological response that depends upon the target tissue modeled and corresponding physiological measure. For example, for gut injury, the physiological measure may be depletion of the cell population level of the intestinal epithelia. A diminution in cell population level may result in impaired tissue function that could cause diarrhea, fluid loss, and ultimately death for complete denudation conditions that are associated with high exposure levels. Another example involves the irradiation involving the midepigastic region of the body which is believed to be where the target tissue for vomiting is predominately located. Here the physiological measure would be a toxic or humoral agent capable of producing an effect that triggers an emetic response when present in sufficient quantity.

3.1 PHYSIOLOGICAL CHANGES AND MODELING.

The modeling objective of this effort is to develop mathematical relationships between protracted radiation exposure and sign/symptom endpoints. In order to do this effectively, the modeling approach must have a sound physiological basis and, thus, be mechanistic in nature. All things being equal, a mechanistic biological response model is not only always preferable to an empirical one, but becomes essential when the available data are quite sparse and uncertain over the region of importance, as is the situation here for protracted dose experience. A model based on a mathematical description of the underlying physiology of response can provide accurate interpolation between widely distributed data points and can be extrapolated with confidence in limited cases. It is important, then, to understand the physiological changes induced by ionizing radiation.

The effects of ionizing radiation follow from a cascade of physical, chemical, and biological processes beginning with the transfer of energy to electrons and atomic nuclei along the path of the incident particle and its secondaries. The deposited ionization energy produces a complex array of molecular disruptions in a biological system ranging in size from free radicals to directly produced lesions on biologically active macromolecules including the genome. Observed physiological changes result from the chemical stabilization and subsequent biochemical activity of these molecular disruptions.

Two general categories of radiation-induced biochemical abnormalities of particular interest to the Human Response Program are humoral changes and chromosome damage. Humoral changes, such as the level of histamines in the blood, are caused by abnormal secretory activity of damaged tissues and by the decay products of killed cells. The resulting abnormal levels of toxins and neurologically active substances induce signs and symptoms of radiation sickness. The humoral changes are gradually brought under control by normal metabolic processes if the organism survives. Upper gastrointestinal distress and some aspects of fatigability and weakness are believed to follow this pattern. Response modeling of such symptoms is based on the kinetics of toxins in the body in the same way that the effects of drugs are modeled in pharmacokinetics. We refer to such models that address radiation-induced symptoms based on humoral changes as *toxicokinetic* models.

The other category, chromosome damage, such as single- or double-strand breaks and DNA-protein crosslinks, may be caused either directly by ionization damage to the DNA strands or indirectly by the action of radiation-induced free radicals such as OH^{\bullet} . Chromosome damage may be repaired by cellular processes or, if irreparable, may result in the death of the cell within a time comparable to the cell cycle time. A model of cell survival can be based on the dynamics of the production and repair of lesions on chromosomal DNA. Cell survival, in turn, affects the health of bodily tissues.

Using the link between chromosome damage and cell survival, a second type of symptomatology model is based on tissue functionality. Certain signs and symptoms follow directly from the inability of a specific bodily tissue to function properly. Two prime examples of this are (a) damage to the intestinal mucosa resulting in lower gastrointestinal distress and (b) damage to the hematopoietic system resulting in infection and bleeding. The health of a tissue is directly attributable to the health of the cells comprising a tissue and their ability to proliferate in a controlled fashion to maintain the cellular population of the tissue. Since cell survival affects the health and functionality of bodily tissue, some of the symptomatology of radiation sickness is describable through the dynamics of chromosome damage. We refer to such symptomatology models based on the dynamics of chromosome lesions and cellular proliferation as *tissue functionality*, or *target tissue* models. These models are based on target-cell depletion as the determinant of tissue response and have been put forth according to the "target-cell hypothesis" discussed in the section which follows.

3.2 TARGET CELL HYPOTHESIS.

A key consideration for a protracted dose modeling approach involving tissue and organ response is the evidence for target-cell depletion as the determinant of tissue response. Thames and Hendry [1987] provide a review of this evidence and indicate the formulation of the target-cell hypothesis as follows:

"The responses of tissues to irradiation are quantitatively related to dosage. The increase in response will reflect the increase in the number of cells affected, primarily regarding their replicative ability. The important cells in the tissue regarding this endpoint may be a small proportion of the cells, as in type H tissues, or the majority of cells, as in type-F tissues. In both cases those cells capable of replication and regeneration of the tissue are the *target cells*. The effects on tissue response of alterations in radiation quality or distribution of dose in time can be described in terms of alterations in survival probability of the target cells."

Evidence that observed tissue effects can be described on a cellular basis is of the necessary, but not sufficient type since all the ancillary influences and intermediate processes are not well known. Therefore, a detailed, comprehensive correlation involving all the mechanisms from cellular damage to tissue dysfunction is not yet possible. However, the evidence that does exist falls into the following three categories:

- D_0 values derived from the functional response of tissues (e.g., organism lethality) are numerically equivalent to those measured for their renewing populations of cells (e.g., cell survival).
- Clonogen survival remains essentially fixed even though the tissue isoeffect dose varies when changes are made in exposure time (i.e., dose rate).
- The limiting slopes of isoeffect plots of tissue response to fractionated exposure are consistent with those values deduced from target-cell models.

In their review of target-cell hypothesis, Thames and Hendry [1987] provide convincing evidence in the first two categories based on a number of types of tissues from various investigations; these include the intestine, epidermis, bone marrow, and others. A mathematical relationship can be derived that quantitatively links the incidence of tissue failure to target-cell survival. Evidence for target-cell hypothesis is then provided applying the incidence relationship derived from target-cell survival to tissue failure data, such as lethality.

Derivation of the incidence relationship for a tissue response function is illustrated based on assuming random processes to specify target-cell survival and, in turn, aggregated to the tissue response level employing the tissue-rescuing unit (TRU) concept. In H-tissues, the TRU is assumed to be comprised of a certain number of clonogens capable of producing a life-saving (or tissue-function-maintaining) number of mature cells; in H-tissues the precursor cells that comprise

the TRU are a minority population; in F-tissues, the TRU precursor cells are considered to be functional and, therefore, constitute a majority population. A relationship for the incidence or probability of tissue failure can be derived given by:

$$p = \exp \left[-K \exp(-D/D_0) \right] ,$$

where,

K = an initial number of TRUs

D = dose

D₀ = refers to inactivation of TRUs (not cells)

The above relationship is known as a Poisson model that gives a sigmoid dose response curve. The initial number of TRUs is proportional to the number of clonogenic rescuing cells, k, i.e., K = ck, where c is a constant. The Poisson model can be linearized by a double logarithmic transformation, given by the form below,

$$-\ln(-\ln p) = D/D_0 - \ln ckN$$

where N is the extrapolation number utilized in cell survival modeling. This relationship provides a means of testing the target-cell hypothesis by determining the extent to which the D₀ values are equivalent measured independently from target-cell response data (i.e., cell survival) and tissue failure incidence data due to cell depletion.

The hypothesis has been tested in three normal mammalian tissues (H-tissues) including bone marrow, intestinal, and epidermis. In general, the finding is that the steepness of the incidence curve for tissue failure closely corresponds to the D₀ deduced from clonogen assays for H-tissues. As an example, Fig. 59 for mice irradiation shows that the changes in slopes of the cell-survival and dose-incidence curves are related. Also, changes in the LD_{50/5} are seen to correspond closely to the changes in survival as measured by the microcolony assay of crypt cell survival at the 0.01 fractional

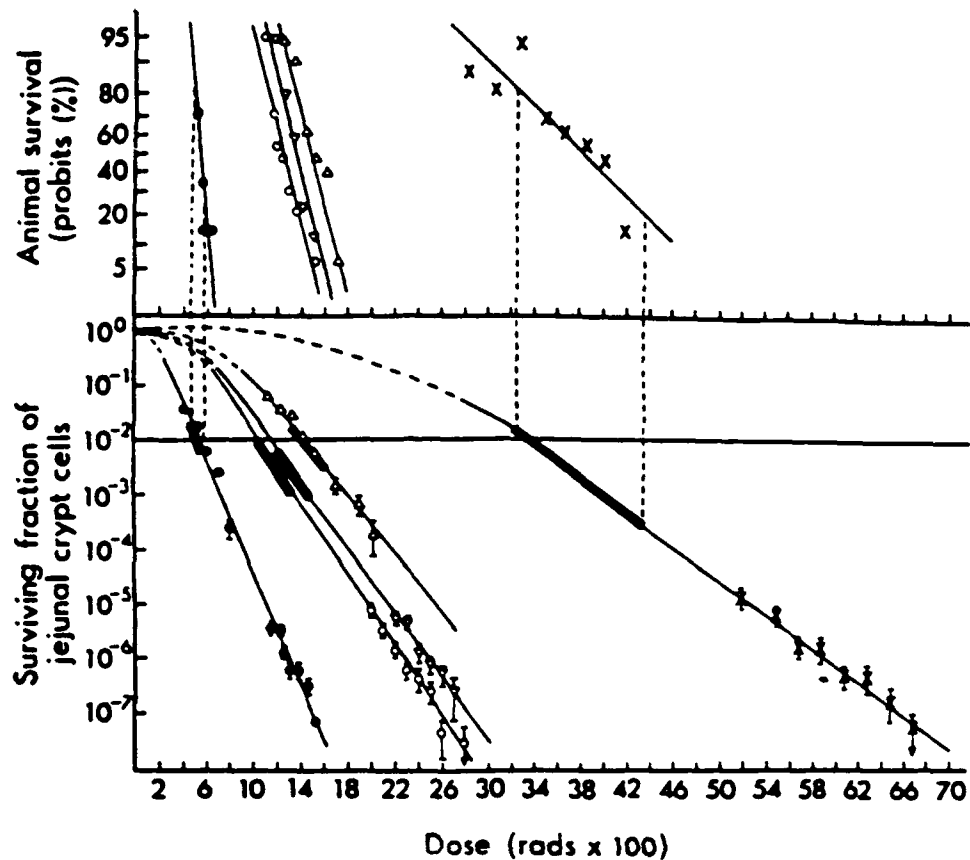


Figure 59. Isosurvival relationship for mice and jejunal crypt cells (Thames and Hendry, 1987).*

*Survival of mice five days after irradiation (upper section of diagram) matched with survival curves for jejunal crypt cells (lower section). The curves show, from left to right, the results of mice breathing oxygen while irradiated with: neutrons (closed circles); electrons, 60 Gy/min (open circles); electrons, 550 cGy/min (inverted triangles); X-rays, 7 MV, 100 cGy/min (triangles). At the right, the curves with the symbol x relate to mice breathing nitrogen while irradiated with electrons, 150 Gy/min. The thickened sections of the curves depicting crypt-cell survival correspond with dose ranges within which animal deaths range from 20 percent to 80 percent as shown by two pairs of vertical dotted lines. For all conditions, animal deaths started to occur at the doses for which cell survival was near 10^{-2} . A horizontal line has been drawn across the diagram at that level. Vertical bars in the lower section represent ± 1 S.E.M.

level. This confirms the close relationship between death from the acute intestinal syndrome and epithelial damage in the small intestine.

The third category of evidence for the target-cell hypothesis presented by Thames and Hendry [1987] is based on the limiting slope of tissue isoeffect curves for fractionated irradiation developed from cell survival considerations. For fractionated exposures, cell survival S based on the linear quadratic (LQ) model is,

$$S(nx) = e^{-n(\alpha x + \beta x^2)}$$

where, n = the number of dose fractions

x = dose per fraction

α, β = LQ parameters,

and the total dose, $D = nx$. A specific isoeffect response endpoint for body tissue can be designated that corresponds to a given isosurvival level of target-cells, S ; for convenience, S may be expressed as $E = -\ln S$. Applying this expression to the LQ cell survival model above, an isoeffect relationship can be obtained, assuming complete intercellular repair between fractions, given by

$$\frac{1}{D} = \alpha/E + (\beta/E)x$$

This linear relationship, known as the "reciprocal-dose," is convenient for the analysis of experimental data involving fractionated irradiation and has been extensively employed in radiobiology for various isoeffect endpoints including lethality of organisms, e.g., typically E corresponds to the ED_{50} or LD_{50} .

This isoeffect relationship can also be represented in the form,

$$D = [\alpha/E + (\beta/E)(D/n)]^{-1}$$

A plot of D vs n suggests limiting slope values for both a large and small number of dose fractions, n . Thames et al. (1982) derived the equation given below for the slope of the isoeffect relationship above to assess the limiting slope values assuming that target-cell response is governed by the LQ model.

$$d\ln D/d\ln n = x/(\alpha/\beta + 2x) \quad .$$

This slope equation corresponds to the exponent of the number-of-fractions given by the "Ellis NSD equation" (Ellis, 1969). However, in the Ellis NSD equation, the exponent (or slope) is fixed at a value to 0.24; whereas in the relationship above, the slope varies according to the size of the dose fraction, x . That is, for smaller dose fractions, x , the slope of the isoeffect curve tends toward zero when proliferation is not a compounding factor; this corresponds to an increasing number of dose fractions n (i.e., $x = D/n$). On the other hand, the relationship also shows that for larger dose fractions (a smaller number of dose fractions), the slope of the isoeffect curve tends toward a limit of 0.5.

The experimental evidence is consistent with the limiting slope values of tissue response to fractioned exposures based on predictions derived from target-cell survival considerations. For an increasing number-of-fractions, there is conclusive experimental evidence that the slope does approach zero. For a decreasing number of fractions, the exponents generally range between 0.4 to 0.5 for late responding tissues, such as the cervical cord, kidney, lung, and bladder, and between 0.2 to 0.3 for early responding ones, such as the jejunum, skin, and lip mucosa. These results provide additional support for the target-cell hypothesis which has encouraged our protracted dose response modeling approach to focus on physiological response mechanisms that are activated by target tissue irradiation.

3.3 RESIDUAL INJURY OR EFFECTIVE RESIDUAL DOSE.

The concept of residual injury in biological systems, discussed in Sec. 2, has been applied extensively in radiobiology to assess radiation damage and recovery. For example, split dose techniques have been employed in animal studies to reveal the extent of damage or injury that remains as a function of time following some arbitrary exposure history. The simplest assessment involves an initial prompt dose D_1 (the conditioning dose) given to a group of animals followed after various recovery periods by another prompt dose D_2 , (the test dose). The size of the test dose is adjusted to produce a certain endpoint, say 50-percent lethality. The additional test dose D_2 required to produce the endpoint is used to calculate the residual injury at the end of the various recovery periods in terms of "prompt dose units," i.e.,

$$\text{Residual Injury} = \text{LD}_{50/30} \text{ (single prompt dose)} - D_2$$

Although, in the example above, D_1 is a single prompt dose, it may very well represent a dose protracted over some period of time or even a dose history consisting of some arbitrary series of doses distributed over the time period.

Residual injury in this context is synonymous with residual dose, being measured in terms of the dose that would produce the net amount of injury that remains unrepaired at the time the assessment is made. Accordingly, residual injury is frequently referred to as the effective residual dose (ERD).

There have been attempts to develop fairly simple models to calculate the ERD associated with lethality, primarily based on the LD_{50} endpoint. Some of these were reviewed in Sec. 2, namely those of Blair [1952], Davidson [1957], and more recently, Broyles and Shapiro [1985]. For protracted radiation exposure, these models apply a single time-dependent recovery function to each increment of dose to continually offset (or discount) the damage incurred by radiation. This implicitly assumes that: (1) all recovery processes, including intracellular repair and cell proliferation, are lumped into a single

time-dependent recovery function, and (2) that the recovery process is independent of the magnitude or duration of the radiation exposure. Also, the empirical determination of recovery function parameters have been restricted to either acute or constant dose rate exposures due to the unavailability of more varied protracted exposure data. This kind of modeling approach predicts the ERD based on a single dynamic step that does not explicitly account for the time delay between the point of damage occurrence and the observed sign/symptom response exhibited by biological systems. Because of these recovery function limitations, ERD models based upon them are only approximations.

Broyles and Shapiro [1985] formulated an ERD model for protracted exposure utilizing the Bateman [1968] recovery function based on the reciprocal cube root of dose rate. This approach prevented the determination of a damage recovery function that was an explicit function of time. However, our review of the LD₅₀ animal data in Sec. 2 on lethality from bone marrow damage has permitted us to develop a simpler empirical relationship that fits the single exposure, constant dose rate data well, permitting the derivation of a damage recovery function that is an explicit function of time. In a subsection below (ERD Modeling with A Recovery Function), we describe the development of this limited ERD model and determine how well it might be applied to exposures involving split-dose histories comprised of different constant dose rate levels.

3.4 EQUIVALENT PROMPT DOSE.

Another noteworthy concept frequently used to express the biological recovery associated with protracted radiation exposure is the equivalent prompt dose (EPD). For a specified protracted dose, the EPD is the prompt dose that produces the same biological endpoint. Because of the repair and recovery that can occur during a protracted exposure, the EPD is nearly always smaller than the accumulated protracted dose. Stated in another way, a given total dose is normally less effective for producing a given endpoint if the dose is fractionated or protracted. In certain unusual cases, the EPD can be larger than the accumulated protracted dose. For example, because the

radiation sensitivity of cells varies during the cell cycle, the tissue damaging potential of a given dose of radiation can be optimized by proper protraction of the dose over the cell cycle.

The EPD is useful for gauging a protracted exposure in terms of a prompt exposure. For example, if certain effects of prompt exposure exist in tabulated form, then an algorithm to compute the EPD for a protracted dose provides a way to use that table for protracted doses. The EPD depends on the endpoint in question. Two different endpoints, say upper gastrointestinal distress and lower gastrointestinal distress, will usually give two different EPDs for the same protracted dose. The difference arises because of the different repair and recovery processes for each endpoint.

3.5 COMPARISON OF EFFECTIVE RESIDUAL DOSE AND EQUIVALENT PROMPT DOSE.

The effective residual dose and the equivalent prompt dose are conceptually related but have important differences. They both arise from the need to quantify the biological repair and recovery that take place during and after radiation exposure. The EPD has been used in a broader context than the ERD regarding biological endpoints. Traditionally, the ERD has been applied to hematopoietic tissue injury leading to lethality as the endpoint, whereas EPD has usually been applied to other defined endpoints such as nausea or vomiting. A second difference is that the ERD depends inherently on postexposure time while the EPD does not. When a protracted exposure is over, the ERD decreases with time as repair and recovery take their course. On the other hand, the EPD, as usually defined, takes a fixed value for a given protracted dose. For example, if the endpoint is a certain incidence of prodromal vomiting, then the EPD for a protracted exposure has a well-defined value that does not change with postexposure time.

Each measure has a use for which it is best suited. As discussed above, the EPD is useful for relating the effects of a protracted dose to existing tables or other forms of data on the effects of prompt exposure. The ERD is useful for specifying residual effects from a previous dose. For example, the Army presently uses a quantity called

the Radiation Exposure Status (RES) number to summarize the condition of units regarding radiation dose received. The RES number is based on the total dose received treated as a single prompt dose.

Presently, Army doctrine provides no means to account for the sparing effects of dose protraction or the downgrading the RES number with the passage of time. Our protracted dose modeling will provide the basis for implementing the EPD and ERD concepts into Army doctrine. The EPD will account for the sparing effect of dose protraction in setting the RES number, and the ERD can be applied to downgrade the RES number as repair and recovery occur.

3.6 ERD MODELING WITH A RECOVERY FUNCTION.

Based on the LD₅₀ endpoint, we have developed a residual injury model using animal data from continuous exposure at a constant dose rate. The model involves the determination of a recovery function utilizing a relationship of LD₅₀ dose as a function of constant dose rate of the form $LD_{50} = D_0(1 + R/r)$, which is discussed above in Sec. 2.

We define residual injury, or ERD, after exposure time t as

$$D_R(t) = \int_0^t r(\tau)f(t - \tau) d\tau ,$$

where $r(\tau)$ is the dose rate and $f(t - \tau)$ is a recovery function that is determined from the LD₅₀ for constant dose rate exposure. The applicability of $f(t - \tau)$ to protracted exposure histories other than a constant applied dose rate is determined below.

Assuming a constant dose rate and fixing the residual injury to be $D_0 = D_R(t)$, where D_0 is the median lethal dose for an acute dose rate level, we have

$$D_0 = r \int_0^t f(t - \tau) d\tau .$$

Dividing by r and differentiating,

$$\frac{d}{dr} \left(\frac{D_o}{r} \right) = \frac{d}{dr} \int_0^{t(r)} f(t - \tau) d\tau .$$

The observation point t is a function of r , which is determined from the assumed relationship of median lethal dose as a function of dose rate, $D_{50}(r) = a/r + D_o$ (used in fitting the animal data discussed previously above); i.e.,

$$t(r) = D_{50}(r)/r = a/r^2 + D_o/r .$$

Completing the differentiation above,

$$\begin{aligned} -\frac{D_o}{r^2} &= f(a/r^2 + D_o) \frac{d}{dr} (a/r^2 + D_o/r) \\ &= f(a/r^2 + D_o) (-2a/r^3 - D_o/r^2) . \end{aligned}$$

Rearranging terms and solving for f , the recovery function can be expressed in the form,

$$f(t) = \frac{r(t)}{r(t) + (2a/D_o)} .$$

Then in order to express f as a pure function of t , we solve for $r(t)$, again utilizing the relationship, $D_{50}(r) = a/r + D_o$; i.e.,

$$\begin{aligned} D_{50} &= a/(D_{50}/t) + D_o \\ &= at/D_{50} + D_o . \end{aligned}$$

Multiplying by D_{50} and rearranging, we have the quadratic form,

$$D_{50}^2 - D_o D_{50} - at = 0 ,$$

which has the solution,

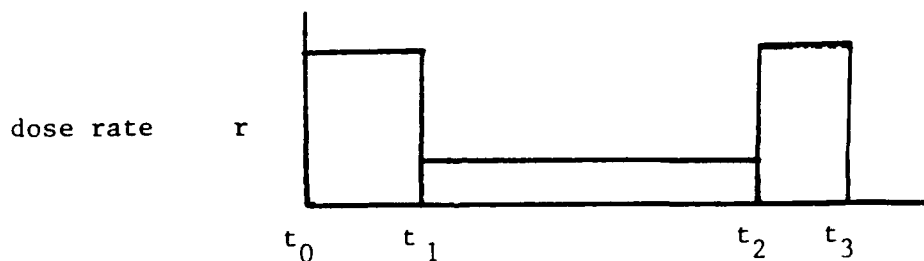
$$D_{50}(t) = \frac{D_o + \sqrt{D_o^2 + 4at}}{2} .$$

Dividing by t provides the relationship of $r(t)$ for the recovery function, $f(t)$ above; then after rearranging terms, the recovery function can be expressed as a pure function of t given as,

$$f(t) = \frac{1 + \sqrt{1 + kt}}{1 + \sqrt{1 + kt} + kt} , \quad f(t) = \begin{matrix} 1, & t \rightarrow 0 \\ 0, & t \rightarrow \infty \end{matrix}$$

where $k = 4a/D_o^2$.

The recovery function $f(t)$ is then derived based on a constant dose rate relationship for LD_{50} of the form which fits a variety of animal data shown in Sec. 2 of this report. We investigated its applicability to split dose studies as depicted in the sketch below:



The residual dose $D_R(t_N)$ was calculated utilizing the following relationship to compare with experimental observations:

$$D_R(t_N) = \int_0^t r(\tau) f(t - \tau) d\tau$$

$$= \sum_{n=1}^N r_n \int_{t_{n-1}}^{t_n} f(t_N - \tau) d\tau .$$

Calculations of residual injury were performed to match the seven split dose cases from sheep and swine irradiation studies listed in Table 25. Values used for the constants, a , D_0 , and k were estimated from the relationship $D_{50} = a/r + D_0$ fit to animal experimental data developed previously above. The values ranged as follows:

Table 25. Split dose irradiation studies.

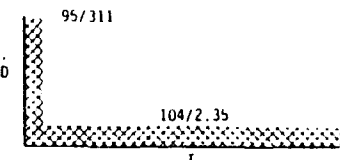
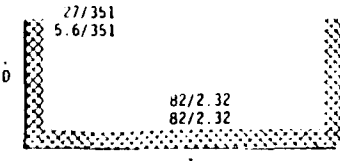
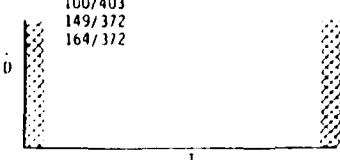
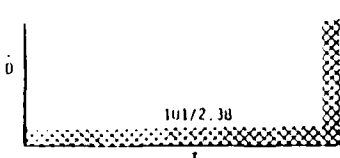
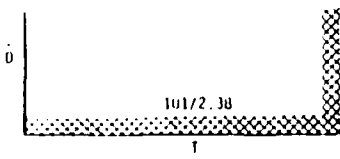
Case	Experimental (Source)	Period									Total Dose (rads)
		1			2			3			
		Duration (h)	Dose Rate (rads/h)	Dose (rads)	Duration (h)	Dose Rate (rads/h)	Dose (rads)	Duration (h)	Dose Rate (rads/h)	Dose (rads)	
1	Sheep Still et al. [1969]	0.304	311.1	94.55	44.55	2.348	104.3				199 ^d (192)
2	Sheep Jones and Krebs [1970]	0.078	351.1	27.45	35.76	2.318	81.74	0.158	351.1	55.51	165 (157)
3	Sheep Jones and Krebs [1970]	0.0158	351.1	5.55	35.26	2.318	81.74	0.234	351.1	82.29	170 (160)
4	Sheep Page et al. [1971]	0.25	402.6	100.7	168	0	0	0.13	402.6	50.3	151 (145)
5	Sheep Hanks et al. [1966]	42.3	2.38	100.7	0.22	366	80.52				181 (145)
6	Swine Nachtway, Ainsworth, and Leong [1967]	0.4	372	149	72	0	0	0.47	372	175	324 (247)
7	Swine Hanks et al. [1966]	0.44	372	164	168	0	0	0.51	372	190	354 (247)

^a Parenthetical values are acute LD₅₀.

	$a(\text{rad}^2 \text{ h}^{-1})$	$D_o(\text{rad})$	$1/k(\text{h})$
Sheep	234-274	145-192	23-38
Swine	4636-4410	235-247	3.3-3.4

We noted, however, that calculated results are not especially sensitive to these ranges. Table 26 compares results from the residual injury calculations with those from the experiments. The diagrams on the left portray the split-dose irradiation profiles. The numbers give dose/dose rate levels; for example, in the upper left of the diagram, 95/311 means a dose of 95 rads given at a rate of 311 rad/h (overall irradiation period 44-47 h). Comparisons were made of the residual accumulated injury relative to the acute LD₅₀, consistent with the residual injury model previously derived. The last column in Table 26 provides the comparisons. For the bulk of the dose delivered toward the end of the period, cases 3 and 5 show the best

Table 26. Protracted dose--experimental/model comparison.

	CASE	SPECIES	TIME (HR)	RESIDUAL INJURY			
				EXP'T	MODEL	DIFFERENCE	PERCENT
	1	SHEEP	44.7	192	149	43	22 LOW
	2	SHEEP	35.5	157	138	19	12 LOW
	3	SHEEP	35.5	160	150	10	6.3 LOW
	4	SHEEP	168.4	145	85	60	42 LOW
	6	SWINE	72.9	247	199	48	19 LOW
	7	SWINE	169	247	205	42	17 LOW
	5	SHEEP	42.5	145	155	10	6.9 HIGH

agreement. In contrast, for a relatively substantial amount of the dose delivered during the initial part of the period, cases 1 and 4 show the least agreement. The model, then, underestimates the residual injury (i.e., overestimates recovery) remaining from the initial radiation exposure. Cases 2, 6, and 7 agree somewhat, for comparable doses given over the initial and latter portions of the exposure period. Again, this probably reflects the model's overestimation of recovery for the initial portion of the dose, which is a relatively smaller portion than for cases 1 and 4.

We conclude from these results that the recovery function derived from constant dose rate data cannot generally be applied to split-dose type irradiation histories. Improvements could be made to the model if supported by the appropriate data, but those data are not available in the required generality. For example, correctly modeling a time-varying dose rate would involve taking second order derivatives to derive an empirical recovery function for radiation-induced damage, and we are unaware of any appropriate experimental results to permit that. An even more fundamental limitation is the nonlinear alteration of repair mechanisms due to varied radiation exposures such as would be present for arbitrary exposure histories. For example, in tissue damage modeling, mitotic delay and homeostatsis play important parts in the damage recovery process. These aspects must be explicitly simulated, including feedback mechanisms that operate in the recovery process.

3.7 SINGLE STEP AND MULTISTEP MODELING.

The complexity of a modeling effort must match the complexity of the essential elements of the system being modeled. This subsection examines the limitations of the ERD modeling approach and establishes requirements for properly modeling radiation sickness.

In the ERD concept, the amount of radiation-induced biological damage in an organism at a given time after an exposure (prompt or protracted) is expressed in terms of the instantaneously applied dose that would produce the same amount of biological damage. The ERD concept implicitly assumes that the condition of the organism in

question can be described by a single variable, namely the ERD. This assumption is justified when the biological effect in question depends on a single type of damage, when the production of that damage is well approximated by a single-step process, and when that damage is repaired by a simple process.

This type of damage and repair is simple to model mathematically. If the amount of damage existing in the organism is known at a given time relative to a protracted exposure history as well as the relationship between prompt dose and the resulting amount of damage, then it is possible to specify the ERD from the protracted dose as the prompt dose that would instantaneously produce the same damage. This unambiguous association of an ERD with a given exposure history assumes that the nature of the biological damage does not change with time.

As an example, consider the ERD concept applied to the case of chromosome damage when the biological endpoint is reproductive survival of cells in a freely growing culture. The actual damage process is quite complex when considered on atomic and molecular time scales. However, when considered for times longer than a minute or so, the damage process is well approximated by the single step production of lethal and potentially lethal lesions on chromosomes. To a good approximation, the cell will not survive if it enters mitosis with any lesion present, so the endpoint depends directly on the damage being modeled. During the time preceding mitosis, the potentially lethal lesions in a cell are eliminated at random at a more or less constant rate by intracellular repair. The ERD, at any given time during or after a protracted exposure, is the prompt dose that would generate the number of lesions present at that time.

Most biological effects, particularly those which determine performance decrement or lethality in mammals, are not as simply modeled as the one-step process discussed above. Usually there is a cascade of biological processes which occur during the time of interest after radiation damage is incurred. Furthermore, the expression, or occurrence, of signs and symptoms is not directly related to the original damage, but rather to one of the subsequent biological

processes in the cascade. In man, important processes in the biological cascade following radiation exposure are still occurring during the hours-to-days-to-weeks time frame when we want to be able to estimate the military operational consequences of exposure.

For example, nausea and emesis occur with a definite dose-dependent delay after a prompt exposure, indicating the need for at least two steps in the link between exposure and symptom expression. Any attempt to model the effects of protracted or fractionated doses must account for the time delay in symptom expression.

As another example, consider bone marrow lethality. For prompt doses around the LD₅₀, lethality in humans occurs mainly several weeks after exposure. The cause of death is usually overwhelming infection. The immediate circumstances determining life or death are quite removed from the initial molecular damage caused by the ionizing radiation exposure. Although there is a clear casual link between exposure and death, an attempt to model it must account for at least one and probably several intervening processes.

The simple concept which works well for a one-step process is not suited for a multistep cascade of processes, especially when characteristic times in the cascade are of the same order as the times being modeled. First of all, the ERD formulation has no provision for an inherent time delay for symptom expression. Secondly, the single-variable description of residual damage implicit in the ERD is not adequate for a multistep cascade. Variables are needed to specify not only the amount of original damage remaining, but also to specify the progress of each of the important processes linking damage repair and recovery to biological endpoint.

For example, consider a mammal that has received the LD₅₀ dose and, after an elapsed time, is in critical condition. More than one variable is needed to describe the state of the mammal regarding its likelihood of survival. Physiological variables such as temperature, blood counts, and fluid balance are important regarding the viable dispositions of the organism. None of these variables is directly related to the initial radiation damage in the sense that there exists a certain prompt radiation dose (an ERD) that would instantaneously

bring the organism to the same state of fever, blood count, and fluid imbalance.

These considerations explain why, from a modeling viewpoint, there is no simple behavior for the experimentally determined ERD for the LD₅₀ endpoint in animals (See Figs. 40 through 42, 45, and 46) and why those ERDs are even sometimes negative. Furthermore, it explains why our ERD modeling of the LD₅₀ with a recovery function described earlier in this section was only partially successful. The ERD concept can be properly applied when either the type of dose protraction or the time frame of interest is limited so that the single step, single variable approximation inherent in the ERD concept is reasonably good. To the best of our knowledge, all of the signs and symptoms of acute radiation sickness and all of the lethality effects of radiation exposure are multistep cascades of processes and must be so treated if the resulting model is to be valid for any protracted exposure.

3.8 SELECTED MODELING APPROACH.

From our review of the modeling efforts of others and from the modeling that we have accomplished under this effort, we conclude that the most promising way to achieve valid, broadly applicable models of the biological response to protracted radiation exposure is to use differential equations (rate equations) which describe in an approximate manner the multistep, physiological processes underlying the radiation response. These equations contain dose rate as a driving term and will, therefore, be applicable to any exposure history. In certain cases, it will be possible to summarize results through approximations such as the effective residual dose and the equivalent prompt dose for ease of application.

Two concrete modeling techniques with immediate application to symptomatology are the toxicokinetic approach and the tissue functionality approach. In Sec. 4, we apply the toxicokinetic approach to develop an uppergastrointestinal distress model (the UGIDM), and in Sec. 5, we apply the tissue functionality approach to develop a gut injury model (the GIM) for lower gastrointestinal distress, fluid loss, and gut death.

Finally, we would like to make some observations regarding future work. The GIM is firmly based on a mathematical description of chromosome damage as it effects mitotic death of cells. Ongoing research in cellular biology may add to our understanding of this problem. A small fraction of chromosome damage is mutagenic and some is carcinogenic. Major advances through molecular genetic biology have been made over the last decade in understanding both aspects of chromosome damage. In particular, the identification of oncogenes and antioncogenes ("suppressor genes") and the elucidation of their role in controlling the cell cycle have resulted in an understanding of the origin of retinoblastoma and a nearly complete picture of the progression of human colorectal cancer. A major role is played by the activation or inactivation by deletion, point mutation, or methylation of genes involved in the control of cell cycling. A perspective on this work was given recently by Stanbridge [1990].

These advances in molecular genetic biology are relevant to our symptomatology modeling for two reasons. First of all, they shed light on the control of the cell cycle and hence the proliferation that is an important part of modeling the response to protracted radiation. The connection is especially relevant since a single cell line, namely intestinal epithelial cells, is the main component of the intestinal mucosa and the source of colorectal cancer. Secondly, some of the DNA lesions that we model in an abstract fashion in our cell survival model surely result in gene deletions and point mutations similar to those involved in carcinogenesis. We may gain valuable insight for our mathematical formulation of cell survival from the explicit characterization of the genetic changes involved in carcinogenesis.

SECTION 4

UPPER GASTROINTESTINAL DISTRESS MODEL (UGIDM)

This section details the development of a unified model to predict the severity of the human emetic response to acute and protracted radiation exposure; we refer to this model as the upper gastrointestinal distress model (UGIDM). Our approach to modeling the UG response was by necessity semiempirical because of the lack of definitive data and reliable information for low dose rates for extended periods of protracted exposure as discussed in the *Prodromal Signs and Symptoms* subsection of Sec. 2 (*Nausea and Vomiting*). However, we have taken the available information into consideration and utilized what human data is available, including that developed by the DNA/IDP for acute radiation exposure. In addition, considerable recent progress has been made that clearly focuses upon the apparent mechanisms and pathways involved in radiation-induced emesis [Andrews, Rapeport, and Sanger, 1988; Harding, 1988; Lang and Marvig, 1989; Bermudez et al., 1988; Davis et al., 1986; Barnes, 1984; Borison, Borison, and McCarthy, 1981]. This progress has guided our effort in structuring an overall dynamic approach to emulate the UG response, although at this stage, the model was devoid of the specific mechanistic details.

Below, we discuss the basis for the modeling, give a description of the model, develop the equations, illustrate computed results of protracted exposures, and outline a means of empirical verification based on suggested laboratory experiments with ferrets.

4.1 BASIS FOR MODELING.

The onset of nausea and vomiting following radiation exposure is generally within the first few hours, ranging from minutes to several hours, depending on dose, as indicated in the *Prodromal Signs and Symptoms* subsection of Sec. 2. This early time frame suggests the involvement of changes in the physiological and biochemical processes due to radiation effects that are not principally due to cell injury

and death, with the possible exception of the extra sensitive lymphatic tissue and lymphocytes discussed in Section 2 (*Damage to Lymphoid Tissue*). Furthermore, the duration over which bouts of nausea and vomiting intermittently occur in humans extends anywhere from hours to a day or two, also depending on dose. The precise reason for this kind of discrete behavior still remains a major question [Andrews, Rapeport, and Sanger, 1988]. Even so, the overall recovery time is much shorter than would be expected for the gross repair and replacement of injured tissue.

Young [1986] provides an overall summary of the mechanisms and treatment of radiation-induced nausea and vomiting. It has been known for some time that the basic physiology of radiation-induced vomiting involved neural control mechanisms located in two distinct areas of the brain known as the chemoreceptor trigger zone (CTZ), located in the area postrema (AP), and the vomiting center. The vomiting or emetic centre is the final common pathway for emesis regardless of whether the afferent input comes from the gastrointestinal tract, a cortical center, or the CTZ that is activated by chemical stimuli from the blood and cerebrospinal fluid. The AP is located outside the blood-brain barrier where its neurons can react to substances in the circulation and transmit signals through the barrier to activate the vomiting motor reflexes via the emetic center.

Davis et al. [1986] point out that very little evidence over the last 30 years actually confirms the existence of a discrete group of cells that make up the vomiting centre or that produce the singular function of the "vomiting center." Rather, more in keeping with the CNS control of other functions such as the respiratory and cardiovascular system, a hierarchial process is envisioned where control arises from the higher expression of the integrated activity (rather than a "black box") which ordinarily serves the separate output functions that are associated with vomiting--such as mouth opening, salivation, gastric relaxation, respiratory control, and abdominal muscle contraction--or the actual act of vomiting. The occurrence of vomiting is a definite threshold effect (i.e., an all or nothing event) which activates the mechanism. Harding [1988] has likened the vomit-

ing response to that of a siphon or toilet whose reservoir empties via an inverted "U"-tube when a certain level is reached; the stimulus (water) entry rate or quantity delivered is not as important as the sum of the stimuli.

A "sequential activation model" described by Davis et al. [1986] seems to offer an interpretation of the vomiting response that provides a mechanism for increasing summation of inputs which eventually trigger the motor neurons. This model is consistent with experimental observation including the difficulty in pinpointing the discrete location of a vomiting center, which, it is argued, may not exist, but is a "higher" function of a number of separate effector nuclei.

Barnes [1984] gives a comprehensive review of vomiting and radiation exposure based on human accidental exposure to ionizing radiation, radiation therapy patients, and animal experimentation. Partial body radiation clinical experience (i.e., upper half body irradiation (UHBI), lower half body irradiation (LHBI), and middle third body irradiation) has amply shown that the upper abdomen is the most radiosensitive area. Further, abdominal vagotomy of irradiated dogs does not prevent early emesis in the dog although the latency is increased. A conclusion is that the vomiting mechanism of early radioemesis must also involve the action at the CTZ of circulating substances liberated in the process of a general tissue reaction to irradiation, the upper intestines being an important source. Since the dog is believed to be more similar to man than the monkey or cat where vomiting induction is concerned, the midepigastlic area of the body would appear to be the primary location of the target tissue for UG distress.

A wide variety of endogenous neuroactive agents may be released as a result of cellular damage by radiation such as serotonin, histamines, prostanoids, vasoactive intestinal polypeptides, free radicals, etc. Serotonin, known chemically as 5-hydroxytryptamine (5HT), is of principal interest because of its known role in the production of nausea and vomiting; it binds to and activates postsynaptic receptors (probably gastrointestinal vagal afferent axons). Besides

directly stimulating gastrointestinal afferents, these agents may also enter the systemic circulation via the portal vein where hepatic afferents can be activated. If they survive degradation by the liver, the emetic agents could then directly activate the area postrema [Andrews, Rapeport, and Sanger, 1988]. Animal experiments provide evidence of parallel pathways that can evoke emesis which may differ in sensitivity or relative prominence in different species. Although radiation may predominantly stimulate one pathway, others may also be involved; Harding [1988] suggests that the relative pathway weighting may have to be differentiated on a molecular level.

The actual detailed mechanisms of 5HT production and release are still unknown. However, recent work in the identification of the neuroreceptors in the brain and gut specifically associated with nausea and vomiting, known as 5HT₃ receptors, have significantly facilitated understanding of the neurophysiology of emesis. Furthermore, the recent work with 5HT₃ antagonists holds promise for quelling the response to radiation exposure significantly since the 5HT₃ receptors are believed to occupy a critical position in the emetic pathway(s).

The radiation-induced UG response is obviously a complicated process involving both humoral and neuronal pathways that at this stage we cannot hope to model in detail. Moreover, in spite of the progress that has recently been made, some details are still missing. However, we view the complexity and missing details as not being overly restrictive for purposes of our modeling effort here. Rather, we have focussed on developing a gross dynamic analogue in an attempt to simulate the irradiation of the target tissue, the production and body clearing of toxic substances, and their role in producing the UG response not associated with any of the specific pathways.

4.2 MODEL DESCRIPTION AND EQUATIONS.

Figure 60 is a schematic that pictures our approach to modeling upper gastrointestinal distress. Elements of the model (UGIDM) are shown which represent our gross interpretation of the phenomenology and mechanistic concepts currently thought to comprise the process of

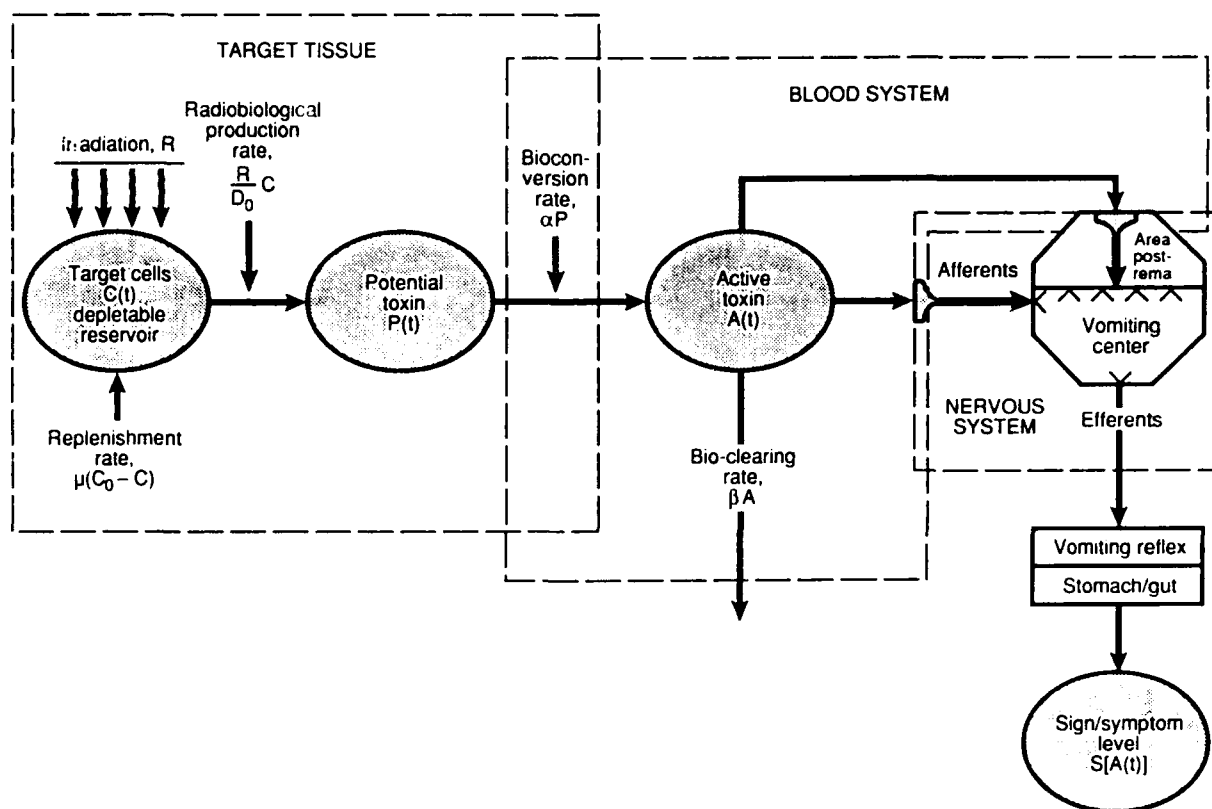


Figure 60. Upper gastrointestinal distress model (UGIDM).

radiation-induced vomiting. An initial version of the model, known as the prodromal response (PR) model, was first presented by McClellan and Anno [1986], and was designed to predict the early-time dependence of severity for three DNA/IDP-defined symptom categories [Anno, Wilson, and Baum, 1985]: uppergastrointestinal distress (UG), fluid loss and electrolyte imbalance (FL), and fatigability and weakness (FW). Significant improvements that have been made to modeling the UG symptom category have resulted in the UGIDM to predict the time-dependent severity level of the UG response. The severity levels are based on an ordinal scale given in Table 27 developed for the DNA/IDP [Anno, Wilson, and Baum, 1985].

As portrayed in Fig. 60, we assume a nonspecific target tissue located in the body that, when irradiated, produces a substance or potential toxin within the tissue cells. A subsequent chain of biochemical events in turn produces an active endogenous substance or humoral toxin that initiates the physiological processes that triggers

Table 27. Severity levels of upper gastrointestinal (UG) distress in humans.

Severity Level	Signs and Symptoms
1	No effect.
2	Upset stomach; clammy and sweaty; mouth waters and swallows frequently.
3	Nauseated; considerable sweating; swallows frequently to avoid vomiting.
4	Vomited once or twice; nauseated and may vomit again.
5	Vomited several times including the dry heaves; severely nauseated and will soon vomit again.

the body response expressed as the signs and symptoms of acute UG distress (nausea and/or vomiting). The blood system and nervous system, consisting of the afferents, neuroreceptors, area postrema, vomiting center, and efferents indicated in Fig. 60, are not explicitly modeled. We assume that the blood circulation (~1 min), nerve receptor response, and nerve impulse transmission all generally take place in a time much shorter than the characteristic times of the rate processes modeled.

Mathematically, the UGIDM is structured as a two-compartment analogue that calculates UG symptomatology based on solving three coupled linear differential equations together with a symptom-severity response relationship. First, a potential toxin P is produced by radiation exposure. This potential toxin is not directly responsible for triggering the expression of symptoms. Second, the potential toxin is converted to an active toxin (or substance) at a rate α that initiates or triggers a UG distress response depending upon the level of A . The level of A also depends on a bio-clearing rate β to simulate degradation of the active toxin (or substance) due to body recovery processes such as those which occur in the renal-hepatic system.

In the UGDIM, we assume that the amount of potential toxin that can be produced by the action of radiation on the target cells is finitely limited. In order to accommodate this limitation in the model, we have introduced an analogue referred to as a hypothetical "depletable reservoir," which is the source of the potential toxin produced by radiation exposure. No specific mechanism(s) and/or process(es) have been identified that would account for this effect of diminishing toxin production with radiation exposure. However, it appears to be present both from experimentation with animals [Borison, McCarthy, and Douple, 1988] and from clinical experience involving fractionated treatment protocols in radiotherapy [Tichelli et al., 1987]. The reservoir level C is assumed to be depleted by radiation exposure with a characteristic dose D_0 analogous to the way in which the cell population of a tissue is depleted by radiation exposure. The rate equation for the reservoir level is:

$$\dot{C} = - \left(\frac{R}{D_0} \right) C + \mu (C_0 - C)$$

The first term on the right hand side of this equation is the depletion caused by the dose rate R . The second term of the equation returns the reservoir to its initial (preirradiation) level C_0 with a time constant μ^{-1} . A feature of the depletable reservoir is that it allows for the "habituation" effect observed with repeated doses of radiation as indicated above, where successive doses tend to be less effective at producing emesis. The depletable reservoir also provides improvement in modeling peak severity levels produced for moderate acute doses.

Some limiting characteristics of the depletable reservoir assumed are pointed out below based on the solution of the differential equation above for a constant dose rate R , given by,

$$C(t) = \frac{\mu C_o}{K} (1 - e^{-Kt}) + C_o e^{-Kt} ,$$

where
$$K = \frac{R}{D_o} + \mu .$$

The equilibrium level of the reservoir (i.e., when $t \rightarrow \infty$) is,

$$C(\infty) = \frac{\mu C_o}{(R/D_o) + \mu} .$$

When the dose rate is large compared to the reservoir reconstitution rate, the equilibrium becomes,

$$C(\infty) \approx \frac{\mu}{(R/D_o)} C_o , \quad (R/D_o) \gg \mu$$

This would correspond to a dominating habitation effect where the reservoir level is low and potential toxin production becomes curtailed due to sustained (high) level of radiation exposure.

On the other hand, when the dose rate is small compared to the reservoir reconstitution rate, the equilibrium level becomes, $C(\infty) \approx C_o$, $(R/D_o) \ll \mu$. This would correspond to a high reservoir level (or absence of the habitation effect) where potential toxin production would not be curtailed by subsequent radiation exposure. Although, the UG severity response would also be determined by the other rate processes modeled if the dose rate were sustained at a low level.

For an acute exposure, the rate equation for the depletable reservoir is,

$$\dot{C} = \mu(C_o - C)$$

The initial condition can be determined from the equation given previously above for a constant dose rate by taking the limits of the dose rate and time along the fixed relationship, $D = Rt$, and where $(R/D_0) \gg \mu$,

$$\begin{aligned} \lim_{R \rightarrow \infty, t \rightarrow 0} C(t) &= C_0 e^{-\left(D/D_0\right)} \\ D &= Rt \end{aligned}$$

The reservoir level solution following an acute exposure is then,

$$C(t) = C_0 - C_0 \left[1 - e^{-\left(D/D_0\right)} \right] e^{-\mu t}.$$

When the dose is small and/or the time is large, the reservoir tends toward its preirradiation capacity, i.e., $C(t) \rightarrow C_0$. When the dose is large, the reservoir reconstitutes according to the relationship,

$$C(t) = C_0 \left(1 - e^{-\mu t} \right).$$

The differential equations for the production and clearing of the potential and active toxin levels (P and A , respectively), are:

$$\dot{P} = \left(\frac{R}{D_0} \right) C - \alpha P \quad (\text{continuous exposure})$$

or $\dot{P} = -\alpha P \quad (\text{acute exposure})$

and, $\dot{A} = \alpha P - \beta A$

The toxin levels for this two-compartment model are described by linear kinetics where the production rate is proportional to the dose rate R and depletable reservoir level C . P is converted to A at the rate α , and A is degraded or eliminated at the bioclearing rate β .

For simplicity, we have chosen to express the C, P, and A levels in terms of dose units. This abstract representation is necessary since we presently have no means of calibrating the actual quantities of these target cell populations (or tissues) and substances hypothesized in our model. Also, we have chosen to make the two constants D_0 and C_0 be equal since we have no *a priori* means of knowing the relationship between D_0 and C_0 . However, by doing so, it is then readily seen that the P production rate, $R(C/C_0)$, is the dose rate weighted by the fractional level of the reservoir that tends to be depleted by radiation exposure. This choice also ensures that when the applied dose rate is small, C is essentially constant at the value C_0 and the source term in the \dot{P} equation (for continuous exposure) reduces to just R. The model then reduces to the case with no depleting reservoir that limits the production of P.

The final relationship in the UGIDM converts the active toxin level A to UG symptom severity level (Table 27), given as follows:

$$S = 1 + 4 \left\{ 1 - \exp \left[-\ln 2 \cdot \left(A/A_{0.5} \right)^\gamma \right] \right\} .$$

Given by this form, the severity S is halfway to maximum expression when the toxin level A is $A_{0.5}$. The shape parameter γ determines how steep the function is near $A_{0.5}$, that is, how markedly the severity level rises as A increases. This form was chosen since it introduces a threshold-like behavior, suppressing early symptoms until the toxin level approaches $A_{0.5}$. The amount of suppression is determined by γ . A threshold-like behavior is in better agreement with the sudden onset of symptoms implied by the IDP severity level curves for acute doses.

Because of the transient nature of the UGIDM, the active toxin A will attain a maximum value at some time postexposure (i.e., after irradiation has stopped) which depends on the model's parameters. Also, the time delay where A maximizes after the radiation terminates will be longer the smaller the time over which the dose is delivered, the longest delay being for an acute dose. Therefore, when calculations are performed with the UGIDM to determine severity level, care must be taken to assure that the maximum value of A is attained.

The UGIDM equations, initial conditions, and parameters are summarized below:

Continuous Exposure

$$\dot{C} = -\left(\frac{R}{D_o}\right) C + \mu (C_o - C)$$

$$C(0) = C_o \geq 0$$

$$\dot{P} = \left(\frac{R}{D_o}\right) C - \alpha P$$

$$P(0) \geq 0$$

Acute Exposure

$$\dot{C} = \mu (C_o - C)$$

$$C(0) = C_o e^{-\left(D/D_o\right)}$$

$$\dot{P} = -\alpha P$$

$$P(0) = C_o \left[1 - e^{-\left(D/D_o\right)}\right]$$

$$\dot{A} = \alpha P - \beta A$$

$$A(0) \geq 0$$

$$S = 1 + 4 \left\{1 - \exp \left[-\ln 2 \cdot \left(A/A_{0.5}\right)^\gamma\right]\right\}$$

Variables

C = depletable reservoir (target tissue) level, Gy

P = potential toxin, Gy

A = active toxin, Gy

R = dose rate, Gy h⁻¹

D = dose, Gy

Parameters

α = potential toxin conversion rate/active toxin production rate, h⁻¹

β = active toxin clearing rate, h⁻¹

μ = depletable reservoir reconstitution rate, h⁻¹

C_o = initial reservoir level, Gy

D_o = characteristic target tissue dose (=C_o), Gy

A_{0.5} = half-maximum value of A, Gy

γ = severity response slope

The UGIDM differential equations above are all linear with constant coefficients and can be solved analytically in closed form for an acute dose or a constant dose rate (see Appendix A). However, for a time-dependent dose rate such as the Way-Wigner power law form ($t^{-1.2}$) frequently employed to approximate the gross beta decay of a fission product assembly, numerical methods are employed to obtain computer solutions.

Values for the parameters listed above were obtained by matching the UGIDM equations to appropriate data. For this purpose, we have chosen to apply the UGIDM for acute exposure to match the UG symptom severity data developed by the DNA/IDP. This was necessary since no other data are currently more complete over the dose and time range of interest. Furthermore, since the UGIDM is uniformly applicable for both acute and protracted exposure, the parameter values obtained in this manner enable a self-consistent application of the UGIDM to arbitrary dose histories involving acute and/or protracted exposure(s).

Figure 61 is a plot of the time dependence of the UG distress symptom category originally developed by the DNA/IDP [Anno, Wilson,

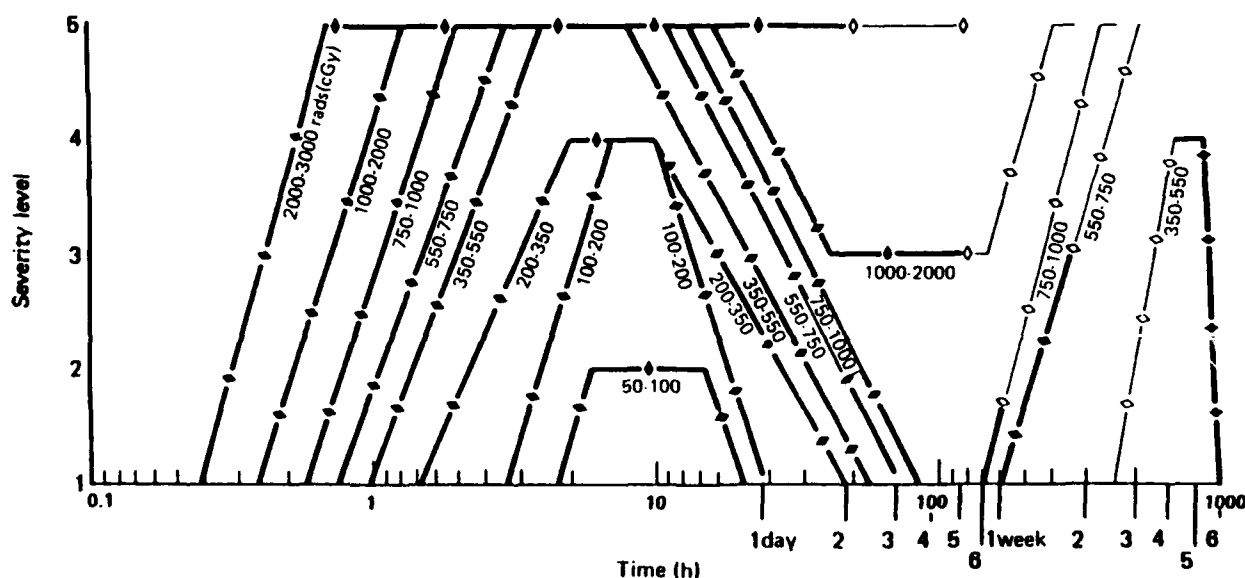


Figure 61. UG severity levels for prompt dose ranges midline tissue (MLT).

and Baum 1985]. Each time profile corresponds to symptom severity for acute dose in the range indicated. In Fig. 61, dose is referenced to midline tissue (MLT), which corresponds to the dose absorbed in the midepigastic portion of the body since that area represents the likely sensitive body region of target tissue for UG distress. We utilized the MLT dose reference in dealing with clinically derived information to formulate the UGIDM due to radiobiological precedence. Later in this section, when operational applications of the UGIDM are considered, illustrations are given in terms of free-in-air (FIA) dose values consistent with the dose reference employed by the military where the assumed conversion is $\text{dose(MLT)} = 0.66 \times \text{dose(FIA)}$.

During the prodromal phase of acute radiation sickness, UG distress symptoms begin within hours after prompt radiation exposure and then fade in a few days or less. Remission of symptoms lasts about a week, then the manifest illness phase brings on new symptoms. In formulating the UGIDM, we have not attempted to model UG distress during the manifest illness phase that involves other confounding degenerate body processes. Furthermore, since UG distress that occurs during the prodromal phase is the primary focus of interest, we have concentrated on a postexposure response time-frame of less than or equal to about three days duration. Accordingly, we have utilized the DNA/IDP data including acute doses up to the 5.5 to 7.5 Gy range from which to develop UGIDM parameter values.

We have also made some minor modifications in the severity profiles for UG distress represented in Figure 61 in order to remove undue analysis constraints in using the data to determine values for the UGIDM parameters. In the development of the DNA/IDP profile (Fig. 61), an effort was made to attach meaning to UG distress at only integer levels consistent with the discrete levels chosen to ordinally scale severity; accordingly, UG distress was essentially "quantitized" where noninteger states (or levels) were interpreted to have no meaning. This notion is reflected in the flat horizontal portions and sharp corners of the profiles. However, in our modeling effort here, noninteger values do have mathematical meaning in terms of continuous functional forms consistent with solutions of the UGIDM equations.

Since the UGIDM solutions are time-dependent profiles that may attain integer levels, the discrete response characterization of UG distress is preserved and the modifications made do not alter that interpretation.

The dashed lines given in Fig. 62 represent the modified time-dependent profiles for UG distress. They reflect some smoothing of profile data around the peaks, and in the case of the 2.0-3.5 Gy profile, the peak was extended to between severity levels 4 and 5. Using this profile data, optimization calculations were carried out with the acute dose form of the UGIDM to obtain parameter values based on minimizing the objective function specified as the root-mean-square deviation of the difference between the DNA/IDP data and UGIDM severity level prediction. All of the UGIDM parameters, except the reservoir reconstitution rate μ , influence the predictions for the case of acute dose. Since μ cannot be determined from the acute dose

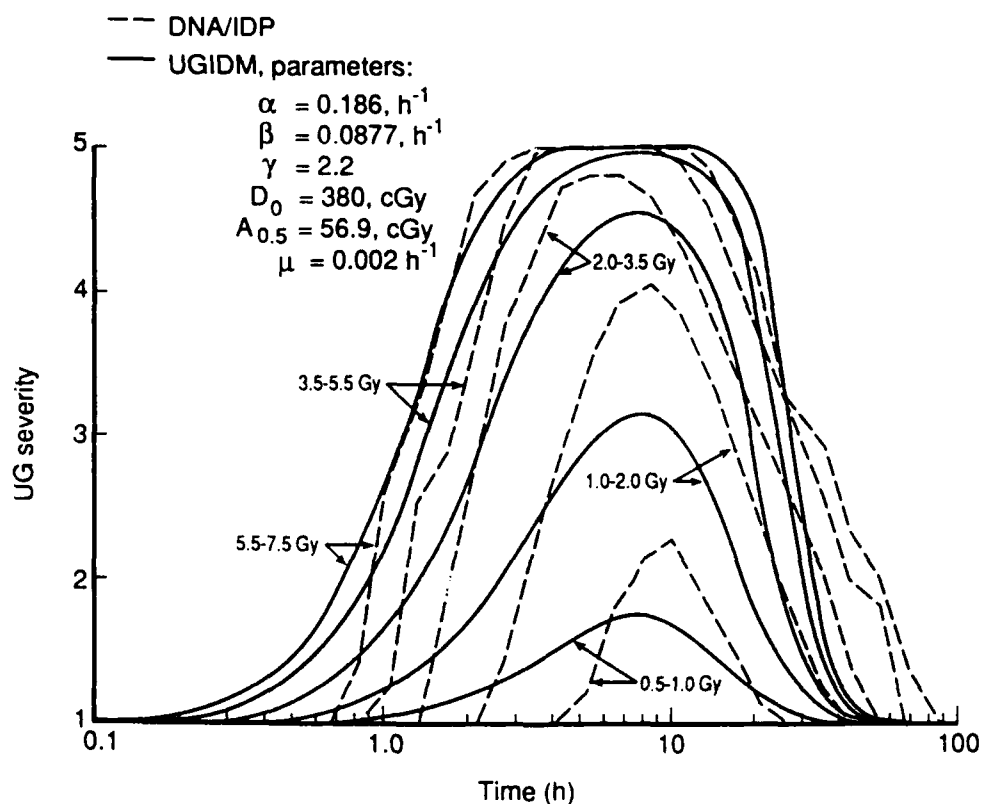


Figure 62. The severity level of upper gastrointestinal (UG) distress in humans.

data, we arbitrarily chose $\mu = 0.002 \text{ h}^{-1}$ and determined the other parameters. This value corresponds to a reservoir reconstitution half-time of about two weeks, although without appropriate protracted dose data this value cannot be empirically reconciled.

Variations in the form of equations for the potential toxin A and active P (other than those summarized above) were investigated for fitting the DNA/IDP data including the following:

Saturable active toxin clearing:

$$\begin{aligned}\dot{P} &= -\alpha P \\ \dot{A} &= \alpha P - \frac{\beta_1 A}{\beta_2 + A}\end{aligned}$$

Quadratic conversion:

$$\begin{aligned}\dot{P} &= -\alpha P^2 \\ \dot{A} &= \alpha P^2 - \beta A\end{aligned}$$

Polynomial quadratic clearing:

$$\begin{aligned}\dot{P} &= -\alpha P \\ \dot{A} &= \alpha P - \left(\beta_1 A + \beta_2 A^2 \right)\end{aligned}$$

None of the above forms provided any improvement in fitting the data and were not pursued for the UGIDM.

Figure 62 gives acute dose plots (solid line curves) of UG severity calculated with the parameter values obtained by fitting the data. The UGIDM predicts a somewhat less abrupt rise in severity compared to the DNA/IDP profiles, particularly for lower dose levels. On the other hand, the UGIDM indicates a more abrupt drop in severity, particularly apparent for higher doses. The UGIDM predicts a somewhat lower peak of severity, particularly apparent at the 1.0-2.0 Gy dose level. Also, the DNA/IDP curves indicate a shift in the peak position to somewhat later times as the dose decreases; because of the linear nature of the UGIDM, this shift is not predicted.

Exact agreement should not be demanded since the original DNA/IDP data [Baum et al., 1984] themselves are partially based on qualitative observations of many different experts without benefit of a common symptom severity scale. In fact, a UG distress response model that details all the appropriate biological processes may be capable of producing more realistic shapes of the symptom severity curves than those given by the DNA/IDP.

We believe that the agreement of the UDGIDM with the DNA/IDP data is reasonable given the nature of the data and the simplicity of the model. Also, it must be kept in mind that the IDP symptom severity scale is only an ordinal scale. Although constructed with reasonableness in mind, there is no quantitative assurance of the implied linearity. Thus, detailed agreement between the model and the data representing the DNA/IDP should not be expected. This point is discussed further in this section below in conjunction with suggested experiments with the ferret as a possible means of model verification.

4.3 PROTRACTED DOSE RESPONSE.

Calculations were performed with the UGIDM to severity predictions for protracted radiation including continuous constant dose rate and fractionated exposure (MLT). Some calculations were also performed to illustrate UG distress severity from radiation exposure (FIA) protracted in a fallout field.

4.3.1 Continuous Exposure.

The UGIDM predictions for the severity of UG distress for continuous exposure applied at a constant dose rate are shown as the three curves (solid lines with dashed extensions) in Fig. 63. These curves show the dose rate required to reach severity levels 2, 3, and 4 as a function of dose rate (MLT). As the dose rate is decreased to around 20 cGy h^{-1} and below, the required isoeffect dose (MLT) increases very rapidly.

We interpret this rapid increase in UG severity level 3 to define a dose rate threshold below which prodromal emesis in humans is predicted to not occur. Below this dose rate, the toxin bioclearing

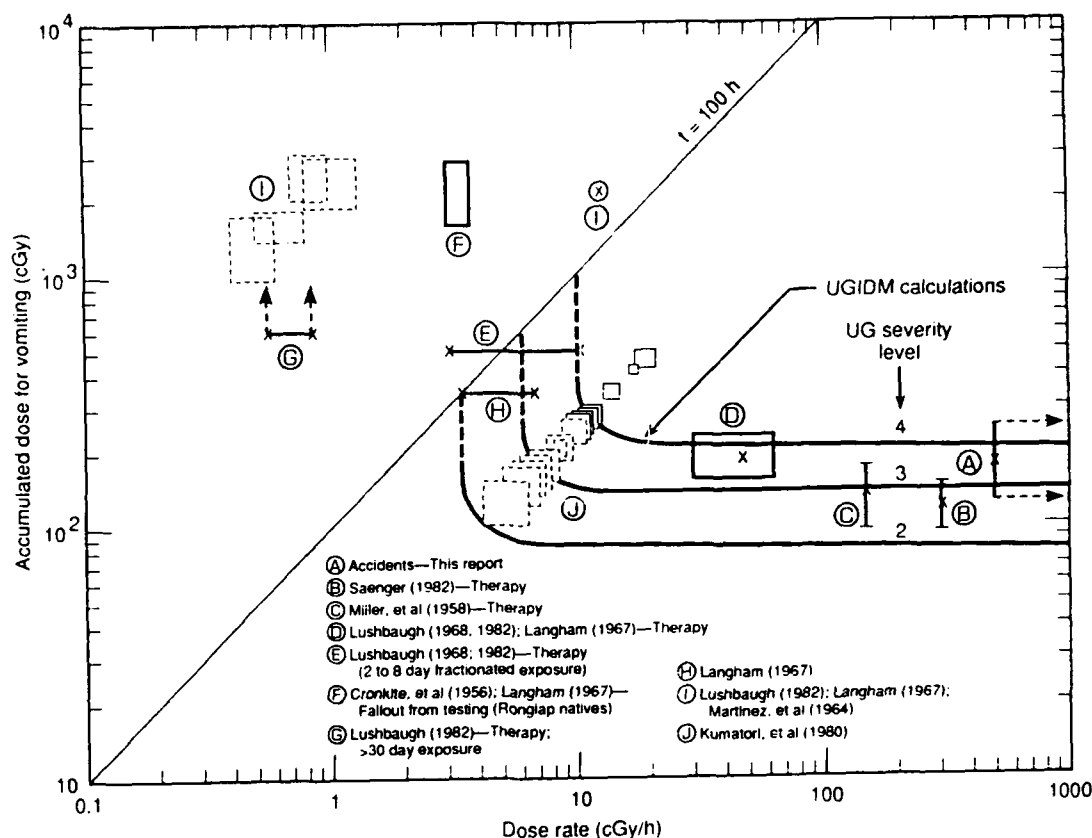


Figure 63. Accumulated dose versus dose rate: UGIDM-predicted severity levels and data from humans.

rate simulated by β in the UGIDM prevents the accumulation of a body toxin level sufficient to trigger emesis.

Figure 63 contains the same data discussed and displayed in Fig. 6 of Section 2, some of which are for emesis ED_{50} (i.e., (A), (B), (C), and (D)). A direct comparison cannot be made between the UGIDM and the ED_{50} data, particularly for low dose rates (less than about 30 cGy h^{-1}), for two main reasons. First, comprehensive data for ED_{50} at low dose rates is lacking. Second, also because of the lack of appropriate data, specific correlation cannot be made jointly for the incidence and severity level of emesis. That is, for a given level of emesis, the incidence distribution is generally unknown; the converse is also true. However, it is generally assumed that severity and incidence of emesis do go hand-in-hand according to the DNA/IDP investigations. Accordingly, we feel that the ED_{50} may generally correspond to UG severity level between 3 and 4. This is indirectly

supported by an independent determination of the incidence for vomiting made from accident victims exposed to acute doses. Based on a log-likelihood analysis of quantal response for the first 24 h postexposure, we obtained an ED₅₀ of 170 (+61, -45) cGy for emesis by fitting a lognormal distribution to the data (see Appendix B). This result, given in Fig. 63 by the (A) designation, falls between severity levels 3 and 4 predicted independently by the UGIDM. The data designated (E) through (J) in Fig. 63, discussed previously in conjunction with Fig. 6 in Section 2, serve as a guide as to the reasonableness of the UGIDM predictions.

The diagonal line in Fig. 63 corresponds to an exposure time of 100 h. It emphasizes that UGIDM predictions for humans are expected to be valid only for doses less than about 1000 cGy h⁻¹ and for times less than four days or so. Vomiting that may occur beyond four days at greater doses may arise from subsequent effects not specifically considered in the UGIDM.

4.3.2 Fractionated Exposure.

There is almost no appropriate quantitative data for the severity of UG distress after fractionated exposures that do not include the use of chemotherapy and/or drugs to mitigate prodromal reactions. However, there are ample anecdotal reports from both radiotherapists [Tichelli et al., 1987; Anno, 1983] and animal experimenters [Borison, McCarthy, and Duple, 1988] indicating that when moderate fractionated doses are given daily, the intensity and frequency of emesis diminish substantially after the second or third fraction. That is, the irradiated patient becomes in some way habituated to successive dose fractions and does not respond as readily to later fractions. Figure 64 shows the prediction of the UGIDM based on the parameters shown in Fig. 63. The model clearly predicts the habituation effect; however, we do not have data at present to validate or improve the model in this regard.

Calculations were also performed to illustrate the UGIDM predictions for the response to fractionated radiation exposure assuming a nondepletable reservoir. The results, calculated for the same ir-

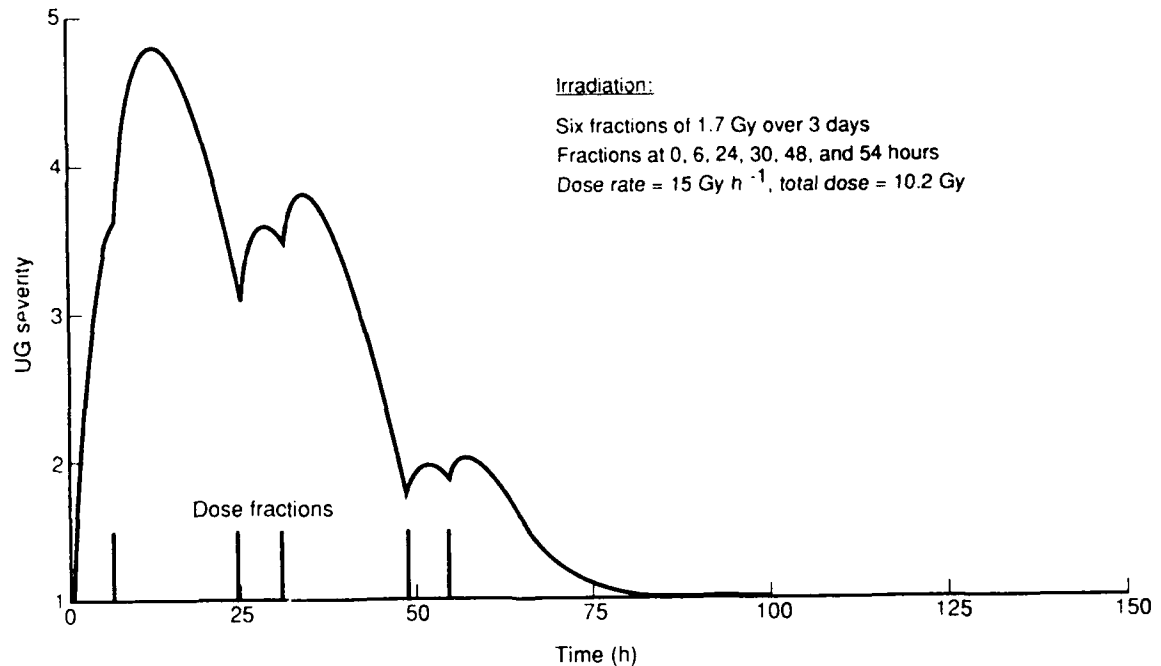


Figure 64. UGIDM prediction of severity level for upper gastrointestinal (UG) distress/fractionated doses.

radiation schedule in Fig. 64 are given in Fig. 65. For these calculations, the UGIDM does not include the \dot{C} equation and the source term for the \dot{P} equation is just the dose rate R . These results show a progressive increase in UG severity with continuing dose fractions where, unlike the case of a depletable reservoir, the only limiting factor is the bioclearing rate β . Assuming a continuation of fractionated exposures, a nondepleting reservoir would allow a progressive buildup to level 5 with no diminution in severity, which would not be biologically reasonable.

4.3.3 Fallout Field Exposure.

Calculations were performed to illustrate the utility of the UGIDM for exposure in a fallout environment following a nuclear weapon detonation where fission product radionuclides are assumed to follow the $t^{-1.2}$ Way-Wigner decay relationship. Dose units for these calculations refer to free-in-air (FIA) values consistent with those employed for military applications.

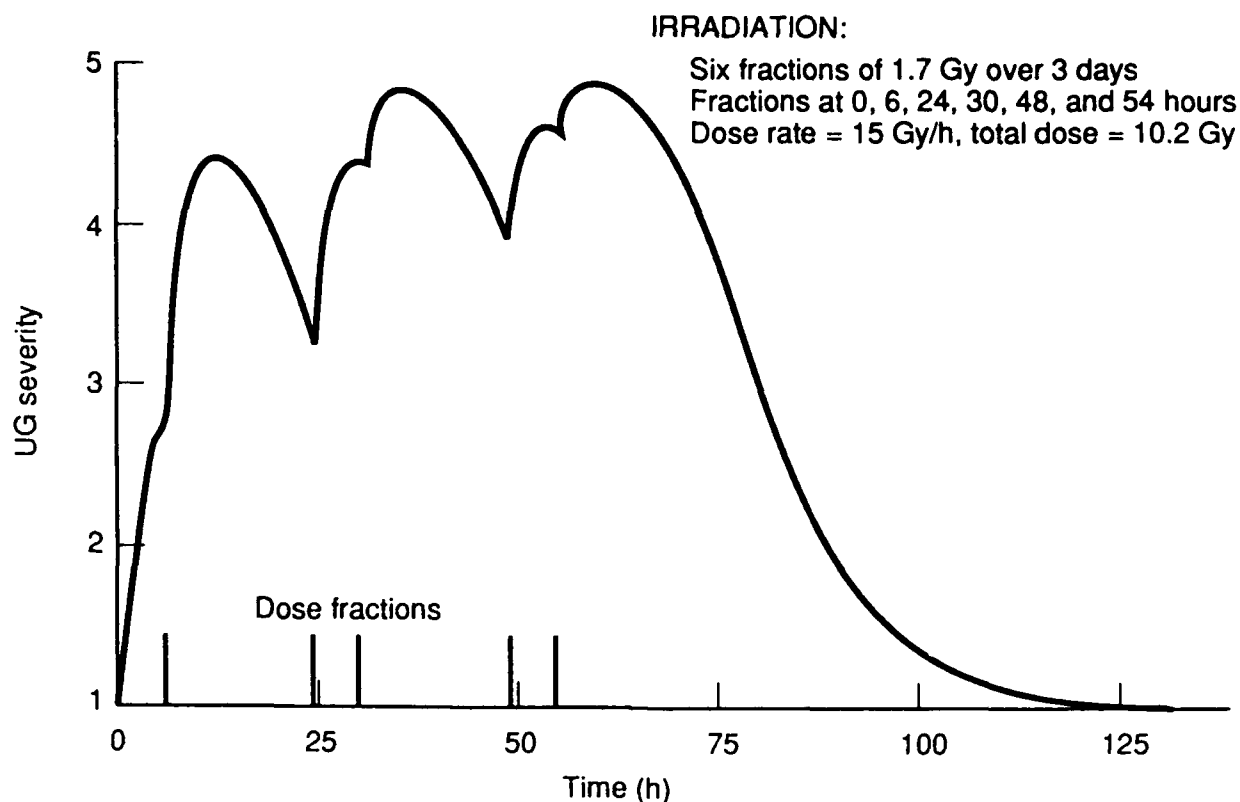


Figure 65. UGIDM prediction of severity level for upper gastrointestinal (UG) distress/fractionated doses--non-depleting reservoir.

Figure 66 is a family of isoeffect curves for a duration of continuous radiation exposure versus initial dose rate. The parameters for the curves of initial time after burst refer to an arbitrary time after detonation at which the (initial) dose rate is known. The specific isoeffect corresponds to a radiation exposure status level of 2 (RES-2) employed by the U.S. Army to designate an emergency risk dose of 150 cGy (EPD)*; this dose value also corresponds approximately to an estimated ED₁₀ for emesis based on our analysis of the accident data. The two quantities that must be known to utilize the curves are the initial dose rate (for example, by measurement or prediction) and the corresponding initial time after burst. The dashed lines in Fig. 66 provide examples. Assuming a dose

*EPD = equivalent prompt dose (discussed in Section 3).

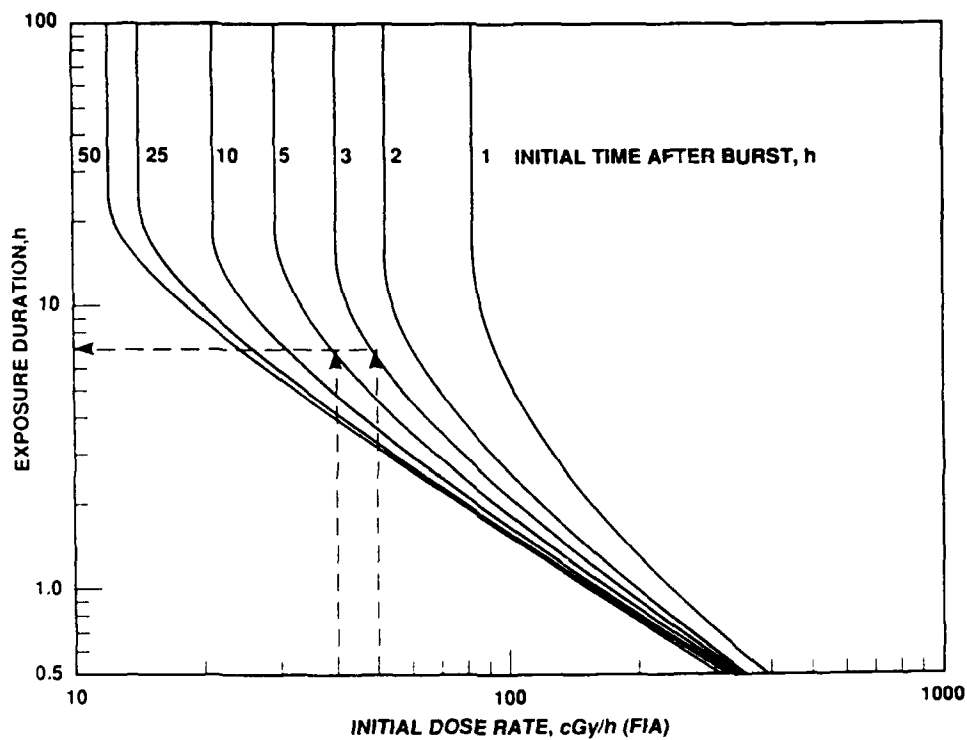


Figure 66. Protracted exposure in a fallout field ($t^{-1.2}$ radioactive decay) UG distress--equivalent prompt dose for RES 2 (emesis ED_{10}): 150 cGy (FIA).

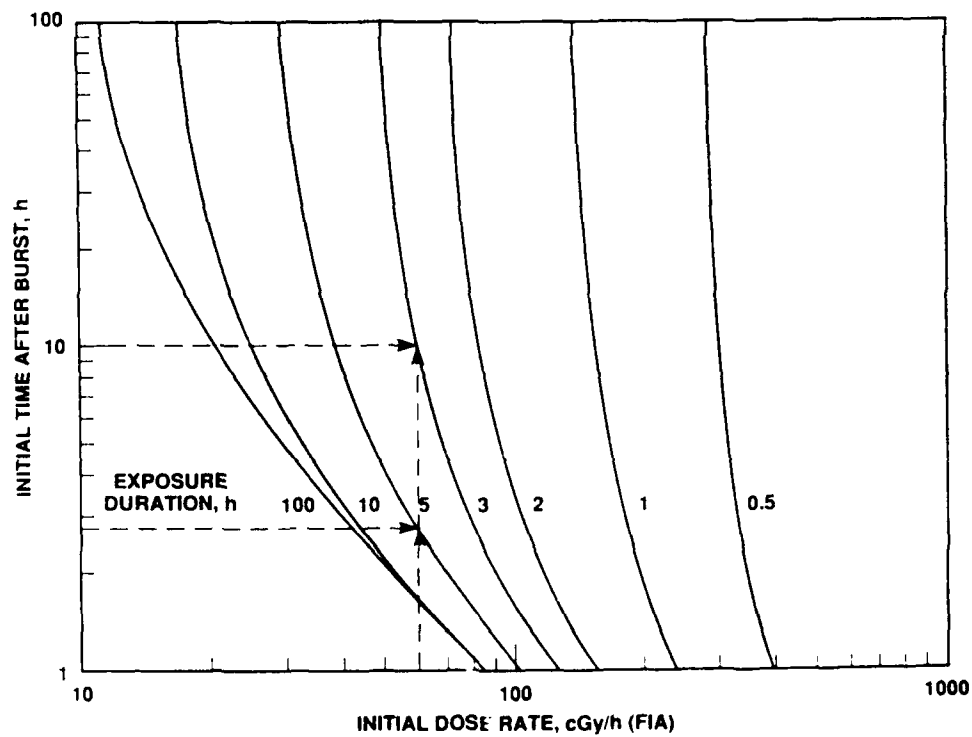


Figure 67. Protracted exposure in a fallout field ($t^{-1.2}$ radioactive decay) UG distress--equivalent prompt dose for RES 2 (emesis ED_{10}): 150 cGy (FIA)).

rate level of 50 cGy h^{-1} were known in a fallout environment at an estimated time of 3 h following weapon burst, a subsequent period of continuous exposure could be tolerated (avoid the isoeffect dose) provided that it was less than 7 h in duration. Operationally, this would also be approximately equivalent to the situation if the initial dose rate is 40 cGy h^{-1} at a time of 5 h subsequent to weapon burst. The curves are quite sensitive to the initial dose rate primarily due to the $t^{-1.2}$ decay law assumed for fission product radionuclides. For example, if the initial dose rate of 50 cGy h^{-1} occurred at an initial time of 2 h or less after detonation, there would be no restriction on the subsequent duration of exposure with regard to avoiding the isoeffect, as exemplified by the vertical rise in the 2 h curve. The same concept applies to the other curves which define specific dose rates for initial times after burst where subsequent durations of exposure in a fallout environment are not restricted in terms of avoiding the isoeffect dose level (150 cGy, EPD).

Figure 67 is another version of the isoeffect dose level of 150 cGy (EPD) which plots initial time after burst versus initial dose rate for a family of parameterized curves of exposure duration. For example, an exposure duration of just under 5 h initially commencing about 1.75 h after burst could be tolerated when the known dose rate is no greater than 60 cGy h^{-1} . If the same dose rate prevailed at a later time of 10 h, the subsequent duration of exposure in a fallout environment must just be under 3 h to avoid the same isoeffect dose level. Like those shown in Fig. 66, these curves are also quite sensitive to dose rate.

Calculations similar to those that correspond to Fig. 66 and 67 were performed for an isoeffect dose of 255 cGy (FIA) which is the ED_{50} EPD value for vomiting within the first 24 h postexposure obtained from the analysis of data for accident victims. Using the UGIDM, with the parameter values given in Fig. 62, we determined a severity level that corresponds to the ED_{50} (255 cGy) EPD of $S = 3.67$. The curves given in Fig. 68 and 69 then correspond to that isoeffect severity level. These are used in the same manner as discussed for Figs. 66 and 67.

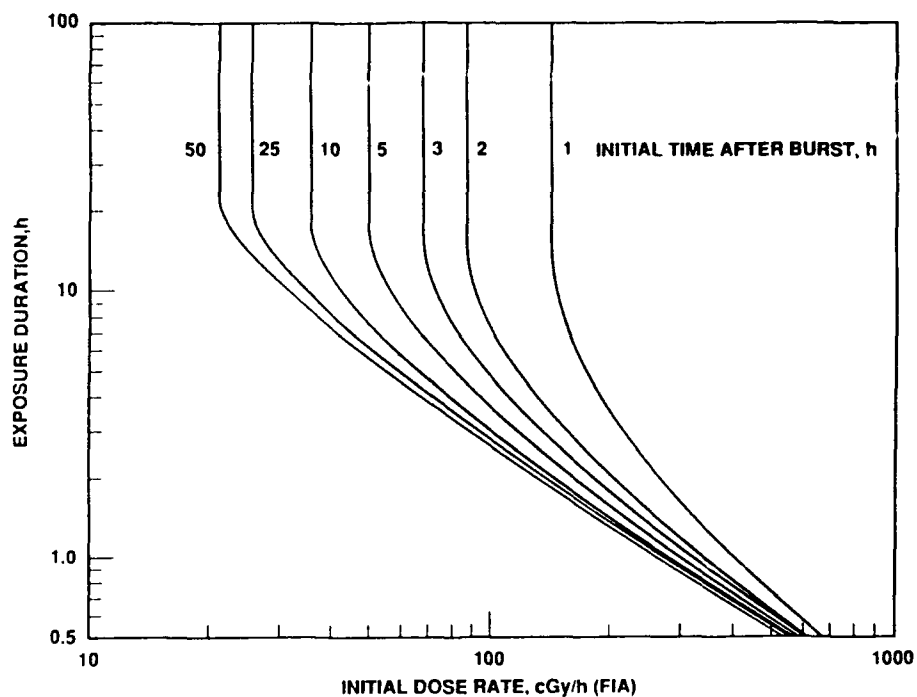


Figure 68. Protracted exposure in a fallout field ($t^{-1.2}$ radioactive decay) UG distress--equivalent prompt dose for emesis: $ED_{50} = 255$ cGy (FIA).

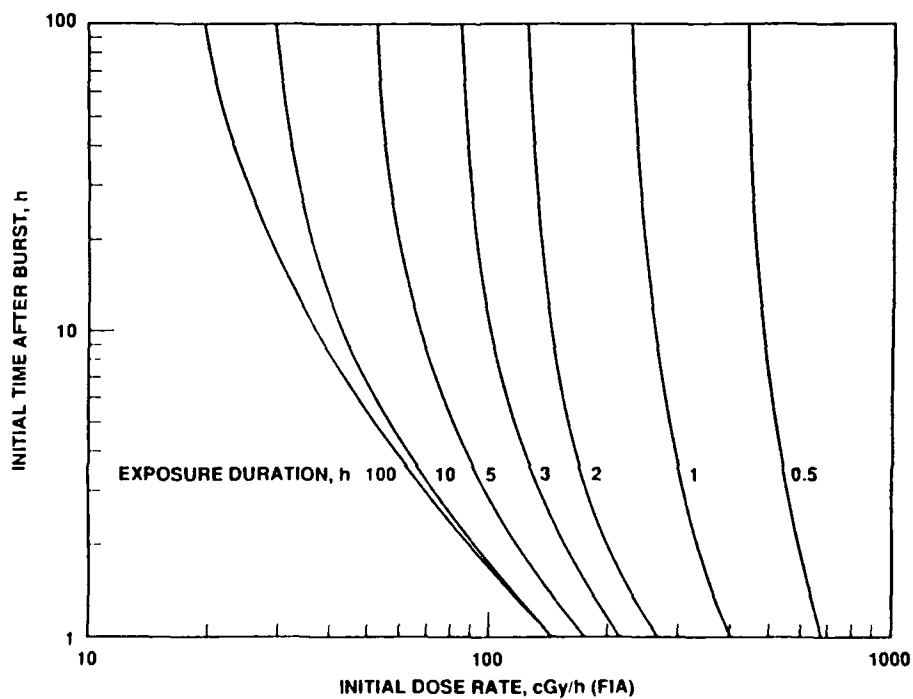


Figure 69. Protracted exposure in a fallout field ($t^{-1.2}$ radioactive decay) UG distress--equivalent prompt dose for emesis: $ED_{50} = 255$ cGy (FIA).

The UGIDM was used to perform calculations to predict the severity profile for two hypothetical protracted dose scenarios expressed in Fig. 70. Four daily exposure periods are shown that take place following a nuclear weapon detonation where an initial $H + 1$ h dose rate of 400 cGy h^{-1} is assumed. Scenario A differs from Scenario B where, in addition to the four protracted dose exposure periods, Scenario B adds an acute exposure of 100 cGy assumed to occur at 1200 h midway through the second protracted dose period on day 2 following the initial weapon detonation; no additional fallout-source radiation is assumed to result. The unshaded time intervals assume a fallout radiation protection factor of $\text{PF} = 0.01$ for shelter and no protection for unsheltered periods given by the shaded time intervals.

Results of the scenario A and Scenario B calculations to predict severity for UG distress are given in Figs. 71 and 72, respectively. These results predict vomiting to onset during day 1 and to continue

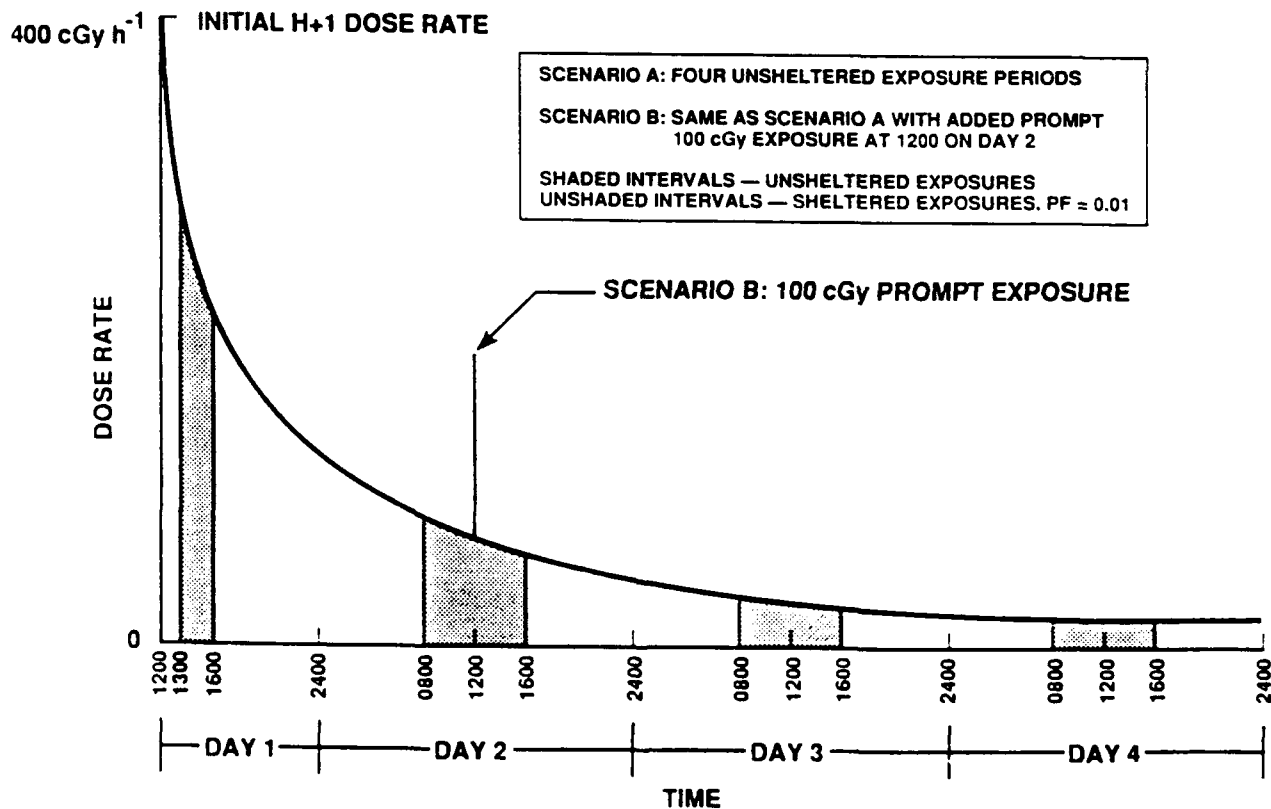


Figure 70. Fallout exposure scenarios (A and B) ($t^{-1.2}$ radiodecay).

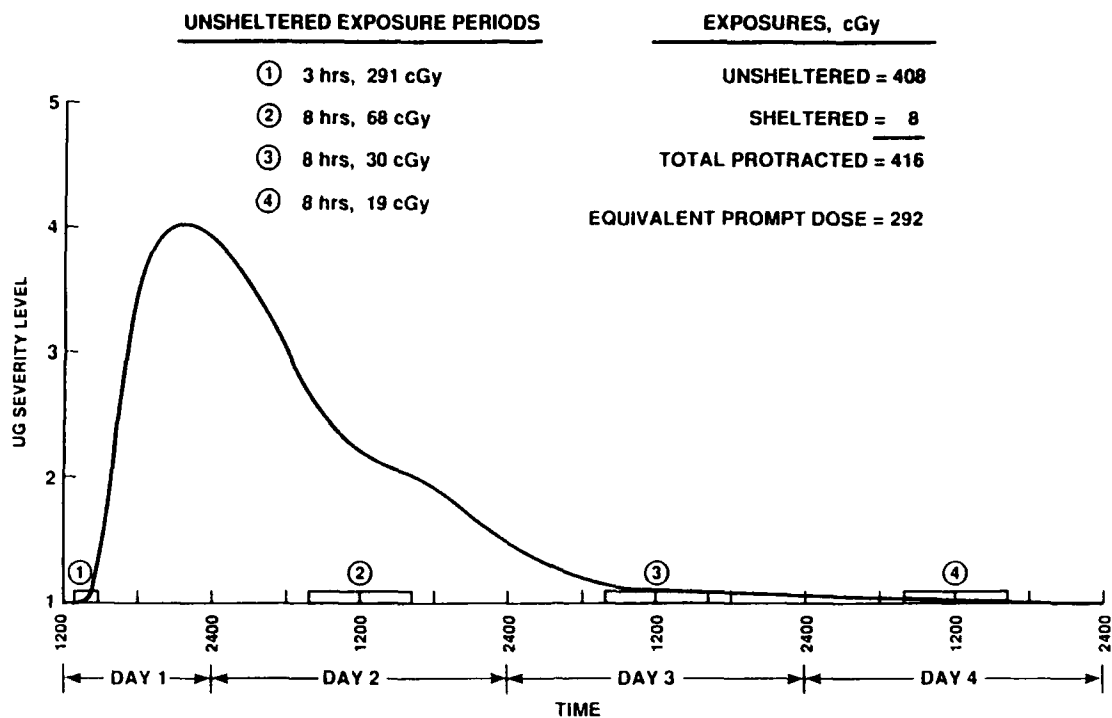


Figure 71. UGIDM prediction of upper gastrointestinal distress (UG) severity level for scenario A.

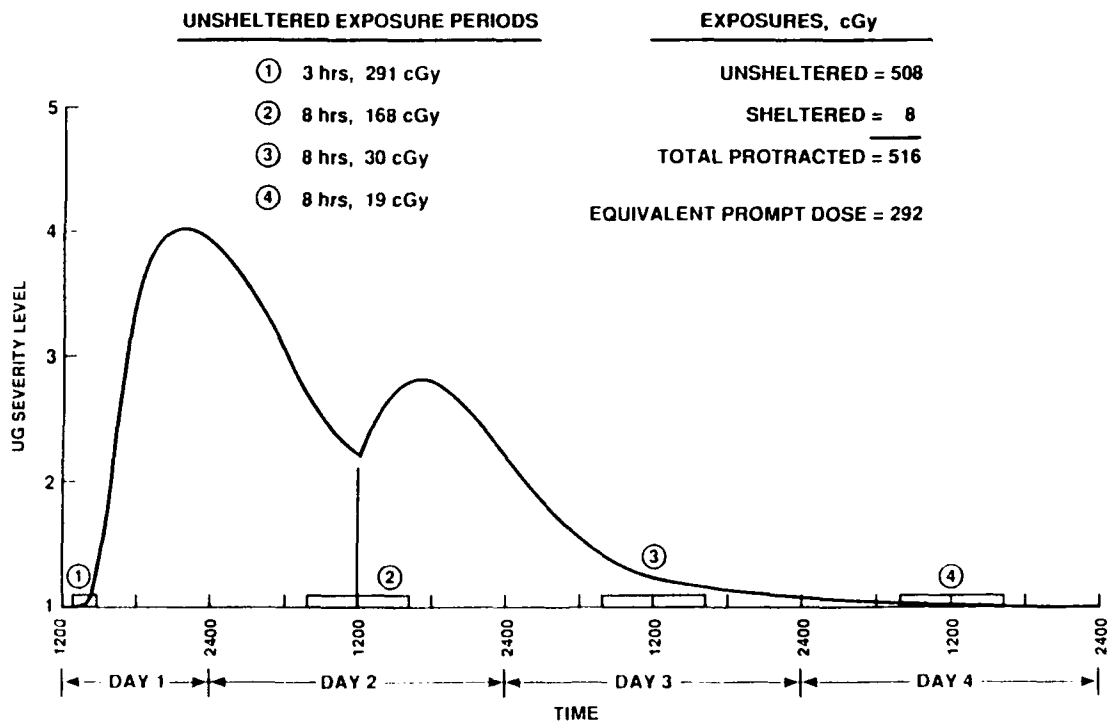


Figure 72. UGIDM prediction of upper gastrointestinal distress (UG) severity level for scenario B.

into the first part of day 2 due to the initial short 3 h period of exposure to early fallout radiation during an unsheltered posture. The UGIDM calculations do not predict a likely emetic bout due to the added 100 cGy acute exposure assumed for Scenario B. Also since the maximum levels are the same for Scenarios A and B, both have the same EPD value of 292 cGy.

4.4 THE FERRET--AN EXPERIMENTAL MODEL.

Both repeated exposures and continuous low dose rate exposures enter into important operational situations relevant to combat in a nuclear environment. Presently no comprehensive models or algorithms exist for predicting the severity of UG distress for mission exposure profiles other than single, acute doses. The UGIDM which we have developed is a means of addressing this problem. It is also important to obtain data which validate and provide confidence in the model in the following areas.

- Determine the low dose rate threshold below which prodromal UG symptoms cease to be expressed.
- Resolve the uncertainty in the shape of the curve of ED₅₀ versus continuous dose rate exposure for low dose rate approach to the threshold.
- Demonstrate the proposed diminishing expression of UG severity with time-separated (fractionated) exposures.

Experimental work by King [1988] and others [Andrews, Davis, and Hawthorne, 1986; Gyls and Gidda, 1986] indicates that the UG response of ferrets is qualitatively very similar to that of humans. Comparison with the human response summarized by Baum, Anno, Young, and Withers [1984] and Anno, Wilson, and Dore [1984] shows that apart from scale factors, the time and dose dependence of the ferret emetic response to acute doses closely resembles that of humans. The differences are mainly that the ED₅₀ is a factor of about 1.7 to 2.2

lower* and the postexposure response time about a factor of ten shorter for ferrets than for humans.

We believe that if the UGIDM can successfully relate the UG response of ferrets to acute and protracted doses, then with reasonable confidence, the model could be extended to humans with the appropriate modifications. To this end, we have outlined a series of fractionated and constant dose rate exposures of ferrets to characterize their UG distress response in the vicinity of the dose rate threshold predicted by the UGIDM. In applying the UGIDM to ferrets, the first task is to construct a severity scale for ferrets analogous to the one already developed for humans. This scale allows the quantification of UG severity curves versus time-after-dose for the presently available acute dose data in ferrets. Both the severity scale and curves for the ferret are patterned after the observations made by King [1988]. Next, these severity curves determine the set of best parameter values for the UGIDM. Finally, with these parameter values, the UGIDM is used to predict the UG distress response of ferrets to fractionated and continuous exposure.

4.4.1 UG Severity Scale.

Quantification of upper gastrointestinal distress in ferrets is based on signs rather than symptoms. Symptoms, by definition, are those feelings reported by the subjects and are not observable except by self-reporting. A sign of illness, on the other hand, is something that can be observed, i.e., an objective measure. Thus, animal experiments are based on signs such as temperature, emesis, muscular contractions, or characteristic behavior patterns.

The ferret UG distress severity level scale is patterned after the one for humans (see Table 28) devised for the DNA/IDP [Anno, Wilson, and Baum, 1985]. Normal, or no sign of illness, is designated level 1. The most severe form of illness is designated level 5.

*For an acute exposure, we estimate an ED₅₀ of 170 cGy for emesis in humans, whereas, in ferrets, King [1988] finds an ED₅₀ of 98 cGy; when retching is included, he finds a value of 77 cGy. Our estimate for humans is based on a probit regression analysis of the emetic response of 40 cases of accidental exposure (see Appendix B).

Table 28. Severity levels of upper gastrointestinal (UG) distress in ferrets.

Severity Level	Signs
1	No effect.
2	Behavioral signs of nausea such as lip-licking, clawing roof of mouth, burrowing motions.
3	Retching, one or two episodes of controlled vomiting.
4	Controlled vomiting, repetitive, preceded by behavioral changes and/or retching.
5	Uncontrolled vomiting, not preceded by retching, sometimes projectile; lethargic between episodes (accompanied by diarrhea).

Level 2 is defined by the mildest (or least behaviorally disruptive) set of signs which are always associated with the UG distress.

Levels 3 and 4 are comprised of signs which are apparently more severe, are more behaviorally disruptive, and generally are associated with higher radiation doses.

The severity scale is properly an ordinal scale rather than a ratio scale. That is, increasing severity level corresponds to increasing severity of illness, but there is no guarantee that illness is quantitatively proportional to the numerical severity level. Accordingly, it must be kept in mind that it is an approximation to use the severity level in numerical calculations as we do below.

Table 28 presents the UG distress severity scale for ferrets that we have constructed. Level 2, associated with nausea (presumed) and its related symptoms in humans, must be cast in terms of observable signs in ferrets. King [1988] reports that the signs shown in Table 28 seem to precede vomiting at lower doses. Since he has not quantified the relationship, it would be illuminating to measure these (and any other signs associated with nausea) at doses around the threshold for emesis. However, at present there is no basis for separating these behaviors to denote different severity levels for

nausea, presumed in the ferret. Therefore, in the ferret, only the single level 2 is designated for nausea alone. On the other hand, for humans, the severity level scale for UG distress (Table 27) is based both on signs and symptoms, where nausea is present at three levels of severity (3, 4, and 5) according to experience related by humans. Accordingly, exactly matching UG severity level cannot be expected other than the common number of severity levels that are invoked.

We assume that severity level 3 is related to the ED₅₀ for emesis in the ferret, whereas in humans, an intermediate severity level between 3 and 4 relates to the ED₅₀ for emesis. Like King [1988], we include retching as well as productive vomiting in the ferret emetic response. By definition, half of the animals in a group receiving the ED₅₀ dose do not have emesis, and we assume that these animals will either have retching without vomiting or will be at severity level 2. Of the animals that do have emesis, most will be at level 3. A small fraction of the animals may be at level 4. Thus, level 3 typifies animals that have emesis for doses in the vicinity of the ED₅₀. Later calculations will be given for the severity level as a function of dose and time; it should be interpreted as the mean severity level over a sample population, since a given dose will induce varying severity levels in different individuals. As the dose is increased to ED₉₀, most animals will be at severity level 3 and quite a few will be at level 4.

For levels 3 and 4, we use the term controlled vomiting to incorporate King's observation that at lower doses, the animals vomit toward the area where they normally defecate; apparently the animal is well enough to make this choice. At higher doses, the animal is so sick (its behavior pattern so disrupted) that it vomits anywhere. In that case, the term uncontrolled vomiting applies.

Level 4 is distinguished from level 3 by more episodes of vomiting and by a longer interval of continuing occurrence. Furthermore, all animals suffer productive vomiting rather than nonproductive retching.

Level 5 corresponds to the most severe form of UG distress reported by King and occurs at doses of 5 to 10 times the ED₅₀ value. Vomiting is uncontrolled as to location and is sometimes projectile. The onset is sudden, not preceded by retching. The animal is lethargic between episodes and usually suffers diarrhea as well.

4.4.2 UG Severity Curves for Acute Dose.

King [1988] presents extensive data on radiation-induced emesis in ferrets for acute doses. In addition to his qualitative description, the following quantitative information is particularly helpful: the percent responding versus dose for emesis and retching, the actual time histories of emetic episodes for individual animals at different doses, and the mean time to first emesis versus dose.

Figure 73 shows ferret curves of average UG severity for five acute doses according to our interpretation of King's data. We constructed the curves by plotting the heavy dots shown in the figure and then connecting them with straight lines. The lines were not extended down to severity level 1 (no effect) because King did not report beginning and ending normal times. In fact, even the times for severity level 2 are mostly guesses at this point. The higher levels

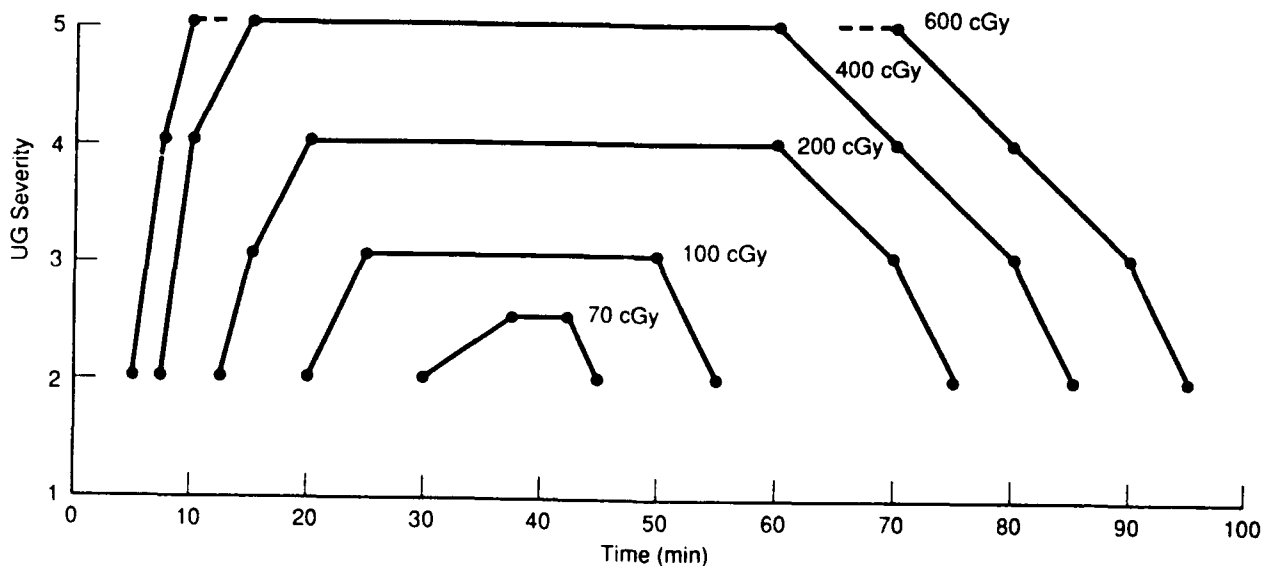


Figure 73. Ferret upper gastrointestinal (UG) distress--postexposure severity levels.

are more directly connected to the data as illustrated in the following discussion.

Considering the severity curve versus time for an acute dose of 200 cGy, King's behavioral observations at 201 cGy and below were used to define severity level 4. Thus, the maximum severity level for 200 cGy is 4. The time at which the 200 cGy curve reaches level 3 is the time of earliest emesis observed in the group of animals exposed at that dose, namely 15 minutes. The time at which the curve reaches level 4 corresponds to the mean time to first emesis for the group. All six of the animals exposed at this dose had emesis. The time at which the severity begins to drop from level 4 corresponds roughly to the mean time of last emesis. The level drops to 3 at about the time of latest emesis observed in the group. Similar considerations were used to locate the 400 and 600 cGy curves.

The peak severity level for a 200 cGy dose is set at 3. At this dose, King's dose-response curves show that about 50 percent of the animals suffer emesis and more than 75 percent suffer retching and/or emesis. The time to reach level 3 is about the time of earliest emesis observed. The time at which the curve drops from level 3 is about the time of the last observed emesis.

The lowest severity curve in Fig. 73 is for a dose of 70 cGy. At this dose, King's dose-response curves show about 20 percent emesis and about 35 percent retching and/or emesis. This situation seems a little worse than level 2 but on the average less than level 3, so we set the peak severity at 2.5. This peak occurs at 40 min, the time of the single observed episode of emesis, and lasts for only 5 min. Obviously, this curve is qualitative and should not be taken too literally.

The extension of all of the curves to severity level 2 is entirely a matter of judgment since King did not report quantitative data on the behavioral signs of nausea. The extensions were based mainly on generating a family of smooth curves.

Figure 73 is our starting point for applying the UGIDM to quantify UG distress in ferrets. These severity level curves should be considered preliminary and subject to improvement. With these curves

as an example, it would be more desirable to formulate an entirely objective procedure for their construction and then to design an experiment to determine the curves. However, in the meantime, we proceeded to fit the UGIDM to the curves keeping our expectations qualitatively consistent with the nature of the data.

4.4.3 UGIDM for Ferrets.

Figure 74 presents the UGIDM fitted to the ferret severity level curves of Fig. 73. The model parameters are included in Fig. 74. The shape parameter γ was held at 2.2; also, the reservoir recovery parameter μ was set at 0.002 h^{-1} . The remaining parameters were set by a least squares fit to the severity curves.

The agreement between the UGIDM and the severity level curves is qualitatively very good. The apparent disagreements are simply the result of the disparity between the two methods of describing UG distress. The curves in Fig. 73 arise from a basically tabular description of experimental observations for acute exposure. There is

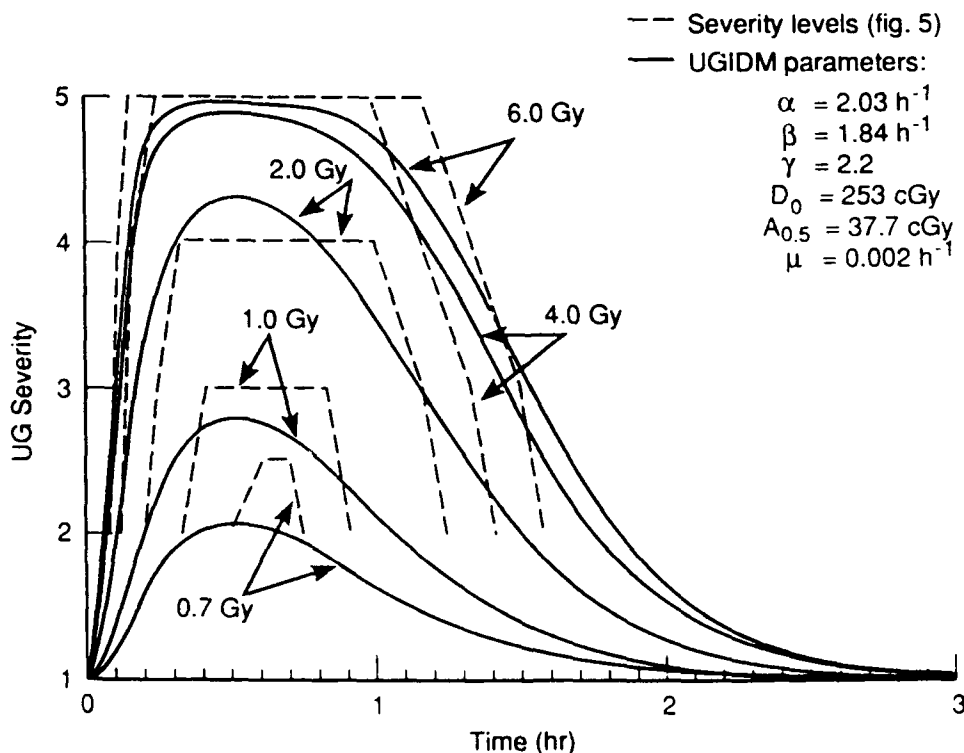


Figure 74. UGIDM acute dose severity levels for ferret--upper gastrointestinal (UG) distress.

no intuitively pleasing way to extend these observations to other exposure histories. The curves given by the UGIDM, on the other hand, arise from a mathematically continuous model for UG severity constructed to mimic the biological processes underlying UG distress. The UGIDM can be straightforwardly extended to any exposure history.

The UG DM predicts how UG severity fades away to low levels that are not presently quantifiable by experiment. These tails given by the UGIDM curves cannot be compared with present data and should not be considered a shortcoming of the model. The tails could be eliminated by a mathematical clipping procedure according to some threshold; however, since there is no firm data to determine the threshold and the tails arise from mathematical continuity essential for the application to continuous or fractionated exposure, they currently remain as shown in Fig. 74.

The utility of the UGIDM is its ability to predict the response to both continuous and fractionated exposures. However, we need to understand what features of that response the UGIDM is likely to predict reasonably well; the primary ones are:

- The approximate onset time of signs of UG distress.
- The approximate peak severity level.
- The approximate time of peak severity.
- The approximate time to recover from the higher levels of UG distress.

We believe that experiments using ferrets can serve to provide an understanding of these features.

4.4.4 Fractionated And Continuous Exposures Predictions.

Figure 75 shows the predicted time dependence of the severity of ferret UG distress for a fractionated exposure consisting 3 fractions of 200 cGy separated by 2 h intervals. The UGIDM parameters shown in Fig. 74 were used for the prediction. Two features are noteworthy. First, the 2 h interval is long enough for the UG distress to almost completely subside before the next dose fraction is delivered.

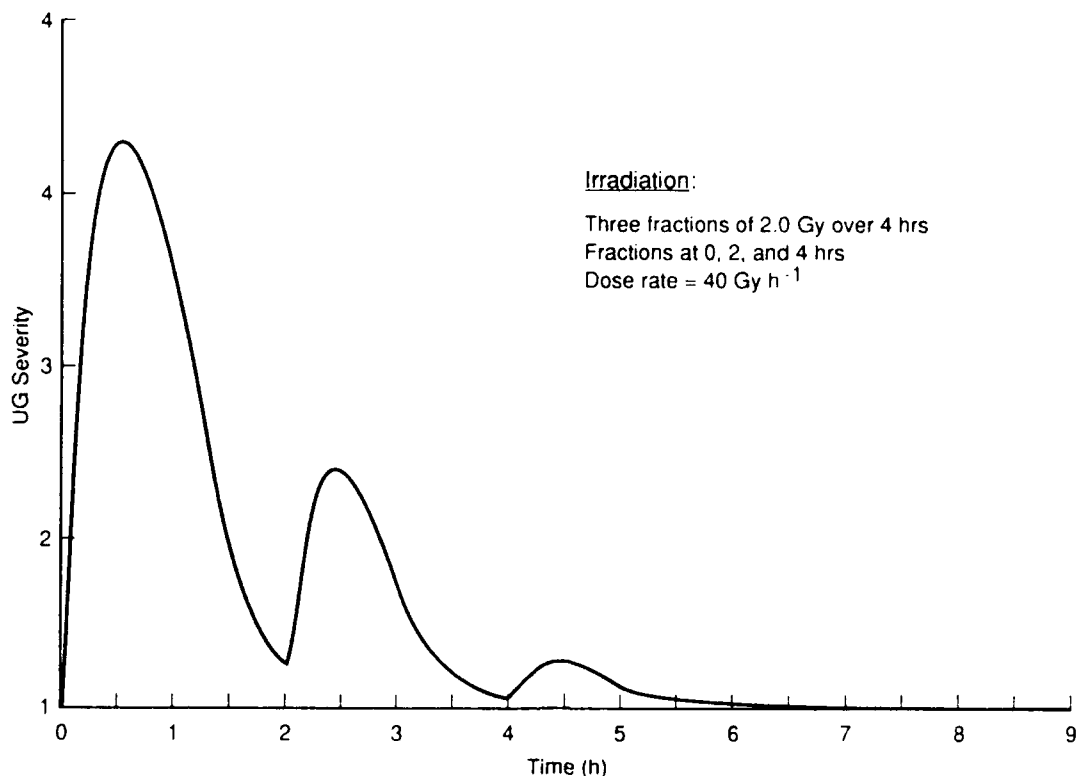


Figure 75. UGIDM prediction of severity level for upper gastrointestinal (UG) distress in the ferret--fractionated dose.

Second, a 200 cGy fraction severely depletes the reservoir from which the hypothetical UG toxins are produced. Thus, the maximum severity level from the second and third fractions are greatly suppressed.

Both of these effects should be easily confirmed or disproved by experiment. This type of experiment with varying time intervals and dose fractions should be effective for the determination of the best values of the reservoir depletion parameter D_0 and the reservoir recovery rate μ . Determination of the reservoir recovery rate will require that other aspects of radiation sickness do not entirely mask the UG distress for later fractions.

For continuous exposures, we used a different method for presenting predictions of the UGIDM. Figure 76 plots the relationship between dose and dose rate for selected levels (2, 3, and 4) of peak UG severity. Accordingly, these curves are isoseverity doses versus dose rate. The high dose rate limits of the isoseverity curves (right hand intercepts of Fig. 76) are values that can be interpolated from the acute dose curves of Fig. 74.

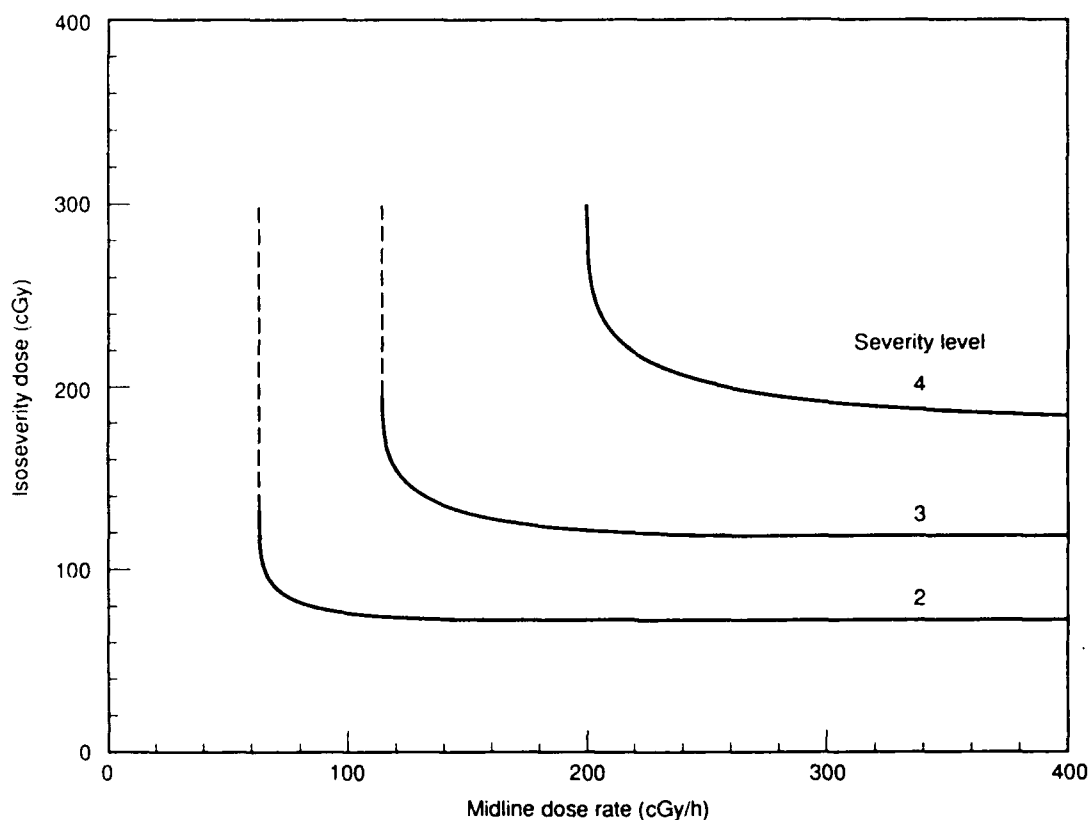


Figure 76. UGIDM calculations of isoseverity dose versus dose rate for UG distress levels (2, 3, and 4) in the ferret.

At an intermediate dose rate ($100\text{--}300\text{ cGy h}^{-1}$), the severity versus time predicted by the UGIDM (not shown) peaks a little later than at high dose rate. Because of toxin clearing during exposure, it requires a higher total dose for the severity to peak at a fixed level. Thus, the isoseverity dose increases as the dose rate decreases.

At low dose rates, the severity versus time (also not shown) predicted by the UGIDM rises slowly and eventually approaches an equilibrium value that depends on the balance between toxin production and clearing rates and that between the reservoir depletion and replenishment rates. Since longer times are required at lower dose rate to achieve a specified severity level, the isoseverity dose curves of Fig. 76 turn upwards. Ultimately, the dose rate becomes too low to induce the specified severity level where the equilibrium severity level is below that specified and, in principle, the dose can get infinitely larger without causing the specified severity. The

results illustrated in Fig. 76 indicate that there are specific threshold dose rates below which particular severity levels are never reached.

This prediction of a threshold dose rate by the UGIDM must be kept in context. It applies to early UG distress only. The validity of the model probably extends just a few hours for the ferret. For longer times, other aspects of radiation sickness will come into play and possibly induce some of the signs of UG distress through other mechanisms not specifically addressed by the UGIDM.

In the UGIDM, the dose rate is an independent variable that directly controls the production rate of the UG toxin. The clearing of this toxin is controlled by the parameter β . Therefore, observations of the UG severity level versus dose rate offer an experimental verification of the value of β determined from acute doses. On the other hand, if the assumptions of the UGIDM are not valid, then these experimental observations should invalidate the model and point the way to a more realistic one. In either case, we believe that experiments with ferrets offer an empirical means for understanding the effects of dose protraction on UG distress.

4.4.5 Suggested Ferret Experiments.

We intend that the experiments suggested below on the occurrence of UG distress in the ferret will provide empirical guidance for estimating UG distress in humans for protracted doses. Our approach is to assume that the prodromal response model is reasonably valid for both humans and ferrets. The important aspect of the UGIDM is that it provides a mathematical response relationship between acute and protracted doses. If this relationship can be demonstrated in ferrets, then it can more reasonably be assumed that it is similarly valid in humans.

It is primarily the mathematical form of the UGIDM that we hope to validate rather than the parameters of the model. The parameters for human UG distress can be determined from the available human data. The ferret experiments are intended to determine if a single set of parameters for the ferret are capable of reproducing UG dis-

tress levels for both acute and protracted doses. If so, then the form according to our theoretical assertions will be validated. Figure 77 shows a UGIDM comparison of isoseverity doses versus dose rate for humans and ferrets. It emphasizes that even though the effective dose levels and threshold dose rates are different, the mathematical form of the model is the same in both cases. If the model proves to be incapable of correctly describing the response to both acute and protracted doses, then we expect the ferret data to suggest alternative modeling approaches.

In the following paragraphs, we present suggested experiments for both fractionated and continuous exposures. Observations should consist of the quantitative data on emesis and retching reported by King [1988], supplemented, if possible, by behavioral changes related to severity level 2 of the UG distress scale. It would also be helpful to quantify the differences in the nature of emesis between severity levels 4 and 5. We assume that gamma rays will be used for all radiation exposures, preferably the same energy for both acute and protracted exposures.

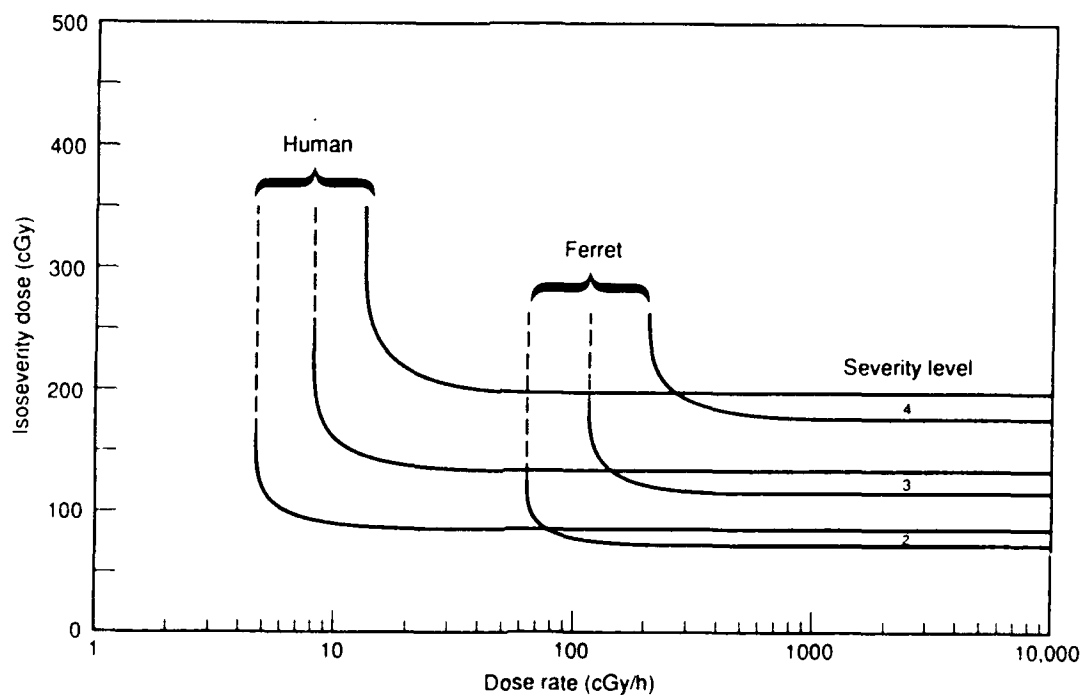


Figure 77. UGIDM calculations of isoseverity dose versus dose rate for UG distress levels in ferrets and humans.

Fractionated Exposures. The purpose of experiments with fractionated exposure is to quantify the expected habituation effect, that is, the reduction in response to repeated exposures. Based on the UGIDM, the predicted response of ferrets to fractionated doses was discussed previously in this section. Figure 75 presents the particular case for 3 fractions of 200 cGy each separated by 2-h radiation-free periods. The total observation time for an experiment paralleling the exposure protocol represented in Fig. 75 would be 6 h or so. There should be a control group receiving one 200 cGy dose and a control group receiving 2 fractions of 200 cGy each separated by 2 h. Both control groups would be observed for 6 h also.

The dose rate at which each fraction is delivered should be high enough that the exposure time is much less than the onset time for emesis after each dose fraction. Two hundred cGy delivered at 40 cGy/h would be an exposure time of 3 min, comfortably less than the onset time of about 15 min reported by King [1988].

If practical considerations argue for a lower dose rate for each fraction, it might be possible to get useful data for exposure times as long as 10 min and doses per fraction as low as 100 cGy. The corresponding dose rate is 6 cGy/h or 10 cGy/min. Lower dose rates would move into the realm of continuous exposure.

Continuous Exposures. The purpose of experiments with continuous exposures is to quantify the expected reduction in severity of UG distress for continuous exposures at low dose rate. The predictions of the UGIDM for continuous exposures were presented above in this section. Figure 76 shows that the dose required to reach a given severity level increases as the dose rate is reduced until finally a threshold dose rate is reached below which the given severity level does not occur as an early response.

One way to experimentally determine the isoseverity curves of Fig. 76 is to start at a dose rate 4 Gy/h where the dose to reach severity level 3 (approximately the ED₅₀ for emesis) is still close to the acute value, about 100 cGy. The exposure time would be 15 min, somewhat less than the onset time of 25-30 min at this dose. Only a few animals would be required to verify that the ED₅₀ is still about 100 cGy at this dose rate.

The second step would be to halve the dose rate to 2 Gy/h. The exposure time would then be 30 min for 100 cGy, close to the mean onset time for an acute dose. At this dose rate, the UGIDM predicts a 10-20 percent increase in the ED₅₀. It should still be easy to find the ED₅₀ dose even if the model prediction is inaccurate. It will be necessary to observe the animals during the exposure period as well as after.

The third step would be to halve the dose rate again to 1 cGy/h. The exposure time would then be 1 h for 100 cGy. This dose rate is below the predicted threshold for emesis in the PR model. Figure 76 shows that for a dose of 100 cGy, only severity level 2 is expected, that is, behavioral signs related to nausea. This prediction should be easy to check. Then it would be informative to see if emesis reappears at higher doses, such as around 200 cGy, that would require a couple h of exposure.

The experimental procedure from this point on would be dependent on the collective results obtained. If emesis is still observed on the third step at 1 cGy, then another halving of the dose rate is indicated. Otherwise, an elaboration of the shape of the severity level 3 (ED₅₀) curve at dose rates just above the threshold would help to reveal the correct modeling. The shape of the curve at these dose rates is important whether or not there is a distinct dose rate threshold for emesis.

It is sometimes more useful to think about and plan experiments based on exposure time rather than dose rate. The above discussion points out that the exposure periods where significant dose rate effects are predicted range from 15 min to a few h for the ferret. Figure 74 shows that the characteristic response time of a ferret to an acute dose lies within this range of exposure periods.

In this section, we have presented a model (UGIDM) for upper gastrointestinal distress and suggested means of additional model verification. In the following section, we describe another model for lower gastrointestinal distress.

SECTION 5

GUT INJURY MODEL

Our gut injury model (GIM) of the symptoms of lower gastrointestinal (LG) distress is based on the anatomy and physiology of the intestinal mucosa, in particular, of the layer of epithelial cells forming the surface of the mucosa. Both the incidence and severity of diarrhea and fluid loss will be related to the epithelial cell population level of the mucosa, as will the incidence of lethality from gut injury. Although we have considered the possible effects of reduced functionality of mature epithelial cells and of reduced vascularity of the villi after radiation exposure, these effects are not yet included in the GIM.

The following subsections describe the human symptomatology that is modeled, the physiological basis of that symptomatology, the structure of the model, and the validations that have been done so far with animal data.

5.1 SYMPTOMATOLOGY OF LG DISTRESS.

Figure 78 summarizes the symptomatology of LG distress by plotting the severity level versus time of LG distress in humans after an acute dose (FIA) in the indicated ranges [Anno, Wilson, and Baum, 1985]. The primary sign/symptom is diarrhea with accompanying discomfort and cramping. The symptoms occur in three phases.

First, at doses higher than about 3 Gy, there is a relatively low incidence of early LG distress occurring a few hours after exposure. There is some tendency for the incidence to increase with dose; however, it does not exceed 30 percent even at doses of 30 to 45 Gy and lasts only a few hours.

The second and most prominent phase of LG distress occurs about four days after acute exposure. At doses in the 8 to 11 Gy range and above, diarrhea occurs with essentially 100 percent incidence. Severity increases at higher doses, and the onset time advances somewhat, beginning as early as three days in the 30 to 45 Gy dose range.

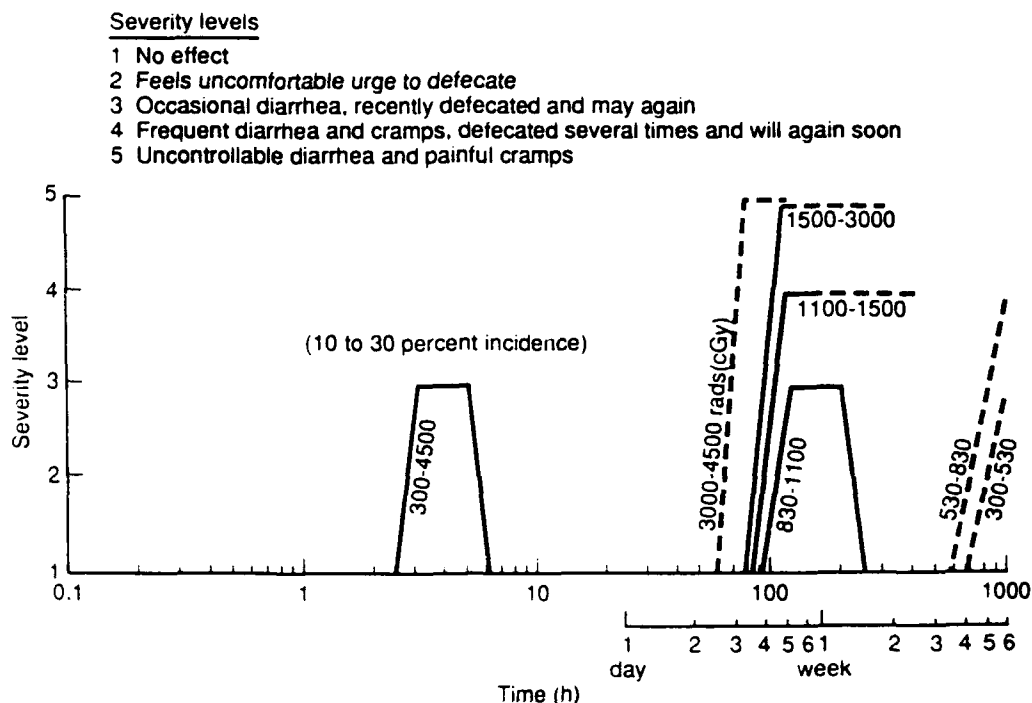


Figure 78. Lower gastrointestinal (LG) severity levels for acute dose ranges cGy (free-in-air).

This consistent pattern of diarrhea is followed within a day or two by symptoms of fluid loss and electrolyte imbalance.

Finally, at doses in the 3 to 8 Gy range, LG distress is again prevalent four or five weeks postexposure during the manifest illness phase of radiation sickness.

For the dose and time-after-dose regions indicated with dashed lines in Fig. 78, there is a significant rate of mortality so that the indicated severity levels are relevant only for survivors.

5.2 CAUSES OF LG DISTRESS AND LETHALITY.

The origin of the early LG distress occurring a few hours after exposure is not known. It may be secondary to the toxicokinetic effects that lead to UG distress or it may be a psychological response to radiation exposure. The effect is reported over a wide range of doses with only a weak dependence of incidence on dose level [Anno et al., 1989]. Since it is not directly related to the level of the epithelial cell population in an apparent way and the incidence is low, we leave modeling of this early response to a future effort.

The last phase of LG distress at four to five weeks is secondary to the immune system collapse that results from radiation damage to the hematopoietic system. The intestinal mucosa deteriorates because of failing physiological support from the blood system. This phase of GI distress occurs only in a narrow range of doses. The dose must be high enough to cause lethality from the bone marrow syndrome in untreated individuals but low enough to permit survival out to the four to five week time frame. The modeling of this interaction between the mucosa and the blood system will also be left to future work when a suitable model of the hematopoietic system becomes available.

The middle and most prominent phase of LG distress occurs for doses above 8 Gy approximately and is caused primarily by radiation damage to cells of the intestinal epithelium. This population of epithelial cells forms a continuous layer, one cell thick, which separates the lumen, or interior space, of the intestine from the interior of the body. Although there is a hierarchy of projections and folds in the layer of epithelial cells, the layer is topologically a simple tube that separates the partially digested contents of the lumen from a dense layer of lymph and blood vessels in the intestinal wall. The epithelial layer maintains the proper fluid and electrolyte balance between lumen and the body and transports nutrients from the lumen to the blood stream. In addition, the epithelial cells play an active role in processing nutrients by breaking down both complex sugars and polypeptides. Also, since the lumen is topologically connected to the outside world, the epithelial layer is a crucial barrier against microbial infection of the body. For all of these reasons, the integrity and functionality of the intestinal epithelium is critical for maintaining bodily health. Radiation exposure induces LG distress and gut death by damaging and killing the cells of the intestinal epithelium.

Lethality from radiation damage to the intestines (gut death) is clearly linked to denudation of the mucosa, that is, the complete disappearance of the epithelial cells covering the villi. Gut death for rats and most likely other mammals is due to hypovolemic shock caused by the inability of the denuded mucosa to absorb fluid and

electrolytes [Jackson and Geraci, 1986]. The correlation between clonogen survival in the intestinal crypts and lethality [Withers and Elkind, 1969; Thames and Hendry, 1987] was discussed in Sec. 2.

We assume that the symptomatology of LG distress is also related to the loss of epithelial cells, although it is possible that some LG distress may be caused by reduced functionality of mature epithelial cells. There is some evidence from animal data of impaired functionality of the intestinal epithelium after irradiation but before a significant change in cell number. Experiments with rabbit ileum in vitro [Gunter-Smith, 1989] have shown a switch in Cl transport from absorption to secretion 24 h after doses in the range of 8.5 to 12 Gy. Cl excretion in vivo would cause osmotic loss of water to the lumen and is associated with diarrheal diseases. On the other hand, no change was observed in net Na transport and at 10 Gy there was no significant reduction in the absorption of the actively transported amino acid, alanine, until 96 h postexposure when denudation of the villi becomes a factor.

Jackson and Geraci [1986] report an ED₅₀ for diarrhea in conventional rats of about 11 Gy at 24.6 Gy/h dose rate versus an LD_{50/5} of 14.1 Gy. The fact that diarrhea occurs at a lower dose than lethality apparently indicates that diarrhea is associated either with some functional impairment of the mucosa as indicated by the in vitro work of Gunter-Smith or with a moderate reduction in the cell population short of denudation. Jackson and Geraci report that the onset of fluid loss and diarrhea is three to four days, consistent with the expected time of minimum cell population of the intestinal epithelium after acute doses of this size.

At this point, we do not have conclusive evidence that radiation causes enough functional impairment of mature epithelial cells on the villi to cause noticeable signs/symptoms that would lead to performance decrement before there is significant atrophy and denudation of the villi. Since the possibility is not ruled out, we expect to consider this question again in the future.

The vasculature of the intestinal mucosa is also crucial to proper gut function. The vascular system is known to respond to doses of 5 to 10 Gy over the day or two time frame [Griem, 1989]. There is a clear reduction in the vascularity of the crypt and villi as the epithelial cell population drops [Boyer and Conger, 1972]. This reduced vascularity may be a primary effect of radiation exposure of the vascular system or a secondary phenomena of other mucosal damage. In any case, it is neglected in the present GIM. Since dose protraction might alter the nature of the interaction between the epithelium and the mucosal vasculature, this uncertainty deserves attention in future work.

In the meantime, we assume that the dominant physiological change causing the symptomatology of LG distress is the reduction in epithelial cell number. At the very least, we expect that the consequences of any functional impairment of mature cells on the villi will be correlated with reductions in cell number. This assumption results in a model of the intestinal epithelium based on cell number that is related to diarrhea, fluid loss, and gut death in mice and rats.

5.3 MODEL DESCRIPTION.

The GIM unifies mathematical expressions of the proliferation, radiation damage and repair, and hierarchy of the intestinal epithelial cell population as a set of differential equations and subsidiary conditions. Since dose rate is a driving term in the equations, the GIM accommodates any dose protraction. Solutions to the equations are computed with standard difference techniques. This subsection provides a description of the structure of the intestinal epithelium, its dynamic equilibrium properties, and its radiation response as represented by the GIM equations.

5.3.1 Anatomical And Physiological Modeling Basis.

Figure 79 is a simplified version of a cross section of a small part of the intestinal wall that we use for modeling purposes. Our primary reference for the anatomical structure and dynamics of the

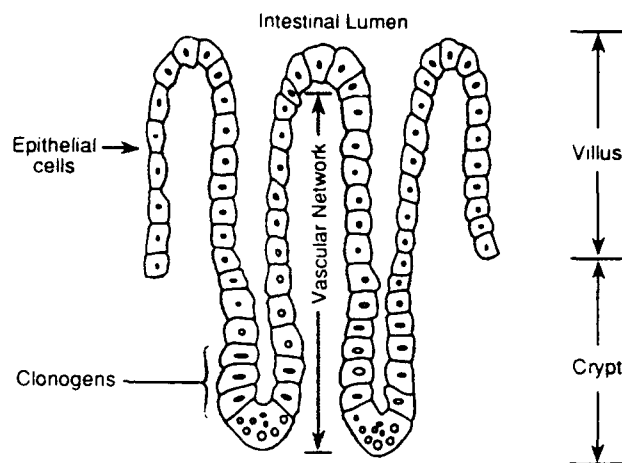


Figure 79. The villus/crypt structure of the intestinal epithelium.

intestinal epithelium is Chapter 3 of the book "Cytotoxic Insult to Tissue: Effects on Cell Lineages" [Potten and Hendry, 1983]. The intestinal epithelium is a dynamic, single-layer cell population having one of the highest turnover rates in the body. This high turnover rate results in an early response of the tissue to radiation exposure.

The compartment of functional epithelial cells is located on the surface of the villi. These cells continually move up the finger-like villi and are cast off the tip and lost to the intestinal lumen. Around the base of each villus are ten or twenty crypts, or well-like depressions, lined with epithelial cells that form a continuous sheet with those covering the villi. Roughly the bottom one-third of cells lining the crypt are clonogenic. This compartment of clonogenic cells is rapidly proliferating and is the source of new cells to replace those lost at the tip of the villi. The epithelial cells in the upper two-thirds or so of the crypt are called transit cells. As cells move through this transit compartment, they differentiate to a mature, functional state and their proliferation ceases. A tissue with this separation between proliferating, clonogenic cells and nonproliferating, functional cells is referred to as a hierarchal, or "H" tissue.

The cells of the clonogen population are the most sensitive to radiation because of their high rate of proliferation, or cell cycling. The D_0 , or dose that reduces survival by a factor of e , is about 1.1 Gy (110 rads). Since there are only 100 to 300 cells in the clonogenic compartment of a crypt, a dose of 5 or 6 Gy leaves only about one surviving clonogenic cell per crypt. If one or more cells survive in a crypt, a new colony of clonogens will develop and allow regeneration of the crypt after a sufficient number of cell cycles. Until recovery of the crypts, the villus will atrophy because of the normal attrition rate of functional cells. Withers and Elkind (1970) developed a microcolony technique to assay crypt survival in mice after radiation exposure and to deduce cell survival from the observations through a statistical (Poisson) correction for colony formation by multiple clonogenic cells.

Cells in the transit compartment and on the villi continue their upward migration to the villus tip after doses as high as 30 Gy. Since these cells do not proliferate or suffer gross damage even at this high dose level, the intestinal epithelium maintains its structural integrity until it is depleted by normal attrition of cells into the lumen. While the epithelial layer is still intact on the atrophying villi, it provides some level of functionality and an effective barrier against microbial invasion. However, at high doses within a period of a few days, the villi become denuded of epithelial cells, typically leading to fluid and electrolyte imbalance, infection, and death within about five days postexposure. Jackson and Geraci [1986] have concluded that, in mice and rats, this so-called gut death is due predominately to hypovolemic shock brought on by loss of the intestinal epithelium.

Withers [1989] and others have shown that the $LD_{50/5}$ in mice corresponds to the survival of about one-third of the crypts in the jejunum. For doses less than the $LD_{50/5}$, crypt recovery occurs soon enough to prevent serious mucosal denudation.

The GIM is constructed to match the structure and dynamics of this somewhat simplified picture of the intestinal epithelium. Since we found an abundance of data for the jejunum, which is the central

section of the small intestine, we have used it as the basis for the GIM. Straightforward parameter changes can be applied to adapt the model to other portions of the gut.

5.3.2 Modeling Arrangement of the GIM.

The computer implementation of the GIM consists of a nested arrangement of component models. The full set of equations is presented in Appendix C. We use the lethal potentially lethal (LPL) model of Curtis [1986] to calculate cell survival after radiation exposure. The LPL model is a unified damage and repair model for chromosome lesions. Both repairable and irreparable lesions are modeled. The LPL model provides the dose rate dependence of cell survival through a lesion repair rate with first order, or linear, kinetics and a misrepair rate with second order kinetics. It is a state-of-the-art model for radiation action in mammalian cells [Hall, 1988].

At the first level of model aggregation is PSR's Proliferation And Intracellular Repair (PAIR) model. The PAIR model combines the LPL equations for cell survival with equations describing cell proliferation and radiation-induced mitotic delay. The equations of the PAIR model are obtained from a mathematical derivation accounting for the statistical distribution of lesions among cells and how that distribution is influenced by the appearance of daughter cells and the disappearance of mitotically dead cells.

Finally, the PAIR model is combined with a compartmental description of the hierarchial structure of the intestinal epithelium. At this final level of aggregation, the inclusion of homeostatic control of the cell population and the linkage of symptomatology and lethality with villi population level results in the full GIM.

Figure 80 illustrates this nested arrangement of models for the GIM. The same arrangement can be used to model any other tissue of the body or *in vitro* cell line, where a separate PAIR model would be used for each proliferating compartment of the tissue. Linkage of the compartments and homeostatic control according to the physiology of the tissue provides an overall model tailored to the particular tissue.

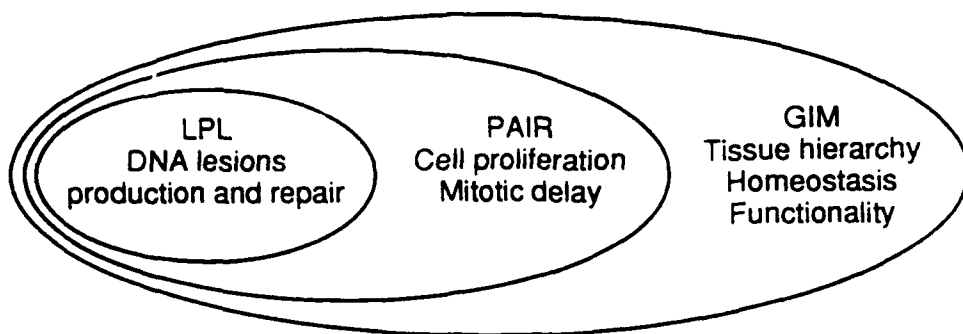
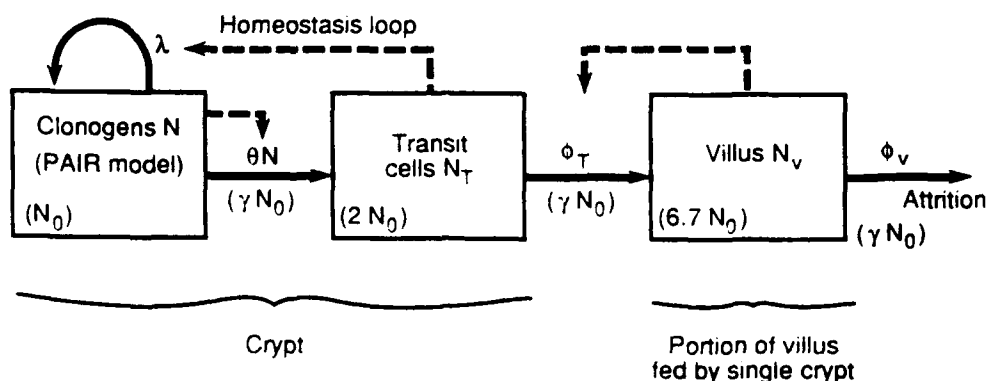


Figure 80. A nested arrangement of models provides the overall description of the response of the intestinal epithelium to protracted radiation exposure.

5.3.3 Compartmental Structure.

The GIM tracks the number of cells in three linked compartments: clonogens in the crypts, transit cells in the crypts, and functional cells on the villi. Figure 81 is a schematic diagram of the GIM, illustrating the compartments linked by fluxes of epithelial cells and feedback controls. Appendix C presents the equations for these fluxes. The linear arrangement of compartments is possible because of the simple geometry of the intestinal epithelium.

The cell populations of the compartments are normalized to the equilibrium number N_0 of clonogenic cells in a single crypt. The time dependent number of clonogens N is calculated by the PAIR model. The



Note: Equilibrium values in parentheses.

Figure 81. Schematic diagram of the cell compartments comprising the gut injury model (solid arrows represent cell movements; dashed arrows represent control signals).

time dependent number of transit cells N_T has an equilibrium value of $2N_0$, so that the fraction of clonogenic cells in each normal crypt is one-third. As discussed in Sec. 2, various data are available from both conventional and germfree mice. Germfree mice have larger crypts and longer survival times before gut death. The time dependent number N_V of functional cells on the villi has an equilibrium value of $1.7N_0$ for conventional mice, $6.7N_0$ for germfree mice, and $3N_0$ for man. The equilibrium number of cells in the compartments and the attrition rate from the villi are chosen to match available physiological data and to reproduce observed denudation times after large acute doses.

Radiation sensitivity in the model is confined to the clonogens. Clonogens are the most susceptible to radiation damage because of their high rate of proliferation, or cell division. A tissue dose greater than 15 Gy or so will kill nearly all clonogens in most crypts. With the supply of new cells interrupted, villi will atrophy and become denuded of epithelial cells in about 3.5 days in conventional mice, seven days in germfree mice, and six to seven days in man.

5.3.4 Symptomatology and Lethality.

The symptomatology of LG distress and the likelihood of gut death are assumed to depend on the number of cells in the villus compartment. The onset of the symptomatology occurs during the latter stages of villi atrophy just before denudation; mortality then follows denudation. We used the time-dependent cell population level to associate with these effects.

We expect that the frequency of diarrhea can be associated with the changing cell population level of the villi. In the present work we have taken only the first step by assuming that the ED_{50} for diarrhea corresponds to a certain minimum cell population regardless of the exposure history. The value of the minimum is determined from a GIM calculation of the villi population as a function of time after an acute dose that is equal to the known ED_{50} for diarrhea. For that dose, the GIM predicts a population nadir of about 27 percent occurring at a time consistent with the observed onset of diarrhea. We

therefore assume the 27 percent nadir in villi cell population to be the isoeffect indicating the ED₅₀ for diarrhea for protracted exposures. The resulting model prediction for the dose rate dependence of the ED₅₀ is presented in the next subsection.

In a similar manner, we determined an isoeffect that would predict lethality. Experience with mice indicates that a high incidence of lethality from gut death sets in only after a significant period of mucosal denudation [Withers, 1989; Matsuzawa and Wilson, 1965]; gut death may be avoided for only a brief period of denudation. Consequently, the LD₅₀ cannot simply be identified with a zero-level villi cell population. We therefore assumed that the isoeffect for predicting LD₅₀ for gut death corresponds to zero villi cell population over a certain time interval. This isoeffect is then used to predict LD₅₀ dose rate dependence for gut death. The next subsection presents the comparison of that model calculation with data, as well as other other validations of the model. We expect that future work will link the time dependent incidence of lethality with the villi population level.

5.4 VALIDATION OF THE GIM.

This subsection presents the application of the GIM to an extensive set of data on GI response to radiation in mice and rats.

5.4.1 Decline of Mucosa.

Mouse data on the morphological response of the intestinal mucosa validate the ability of the GIM to describe cell population levels after high doses. Figure 82 shows the GIM calculated crypt and villi cell counts versus time for mice after an acute dose of 30 Gy compared to the data of Matsuzawa and Wilson [1965]. This dose is large enough to kill essentially all clonogenic cells, so that the data represent crypt and villi atrophy rates in the absence of recovery. For simplicity, we have used identical crypt cell parameters for both conventional and germfree mice even though the data in Fig. 82 shows a small systematic difference in the crypt atrophy rates. However, the GIM does account for the nearly factor of two difference in the times

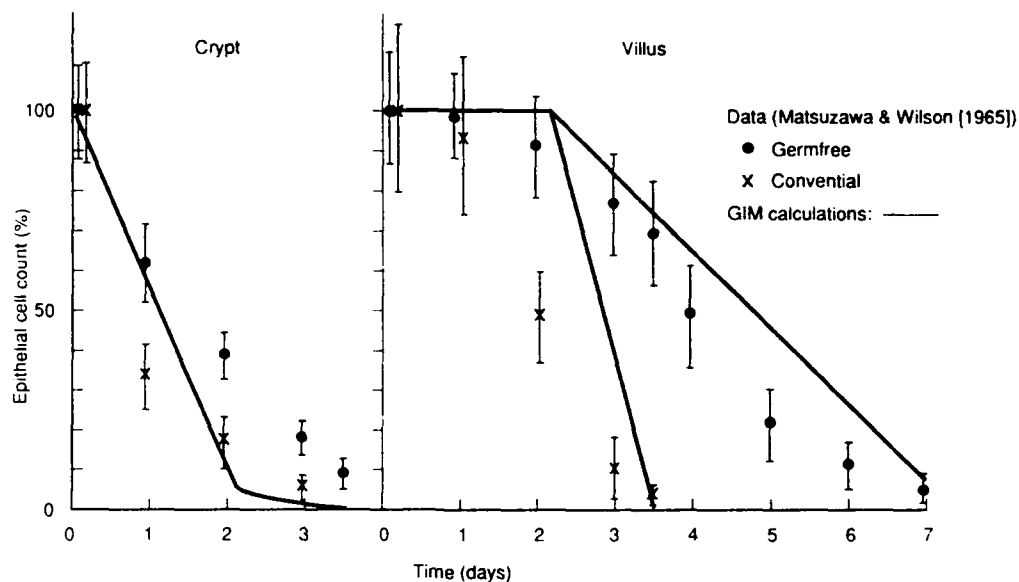


Figure 82. Crypt and villus cell counts of mouse ileum after sterilizing dose: 33.5 Gy @ 26.8 Gy/h, 250 kVp X-rays.

for complete denudation of the villi. As seen from Fig. 82, the GIM curves are in good qualitative agreement with the mouse data.

5.4.2 Crypt Recovery.

The recovery, or regeneration, of crypts after an acute dose provides information on the maximum rate of compensatory proliferation of epithelial cells and on the time delay before this high rate of proliferation is effective. Figure 83 compares the GIM calculation with crypt recovery data obtained by the split dose technique [Withers and Elkind, 1969]. The GIM curve shows the number of clonogens as a function of time after a single acute dose of 660 cGy of 200 kVp X-rays. The curve is normalized relative to the survival number from a single dose of 2075 cGy (without proliferation). After the completion of intracellular repair in a few hours, there is slow proliferative recovery over the first two days until the drop in transit compartment population induces rapid proliferation on the third day. This delayed recognition of damage is an important feature of the hierarchical structure of the GIM. The calculated clonogen population overshoots equilibrium by about a factor of two on the fourth day then settles back to equilibrium in a few days.

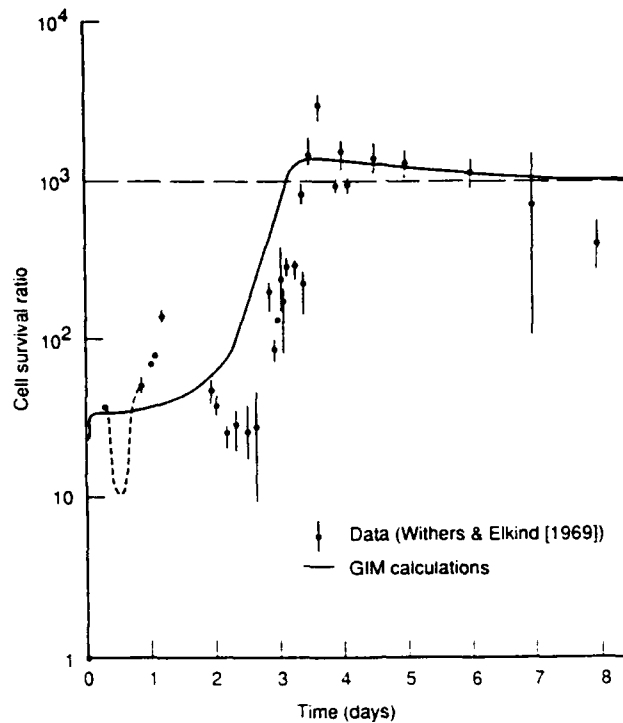


Figure 83. Cell survival ratio for recovery of jejunal crypt cells after 660 cGy acute dose, conventional mice, 220 kVp X-rays.

The data in Fig. 83 for surviving clonogens after a dose of 660 cGy were obtained by Withers and Elkind [1969] by assaying cell survival with the macrocolony technique. The experimental procedure applied a total dose of 2075 cGy split into a conditioning dose of 660 cGy and a test dose of 1415 cGy. The conditioning and test doses were separated by a fractionation interval equal to the time plotted in Fig. 83. The data show a sustained repopulation rise beginning about 2.5 days after exposure. The maximum rate of this compensatory proliferation occurs between 64 and 88 hours after exposure and has an e-folding time of about 6.1 h. Although the model curve starts to recover somewhat earlier than the data, the GIM has a maximum proliferation rate of $\lambda_M = .17$ inverse hours, or an e-folding time of 5.9 h, in close agreement with the data. The data in the overshoot region after 3.5 days have substantial variability, but there is good qualitative agreement between the GIM and the data. The homeostatic control mechanisms presented in Appendix C were adjusted to produce the overshoot.

The data in Fig. 83 show large fluctuations in the survival ratio before 2.5 days. The trend of the data between 8 and 16 h is represented by the dashed curve. These fluctuations are not reproduced by the GIM curve. Some of this variation, especially during the first few cell cycle times after exposure, likely originates in the differences in radiation sensitivity of the cell during the different phases of the cell cycle (see, for example, Bedford et al., 1980). Because of these sensitivities, the conditioning dose causes a redistribution of cells among the phases of the cycle. The resulting partial synchronization of the population leads to a systematic variation of the survival ratio with time that disappears after a few cell cycles when the population loses synchrony. We believe another cause of variation may be changes in the oxygen partial pressure within the clonogen population caused by the radiation response of the mucosal vasculature mentioned earlier. Neither of these sources of varying radiosensitivity are presently accounted for in the GIM. Thus, during the first two days or so, the model curve describes only the average behavior of the survival ratio.

5.4.3 Clonogen Response to Exposure at Constant Dose Rate.

Figure 84 illustrates the effectiveness of the GIM to describe the clonogen response to protracted radiation exposure. The figure compares GIM calculated curves for continuous exposure to data on the number of surviving clonogens versus exposure time at several dose rates between 0.5 and 6.0 Gy/h. The GIM correctly models the influence of intracellular repair at dose rates of a few Gy/h. Furthermore, it correctly describes the onset of compensatory proliferation after about 50 h at dose rates of 0.6 Gy/h and below. Since the present GIM does not include any variation of radiosensitivity during the cell cycle, there are systematic deviations of the data from the GIM curves when the exposure time is 20 to 50 h, comparable to the *in vivo* cell cycle time.

The data in Fig. 84 were used to determine eight of the parameters of the GIM for mice based on a weighted least squares fit. These parameters and their values are shown in the figure; also, a complete set of values of GIM parameters for mice and estimates for

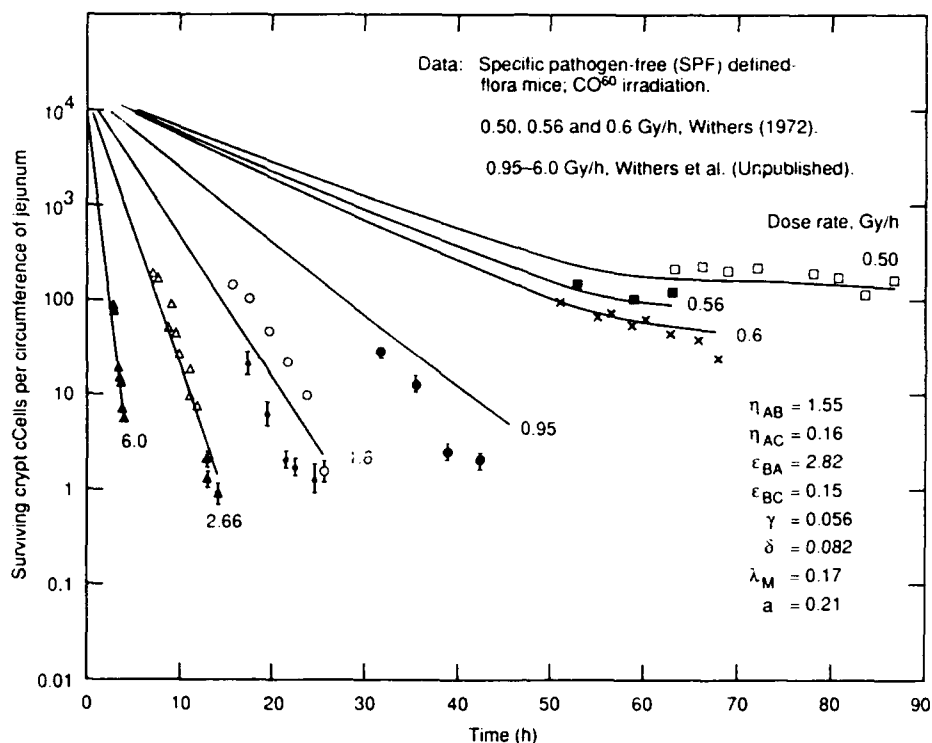


Figure 84. Crypt cell survival in mouse jejunum for varying dose rates, ^{60}Co radiation.

humans are given below in Table 30 of this section. The definitions of the parameters are given in Appendix C.

5.4.4 Dose Rate Dependence of $\text{LD}_{50/5}$ for Mice.

Invoking the link between denudation of the villi and gut death as described earlier in this section, we use the GIM to predict the dose rate dependence of the $\text{LD}_{50/5}$. The procedure is to find the denudation time corresponding to the $\text{LD}_{50/5}$, then determine the corresponding isoeffect dose as a function of dose rate.

Figure 85 shows the GIM calculations versus time of the villus cell population for conventional mice after a dose delivered at 30 Gy/h. The number plotted corresponds to the portion of a villus that is supplied with epithelial cells by a single crypt. The five doses shown in the figure include the $\text{LD}_{10/5}$ and the $\text{LD}_{90/5}$ obtained by scaling rat data given for these values in proportion to the mouse and rat $\text{LD}_{50/5}$ ratio at 30 Gy/h. For the four larger doses, the villus cell population drops to zero after 3.5 days. At the $\text{LD}_{50/5}$,

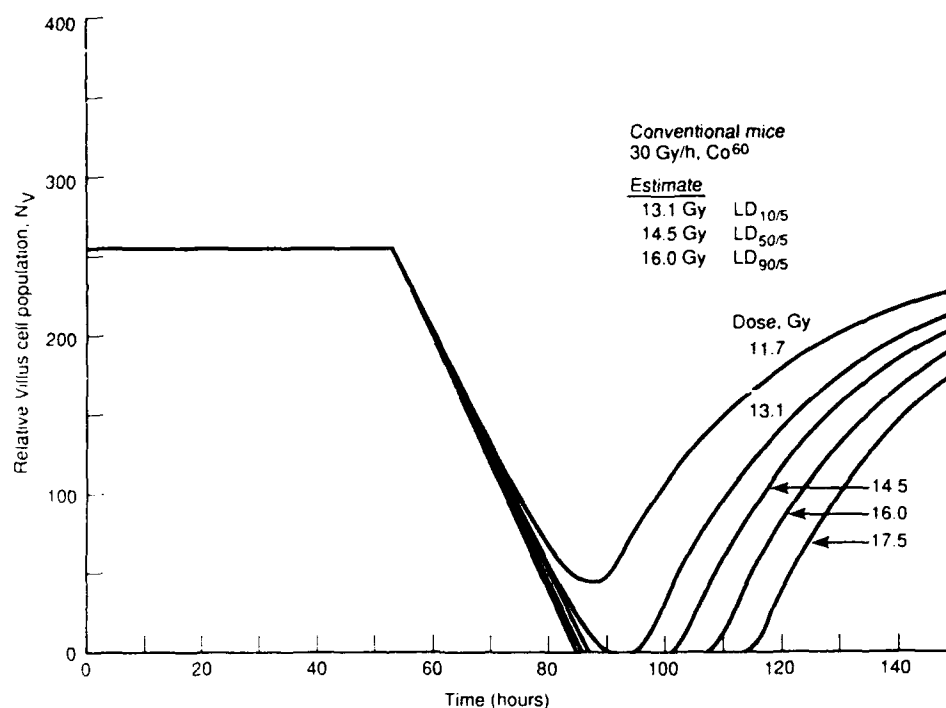


Figure 85. Relative villus cell population for conventional mice, 30 Gy/h, ^{60}Co radiation.

the villus remains denuded of epithelial cells for 14 h until the recovering crypt begins replenishment of cells. At the $\text{LD}_{10/5}$ dose, which is 1.4 Gy below the $\text{LD}_{50/5}$, the denudation lasts only 5 h. If the dose is reduced another 1.4 Gy to 11.7 Gy, denudation does not occur. The denudation time increases with dose above the $\text{LD}_{50/5}$. These denudation times have not been matched with laboratory data, but are within reason [Withers, 1989]. From Fig. 85, we conclude that the GIM provides a reasonable variation of the denudation time with dose and that the denudation time associated with the $\text{LD}_{50/5}$ in conventional mice is 14 h.

Table 29 presents the $\text{LD}_{50/5}$ dose as a function of dose rate based on the 14 h denudation period as predicted by the GIM. Figure 86 compares these data with the measured dose rate dependence of the $\text{LD}_{50/5}$ for mice [Krebs and Leong, 1970] in terms of the ratio of the $\text{LD}_{50/5}$ at constant dose rate to the $\text{LD}_{50/5}$ for prompt exposure. This measure was chosen in order to illustrate the dose rate effect while minimizing the influence of other factors such as dosimetry, RBE, experimental conditions, and variations in mouse strains.

Table 29. GIM calculated LD_{50/5} versus dose rate for conventional mice.

Dose Rate (Gy/h)	LD _{50/5} (Gy)	Dose Rate (Gy/h)	LD _{50/5} (Gy)
prompt	12.5	8.0	19.2
63.4	13.5	4.0	23.6
30.0	14.5	2.0	28.6
15.0	16.4	1.0	33.8

Although the data below 10 Gy/h deviate somewhat from the GIM curve in Fig. 86, it is clear that the GIM reproduces the trend of the data for protracted exposure. This agreement is significant since no lethality data for protracted exposure were used to obtain the GIM parameters for the lethality prediction calculations. The GIM uses only cell survival data and various anatomical and physiological features of the gut to predict gut lethality variation with dose rate.

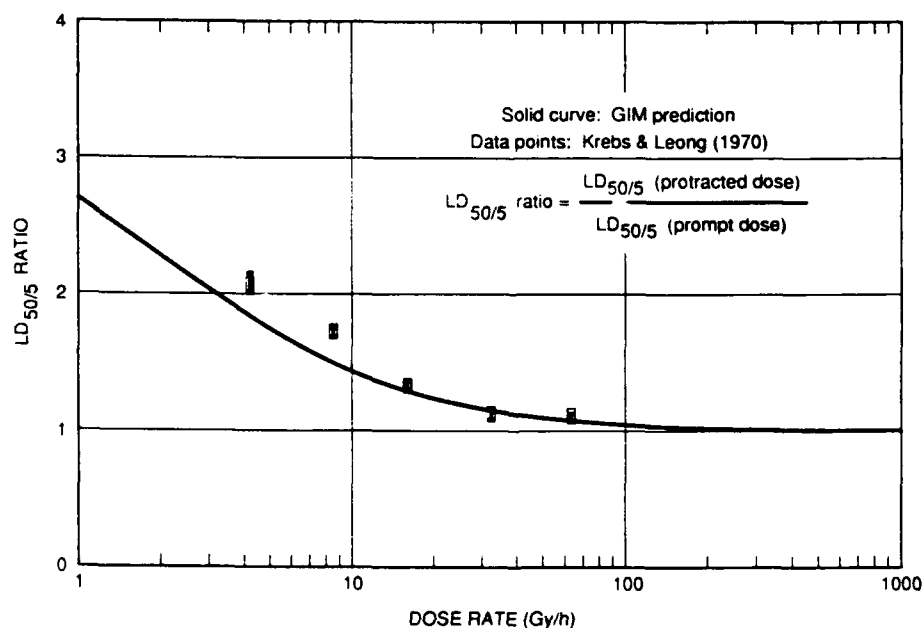


Figure 86. LD_{50/5} ratio related to constant dose rate exposure for mice.

5.4.5 LG Distress Symptomatology in Mice and Rats.

Figure 87 summarizes data on diarrhea and fluid loss in mice and rats [Matsuzawa and Wilson, 1965; Jackson and Geraci, 1986]. The following paragraphs describe GIM calculations and their relationship to this data.

Jackson and Geraci observed fluid loss in rats for doses of 17.3 and 11.5 Gy (Cs-137 gammas, 24.6 Gy/h) at both 3 and 4 days after irradiation but not earlier. At 11.5 Gy, no fluid loss was observed 5, 6, and 7 days after irradiation. At 17.3 Gy, the rats did not survive to 5 days postirradiation. No fluid loss was observed within one week of irradiation at a dose of 5.76 Gy. We have scaled these doses to mice using the mouse to rat LD_{50/5} ratio (15.0 Gy/14.1 Gy) at the dose rate of 24.6 Gy/h. The resulting doses for mice are 18.4, 12.2, and 6.1 Gy. From this rather coarse data, we estimate that the ED₅₀ for fluid loss in mice is between 6 and 12 Gy, and that the duration is 1 or 2 days for animals that survive the gut injury.

Figure 88 shows GIM calculations of villus cell population versus time in mice for four doses bracketing this dose range. For doses of about 10 to 15 Gy, the population stays normal for two full days, then

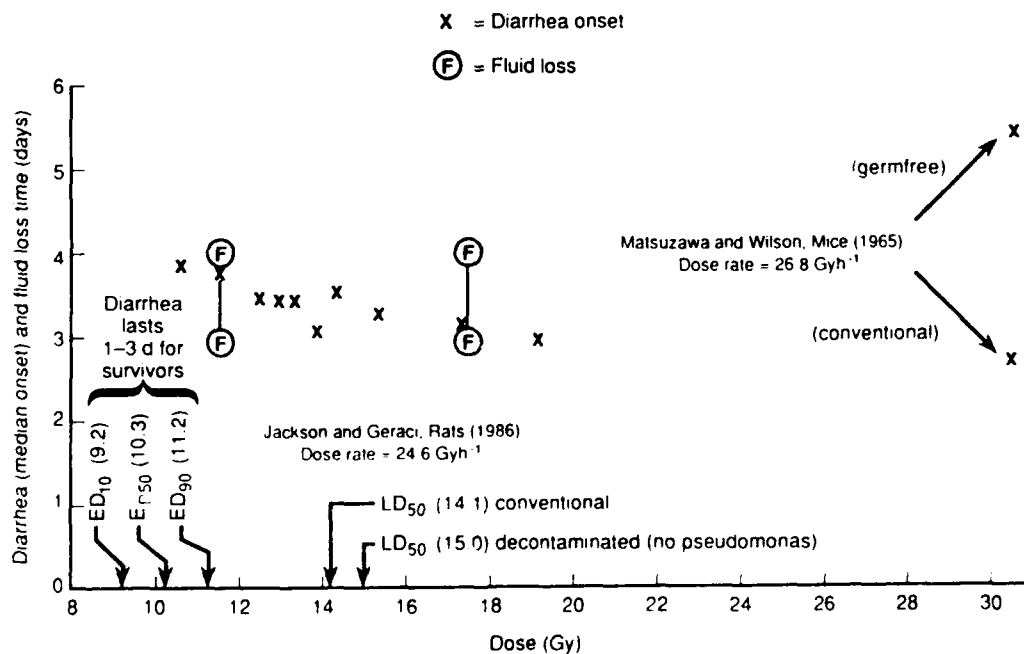


Figure 87. Diarrhea and fluid loss in rats and mice.

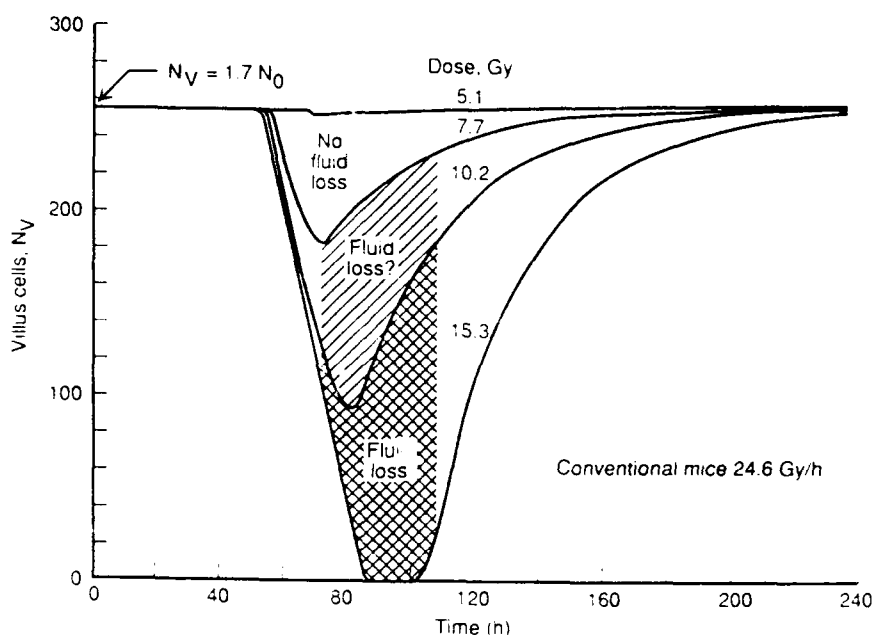


Figure 88. Estimated fluid loss in mice.

begins to fall, dropping below one-half about 3 days postexposure but not on the fifth through seventh days. This observation correlates well with the GIM calculation for mice. Interpolation in Fig. 88 shows that the villus population after 12.2 Gy is recovering rapidly on the fourth day, reaching one-half by about 4.5 days, consistent with the cessation of fluid loss 5 days after exposure. We conclude that the epithelial cell populations according to the GIM calculations are consistent with the onset, duration, and dose response characteristics (roughly) of the intestinal fluid loss observations.

Figure 87 indicates that the time of onset of diarrhea is about the same as or maybe a little later than that of fluid loss. The data for diarrhea onset is more detailed, however, and shows that the dose increase causes a slight trend toward earlier onset. Figure 85 shows that the GIM calculations exhibit the same trend if onset is associated with drop in villus population through a fixed level.

Jackson and Geraci [1986] report that the ED₅₀ for diarrhea in rats exposed to gamma rays at 24.6 Gy/h is 10.3 Gy. Scaling this value to an acute ED₅₀ for mice using the ratio of LD_{50/5}'s as above, gives an estimated mouse ED₅₀ for diarrhea of 11 Gy at the same dose

rate. Figure 89 shows the cell populations versus time for all three cell compartments of the GIM after a somewhat smaller dose of 9 Gy. The cell populations are scaled to the normal clonogen population level of 150. This presentation clearly shows how the declining clonogen and transit populations are able to maintain the villi population for more than two days. It also shows how the declining transit population triggers a rapid recovery and overshoot of the clonogen population and the eventual return to equilibrium of the compartments eight to ten days after exposure.

We concentrated on the villus compartment to analyze the ED₅₀ for diarrhea. By interpolating the data in Fig. 88, we found that the nadir of the villus population calculated by the GIM is 27 percent for 11 Gy, the estimated mouse ED₅₀ for diarrhea. As discussed earlier in this section, we estimated the ED₅₀ for other protracted exposures by finding the dose that reproduces the same nadir value of the villus population. This procedure provides the dose rate dependence of the ED₅₀ for diarrhea as plotted in Fig. 90.

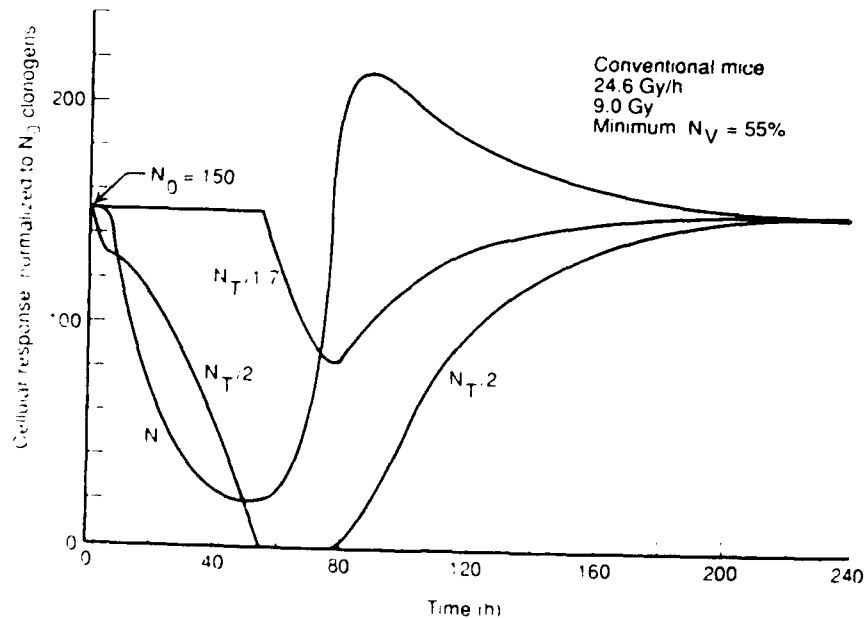


Figure 89. Normalized compartment population response to a 9 Gy dose.

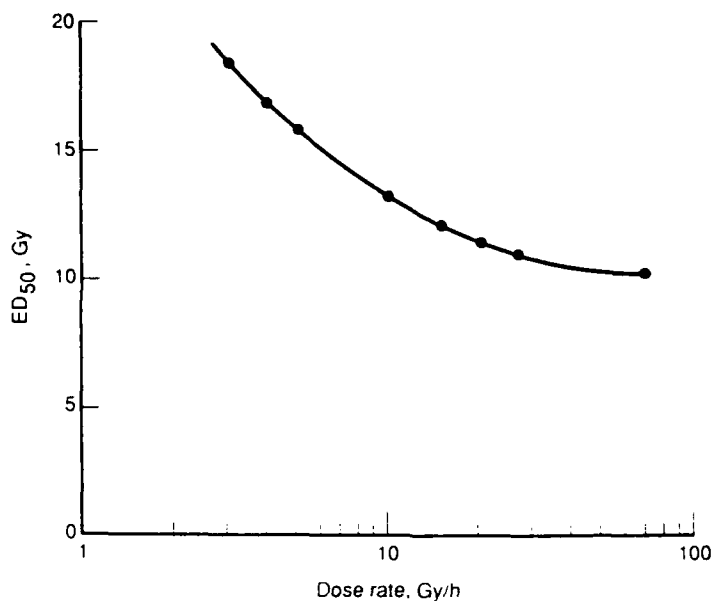


Figure 90. Predicted ED_{50} for diarrhea (conventional mice; isoeffect = 27% villi level).

Figure 90 shows that the predicted ED_{50} increases smoothly by almost a factor of two as the dose rate is reduced from 100 Gy/h to 3 Gy/h. The corresponding increase in exposure time is from 0.1 h to about 6 h. This result indicates how dose protraction can substantially influence symptomatology for protracted exposure.

Because of the similarity of the lower gastrointestinal syndrome among mammals, the GIM should be as effective for modeling GI distress in humans as it is for mice. However, it is necessary to adjust the model parameters to the human gut and to validate the model with available human data. As a first step in this effort, we have chosen a set of parameters for man and predicted the dose rate dependence of the LD_{50} for gut death and the ED_{50} for diarrhea, as discussed in the following subsection.

5.5 LETHALITY AND DIARRHEA ESTIMATES FOR HUMANS.

We performed calculations with the GIM to make estimates of GI syndrome lethality ($LD_{50/7-14}$) and diarrhea (ED_{50}) for constant dose rate exposures of humans. Table 30 lists the GIM parameters used in the calculations; GIM parameters derived for mice discussed above in

Table 30. GIM parameters.

		Mice		Human
		Germfree	Conventional	
η_{AB}	Gy^{-1}	1.55	1.55	1.55
η_{AC}	Gy^{-1}	0.16	0.16	0.16
ϵ_{BA}	h^{-1}	2.82	2.82	2.82
ϵ_{BC}	h^{-1}	0.15	0.15	0.15
γ	h^{-1}	0.056	0.056	0.0418 ¹
λ_m	h^{-1}	0.171	0.171	0.076 ²
δ	Gy^{-1}	0.082	0.082	0.0612 ¹
A	--	0.1	0.1	0.1
a	--	0.21	0.21	0.21
Crypt cells ³		N_0	N_0	N_0
Transit cells ⁴		$2N_0$	$2N_0$	$2N_0$
Villus cells ⁵		$6.7N_0$	$1.7N_0$	$3N_0$

¹Assumes normal cell cycle time 34% longer in man than in mice; assumes mitotic delay parameter 34% smaller in man than in mouse.

²Adjusted from GIM calculations for 9.0 Gy (LD_{50/7-14}) and 23 h dwell time for villi denudation.

³ $N_0 = 2.08 \times 10^4$, number of crypt clonogenic cells per circumference of jejunum for mice.

⁴ $2N_0$, estimates based on Quastler and Sherman [1959], Potter and Hendry [1983], and Fabrikant [1987].

⁵ $6.7N_0$, estimate for germfree mice based on Quastler and Sherman [1959]; $1.7N_0$, estimate for conventional mice based on Matsuzawa and Wilson [1965]; $3N_0$, estimate for human based on Ingram [1965].

this section (Clonogen Response to Exposure at Constant Dose Rate) are also listed in Table 30 along with some explanatory footnotes relevant to the model.

Table 22 (Sec. 2) gives dosage and time estimates for GI syndrome lethality in man following acute irradiation. Compared to mice, the time of GI-syndrome lethality for man following irradiation is expected to be about twice as long [Lushbaugh, 1973] or about 7-14 days. Withers [1989] estimates that the LD_{50/7-14} for humans may be about 8-10 Gy (MLT) for acute gamma irradiation; we chose 9.0 Gy (MLT)

for our purposes. Withers [1989] also indicated that GI death occurs when the intestinal epithelium (villi) fails to regenerate and remains denuded over a certain period of time following irradiation. Using the GIM, we estimated this period for conventional mice to be about 14 h based on the $LD_{50/5} = 12.5$ Gy [Withers and Elkind, 1969]*, according to the procedure discussed above in this section (Dose Rate Dependence of $LD_{50/5}$ for Mice). Applying the same GIM calculational procedure with the estimated parameters for humans, we determined a denudation period of 23 h for the isoeffect corresponding to the assumed human $LD_{50/7-14}$ value of 9.0 Gy (MLT) for prompt radiation.

A series of calculations were performed to estimate the dependence of $LD_{50/7-14}$ on dose rate as shown in Fig. 91. The dose values on the ordinate were all determined for a villi denudation period of 23 h (i.e., the isoeffect for prompt exposure). All the dose values are expressed as free-in-air (FIA) exposures which can be converted to midline tissue (MLT) absorbed dose, multiplying by 0.67. According to the measure of 50 percent lethality based on the GI syndrome, protracted exposures can amount to a factor of about 2.4 in dose to effect median lethality over the range of dose rate shown in Fig. 91 (i.e., from about 1.5 to 60 Gy/h).

We also performed calculations with the GIM to estimate the dose rate dependence of the ED_{50} for diarrhea in humans. Here we assumed, as determined for mice, a 27 percent atrophy nadir of the normal (jejunum) villi epithelial complement for the isoeffect corresponding to the ED_{50} for diarrhea. The results are given in Fig. 91 where all dose values are expressed as FIA exposures. These results indicate that protracted exposures can amount to a factor of about two in dose to effect the ED_{50} for diarrhea over the range of dose rate from 1.0 to 60 Gy/h. Although qualitatively similar, the quantitative difference in the dose rate effect between the $LD_{50/7-14}$ and ED_{50} for diarrhea are due to the two different isoeffects upon which the two

*Withers and Elkind obtained an $LD_{50/5}$ of 10.6 Gy for 200 kVp X-rays; 12.5 Gy reflects an RBE adjustment by a factor of 1.18 to express the $LD_{50/5}$ in terms of ^{60}Co radiation.

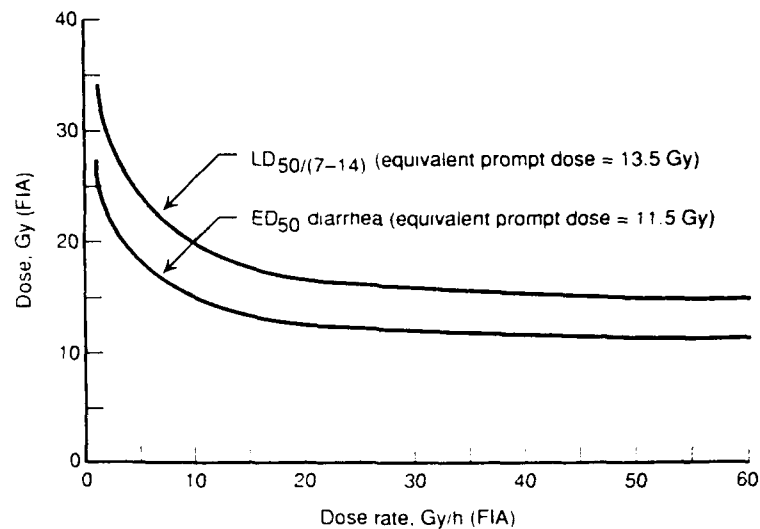


Figure 91. Estimated protracted radiation exposure effects for GI tract injury in humans.

endpoints are based. It is also interesting to note the similarity in the prompt dose ratios of ED₅₀ (diarrhea)/LD_{50/7-14} for humans and mice. For mice, this ratio is $10.5/12.5 = 0.84$ based on extrapolating the ED₅₀ in Fig. 90 to essentially a prompt dose (i.e., ≥ 100 Gy/h); and for humans, the ratio is $11.5/13.5 = 0.85$ (see Fig. 91). This suggests that if the damage mechanisms are similar for radiation-induced gastrointestinal damage in mice and humans, the GIM provides a reasonably consistent means for making such endpoint predictions (i.e., lethality and diarrhea) for humans. Furthermore, the GIM calculations indicate that the model yields results that are consistent with the data.

5.6 FUTURE DEVELOPMENTS.

Several avenues of improvement are apparent for the GIM. First of all, the model needs to account for the variations in radiosensitivity of cells during the cell cycle and the consequent redistribution of the cell population. The need for this development is illustrated in Fig. 84 by the systematic deviation of the cell survival data from the model predictions at dose rates of around 1 Gy/h. For this data, the exposure times of 20 to 50 h are comparable to the cell cycle times (as modified by homeostasis and

mitotic delay). Variations in cell sensitivity during the exposure time are likely to account for the deviations.

The second need for the GIM is provided for the response to mixed gamma/neutron exposures. This RBE effect can be handled conveniently in the LPL equations for cell survival. The two lesion production rates can be adjusted for the RBE of the particular gamma/neutron mixture. The rest of the GIM remains the same. Available human data and guidance from animal experiments can be used to adjust the rates.

Other areas for improvement are the homeostasis terms, statistical effects on crypt survival, saturation of lesion repair rates, the possibility of a few divisions before mitotic death of all daughter cells, the mitotic delay formulation, differences among the various parts of the large and small intestines, and the influence of the vascular system on the intestine.

SECTION 6

CONCLUSIONS

We reviewed and analyzed a large body of radiobiological literature relevant to radiation-induced damage, repair, and recovery in biological systems ranging from the cell to organism level. The focus was on empirical data, biological response mechanisms, and existing models to address the requirements undertaken in this effort for developing and demonstrating modeling approaches for predicting the symptomatology response to protracted radiation exposure. Both acute and protracted exposure information were relevant since any model developed should be valid regardless of exposure duration.

The need to accommodate a multitude of possible protracted exposure histories was the determining factor requiring mathematical modeling approaches employing differential equations. This requirement and the nature and empirical characteristics of the response to be modeled established the specific mathematical formulation to emulate response dynamics.

We developed two approaches to modeling the symptomatology response to protracted radiation exposure. Each is based on fundamentally different mechanisms of radiobiological and physiological changes.

One type of model, the UGIDM, considers radiation exposure-induced humoral changes that cause symptoms of upper gastrointestinal distress. The response is expressed as the severity of nausea and vomiting. We refer to this type of model based on humoral changes as a *toxicokinetic* model.

Another type of model, the GIM, considers radiation exposure-induced chromosome damage that triggers various cellular processes, including cell damage and repair, cell death, and proliferative tissue recovery. These processes have been modeled for the intestinal epithelium to predict the changes in the tissue population that may result in either lethality or symptomatology such as diarrhea and fluid loss. We refer to this type of model, based on the dynamics of

chromosome damage and cellular proliferation, as a *target tissue* model.

The recovery of biological systems from the injurious effects of ionizing radiation exposure has been represented in various ways. Next, we summarize them from our literature review.

6.1 LITERATURE REVIEW.

The effect of biological recovery from ionizing radiation insult are demonstrated in the literature based on primarily two extreme ends of the biological scale: cell level, and sign/symptom response of an organism. Observed physiological and anatomical changes, important from a modeling standpoint, have received relatively less attention. Also, the preponderance of investigations that are relevant to mechanistic modeling approaches are primarily on the hematopoietic system and secondly on the GI-system.

In both systems, the stem cells (in the bone marrow and intestinal crypts) are sensitive to radiation and undergo changes that dramatically affect their survival, largely dependent upon the time course of exposure. For protracted compared to prompt exposures, stem survival fractions on the order of one percent can result in factors of 2 to 3 higher dose levels to affect lethality in mammalian organisms as measured by the median lethal dose level.

Both the bone marrow and gut are hierarchical tissue systems that regenerate according to a progression of cellular maturation stages to attain functional maturity. Stem cell behavior and subsequent cellular maturation processes altered by severe physical stress such as that induced by radiation exposure are essential for modeling the dynamics of damage, repair, and recovery. In the bone marrow, the behavior of maturing cells destined for specific functions (i.e., neutrophils, erythrocytes, and platelets, etc.) is more difficult to assay than are those developed for the maturing cellular phases of the GI system. Therefore, mechanistic insights for modeling based on empirical data must be inferred largely from measurements of the mature blood cell components in circulation. For humans, average neutrophil and platelet dynamic response levels have been profiled by

investigators for various levels of acute exposure, and there is general agreement, although some significant disagreement does remain to be resolved.

A variety of dynamic models for modeling H tissue response does exist, primarily for hematopoiesis. Two of the most comprehensive models described in Sec. 2 (Blood Cell Modeling) are for hematopoiesis. Both are based on multicompartment cellular dynamics mathematically developed with coupled differential rate equations and feedback controls to regulate cell production and homeostasis. One of the two models provides a more detailed simulation of stem cell injury and has been applied to analyze human accident cases for acute and protracted exposures. Based on granulopoiesis, the acute exposure cases are modeled significantly better than the protracted exposure cases. We believe improvements can be made by more explicit modeling of the intracellular damage and Elkind-type repair processes. We have incorporated these kinds of improvements in modeling the crypt changes in cells of the GIM.

From the 1950s up until the 1970s, a considerable amount of work was done with mammals ranging from mice to large animals to demonstrate recovery of the hematopoietic system based upon ED₅₀ endpoint measurements for acute, split dose, and constant dose rate exposures. Review and analysis of this work was quite useful for establishing our modeling approaches. Based on these investigations, a variety of protracted dose empirical models were developed which demonstrate increasing organism recovery with decreasing dose rate, i.e., with increasing exposure period.

Some of the existing models have been suggested for application to humans with some parameter adjustments. One model in particular (developed by Soviet investigators) provides a model for humans based on a complex multifactor extrapolation procedure from animals involving a variety of physiological and anatomical parameters. Some of these models have been applied to operations analysis involving protracted exposures in a fallout environment. We derived an empirical recovery function from constant dose rate data of large animals (sheep and swine) and investigated the utility of applying it to split

dose and varied dose rate histories based on the equivalent residual dose (ERD) concept. We concluded that the recovery function derived from constant dose rate exposure data cannot generally be applied to split dose and varied dose rate histories since the dynamics and some significant details are not explicitly modeled in this simple approach.

Split dose lethality data from various animals also result in varying degrees of recovery, including over-recovery (or negative residual injury) indicated by measurements of residual injury as a function of time following acute and constant dose rate exposures. Similar undulating patterns are also seen in bone marrow stem cells. Although no concrete explanation has been developed regarding this varying postexposure behavior, most attribute it to unknown underlying physiological processes; we believe that stem cell cycling redistribution could also play a significant role. A lot of the measurements for constant dose rate animal exposures do not show the varied behavior in recovery, probably because of the lack of data.

Similar oscillatory behavior has been demonstrated for the response of clonogen cells in the crypt of the jejunum of mice that correlates with cell cycle times for both split dose and constant dose rate exposures (cell cycling redistribution has also been demonstrated in other cell lines for constant dose rate exposure). However, we are not aware of any data for GI-syndrome lethality that demonstrates the effect of varying recovery, such as for the hematopoietic syndrome.

A central consideration for modeling development is the proper dynamic response for the symptomatology. Unlike the single step ERD approach, a multistep mathematical modeling structure is required to explicitly account for the time delay and regulating processes that determine most radiobiological response dynamics. To address this requirement, we developed multicompartment modeling structures of coupled rate equations with subsidiary functional relationships and constraints.

Our review and analysis of the literature supports the two symptomatology modeling approaches we developed in this effort. Below we summarize some key aspects of the modeling approaches as well as

initial results obtained and provide some concluding remarks for modeling improvement for the UGIDM and GIM. Finally, we provide a discussion regarding approaches for modeling radiation-induced fatigability and weakness.

6.2 UGIDM.

Empirical observations of changes in UG distress induced by protracted radiation exposure provided impetus for developing the UGIDM. Human data indicates significant differences in the emetic response for protracted exposure including onset, incidence, severity, and duration. Constant dose rates less than a few cGy/h over a period of one to two weeks are not enough to cause significant vomiting, where dose rates of about 10 cGy/h over a period of a few days do produce a significant emetic response; between a few cGy/h and about 10 cGy/h, there is considerable uncertainty due to the lack of empirical data. The postulated habituation effect of emesis for repeated intermittent exposures lacks quantitative empirical verification, except in the cat. However, anecdotal radiation therapy experience based on fractionated TBI suggests the effect.

The UGIDM is based on a semiempirical modeling approach guided by recent advances in understanding the process of radiation-induced emesis. The response time frame suggests that target tissues primarily in the midepigastic area of the body produce toxic substances that stimulate the emetic response based on more than one pathway.

A set of three differential rate equations were developed based on a simplified two-compartment analogue consisting of potentially active and active toxin levels and a "depletable reservoir" of target tissue. A potential toxin (normalized to units of dose) is assumed produced at a rate proportional to dose rate, transformed to an active form, and then biologically deactivated or cleared. Rate parameters for these processes are derived from severity data of UG distress developed by the DNA/IDP for acute radiation exposure. A two-parameter Weibull response function relates the active toxin level to UG distress in terms of sign/symptom severity.

Calculations for constant dose rate exposure compare reasonably with various data for emesis from radiation therapy and accidents, where valid comparisons can be made. However, considerable uncertainty in the human data reviewed in the critical dose rate region between a few to about 30 cGy/h prevents a more precise validation of the UGIDM. This region is critical because we believe it is where dramatic changes in response take place as a low dose rate threshold is approached where emesis disappears.

Another aspect of the UGIDM that requires additional attention includes verification of the habituation effect for fractioned exposures as modeled by the "depletable reservoir" approach. Also, we have focussed primarily on gamma radiation exposure, and as such, assumed the neutron RBE = 1 for UG distress. Once established, however, RBE variations can readily be incorporated in the UGIDM.

Extension of the UGIDM to include the incidence of UG distress should also be given attention to provide a more complete picture of UG distress. Conceptually, we have developed such an approach that is based on the active toxin level as a function of time as calculated by the UGIDM.

The improvements for the UGIDM will require the acquisition and analysis of additional human and animal data. As far as animal data are concerned, we applied the UGIDM to some acute exposure ferret data and believe that some recommended experiments for protracted exposures can be utilized to verify or guide UGIDM improvement.

6.3 GIM.

Empirical observations, involving rats, mice, and humans, of the symptomatology of LG distress that include diarrhea and fluid loss correlate well with dynamic changes in the intestinal epithelium and the loss of mature villi cells. Furthermore, variations in protracted irradiation exposure of mice result in changes in the survival level of clonogen crypt cells and the loss of villi epithelia that correlate well with the progression of the GI syndrome, culminating in early (3-5 days) lethality. These observations provided impetus for developing the GIM.

We recognize that other physiological changes not explicitly modeled, such as damage to the membrane of mature functional cells and vasculature of the intestinal mucosa, may play a significant role in the symptomatology. Such causal mechanisms deserve attention in future modeling efforts. In the meantime, we assume the dominant physiological change is attributed to the reduction in the epithelial cell population.

The GIM is structured as an H-type tissue to track the number of cells in three linked compartments, including clonogens in the crypts, transit cells in the crypts, and functional cells on the villi. The modeling is based on a nested arrangement of three models that unify cell radiation damage and repair (LPL), mitotic delay and proliferation (PAIR), and tissue hierarchy, homeostasis and functionality (GIM). Mathematically, the model is expressed by a set of nine coupled differential rate equations and several subsidiary functional linking relationships.

Radiobiological, anatomical, and physiological considerations form the foundation for the GIM development. Damage and repair of chromosome lesions are calculated by the lethal potentially lethal (LPL) model to yield dose rate dependence of cell survival. Damage includes the production of both repairable and irreparable lesion production. Lesion repair rate is simulated according to first order kinetics; misrepair rate is simulated according to second order kinetics.

The PAIR model combines the cell survival equations of the LPL model with those that describe cell proliferation and radiation-induced mitotic delay. The equations are derived from statistical considerations of the changing lesion distribution among cells brought on by cell mitosis and mitotic death. The PAIR model relationships are combined based on a compartmental description of the hierarchical structure of the intestinal (jejunal) epithelium. At this final level of model aggregation, homeostatic control of the cell population and linkage of symptomatology and lethality with the villi population complete the current version of the GIM.

The GIM includes eight basic parameters whose values were determined based on optimal fitting of dose rate dependent survival data for (jejunal) crypts of mice, together with guidance from empirical data for the capacities and dynamics of the crypt clonogen, transit, and villi cell populations for both germ-free and conventional mice. Here, more than one purpose was served. Aside from obtaining the optimum parameter values, parameter sensitivities were determined, and the model was validated over a large range of dose rates, which also revealed the effect of cell cycle redistribution not explicitly modeled.

Also based on crypt clonogen levels, GIM calculations were compared with split dose crypt recovery data of mice, and generally good central agreement was obtained. However, oscillations in the dynamic recovery profile further suggest the effect of cell cycle redistribution and other possible transient physiological mechanisms.

Another independent validation assessment of the GIM was performed comparing the morphological decline of the crypt and villi mucosa with empirical data based on a high, sterilizing dose of 33.5 Gy at 26.8 Gy/h. Good qualitative agreement was obtained with mouse data.

The GIM model was applied to perform protracted exposure calculations of LG symptomatology and lethality. Empirical data indicate that lethality in mice correlates with a sustained period of mucosal denudation (or villi atrophy). Based on a reference exposure rate (30 cGy/h), we estimated a villi denudation period of 14 h corresponds to the LD_{50/5}. Using this isoeffect value, dose rate dependent LD_{50/5} values were calculated with the GIM that provided reasonable agreement with empirical data. This agreement is significant and indicates the GIM is reasonably sound mechanistically in that parameter values were determined independently of lethality data.

LG distress calculations for mice were made with the GIM to correlate villi cell levels with observed fluid loss and diarrhea. Since data on these responses were available only for rats, we extrapolated to mice based on the ratio of LD_{50/5} values for the experimental dose rate of 24.6 Gy/h. Based on the dynamic response of

the villi population, the calculated results correlated well with the observed postexposure fluid loss times and dose levels.

In rats, the empirical ED₅₀ for diarrhea was determined to be 10.3 Gy at 24.6 Gy/h, which extrapolates to 11 Gy for mice based on the LD_{50/5} ratios. Using GIM calculations, we found that 11 Gy (at 24.6 Gy/h) corresponds to a villi population that recedes to 27 percent of the normal and then returns to normal after several days. Using this nadir as the isoeffect, we applied the GIM to calculate the ED₅₀ dependence on dose rate. Over a dose rate range of from 100 to 3 Gy/h, the ED₅₀ was found to vary by a factor of about 2.

Similar calculations were made with the GIM for diarrhea (ED₅₀) and lethality (LD_{50/7-14}) for humans based on the similarity of the lower gastrointestinal syndrome among mammals. These calculations were made with parameter adjustments estimated for humans involving cell cycling rates, mitotic delay, and homeostatic ratios of the epithelial compartments.

Based on the same isoeffect value found for mice (27 percent villi population nadir), dose rate dependent calculations were made for the ED₅₀ for diarrhea in humans. The ED₅₀ varied by about a factor of 2 (as in mice) over a dose rate range of from 60 to 1.0 cGy/h.

LD_{50/7-14} dose rate dependent calculations were made with the GIM based on an isoeffect of 23 h period of villi denudation. This value was determined by GIM calculations corresponding to an estimated LD_{50/7-14} of 9.0 Gy (MLT) for prompt exposure. Over the range of dose rate from 60 to 1.5 Gy/h, the LD_{50/7-14} is estimated to vary by a factor of about 2.4. These calculations for humans have not been explicitly validated with human data, but represent a first step in the process.

We are encouraged with the GIM results obtained thus far; however, some areas for likely improvements have been identified and are pointed out below.

- Variations in cell radiosensitivity due to cell cycle redistribution.
- The effects of neutron RBE for mixed neutron/gamma exposures.
- The role and functional effects that physiological mechanisms, including vascular damage of the crypt and villus, other than epithelial atrophy might have upon LG symptomatology.
- Statistical effects on crypt survival, homeostasis, lesion repair rate saturation, mitotic delay, and mitotic death definition.
- Physiological effects from combined LG and hematopoietic system radiation damage and consequent effects on symptomatology.

6.4 FATIGABILITY AND WEAKNESS.

Qualitative data on radiation-induced fatigability and weakness (FW), primarily for acute exposure, provide guidance for symptomatology model approaches. A limited amount of protracted exposure data from TBI therapy and accidental exposures suggests a significant difference (10 to 90 percent) for the incidence of FW over dose rates ranging from a few to 150 cGy/h. Acute exposure data indicates a biphasic time response profile for the severity of FW following irradiation, suggesting at least two causal mechanisms are likely: one for an initial period of FW severity that coincides with UG distress, and another for an intermediate to longer period of expressed symptoms.

The lack of appropriate protracted dose data will require that the modeling of the FW response rely primarily on a mechanistic approach. More than one modeling approach will likely be necessary to properly address the observed duality in dynamic behavior. Two possible approaches that appear attractive, based on the observed behavior and physiological considerations, are *toxicokinetic* modeling for the initial FW phase and *target tissue* modeling for the subsequent FW phase(s). For the latter approach, the capillaries and small blood vessels appear to be reasonable candidates for the target tissue (F-type tissue), based on tissue sensitivity to radiation and recent physiological observations.

There are some miscellaneous objective data associated with radiation-induced FW that could be relevant but require further exploration. These include some work capacity assessments made in the Soviet Union with Chernobyl accident victims, and those made obtained from therapy patients and accidental exposures based on pulmonary impedance measurements under an exercise/stress protocol (bicycle ergometry). Measurements have also shown that creatinura correlates with radiation-induced fatigue in therapy patients, and ATP depression occurs with radiation exposure in rats.

In this work, we have shown how to construct effective models of the symptomatology of both upper and lower gastrointestinal distress for protracted exposure to ionizing radiation. We believe that a similar approach applies for fatigability and weakness. We conclude that it is possible to develop and validate a unified model of the symptomatology response to protracted exposure that will be sufficient for estimation of human performance decrement.

SECTION 7

BIBLIOGRAPHY

- ADAMS, G.E., 1984.
LETHALITY FROM ACUTE AND PROTRACTED RADIATION EXPOSURE IN MAN.
INT. J. OF RADIATION BIOLOGY, Vol 46, 1984, Pages 209-217.
- AINSWORTH, E.J., G.F. LEONG, 1966.
RECOVERY FROM RADIATION INJURY IN DOGS AS EVALUATED BY THE SPLIT-DOSE TECHNIQUE.
RADIATION RESEARCH, Vol 29, 1966, Pages 131-142.
- AINSWORTH, E.J., G.F. LEONG, E.L. ALPEN, 1984.
EARLY RADIATION MORTALITY AND RECOVERY IN LARGE ANIMALS AND PRIMATES.
"RESPONSE OF DIFFERENT SPECIES TO TOTAL BODY IRRADIATION", J.J. BROERSE & T.J. MACVITTIE, EDS.
MARTINUS NIGHOFF PUBLISHERS, DORDRECHT, THE NETHERLANDS, Vol 4, 1984, Pages 87-109.
- AINSWORTH, E.J., G.F. LEONG, K. KENDALL, E.L. ALPEN, 1965.
COMPARATIVE LETHALITY RESPONSES OF NEUTRON AND X-IRRADIATED DOGS INFLUENCE OF DOSE RATE AND EXPOSURE ASPECT.
RADIATION RESEARCH, Vol 26, 1965, Pages 32-43.
- AINSWORTH, E.J., N. PAGE, J. TAYLOR, G.F. LEONG, E. STILL, 1968.
DOSE-RATE STUDIES WITH SHEEP AND SWINE.
DOSE RATE IN MAMMALIAN RADIATION BIOLOGY, A SYMPOSIUM CO-SPONSORED
BY UT-AEC AGRICULTURAL RESEARCH LABORATORY, OAK RIDGE, TN: CONF-680410.
U.S. ATOMIC ENERGY COMMISSION, DIV. OF TECHNICAL INFORMATION, July 12, 1968.
- AL BARWARI, S.E., C.S. POTTEN, 1979.
A CELL KINETIC MODEL TO EXPLAIN THE TIME OF APPEARANCE OF SKIN REACTION AFTER X-RAYS OR ULTRAVIOLET LIGHT IRRADIATION.
CELL AND TISSUE KINETICS, Vol 12, 1979, Pages 281-289.
- ALPER, T., 1980.
KEYNOTE ADDRESS: SURVIVAL CURVE MODELS.
"RADIATION BIOLOGY IN CANCER RESEARCH", RAYMOND E. MEYN & H. RODNEY WITHERS, EDS.
RAVEN PRESS, NEW YORK, 1980, Pages 3-16.
- ANDREWS, A., 1965.
TOTAL BODY IRRADIATION IN THE HUMAN BEING.
PROCEEDINGS OF THE XITH INTERNATIONAL CONGRESS OF RADIOLOGY, ROME, SEPTEMBER 1965
September 1965.
- ANDREWS, G.A., 1964.
MEXICAN CO60 RADIATION ACCIDENT
ISOTOPES AND RADIATION TECHNOLOGY
Vol 1, 1964, Pages 200-201.
- ANDREWS, G.A., B.W. SITTERSON, A.L. KRETCHMAR, M. BRUCER, 1959.
ACCIDENTAL RADIATION EXCURSION AT THE OAK RIDGE Y-12 PLANT--IV:
PRELIMINARY RPT. ON CLINICAL AND LABORATORY EFFECTS IN THE IRRADIATED EMPLOYEES.
HEALTH PHYSICS, Vol 2, 1959, Pages 134-138.
- ANDREWS, P.L.R., W.G. RAPEPORT, G.J. SANGER, 1988.
NEUROPHARMACOLOGY OF EMESIS INDUCED BY ANTI-CANCER THERAPY.
TRENDS IN PHARMACOLOGICAL SCIENCE, Vol 9, 1988, Pages 334-341.
- ANNO, G.H., 1983.
NUCLEAR WEAPON EFFECT RESEARCH AT PSR-1982, VOLUME XIV:
ACUTE RADIATION RESPONSE IN HUMANS: INFORMAL COMMENTS BY PHYSICIANS AND RADIOBIOLOGISTS; DNA-TR-82-179-V14.
DEFENSE NUCLEAR AGENCY, WASHINGTON, DC, June 1, 1983.
- ANNO, G.H., S.J. BAUM, 1986.
EFFECTS OF PROTRACTED IONIZING RADIATION DAMAGE ON HUMANS AND ANIMALS:
A BRIEF REVIEW OF SELECTED INVESTIGATIONS; DNA-TR-87-28.
DEFENSE NUCLEAR AGENCY, WASHINGTON, DC, July 31, 1986.
- ANNO, G.H., S.J. BAUM, H.R. WITHERS, R.W. YOUNG, 1989.
SYMPTOMATOLOGY OF ACUTE RADIATION EFFECTS IN HUMANS AFTER DOSES OF 0.5-30 GY.
HEALTH PHYSICS, Vol 56, 1989, Pages 821-838.
- ANNO, G.H., M.A. DORE, 1988.
INCIDENCE OF NAUSEA AND VOMITING IN NUCLEAR ACCIDENTS.
PSR NOTE 781
PACIFIC-SIERRA RESEARCH CORPORATION, LOS ANGELES, CA., November 1988.
- ANNO, G.H., D.B. WILSON, S.J. BAUM, 1985.
SEVERITY LEVELS AND SYMPTOM COMPLEXES FOR ACUTE RADIATION SICKNESS:
DESCRIPTION AND QUANTIFICATION; DNA-TR-86-94.
DEFENSE NUCLEAR AGENCY, WASHINGTON, DC, 1985.

- ANNO, G.H., D.B. WILSON, M.A. DORE, 1984.
NUCLEAR WEAPON EFFECT RESEARCH AT PSR, 1983:
ACUTE RADIATION EFFECTS ON INDIVIDUAL CREWMEMBER PERFORMANCE; DNA-TR-85-52.
DEFENSE NUCLEAR AGENCY, WASHINGTON, DC, August 31, 1984.
- APPLEBAUM, F., J. MEYERS, A. FEFER, N. FLOURNOY, M. CHEEVER, M. GREENBERG, 1982.
NONBACTERIAL NONFUNGAL PNEUMONIA FOLLOWING MARROW TRANSPLANTATION IN 100 IDENTICAL TWINS.
TRANSPLANTATION, Vol 33, 1982, Pages 265-268.
- ARINO, O., M. KIMMEL, 1986.
STABILITY ANALYSIS OF MODELS OF CELL PRODUCTION SYSTEMS
MATHEMATICAL MODELLING
Vol 7, 1986, Pages 1269-1300.
- ARMY, U.S., 1951.
JOINT COMMISSION FOR THE INVESTIGATION OF THE EFFECTS OF THE ATOMIC BOMB IN JAPAN:
MEDICAL EFFECTS OF ATOMIC BOMBS.
ARMY INSTITUTE OF PATHOLOGY, April 19, 1951.
- BARANOV, A.E., A.K. GUSKOVA, 1988.
ACUTE RADIATION DISEASE IN CHERNOBYL ACCIDENT VICTIMS. INTERNAT. REACTS CONF.
THE MEDICAL BASIS FOR RADIATION PREPAREDNESS II. ...FOLLOW-UP SINCE 1979.
MEDICAL AND HEALTH SCIENCES DIV., OAK RIDGE ASSOC. UNIVERSITIES, OAK RIDGE, TN, October 20, 1988.
- BARENDSSEN, G., 1966.
DOSE RATE AND SURVIVAL CURVES.
BRITISH JOURNAL OF RADIOLOGY, Vol 39, 1966, Pages 155-156.
- BARENDSSEN, G., 1982.
DOSE FRACTIONATION, DOSE RATE AND ISOEFFECT RELATIONSHIPS FOR NORMAL TISSUE RESPONSES.
INT. J. OF RADIATION BIOLOGY, Vol 8, 1982, Pages 1981-1997.
- BARNES, J.H., 1984.
THE PHYSIOLOGY AND PHARMACOLOGY OF EMESIS
MOLECULAR ASPECTS OF MEDICINE, 1984, Pages 397-508.
- BARNETT, T.B., 1949.
EXPERIMENTAL RADIATION PATHOLOGY
AEC-D-2614
U.S. ATOMIC ENERGY COMMISSION, WASHINGTON, DC, 1949.
- BARRET, R.L., R. POWLES, 1979.
TOTAL BODY IRRADIATION AND MARROW TRANSPLANTATION FOR ACUTE LEUKAEMIA. THE ROYAL MARSDEN HOSPITAL EXPERIENCE.
PATHOLOGIE BIOLOGIE, Vol 27, 1979, Pages 357-359.
- BARRETT, A., 1982.
TOTAL BODY IRRADIATION (TBI) BEFORE BONE MARROW TRANSPLANTATION IN LEUKEMIA:
A CO-OPERATIVE STUDY FROM THE EUROPEAN GROUP FOR BONE MARROW TRANSPLANTATION.
BRITISH JOURNAL OF RADIOLOGY, Vol 55, 1982, Pages 562-567.
- BARRETT, A., M. DEPLEDGE, R. POWLES, 1983.
INTERSTITIAL PNEUMONITIS FOLLOWING BONE MARROW TRANSPLANTATION AFTER LOW DOSE RATE TOTAL BODY IRRADIATION.
INT. J. OF RADIATION ONCOLOGY, BIOLOGY, AND PHYSICS, Vol 9, 1983, Pages 1029-1033.
- BATEMAN, J., 1968.
A RELATION OF IRRADIATION DOSE-RATE EFFECTS IN MAMMALS AND IN MAMMALIAN CELLS.
DOSE RATE IN MAMMALIAN RADIATION BIOLOGY, A SYMPOSIUM CO-SPONSORED BY UT-AEC AGRICULTURAL RESEARCH LABORATORY, OAK RIDGE,
TN; CONF-680410.
U.S. ATOMIC ENERGY COMMISSION, DIV. OF TECHNICAL INFORMATION, July 12, 1968.
- BATEMAN, J., V. BOND, J. ROBERTSON, 1962.
DOSE RATE DEPENDENCE OF EARLY RADIATION EFFECTS IN SMALL MAMMALS.
RADIOLOGY, Vol 79, 1962, Pages 1008-1014.
- BAUCHINGER, M., E. SCHMID, J. DRESP, 1979.
CALCULATION OF THE DOSE-RATE DEPENDENCE OF DICENTRIC YIELD AFTER CO GAMMA IRRADIATION OF HUMAN LYMPHOCYTES.
INT. J. OF RADIATION BIOLOGY, Vol 35, 1979, Pages 229-233.
- BAUM, S., 1961.
ERYTHROPOIETIC RECOVERY AND RESIDUAL INJURY IN RATS EXPOSED REPEATEDLY TO X-RAYS.
AMERICAN JOURNAL OF PHYSIOLOGY, Vol 200, 1961, Pages 155-158.
- BAUM, S., 1967.
A MEASURE OF NONREPARABLE INJURY TO HEMATOPOIETIC STEM CELLS IN RATS EXPOSED REPEATEDLY TO X-RAYS.
RADIATION RESEARCH, Vol 32, 1967, Pages 651-657.
- BAUM, S., E. ALPEN, 1959.
RESIDUAL INJURY INDUCED IN THE ERYTHROPOIETIC SYSTEM OF THE RAT BY PERIODIC EXPOSURES TO X-RADIATION.
RADIATION RESEARCH, Vol 11, 1959, Pages 844-860.
- BAUM, S., A. DAVIS, L. ALPEN, 1961.
EFFECT OF REPEATED ROENTGEN OR NEUTRON IRRADIATION ON THE HEMATOPOIETIC SYSTEM.
RADIATION RESEARCH, Vol 15, 1961, Pages 97-108.
- BAUM, S., D. KIMELDORF, 1957.
EFFECT OF DOSE RATE ON IRON INCORPORATION INTO NEWLY FORMED ERYTHROCYTES OF RATS EXPOSED TO GAMMA RADIATION.
AMERICAN JOURNAL OF PHYSIOLOGY, Vol 190, 1957, Pages 13-16.

- BAUM, S., M. VARON, D. WYANT, 1970.
RADIATION INDUCED ANEMIA IN RATS EXPOSED REPEATEDLY TO MIXED GAMMA-NEUTRON RADIATION.
RADIATION RESEARCH, Vol 41, 1970, Pages 492-499.
- BAUM, S., D. WYANT, 1970.
HEMATOPOIETIC RECOVERY IN IRRADIATED DOGS.
RADIATION RESEARCH, Vol 44, 1970, Pages 531-544.
- BAUM, S., D. WYANT, J. VAGHER, 1969.
COMPARATIVE HEMATOPOIETIC CYTOKINETICS IN RATS EXPOSED TO EITHER 250 KVP X-RAY OR MIXED GAMMA-NEUTRON IRRADIATION
AMERICAN JOURNAL OF PHYSIOLOGY, Vol 216, 1969, Pages 582-588.
- BAUM, S.J., G.H. ANNO, R.W. YOUNG, H.R. WITHERS, 1984.
SYMPTOMATOLOGY OF ACUTE RADIATION EFFECTS IN HUMANS AFTER EXPOSURE TO DOSES OF
75 TO 4500 RADS (CGY) FREE-IN AIR. DNA-TR-85-56.
DEFENSE NUCLEAR AGENCY, WASHINGTON, DC, August 1984.
- BAUM, S.J., G.H. ANNO, R.W. YOUNG, H.R. WITHERS, 1984.
SYMPTOMATOLOGY OF ACUTE RADIATION EFFECTS IN HUMANS AFTER EXPOSURE TO DOSES OF 50 TO 3000 RADS (CGY) FREE-IN-AIR.
29TH ANNUAL MEETING OF HEALTH PHYSICS SOCIETY, NEW ORLEANS, LOUISIANA, JUNE 3-8, 1984.
PERGAMON PRESS, NEW YORK, NY, 1984.
- BAUM, S.J., G.E. MCCLELLAN, G.H. ANNO, 1990.
PROTRACTED EXPOSURE ANNOTATED BIBLIOGRAPHY.
PSR REPORT 1774.
PACIFIC-SIERRA RESEARCH CORPORATION, LOS ANGELES, CA., February 28, 1990.
- BAVERSTOCK, K.F., 1984.
THE RESPONSE OF MAN TO ACCIDENTAL IRRADIATION.
"RESPONSE OF DIFFERENT SPECIES TO TOTAL BODY IRRADIATION", J.J. BROERSE & T.J. MACVITTIE, EDS.
MARTINUS NIGHOFF PUBLISHERS, DORDRECHT, THE NETHERLANDS, 1984.
- BAVERSTOCK, K.F., P.J.N.D. ASH, 1983.
A REVIEW OF RADIATION ACCIDENTS INVOLVING WHOLE BODY EXPOSURE AND THE RELEVANCE TO THE LD50/60 FOR MAN
BRITISH JOURNAL OF RADIOLOGY, Vol 56, 1983, Pages 837-849.
- BAVERSTOCK, K.F., D. PAPWORTH, K. TOWNSEND, 1985.
MAN'S SENSITIVITY TO BONE MARROW FAILURE FOLLOWING WHOLE BODY EXPOSURE
TO LOW LET IONISING RADIATION: INTER. TO BE DRAWN FROM ANIMAL EXPER.
INT. J. OF RADIATION BIOLOGY, Vol 47, 1985, Pages 397-411.
- BAVERSTOCK, K.F., D. PAPWORTH, J. VENNART, 1981.
RISKS OF RADIATION AT LOW DOSE RATES
LAUCET, February 21, 1981, Pages 430-433.
- BAVERSTOCK, K.F., H. SMITH, R. MOLE, P. LINDOP, J. ROTBLAT, P. WEBER, 1984.
LETHALITY FROM ACUTE AND PROTRACTED RADIATION EXPOSURE IN MAN.
INT. J. OF RADIATION BIOLOGY, Vol 46, 1984, Pages 209-217.
- BAZIN, H., B. PLATTEAU, G. PINON-LATAILLAE, J. MAAS, 1986.
STUDIES OF LONG-TERM CONTINUOUS IRRADIATIONS USING DAILY DOSES RANGING FROM 0.07 TO 0.30 GY
ON THE B LYMPHOID SYSTEM OF THE RAT.
INT. J. OF RADIATION BIOLOGY, Vol 49, 1986, Pages 433-447.
- BEDFORD, J.S., J.B. MITCHELL, M.H. FOX, 1980.
VARIATIONS IN RESPONSES OF SEVERAL MAMMALIAN CELL LINES TO LOW DOSE-RATE IRRADIATION
"RADIATION BIOLOGY IN CANCER RESEARCH", RAYMOND E. MEYN & H. RODNEY WITHERS, EDS.
RAVEN PRESS, NEW YORK, 1980, Pages 251-262.
- BERMUDEZ, J., E.A. BOYLE, W.D. MINER, G.J. SANGER, 1988.
THE ANTI-EMETIC POTENTIAL OF THE 5-HYDROXYTRYPTAMINE-3 RECEPTOR ANTAGONIST, BRL 43694.
BRITISH JOURNAL OF CANCER, Vol 58, 1988, Pages 644-650.
- BERRY, R.J., R.H. MOLE, D.W.H. BARNES, 1976.
SKIN RESPONSE TO X-IRRADIATION IN THE GUINEA-PIG
INT. J. OF RADIATION BIOLOGY, Vol 30, 1976, Pages 535-541.
- BIGATELLO, L., ET AL., 1987.
PHOSPHORUS AND ATP DEPLETION IN BLOOD TISSUE FOLLOWING WHOLE BODY IRRADIATION.
AMERICAN COLLEGE OF SURGEONS 1987 SURGICAL FORUM, Vol 38, 1987, Pages 8-10.
- BLACKETT, N.M., 1971.
HAEMATOLOGICAL EFFECTS OF CONTINUOUS RADIATION EXPOSURE
MANUAL ON RADIATION HAEMATOLOGY, CHAPTER 10, TECHNICAL REPORTS SERIES NO. 123, INTERN. ATOMIC ENERGY AGENCY
1971, Pages 123-128.
- BLAIR, H., 1954.
RECOVERY FROM RADIATION INJURY IN MICE AND ITS EFFECT ON LD50 FOR DURATION OF EXPOSURE UP TO SEVERAL WEEKS
UNIVERSITY OF ROCHESTER REPORT, U-R-312
February 1954.
- BLAIR, H., 1964.
THE CONSTANCY OF REPAIR RATE AND OF IRREPARABILITY DURING PROTRACTED EXPOSURE TO IONIZING RADIATION.
(AEC RESEARCH AND DEVELOPMENT REPORT UR-621, 1/7/63)
ANNALS OF THE NEW YORK ACADEMY OF SCIENCES, Vol 114, 1964, Pages 150-157.

- BLAIR, H.A., 1952.
A FORMULATION OF THE INJURY, LIFE SPAN, DOSE RELATIONS FOR IONIZING RADIATION.
ATOMIC ENERGY PROJECT, UR-206.
UNIVERSITY OF ROCHESTER, ROCHESTER, NY, May 13, 1952.
- BOCHE, R.D., 1954.
EFFECTS OF CHRONIC EXPOSURE TO X RADIATION ON GROWTH AND SURVIVAL, CHAPTER 10
BIOLOGICAL EFFECTS OF EXTERNAL RADIATION, (EDITOR: H.A. BLAIR)
1954, Pages 222-252.
- BOND, V., 1969.
RADIATION MORTALITY IN DIFFERENT MAMMALIAN SPECIES
COMPARATIVE CELLULAR AND SPECIES RADIOSENSITIVITY, V.P. BOND & T. SUGAHARA (EDITORS)
IGAKU SHOIN LTD., TOKYO, JAPAN, 1969.
- BOND, V., 1969.
THE GASTROINTESTINAL SYNDROME
COMPARATIVE CELLULAR AND SPECIES RADIOSENSITIVITY, V.P. BOND & T. SUGAHARA (EDITORS)
IGAKU SHOIN LTD., TOKYO, JAPAN, 1969.
- BOND, V.P., T.M. FLIEDNER, J.O. ARCHAMBEAU, 1965.
MAMMALIAN RADIATION LETHALITY:
A DISTURBANCE IN CELLULAR KINETICS.
ACADEMIC PRESS, NEW YORK, NY, 1965.
- BORISON, H.L., R. BORISON, L.E. MCCARTHY, 1981.
PHYLOGENIC AND NEUROLOGIC ASPECTS OF THE VOMITING PROCESS.
JOURNAL OF CLINICAL PHARMACOLOGY, Vol 21, 1981, Pages 235-295.
- BORISON, H.L., L.E. MCCARTHY, E.B. DOUPLE, 1988.
RADIOEMETIC PROTECTION AT 24 H AFTER 60 CO IRRADIATION IN BOTH NORMAL AND POSTREMECTOMIZED CATS.
RADIATION RESEARCH, Vol 114, 1988, Pages 77-83.
- BORTIN, M., 1973.
FACTORS ASSOCIATED WITH INTERSTITIAL PNEUMONITIS AFTER BONE-MARROW TRANSPLANTION FOR ACUTE LEUKAEMIA.
Vol 2, 1973, Pages 437.
- BOYER, N.H., A.D. CONGER, 1972.
LOW-DOSE X-IRRADIATION DAMAGE TO CAPILLARIES OF MOUSE SMALL INTESTINE:
A CORRELATED HISTOLOGIC AND MICROANGIOGRAPHIC STUDY.
INVESTIGATIVE RADIOLOGY, Vol 7, 1972.
- BRABY, L.A., J.M. NELSON, W.C. ROESCH, 1980.
COMPARISON OF REPAIR RATES DETERMINED BY SPLIT-DOSE AND DOSE-RATE METHODS
RADIATION RESEARCH, Vol 82, 1980, Pages 211-214.
- BRABY, L.A., W.C. ROESCH, 1978.
TESTING OF DOSE RATE MODELS WITH CHLAMYDOMONAS REINHARDI
RADIATION RESEARCH, Vol 76, 1978, Pages 259-270.
- BRECHER, G., C.E. BRAMBEL, F.D. BRAMBEL, 1964.
PATTERNS OF HAEMATOPOIETIC RESPONSE TO CONTINUOUS WHOLE-BODY IRRADIATION
ANNALS OF THE NEW YORK ACADEMY OF SCIENCES, Vol 114, 1964, Pages 549-556.
- BRENNAN, D., C.M.A. YOUNG, J.W. HOPEWELL, G. WIERNIK, 1976.
EFFECTS OF VARIED NUMBERS OF DOSE FRACTIONS ON THE TOLERANCE OF NORMAL HUMAN SKIN.
CLINICAL RADIOLOGY, Vol 27, 1976, Pages 27-32.
- BREWER, J., H. LUTPOLD, 1971.
RADIATION INDUCED HUMAN CHROMOSOMIA ABERRATIONS:
IN VITRO DOSE-RATE STUDIES.
EXCERPTA MEDICA AMSTERDAM, Vol 12, 1971, Pages 305-314.
- BRIT. MED. AS., 1983.
THE MEDICAL EFFECTS OF NUCLEAR WAR:
REPORT OF THE BRITISH MEDICAL ASSOCIATION'S BOARD OF SCIENCE AND EDUCATION.
JOHN WILEY AND SONS, NEW YORK, NY, 1983.
- BROERSE, J., H. ROELSE, 1971.
SURVIVAL OF INTESTINAL CRYPT CELLS AFTER FRACTIONATED EXPOSURE TO X-RAYS AND 15 MEV NEUTRONS
INT. J. OF RADIATION BIOLOGY, Vol 20, 1971, Pages 391-395.
- BROERSE, J., J. ZOETELIEF, 1984.
THE OCCURENCE OF RADIATION SYNDROMES IN RODENTS AND MONKEYS IN DEPENDENCE ON DOSE RATE AND RADIATION QUALITY.
"RESPONSE OF DIFFERENT SPECIES TO TOTAL BODY IRRADIATION," J.J. BROERSE & T.J. MACVITTIE, EDS.
MARTINUS NIGHOFF PUBLISHERS, DORDRECHT, THE NETHERLANDS, 1984.
- BROWN, D., R.G. CRAGLE, 1968.
SOME OBSERVATIONS OF DOSE-RATE EFFECT ON BURROS, SWINE AND CATTLE.
DOSE RATE IN MAMMALIAN RADIATION BIOLOGY, A SYMPOSIUM CO-SPONSORED
BY UT-AEC AGRICULTURAL RESEARCH LABORATORY, OAK RIDGE, TN; CONF-680410.
U.S. ATOMIC ENERGY COMMISSION, DIV. OF TECHNICAL INFORMATION, July 12, 1968.
- BROWN, D., W.A. GRAMLY, F.H. CROSS, 1964.
RESPONSE OF 3 BREEDS OF SWINE EXPOSED TO WHOLE-BODY COLBALT 60 GAMMA RADIATION IN DAILY DOSES OF 100 ROENTGENS.
AMERICAN JOURNAL OF VETERINARY RESEARCH, Vol 25, 1964, Pages 1347-1353.

- BROWN, J., M. CORP, D. WESTGARTH, 1960.
EFFECTS OF DOSE-RATE AND FRACTIONATION OF X-RAY DOSE ON ACUTE LETHALITY IN MICE.
INT. J. OF RADIATION BIOLOGY, Vol 4, 1960, Pages 371-381.
- BROWN, J.A.H., M.J. CORP, D.R. WESTGARTH, 1960.
EFFECTS OF DOSE RATE AND FRACTIONATION OF X-RAYS ON ACUTE LETHALITY IN MICE.
INT. J. OF RADIATION BIOLOGY, Vol 2, 1960, Pages 371-381.
- BROYLES, A., 1986.
RADIATION SURVIVAL PROBABILITY IN A NUCLEAR WAR
UCRL - 15859
November 1986.
- BROYLES, A., 1987.
SENSITIVITY TO RADIATION AND RECOVERY OF HEMATOPOIETIC STEM CELLS.
RADIATION RESEARCH, Vol 109, 1987, Pages 12-18.
- BROYLES, A., C. SHAPIRO, 1985.
BIOLOGICAL REPAIR WITH TIME-DEPENDENT IRRADIATION.
HEALTH PHYSICS, Vol 49, 1985, Pages 701-705.
- BRUCER, M.B., 1959.
THE ACUTE RADIATION SYNDROME: A MEDICAL REPORT ON THE Y-12 ACCIDENT, JUNE 16, 1958.
OAK RIDGE INSTITUTE OF NUCLEAR STUDIES, REPORT ORINS-25, OAK RIDGE, TN.
U.S. ATOMIC ENERGY COMMISSION, WASHINGTON, DC, 1959.
- BRUNER, A., 1977.
IMMEDIATE DOSE RATE EFFECTS OF CO60 ON PERFORMANCE AND BLOOD PRESSURE IN MONKEYS
RADIATION RESEARCH, Vol 70, 1977, Pages 378-390.
- BRUNER, A., V. BOGU, E.A. HENDERSON, 1975.
DOSE-RATE EFFECTS OF 60 CO IRRADIATION ON PERFORMANCE AND PHYSIOLOGY IN MONKEYS
DEFENSE NUCLEAR AGENCY REPORT DNA 3660T
July 30, 1975.
- BURNS, T., 1965.
NOMOGRAM FOR RADIOBIOLOGICALLY-EQUIVALENT FRACTIONATED DOSES.
BRITISH JOURNAL OF RADIOLOGY, Vol 38, 1965, Pages 545-547.
- BURYKINA, L.N., 1971.
REMOTE AFTEREFFECTS OF DAMAGE OF DOGS BY STRONTIUM-90
OTDALENNYYE POSLEDSTVIYA LUCHEVYKH PORAZHENIY, ATOMIZDAT
U.S. ATOMIC ENERGY COMMISSION, DIV. OF TECHNICAL INFORMATION, 1971, Pages 232-250.
- CARPENTER, D.O., D.B. BRIGGS, A.P. KNOX, N.L. STROMINGER, 1986.
RADIATION INDUCED EMESIS IN THE DOG: EFFECTS OF LESIONS AND DRUGS.
RADIATION RESEARCH, Vol 108, 1986, Pages 307-316.
- CARSTEN, A.L., T.R. NOONAN, 1959.
RECOVERY FROM PARTIAL-BODY X-IRRADIATION AS MEASURED BY THE LETHALITY OF TWO EXPOSURES
RADIATION RESEARCH, Vol 11, 1959, Pages 165-176.
- CASARETT, A.P., 1968.
RADIATION BIOLOGY
PRENTICE HALL, INC., ENGLEWOOD CLIFFS, NJ, 1968.
- CASARETT, G.W., 1969.
PATTERNS OF RECOVERY FROM LARGE SINGLE DOSE EXPOSURE TO RADIATION
COMPARATIVE CELLULAR AND SPECIES RADIOSENSITIVITY, V.P. BOND, & T. SUGAHARA (EDITORS)
IGAKU SHOIN LTD., TOKYO, JAPAN, 1969.
- CASARETT, G.W., H.A. EDDY, 1968.
FRACTIONATION OF DOSE IN RADIATION-INDUCED MALE STEER LETHALITY.
DOSE RATE IN MAMMALIAN RADIATION BIOLOGY, A SYMPOSIUM CO-SPONSORED
BY UT-AEC AGRICULTURAL RESEARCH LABORATORY, OAK RIDGE, TN: CONF-680410.
U.S. ATOMIC ENERGY COMMISSION, DIV. OF TECHNICAL INFORMATION, July 12, 1968, Pages 14.1-14.10.
- CASSADY, J.R., S. ORDER, B. CAMITTA, A. MARCK, 1976.
MODIFICATION OF GASTROINTESTINAL SYMPTOMS FOLLOWING IRRADIATION BY LOW DOSE RATE TECHNIQUE
INT. J. OF RADIATION ONCOLOGY, BIOLOGY, AND PHYSICS, Vol 1, 1976, Pages 15-20.
- CHAMBERS, F.W., C.R. BILES, L.J. BODENLOS, J.H. DOWLING, 1964.
MORTALITY AND CLINICAL SIGNS IN SWINE EXPOSED TO TOTAL BODY COBALT-60 GAMMA IRRADIATION
RADIATION RESEARCH, Vol 22, 1964, Pages 316-333.
- CHENG, W., W. YOUMING, C. XIAOHENG, L. QUINGMEI, 1982.
EFFECT OF CHRONIC IRRADIATION OF 60 CO GAMMA-RAY AT LOW DOSE RATE ON RHESUS MONKEY.
SCIENTIA SINICA, Vol 25, 1982, Pages 376-384.
- CHU-TSE, W., L. LAJTHA, 1975.
HEMOPOIETIC STEM-CELL KINETICS DURING CONTINUOUS IRRADIATION.
INT. J. OF RADIATION BIOLOGY, Vol 27, 1975, Pages 41-50.

- CHU-TSE, W., T. SHAO-ZHI, J. XUE-YING, 1983.
KINETIC STUDIES OF RADIATION DAMAGE AND RECOVERY OF MURINE HAEMOPOIETIC STEM CELLS DURING AND AFTER CONTINUOUS IRRADIATION AT LOW DOSE RATE
CELL TISSUE KINET.
Vol 16, 1983, Pages 199-207.
- CLARK, S.C., R. KAMEN, 1987.
THE HUMAN HEMATOPOIETIC COLONY-STIMULATING FACTORS
SCIENCE, Vol 236, June 5, 1987, Pages 1229-1237.
- COHEN, L., M. CREDITOR, 1983.
ISOEFFECT TABLES FOR TOLERANCE OF IRRADIATED NORMAL HUMAN TISSUES.
INT. J. OF RADIATION ONCOLOGY, BIOLOGY, AND PHYSICS, Vol 9, 1983, Pages 233-241.
- COLLIS, C., J. DOWN, 1984.
THE EFFECT OF DOSE RATE AND MULTIPLE FRACTIONS PER DAY ON RADIATION-INDUCED LUNG DAMAGE IN MICE.
BRITISH JOURNAL OF RADIOLOGY, Vol 57, 1984, Pages 1037-1039.
- CONRAD, R., 1980.
THE 1954 BIKINI ATOL INCIDENT: AN UPDATE OF THE FINDINGS IN THE MARSHALLESE PEOPLE
THE MEDICAL BASIS FOR RADIATION ACCIDENT PREPAREDNESS, K.F. HUBNER & S.A. FRY (EDITORS)
ELSEVIER NORTH HOLLAND, INC., NEW YORK, 1980, Pages 55-58.
- COOP RES GROUP, 1980.
EFFECT OF CHRONIC IRRADIATION OF CO 60 GAMMA-RAY AT LOW DOSE RATE ON THE RHESUS MONKEY.
SCIENTIA SINICA, Vol 23, 1980, Pages 1170-1181.
- CORDTS, R.E., K.P. FERLIC, M.G. YOCKMOWITZ, J.L. MATTSSON, 1985.
EMESIS ED50 OF NEUTRON IRRADIATION AND PROPHYLACTIC EFFECTIVENESS.
AEROSPACE MEDICAL DIVISION (AFSC), USAFSAM-TR-85-46.
U.S.A.F. SCHOOL OF AEROSPACE MEDICINE, BROOKS AF BASE, TX, August 1985.
- COURT BROWN, W.M., 1953.
SYMPTOMATIC DISTURBANCE AFTER SINGLE-THERAPEUTIC DOSE OF X-RAYS.
BRITISH MEDICAL JOURNAL, 1953, Pages 802-805.
- COURT BROWN, W.M., R. DOLL, 1965.
MORTALITY FROM CANCER AND OTHER CAUSES AFTER RADIOTHERAPY FOR ANKYLOSING SPONDYLITIS
BRITISH MEDICAL JOURNAL, Vol 2, December 1965, Pages 1327-1332.
- COURTENAY, V., 1963.
STUDIES ON THE PROTECTIVE EFFECT OF ALLOGENEIC MARROW GRAFTS IN THE RAT
FOLLOWING WHOLE-BODY IRRADIATION AT DIFFERENT DOSE-RATES.
BRITISH JOURNAL OF RADIOLOGY, Vol 36, 1963, Pages 440-447.
- COX, D.R., 1983.
ANALYSIS OF BINARY DATA
CHAPMAN AND HALL, LONDON, 1983.
- CRAGLE, A.G., T.R. NOONAN
DOSE RATE IN MAMMALIAN RADIATION BIOLOGY
Pages 5.1-5.16.
- CRONKITE, E.P., 1982.
THE EFFECTS OF DOSE, DOSE RATE AND DEPTH DOSE UPON RADIATION MORTALITY.
THE CONTROL OF EXPOSURE OF THE PUBLIC TO IONIZING RADIATION IN THE EVENT OF ACCIDENT OR ATTACK, RESTON, VA, APRIL 1981
NATIONAL COUNCIL ON RADIATION PROTECTION AND MEASUREMENT, BETHESDA, MD, May 15, 1982.
- CRONKITE, E.P., V.P. BOND, 1960.
DIAGNOSIS OF RADIATION INJURY AND ANALYSIS OF THE HUMAN LETHAL DOSE OF RADIATION.
U.S. ARMED FORCES MEDICAL JOURNAL, Vol 11, 1960, Pages 249-260.
- CRONKITE, E.P., V.P. BOND, A.L. CARSTEN, T. INOUE, M.E. MILLER, J.E. BULLIS, 1987.
EFFECTS OF LOW LEVEL RADIATION UPON THE HEMATOPIETIC STEM CELL:
IMPLICATIONS FOR LEUKEMOGENESIS
RADIATION ENVIRONMENTAL BIOPHYSICS, Vol 26, 1987, Pages 106-114.
- CRONKITE, E.P., V.P. BOND, R.A. CONRAD, R. SHULMAN, R.S. FARR, S. COHN, 1955.
RESPONSE OF HUMAN BEINGS ACCIDENTALLY EXPOSED TO SIGNIFICANT FALL-OUT RADIATION
J.A.M.A.
Vol 159, October 1, 1955, Pages 430-434.
- CRONKITE, E.P., V.P. BOND, C.L. DUNHAM, 1956.
SOME EFFECTS OF IONIZING RADIATION ON HUMAN BEINGS.
TID-5358.
U.S. ATOMIC ENERGY COMMISSION, WASHINGTON, DC, July 1956.
- CRONKITE, E.P., C.R. SIPE, D.C. ELTZHOLTZ, W.H. CHAPMAN, F.W. CHAMBERS, 1950.
INCREASED TOLERANCE OF MICE TO LETHAL X-RADIATION AS A RESULT OF PREVIOUS SUBLETHAL EXPOSURE, P.S.E.B.M
Vol 73, 1950.
- CURTIS, H.J., K. GEBHARD, 1958.
THE RELATIVE BIOLOGICAL EFFECTIVENESS OF FAST NEUTRONS AND X-RAYS FOR LIFE SHORTENING IN MICE
RADIATION RESEARCH, Vol 9, 1958, Pages 278-284.

- CURTIS, H.J., J. TILLEY, C. CROWLEY, 1964.
THE CELLULAR DIFFERENCES BETWEEN ACUTE AND CHRONIC NEUTRON AND GAMMA-RAY IRRADIATION IN MICE
BIOLOGICAL EFFECTS OF NEUTRON AND PROTON IRRADIATIONS, IAEA, VIENNA
Vol 2, 1964, Pages 143-155.
- CURTIS, S.B., 1982.
IDEAS ON THE UNIFICATION OF RADIOBIOLOGICAL THEORIES.
LBL-15913 OR LBL-13159
LAWRENCE BERKELEY LABORATORY, 1982.
- CURTIS, S.B., 1986.
LETHAL AND POTENTIALLY LETHAL LESIONS INDUCED BY RADIATION - A UNIFIED REPAIR MODEL
RADIATION RESEARCH, Vol 106, 1986, Pages 252-270.
- DALE, R., 1985.
THE APPLICATION OF THE LINEAR-QUADRATIC DOSE-EFFECT EQUATION TO FRACTIONATED AND PROTRACTED RADIOTHEAPY.
BRITISH JOURNAL OF RADIOLOGY, Vol 58, June 1985, Pages 515-528.
- DALE, R., J. HUCZKOWSKI, K.R. TROTT, 1988.
POSSIBLE DOSE RATE DEPENDENCE OF RECOVERY KINETICS AS DEDUCED FROM A PRELIM. ANALYSIS
OF THE EFFECTS OF FRACT. IRRAD. AT VARYING DOSE RATES
BRITISH JOURNAL OF RADIOLOGY, Vol 61, 1988, Pages 153-157.
- DALRYMPLE, G., I. LINDSAY, J. GHIDONI, 1965.
THE EFFECT OF 2-MEV WHOLE BODY X-IRRADIATION ON PRIMATES.
RADIATION RESEARCH, Vol 25, 1965, Pages 377-400.
- DANJOUX, C.E., W.D. RIDER, P.J. FITZPATRICK, 1979.
THE ACUTE RADIATION SYNDROME.
CLINICAL RADIOLOGY, Vol 30, 1979, Pages 581-584.
- DAQUISTO, M., E. BLACKBURN, 1960.
THE INFLUENCE OF DELIVERY RATE OF WHOLE BODY 250KV.ROENTGEN IRRADIATION (30 OR 3 ROENTGEUS PER MINUTE) ON
MICE, RATS, GUINEA PIGS.
AMERICAN JOURNAL OF ROENTGENOLOGY, Vol 84, 1960, Pages 699-704.
- DAVIDSON, H.O., 1957.
BIOLOGICAL EFFECTS OF WHOLE-BODY GAMMA RADIATION ON HUMAN BEINGS
OPERATIONS RESEARCH OFFICE, THE JOHNS HOPKINS UNIVERSITY.
THE JOHNS HOPKINS PRESS, BALTIMORE, MD, 1957.
- DAVIS, C.J., R.K. HARDING, R.A. LESLIE, P.L.R. ANDREWS, 1986.
THE ORGANIZATION OF VOMITING AS A PROTECTIVE REFLEX: A COMMENTARY OF THE FIVE DAYS DISCUSSIONS.
NAUSEA AND VOMITING: MECHANISMS AND TREATMENT, C. DAVIS, G. LAKE-BAKAAR, G. GRAHAME-SMITH, EDS.
SPRINGER-VERLAG, BERLIN, HEIDELBERG, 1986.
- DE BRUYN, P.P.H., 1948.
THE EFFECT OF X-RAYS ON THE LYMPHATIC NODULE WITH REFERENCE TO DOSE AND
RELATIVE SENSITIVITIES OF DIFFERENT SPECIES.
ANATOMICAL RECORD, Vol 101, 1948, Pages 373-404.
- DECQ, M., R. STORER, P. WEIDEN, D. SCUHMACHER, H. SHULMAN, T. GRAHAM, 1981.
HIGH-DOSE TOTAL BODY IRRADIATION AND MARROW RECONSTITUTION IN DOGS:
DOSE RELATED ACUTE TOXICITY AND FRACTIONATION-DEPENDENT LONG TERM SURVIVAL.
RADIATION RESEARCH, Vol 88, 1981, Pages 385-391.
- DEEG, H.J., N. FLOURNOY, K. SULLIVAN, K. SHEEHAN, C.D. BUCKNER, J.E. SANDERS, 1984.
CATARACTS AFTER TOTAL BODY IRRADIATION AND MARROW TRANSPLANTATION: A SPARING EFFECT OF DOSE FRACTIONATION
INT. J. OF RADIATION ONCOLOGY, BIOLOGY, AND PHYSICS, Vol 10, 1984, Pages 957-964.
- DEEG, H.J., 1983.
ACUTE AND DELAYED TOXICITIES OF TOTAL BODY IRRADIATION.
INT. J. OF RADIATION ONCOLOGY, BIOLOGY, AND PHYSICS, Vol 9, 1983, Pages 1933-1939.
- DENEKAMP, J., 1973.
CHANGES IN THE RATE OF REPOPULATION DURING MULTIFRACTION IRRADIATION OF MOUSE SKIN.
BRITISH JOURNAL OF RADIOLOGY, Vol 46, 1973, Pages 381-387.
- DENEKAMP, J., 1986.
CELL KINETICS AND RADIATION BIOLOGY
INT. J. OF RADIATION BIOLOGY, Vol 49, 1986, Pages 357-380.
- DENNIS, J.A., 1987.
LETTER TO THE EDITOR
DOSE RATE EFFECTS: IMPLICATIONS FOR RELATIVE BIOLOGICAL EFFECTIVENESS AND RADIOLOGICAL PROTECTION
INT. J. OF RADIATION BIOLOGY, Vol 51, 1987, Pages 941-946.
- DEPLEDGE, M., A. BARRETT, 1982.
DOSE-RATE DEPENDENCE OF LUNG DAMAGE AFTER TOTAL BODY IRRADIATION IN MICE.
INT. J. OF RADIATION BIOLOGY, Vol 41, 1982, Pages 325-334.
- DOLPHIN, G., 1973.
CHROMOSOME ABERRATIONS ANALYSIS AS A DOSIMETRIC TECHNIQUE IN RADIOLOGICAL PROTECTION.
HEALTH PHYSICS, Vol 25, 1973, Pages 007.

- DOWN, J., F. EASTON, G. STEEL, 1986.
REPAIR IN THE MOUSE LUNG DURING LOW DOSE-RATE IRRADIATION
RADIOTHERAPY AND ONCOLOGY, Vol 6, 1986, Pages 29-42.
- DURAND, R.E., P.L. OLIVE, 1976.
IRRADIATION OF MULTI-CELL SPHEROIDS WITH FAST NEUTRONS VERSUS X-RAYS: A QUALITATIVE DIFFERENCE IN SUB-LETHAL DAMAGE
REPAIR CAP. OR KINETICS
INT. J. OF RADIATION BIOLOGY, Vol 30, 1976, Pages 589-592.
- DUTREIX, J., A. SAHATCHIEV, 1975.
CLINICAL RADIOBIOLOGY OF LOW DOSE RATE RADIOTHERAPY
BRITISH JOURNAL OF RADIOLOGY, Vol 48, 1975, Pages 846-850.
- DUTREIX, J., A. WAMBERSIE, M. LOIRETTE, G. BOISSERIE, 1979.
TIME FACTORS IN TOTAL BODY IRRADIATION
PATHOLOGIE BIOLOGIE, Vol 27, 1979, Pages 365-369.
- DUTREIX, J., A. WAMBESIE, 1973.
RELATIONSHIP BETWEEN ISOEFFECT TOTAL DOSE AND FRACTION NUMBER FOR HUMAN SKIN REACTION.
EXCERPTA MEDICA AMSTERDAM, Vol 2, 1973, Pages 205-209.
- EDMONSON, P.W., A.L. BATCHELOR, 1971.
ACUTE LETHAL RESPONSE OF GOATS AND SHEEP TO BILATERAL OR UNILATERAL WHOLE BODY IRRADIATION
BY GAMMA RAYS AND FISSION NEUTRONS.
INT. J. OF RADIATION BIOLOGY, Vol 20, 1971, Pages 269-290.
- EDSALL, D.L., R. PEMBERTON, 1907.
THE NATURE OF THE GENERAL TOXIC REACTION FOLLOWING EXPOSURE TO X-RAYS.
AMERICAN JOURNAL OF MEDICAL SCIENCE, Vol 133, 1907, Pages 426-431.
- EDWARDS, A., D. LLOYD, 1980.
ON THE PREDICTION OF DOSE-RATE EFFECTS FOR DICENTRIC PRODUCTION IN HUMAN LYMPHOCYTES BY X-AND GAMMA-RAYS.
INT. J. OF RADIATION BIOLOGY, Vol 37, 1980, Pages 89-92.
- ELKIND, M.M., 1977.
THE INITIAL PART OF THE SURVIVAL CURVE
IMPLICATIONS FOR LOW-DOSE, LOW-DOSE-RATE RADIATION RESPONSES
RADIATION RESEARCH, Vol 71, 1977, Pages 9-23.
- ELKIND, M.M., 1980.
CELLS, TARGETS, AND MOLECULES IN RADIATION BIOLOGY
"RADIATION BIOLOGY IN CANCER RESEARCH", RAYMOND E. MEYN & H. RODNEY WITHERS, EDS.
RAVEN PRESS, NEW YORK, 1980, Pages 71-102.
- ELKIND, M.M., A. HAN, K.W. VOLZ, 1963.
RADIATION RESPONSE OF MAMMALIAN CELLS GROWN IN CULTURE.
IV. DOSE DEPENDENCE OF DIVISION DELAY AND POSTIRRADIATION GROWTH OF SURVIVING & NONSURVIVING CHINESE HAMSTER CELLS
JOURNAL OF THE NATIONAL CANCER INSTITUTE, Vol 30, April 1963, Pages 705-721.
- ELLINGER, F., 1947.
INFLUENCE OF DOSE FRACTIONATION ON THE LETHAL X-RAY EFFECT PRODUCED BY TOTAL BODY IRRADIATION IN MICE:
A PRELIMINARY NOTE RADIOLOGY
Vol 49, 1947, Pages 238-241.
- ELLINGER, F., J.C. BARNETT, 1950.
FURTHER STUDIES ON THE INFLUENCE OF DOSE FRACTIONATION ON THE LETHAL X-RAY EFFECT PRODUCED BY TOTAL BODY
IRRADIATION IN MICE.
RADIOLOGY
Vol 54, 1950, Pages 90-92.
- ELLIS, F., 1969.
DOSE, TIME AND FRACTIONATION: A CLINICAL HYPOTHESIS
CLINICAL RADIOL.
Vol 20, 1969, Pages 1-7.
- ELTRINGHAM, R., 1967.
RECOVERY OF THE RHESUS MONKEY FROM AN ACUTE RADIATION INJURY EXPOSURE AS EVALUATED BY THE SPLIT-DOSE TECHNIQUE:
PRELIMINARY RESULTS.
RADIATION RESEARCH, Vol 31, 1967, Pages 533.
- EPSTEIN, L.M., ET AL., 1979.
HALF AND TOTAL BODY RADIATION FOR CARCINOMA OF THE PROSTATE.
JOURNAL OF UROLOGY, Vol 122, 1979, Pages 330-332.
- FABRIKANT, J.I., 1987.
ADAPTATION OF CELL RENEWAL SYSTEMS UNDER CONTINUOUS IRRADIATION
HEALTH PHYSICS, Vol 52, 1987, Pages 561-570.
- FABRY, L., 1986.
CYTOGENETIC DAMAGE INDUCED IN HUMAN LYMPHOCYTES BY LOW DOSES OF 60 CO GAMMA RAYS DELIVERED
AT HIGH AND LOW DOSE RATES.
ACTA RADIOLOGICA ONCOLOGY, Vol 25, 1986, Pages 143-146.
- FAJARDO, L.F., 1982.
PATHOLOGY OF RADIATION INJURY.
MASSON PUBLISHING USA INC., NEW YORK, NY, 1982, Pages 263-265.

- FANG, P., 1970.
ANALYSIS OF DOSE-RATE DEPENDENCE OF RADIATION INJURY.
RADIATION RESEARCH, Vol 44, 1970, Pages 1-3.
- FANGER, H., C.C. LUSHBAUGH, 1967.
RADIATION DEATH FROM CARDIOVASCULAR SHOCK FOLLOWING A CRITICALITY ACCIDENT.
ARCHIVES OF PATHOLOGY, Vol 83, 1967, Pages 446-460.
- FIELD, S.B., 1976.
EFFECTS OF FRACTIONATED IRRADIATION ON MOUSE LUNG AND A PHENOMENON OF SLOW REPAIR.
BRITISH JOURNAL OF RADIOLOGY, Vol 49, 1976, Pages 700-707.
- FIELD, S.B., S. HORNSEY, 1974.
DAMAGE TO MOUSE LUNG WITH NEUTRONS AND X-RAYS.
EUROPEAN JOURNAL OF CANCER, Vol 10, 1974, Pages 621-627.
- FIELD, S.B., R.L. MORGAN, R. MORRISON, 1976.
THE RESPONSE OF HUMAN SKIN TO IRRADIATION WITH X-RAYS OR FAST NEUTRONS
INT. J. OF RADIATION ONCOLOGY, BIOLOGY, AND PHYSICS, Vol 1, 1976, Pages 481-486.
- FITZGERALD, T., M. MCKENNA, L. ROTHSTEIN, C. DAUGHERTY, K. KASE, J. GREENBERGER, 1986.
RADIOSENSITIVITY OF HUMAN BONE MARROW GRANULOCYTE-MACROPHAGE PROGENITOR CELLS AND
STROMAL COLONY FORMING CELLS: EFFECT OF DOSE RATE
RADIATION RESEARCH, Vol 107, 1986, Pages 205-215.
- FITZPATRICK, P.J., W.D. RIDER, 1975.
HALF-BODY RADIOTHERAPY OF ADVANCED CANCER.
JOURNAL OF THE CANADIAN ASSOCIATION OF RADIOLOGISTS, Vol 27, 1975, Pages 670D.
- FITZPATRICK, P.J., W.D. RIDER, 1976.
HALF-BODY RADIOTHERAPY.
INT. J. OF RADIATION ONCOLOGY, BIOLOGY, AND PHYSICS, Vol 1, 1976, Pages 197-207.
- FLIEDNER, T.M., K.H. STEINBACH, T. SZEPESI, 1988.
HEMATOLOGICAL INDICATORS IN THE DETERMINATION OF CLINICAL MANAGEMENT STRATEGIES IN RADIATION ACCIDENTS.
PRESENTED AT INTERNATIONAL CONFERENCE, HANGZHOU, PRC, MARCH 27 - APRIL 1, 1988.
UNIVERSITY OF ULM, D-7500 ULM, FRG, 1988.
- FOWLER, J.F., 1968.
EFFECTS OF FRACTIONATED IRRADIATION ON THE SKIN OF PIGS AND OTHER ANIMALS AND ON TUMOURS IN RATS.
DOSE RATE IN MAMMALIAN RADIOBIOLOGY, A SYMPOSIUM CO-SPONSORED BY
UT-AEC AGRICULTURAL RESEARCH LABORATORY, OAK RIDGE, TN, CONF-680410.
U.S. ATOMIC ENERGY COMMISSION, DIV. OF TECHNICAL INFORMATION, 1968.
- FOWLER, J.F., 1984.
WHAT NEXT IN FRACTIONATED RADIOTHERAPY?
BRITISH JOURNAL OF CANCER, Vol 49, 1984, Pages 285-300.
- FOWLER, J.F., D.K. BEWLEY, R.L. MORGAN, J.A. SILVESTER, 1965.
EXPERIMENTS WITH FRACTIONATED X-IRRADIATION OF THE SKIN OF PIGS. II- FRACTIONATION UP TO FIVE DAYS.
BRITISH JOURNAL OF RADIOLOGY, Vol 38, 1965, Pages 278-284.
- FOWLER, J.F., J. LAWREY, 1960.
DOSE-RATE EFFECTS ON MICE AND RATS IN THE RANGE 2 TO 340 RADS/MINUTE.
BRITISH JOURNAL OF RADIOLOGY, Vol 33, 1960, Pages 382-388.
- FOWLER, J.F., E.L. TRAVIS, 1982.
REPAIR OF LATE AND EARLY RADIATION INJURY IN LUNGS OF EXPERIMENTAL MICE
BRITISH JOURNAL OF RADIOLOGY, 1982, Pages 297-298.
- FRINDEL, E., G.M. HAHN, D. ROBAGLIA, M. TUBIANA, 1972.
RESPONSES OF BONE MARROW AND TUMOR CELLS TO ACUTE AND PROTRACTED IRRADIATION
CANCER RESEARCH, Vol 32, October 1972, Pages 2096-2103.
- FRITZ, T.E., W.P. NORRIS, C.E. REHFELD, C.M. POOLE, 1968.
CERIUM-144-TOXIC MANIFESTATIONS IN BEAGLE DOGS
Vol 4, 1968, Pages 260-261.
- FRITZ, T.E., W.P. NORRIS, D.V. TOLLE, 1973.
MYELOGENOUS LEUKEMIA AND RELATED MYELOPROLIFERATIVE DISORDERS IN BEAGLES CONTINUOUSLY EXPOSED TO CO60 γ -RADIATION
UNIFYING CONCEPTS OF LEUKEMIA, BIBL. HAEMAT. NO. 39
1973, Pages 170-188.
- FRYER, C., ET AL., 1978.
RADIATION PNEUMONITIS:
EXPERIENCE FOLLOWING A LARGE SINGLE DOSE OF RADIATION.
INT. J. OF RADIATION ONCOLOGY, BIOLOGY, AND PHYSICS, Vol 4, 1978, Pages 931-936.
- FU, K., T.L. PHILLIPS, L.J. KANE, V. SMITH, 1975.
TUMOR AND NORMAL TISSUE RESPONSE TO IRRADIATION IN VIVO
VARIATION WITH DECREASING DOSE RATES
RADIOLOGY, Vol 114, March 1975, Pages 709-716.
- GEN-YAO, Y., L. YONG, T. NIE, C. BEN-YUN, CHIEN FENG-WEI, X. CHIEN-LING, 1980.
THE PEOPLE'S REPUBLIC OF CHINA ACCIDENT IN 1963
THE MEDICAL BASIS FOR RADIATION ACCIDENT PREPAREDNESS, K. HUBNER & S.A. FRY (EDITORS)
ELSEVIER NORTH HOLLAND, INC., NEW YORK, 1980, Pages 81-89.

- GENGOZIAN, N., D. CARLSON, E. ALLEN, 1969.
TRANSPLANTION OF ALLOGENEIC AND XENOGENEIC (RAT) MARROW IN IRRADIATED MICE AS AFFECTED BY RADIATION EXPOSURE RATES.
TRANSPLANTATION, Vol 7, 1969, Pages 259-273.
- GENGOZIAN, N., D. CARLSON, C. GOTTLIEB, 1968.
RADIATION EXPOSURE RATES: EFFECTS ON THE IMMUNE SYSTEM.
DOSE RATE IN MAMMALIAN RADIATION BIOLOGY, A SYMPOSIUM CO-SPONSORED
BY UT-AEC AGRICULTURAL RESEARCH LABORATORY, OAK RIDGE, TN; CONF-680410
U.S. ATOMIC ENERGY COMMISSION, DIV. OF TECHNICAL INFORMATION, July 12, 1968.
- GENGOZIAN, N., T. TAYLOR, H. JAMESON, E. LEE, R. GOOD, R. EPSTEIN, 1986.
RADIATION-INDUCED HEMOPOIETIC DEATH IN MICE AS A FUNCTION OF PHOTON ENERGY AND DOSE RATE.
RADIATION RESEARCH, Vol 105, 1986, Pages 320-327.
- GERSTNER, H.B., 1958.
ACUTE RADIATION SYNDROME IN MAN.
U.S. ARMED FORCES MEDICAL JOURNAL, Vol 9, 1958, Pages 313-354.
- GERSTNER, H.B., 1960.
REACTION TO SHORT TERM RADIATION IN MAN.
ANNUAL REVIEWS OF MEDICINE, Vol 11, 1960, Pages 289-302.
- GERSTNER, H.B., 1970.
PRACTICAL IMPLICATION OF THE INITIAL REACTION TO PENETRATING IONIZING RADIATION.
UNPUBLISHED MANUSCRIPT.
U.S.A.F. SCHOOL OF AEROSPACE MEDICINE, BROOKS AF BASE, TX, 1970.
- GIDALL, J., I. BOJTOR, I. FEHER, 1979.
KINETIC BASIS FOR COMPENSATED HEMOPOIESIS DURING CONTINUOUS IRRADIATION WITH LOW DOSES
RADIATION RESEARCH, Vol 77, 1979, Pages 285-291.
- GILBERTI, M.V., 1980.
THE 1967 RADIATION ACCIDENT NEAR PITTSBURGH, PENNSYLVANIA, AND A FOLLOW-UP REPORT
THE MEDICAL BASIS FOR RADIATION ACCIDENT PREPAREDNESS, K. HUBNER & S.A. FRY (EDITORS)
ELSEVIER NORTH HOLLAND, INC., NEW YORK, 1980, Pages 131-140.
- GLASGOW, G., ET AL., 1983.
DOSE RATE EFFECTS ON THE SURVIVAL OF NORMAL HEMOPOIETIC STEM CELLS OF BALBC MICE.
INT. J. OF RADIATION ONCOLOGY, BIOLOGY, AND PHYSICS, Vol 9, 1983, Pages 557-563.
- GLASSTONE, S., P.J. DOLAN, 1977.
THE EFFECTS OF NUCLEAR WEAPONS, 3RD ED.
U.S. DEPARTMENTS OF DEFENSE AND ENERGY, WASHINGTON, DC, 1977.
- GLENN, N.D., H.S. DUCOFF, 1976.
ACUTE LETHALITY AFTER FAST-NEUTRON AND X-IRRADIATION OF TRIBOLIUM CONFUSUM
RADIATION RESEARCH, Vol 65, 1976, Pages 120-129.
- GOLDE, D.W., J.C. GASSON, 1988.
HORMONES THAT STIMULATE THE GROWTH OF BLOOD CELLS
SCIENTIFIC AMERICAN, July 1988, Pages 62-70.
- GOLLEY, F.W., ET AL., 1965.
RESPONSE OF WILD RODENTS TO ACUTE GAMMA RADIATION.
RADIATION RESEARCH, Vol 24, 1965, Pages 350-356.
- GOODHEAD, D.T., 1980.
MODELS OF RADIATION INACTIVATION AND MUTAGENESIS
"RADIATION BIOLOGY IN CANCER RESEARCH", RAYMOND E. MEYN & H. RODNEY WITHERS, EDS.
RAVEN PRESS, NEW YORK, 1980, Pages 231-245.
- GOTTLIEB, C., N. GENGOZIAN, 1972.
RADIATION DOSE, DOSE RATE AND QUALITY IN SUPPRESSION OF THE HUMORAL IMMUNE RESPONSE.
JOURNAL OF IMMUNOLOGY, Vol 109, 1972, Pages 719-727.
- GRAHN, D., 1969.
BIOLOGICAL EFFECTS OF PROTRACTED LOW DOSE RADIATION EXPOSURE OF MAN AND ANIMALS. CHAPTER V
LATE EFFECTS OF RADIATION, R.M. FRY, D. GRAHN, M.L. GRIEM & J.H. RUST (EDITORS)
TAYLOR & FRANCIS LTD., LONDON-NEW YORK-PHILADELPHIA, 1969, Pages 101-136.
- GRAHN, D., J.M. FRY, R.A. LEA, 1972.
ANALYSIS OF SURVIVAL AND CAUSE OF DEATH STATISTICS FOR MICE UNDER SINGLE AND DURATION-OF-LIFE GAMMA IRRADIATION
PROCEEDINGS OF THE OPEN MEETING OF WORKING GROUP 5 OF THE 14TH PLENARY MTG. OF COSPAR, W. VISHNIAC (EDITOR)
AKADEMIE-VERLAG, BERLIN, 1972, Pages 175-186.
- GRALLA, E.J., ET AL., 1979.
THE EFFECT OF SELECTED DRUGS ON FIRST-STAGE RADIOEMESIS IN BEAGLE DOGS.
RADIATION RESEARCH, Vol 78, 1979, Pages 286-295.
- GRANT, G.A., A.B. CAIRNIE, R.K. HARDING, N.T. GRIDGEMAN, W.D. RIDER, 1979.
A PREDICTIVE STUDY OF THE INCIDENCE OF VOMITING IN IRRADIATED MILITARY PERSONNEL.
REPORT 817
DEFENCE RESEARCH ESTABLISHMENT, OTTAWA, CANADA, 1979.

- GRANT, G.A., ET AL., 1979.
A PREDICTIVE STUDY OF THE INCIDENCE OF VOMITING IN IRRADIATED MILITARY PERSONNEL.
REPORT 813
DEFENCE RESEARCH ESTABLISHMENT, OTTAWA, CANADA, October 1979.
- GREENBERG, H.M., P.E. NEWBURGER, L.M. PARKER, T. NOVAK, J.S. GREENBERGER, 1981.
HUMAN GRANULOCYTES GENERATED IN CONTINUOUS BONE MARROW CULTURE ARE PHYSIOLOGICALLY NORMAL
BLOOD, Vol 58, October 1981, Pages 724-732.
- GREENBERGER, J.S., V. KLASSEN, K. KASE, R.K. SHADDUCK, M.A. SAKAKEENY, 1984.
EFFECTS OF LOW DOSE RATE IRRADIATION OF PLATEAU PHASE BONE MARROW STROMAL CELLS IN VITRO:
DEMONSTRATION OF A NEW FORM OF NON-LETHAL, PHYSIOLOGIC DAMAGE TO SUPPORT OF HEMATOPOIETIC STEM CELLS
INT. J. OF RADIATION ONCOLOGY, BIOLOGY, AND PHYSICS, Vol 10, 1984, Pages 1027-1037.
- GREIM, M.L., 1989.
EARLY RESPONSE OF BLOOD VESSELS TO RADIATION.
PREDICTION OF RESPONSE IN RADIATION THERAPY, PART 1: THE PHYSICAL AND BIOLOGICAL BASIS. B.R. PALIWAL, ET AL., EDS.
AMERICAN INSTITUTE OF PHYSICS, INC., 1989.
- GRIFFIN, C., S. HORNSEY, 1986.
THE EFFECT OF NEUTRON DOSE RATE ON JEJUNAL CRYPT SURVIVAL.
INT. J. OF RADIATION BIOLOGY, Vol 49, 1986, Pages 589-595.
- GRIGOREV, Y.G., V.G. GORLOV, A.V. SHAFIRKIN, 1978.
BIOLOGICAL EFFECTIVENESS OF LONG-TERM AND CHRONIC EXPOSURES AS A FUNCTION OF DOSE RATE
AS DETERMINED FOR DIFFERENT ANIMAL SPECIES AND MAN.
RADIOBIOLOGIA, Vol 18, 1978, Pages 591-595.
- GRIGORYEV, Y., B.A. MARKELOV, V.I. POPOV, A.A. AKHUNOV, T.P. TSESSARSKAYA, A.V. ILYUKHIN, 1972.
PHYSIOLOGICAL AND HEMATOLOGICAL EFFECTS OF CHRONIC IRRADIATION
PROCEEDINGS OF THE OPEN MTG. OF WORKING GROUP 5 OF THE 14TH PLENARY MTG. OF COSPAR, W. VISHNIAC
AKADEMIE-VERLAG, BERLIN, 1972, Pages 147-154.
- GUNTER-SMITH, P.J., 1986.
GAMMA RADIATION AFFECTS ACTIVE ELECTROLYTE TRANSPORT BY RABBIT ILEUM:
BASAL NA AND CL TRANSPORT.
AMERICAN JOURNAL OF PHYSIOLOGY, Vol 250, 1986, Pages G540-G545.
- GUNTER-SMITH, P.J., 1989.
GAMMA RADIATION AFFECTS ACTIVE ELECTROLYTE TRANSPORT BY RABBIT ILEUM:
II. CORRELATION OF ALANINE AND THEOPHYLLINE RESPONSE WITH MORPHOLOGY.
RADIATION RESEARCH, Vol 117, 1989, Pages 419-432.
- GUSKOVA, A.K., ET AL., 1987.
MASS RADIATION INJURIES AND PROBLEMS OF THE ORGANIZATION OF MEDICAL AID.
TRANSLATED FROM PUBLISHING HOUSE MEDITSINA, MOSCOW, 1987, PAGES 1-81; DTIC NO. AD-B129 882.
DEFENSE TECHNICAL INFORMATION CENTER, ALEXANDRIA, VA, 1987.
- GUSKOVA, A.K., ET AL., 1988.
ACUTE EFFECTS OF RADIATION EXPOSURE FOLLOWING THE CHERNOBYL ACCIDENT: ...
INTERNAT. REACTS CONF. THE MEDICAL BASIS FOR RADIATION PREPAREDNESS II: ...
MEDICAL AND HEALTH SCIENCES DIV., OAK RIDGE ASSOC. UNIVERSITIES, OAK RIDGE, TN, October 20, 1988.
- GUSKOVA, A.K., ET AL., 1988.
ACUTE RADIATION EFFECTS IN VICTIMS OF THE CHERNOBYL NUCLEAR POWER PLANT ACCIDENT:
APPENDIX TO: SOURCES, EFFECTS, AND RISKS OF IONIZING RADIATION: ISBN 92-1-142143-8.
UNITED NATIONS SCIENTIFIC COMMITTEE ON THE EFFECTS OF ATOMIC RADIATION, 1988.
- GUSKOVA, A.K., ET AL., 1988.
ACUTE EFFECTS OF RADIATION EXPOSURE FOLLOWING THE CHERNOBYL ACCIDENT:
IMMEDIATE RESULTS OF RADIATION SICKNESS AND OUTCOME AND TREATMENT.
May 1988.
- GUYTON, A.C., 1981.
TEXTBOOK OF MEDICAL PHYSIOLOGY
W. B. SAUNDERS CO., PHILADELPHIA, PA, 1981.
- HAGER, E.B., J.W. FERREBEE, E.D. THOMAS, 1963.
DAMAGE AND REPAIR OF THE GASTROINTESTINAL TRACT AFTER SUPRALETHAL RADIATION:
EXPERIENCE WITH DOGS RECEIVING 1800 TO 2400 ROENTGENS OF WHOLE-BODY GAMMA RADIATION
RADIOBIOLOGIA RADIOTHERAPIA, Vol 4, 1963, Pages 1-11.
- HAHN, F.F., D.L. LUNDGREN, R.O. MCCLELLAN, 1980.
REPEATED INHALATION EXPOSURE OF MICE TO CEO₂
II. BIOLOGIC EFFECTS
RADIATION RESEARCH, Vol 82, 1980, Pages 123-137.
- HALEY, T.J., E.F. MCCULLOCH, W.G. MCCORMICK, B.F. TRUM, J.H. RUST, 1955.
RESPONSE OF THE BURRO TO 100 R FRACTIONAL WHOLE-BODY GAMMA RAY IRRADIATION.
AMERICAN JOURNAL OF PHYSIOLOGY, Vol 180, 1955, Pages 403-407.
- HALL, E.J., 1972.
RADIATION DOSE RATE:
A FACTOR OF IMPORTANCE IN RADIOBIOLOGY AND RADIOTHERAPY.
BRITISH JOURNAL OF RADIOLOGY, Vol 45, 1972, Pages 81-97.

- HALL, E.J., 1972.
RADIATION DOSE-RATE:
A FACTOR OF IMPORTANCE IN RADIOBIOLOGY AND RADIOTHERAPY (REVIEW)
BRITISH JOURNAL OF RADIOLOGY, Vol 45, 1972, Pages 81-97.
- HALL, E.J., 1978.
RADIOBIOLOGY FOR THE RADIOBIOLOGIST.
HARPER & ROW, HAGERSTOWN, MD, 1978.
- HALL, E.J., R. BERRY, J. BEDFORD, 1968.
DOSE RATE EFFECTS IN MAMMALIAN CELLS IN VITRO AND IN VIVO.
DOSE RATE IN MAMMALIAN RADIATION BIOLOGY, A SYMPOSIUM CO-SPONSORED
BY UT-AEC AGRICULTURAL RESEARCH LABORATORY, OAK RIDGE, TN, CONF-680410.
U.S. ATOMIC ENERGY COMMISSION, DIV. OF TECHNICAL INFORMATION, 1968.
- HALL, E.J., ED., 1988.
BASIC RADIOBIOLOGY
AMERICAN JOURNAL OF CLINICAL ONCOLOGY (CCT), Vol 11, 1988, Pages 220-252.
- HALL, E.J., M.J. MARCHESE, M.B. ASTOR, T. MORSE, 1986.
RESPONSE OF CELLS OF HUMAN ORIGIN, NORMAL AND MALIGNANT, TO ACUTE AND LOW DOSE RATE IRRADIATION
INT. J. OF RADIATION ONCOLOGY, BIOLOGY, AND PHYSICS, Vol 12, April 1986, Pages 655-659.
- HANKS, G., E. AINSWORTH, G. LEONG, D. NACHTWAY, N. PAGE, 1966.
INJURY ACCUMULATION AND RECOVERY IN SHEEP EXPOSED TO PROTRACTED 60-CO GAMMA-RADIATION.
RADIATION RESEARCH, Vol 29, 1966, Pages 211-221.
- HANKS, G., N. PAGE, E. AINSWORTH, G. LEONG, C. MENKES, E. ALPEN, 1966.
ACUTE MORTALITY AND RECOVERY STUDIES IN SHEEP IRRADIATED WITH COBALT 60 GAMMA OR 1 MVP X-RAYS.
RADIATION RESEARCH, Vol 27, 1966, Pages 397-405.
- HARDING, R.K., 1988.
PRODROMAL EFFECTS OF RADIATION:
PATHWAYS, MODELS, AND PROTECTION BY ANTIEMETICS.
PHARMACOLOGY AND THERAPEUTICS, Vol 37, 1988, Pages 335-345.
- HAUVER, R., V. PENIKAS, W. WALKER, M. NOLD, T. MOBLEY, 1968.
EXPOSURE OF SHEEP TO MILLISECOND VS MICROSECOND FISSION RADIATION.
DOSE RATE IN MAMMALIAN RADIATION BIOLOGY, A SYMPOSIUM CO-SPONSORED
BY UT-AEC AGRICULTURAL RESEARCH LABORATORY, OAK RIDGE, TN; CONF-680410.
U.S. ATOMIC ENERGY COMMISSION, DIV. OF TECHNICAL INFORMATION, July 12, 1968.
- HEMPLEMAN, L.H., H. LISCO, J.G. HOFFMAN, 1952.
THE ACUTE RADIATION SYNDROME:
A STUDY OF NINE CASES AND A REVIEW OF THE PROBLEM.
ANNALS OF INTERNAL MEDICINE, Vol 36, 1952, Pages 279-510.
- HENDRY, J.H., 1979.
THE DOSE-DEPENDENCE OF THE SPLIT-DOSE RESPONSE OF MARROW COLONY-FORMING UNITS (CFU-S):
SIMILARITY TO OTHER ISSUES
INT. J. OF RADIATION BIOLOGY, Vol 36, 1979, Pages 631-637.
- HENDRY, J.H., A. HOWARD, 1971.
THE RESPONSE OF HAEMOPOIETIC COLONY-FORMING UNITS TO SINGLE AND SPLIT DOSES OF X RAYS OR D-T NEUTRONS
INT. J. OF RADIATION BIOLOGY, Vol 19, 1971, Pages 51-64.
- HENDRY, J.H., D. MAJOR, D. GREENE, 1975.
DAILY D-T NEUTRON IRRADIATION OF MOUSE INTESTINE
RADIATION RESEARCH, Vol 63, 1975, Pages 149-156.
- HENDRY, J.H., J.V. MOORE, 1985.
DERIVING ABSOLUTE VALUES OF ALPHA AND BETA FOR DOSE FRACTIONATION, USING DOSE-INCIDENCE DATA
BRITISH JOURNAL OF RADIOLOGY, Vol 58, September 1985, Pages 885-890.
- HENDRY, J.H., C.S. POTTEN, N.P. ROBERTS, 1983.
THE GASTROINTESTINAL SYNDROME AND MUCOSAL CLONOGENIC CELLS:
RELATIONSHIPS BETWEEN TARGET CELL SENSITIVITIES, LD-50, AND CELL SURVIVAL, AND THEIR MODIFICATION BY ANTIBIOTICS.
RADIATION RESEARCH, Vol 96, 1983, Pages 100-112.
- HENKELMAN, R.M., G.K.Y. LAM, R.O. KORNELSEN, C.J. EAVES, 1980.
EXPLANATION OF DOSE-RATE AND SPLIT-DOSE EFFECTS ON MOUSE FOOT REACTIONS USING THE SAME TIME FACTOR
RADIATION RESEARCH, Vol 84, 1980, Pages 276-289.
- HENSHAW, P.S., 1944.
EFFECTS OF REPEATED SMALL DOSE OF X-RAYS ON BLOOD PICTURE, TISSUE MORPHOLOGY, AND LIFE SPAN IN MICE.
JOURNAL OF THE NATIONAL CANCER INSTITUTE, Vol 4, 1944, Pages 513-522.
- HENSHAW, P.S., 1956.
REPAIR ASSOCIATED WITH THE EROSIVE EFFECTS OF FALLOUT DAMAGE IN INDIVIDUALS AND POPULATION GROUPS
THE SHORTER-TERM BIOLOGICAL HAZARDS OF A FALLOUT FIELD, (EDITORS: GORDON M. DUNNING, JOHN A. HILCKEN)
U.S. DEPARTMENT OF DEFENSE, ATOMIC ENERGY COMMISSION, 1956, Pages 87-92.
- HEUSS, K., 1967.
ZUR FRAGE DER ERHOLUNGS VORGAENGE BEI DAUERBESTRAHLUNGEN VON VERSUCHSTIEREN MIT ROENTGENSTRAHLEN
BIOPHYSIK, Vol 4, 1967, Pages 146-154.

- HILL, C.K., F.M. BUONAGURO, C.P. MYERS, A. HAN, M.M. ELKIND, 1982.
FISSION-SPECTRUM NEUTRONS AT REDUCED DOSE RATES ENHANCE NEOPLASTIC TRANSFORMATION
NATURE, Vol 298, July 1, 1982, Pages 67-69.
- HILL, C.K., A. HAN, M.M. ELKIND, 1987.
PROMOTION, DOSE RATE, AND REPAIR PROCESSES IN RADIATION-INDUCED NEOPLASTIC TRANSFORMATION
RADIATION RESEARCH, Vol 109, 1987, Pages 347-351.
- HILL, R., 1983.
RESPONSE OF MOUSE LUNG TO IRRADIATION AT DIFFERENT DOSE RATES.
INT. J. OF RADIATION ONCOLOGY, BIOLOGY, AND PHYSICS, Vol 9, 1983, Pages 1043-1047.
- HOLLOWAY, R., G. LEONG, E. AINSWORTH, M. ALBRIGHT, S. BAUM, 1968.
RECOVERY FROM RADIATION INJURY IN THE HAMSTER AS EVALUATED BY THE SPLIT-DOSE TECHNIQUE.
RADIATION RESEARCH, Vol 33, 1968, Pages 37-49.
- HOME OFFICE, 1985.
THE SCIENTIFIC BASIS FOR THE DEVELOPMENT OF GUIDANCE AND OPERATIONAL PROCEDURES
FOR LIVING UNDER RADIOACTIVE FALLOUT CONDITIONS.
SCIENTIFIC RESEARCH AND DEVELOPMENT BRANCH, PUBLICATION 20/85.
HOME OFFICE, GREAT BRITAIN, 1985.
- HOPPER, J.L., P.J. BROCKWELL, 1978.
A STOCHASTIC MODEL FOR CELL POPULATIONS WITH CIRCADIAN RHYTHMS
CELL AND TISSUE KINETICS, Vol 11, 1978, Pages 205-225.
- HORNSEY, S., 1970.
DIFFERENCES IN SURVIVAL OF JEJUNAL CRYPT CELLS AFTER RADIATION DELIVERED AT DIFFERENT DOSE-RATES.
BRITISH JOURNAL OF RADIOLOGY, Vol 43, 1970, Pages 802-806.
- HORNSEY, S., T. ALPER, 1966.
UNEXPECTED DOSE-RATE EFFECT IN THE KILLING OF MICE BY RADIATION.
NATURE, Vol 210, 1966, Pages 212-213.
- HORNSEY, S., S. VATISTAS, 1963.
SOME CHARACTERISTICS OF THE SURVIVAL CURVE OF CRYPT CELLS OF THE SMALL INTESTINE OF THE MOUSE
DEDUCED AFTER WHOLE BODY X-IRRADIATION.
BRITISH JOURNAL OF RADIOLOGY, Vol 36, 1963, Pages 795-800.
- HORNSEY, S., S. VATISTAS, D. BEWLEY, C. PARNELL, 1965.
THE EFFECT OF FRACTIONATION ON FOUR DAY SURVIVAL OF MICE AFTER WHOLE-BODY NEUTRON IRRADIATION.
BRITISH JOURNAL OF RADIOLOGY, Vol 38, 1965, Pages 878-880.
- HUBNER, K., 1975.
SUPPRESSION AND RECOVERY OF THE IMMUNE RESPONSE AND CFU POTENTIAL OF MICE DURING AND AFTER CHRONIC LOW-DOSE RATE
GAMMA-IRRADIATION.
INT. J. OF RADIATION BIOLOGY, Vol 28, 1975, Pages 301-312.
- HUBNER, K.F., S.A. FRY, EDS., 1980.
THE MEDICAL BASIS FOR RADIATION ACCIDENT PREPAREDNESS
ELSEVIER NORTH HOLLAND, INC., NEW YORK, 1980.
- HUCZKOWSKI, J., K. TROTT, 1984.
DOSE FRACTIONATION EFFECTS IN LOW DOSE RATE IRRADIATION OF JEJUNAL CRYPT STEM CELLS.
INT. J. OF RADIATION BIOLOGY, Vol 46, 1984, Pages 293-298.
- HUCZKOWSKI, J., K. TROTT, 1987.
JEJUNAL CRYPT STEM-CELL SURVIVAL AFTER FRACTIONATED GAMMA-IRRADIATION PERFORMED AT DIFFERENT DOSE RATES.
INT. J. OF RADIATION BIOLOGY, Vol 51, 1987, Pages 131-137.
- HUPP, E., J. AUSTIN, G. KRISSE, S. BROWN, M. SZABUNIEWICZ, 1971.
SURVIVAL OF SPANISH GOATS EXPOSED TO CONTINUOUS OR ACUTE IRRADIATION.
INT. J. OF RADIATION BIOLOGY, Vol 20, 1971, Pages 475-484.
- HURSH, J., G. CASARETT, A. CARSTEN, T. NOONAN, S. MICHAELSON, J. HOWLAND, 1958.
OBSERVATION ON RECOVERY AND IRREVERSIBLE RADIATION INJURY IN MAMMALS.
UNIVERSITY OF ROCHESTER, SCHOOL OF MEDICINE AND DENTISTRY REPORT
1958.
- IAEA, 1988.
THE RADIOLOGICAL ACCIDENT IN GOIANA.
STI/PUB/815, ISBN 92-0-127088-8.
INTERNATIONAL ATOMIC ENERGY AGENCY, VIENNA, 1988.
- IBERALL, A.S., 1967.
QUANTITATIVE MODELING OF THE PHYSIOLOGICAL FACTORS IN RADIATION LETHALITY
ANNALS OF THE NEW YORK ACADEMY OF SCIENCES, Vol 147, October 1, 1967, Pages 1-81.
- IMLAY, J.A., S. LINN, 1988.
DNA DAMAGE AND OXYGEN RADICAL TOXICITY
SCIENCE, Vol 240, June 3, 1988, Pages 1302-1309.
- INGRAM, M., 1969.
THE GASTROINTESTINAL SYNDROME IN ACUTE RADIATION INJURY, PART II:
A STUDY OF THE METABOLIC ASPECTS OF THERAPY OF RADIATION INJURY IN THE SOLDIER; AD 696 445.
NATIONAL TECHNICAL INFORMATION SERVICE, SPRINGFIELD, VA, September 1969.

- INGRAM, M., W.B. MASON, 1954.
EFFECTS OF CHRONIC EXPOSURE TO X RADIATION ON THE PERIPHERAL BLOOD OF EXPERIMENTAL ANIMALS. CHAPTER 11:
BIOLOGICAL EFFECTS OF EXTERNAL RADIATION, (EDITOR: HENRY A. BLAIR)
MCGRAW-HILL, NEW YORK, NY, 1954. Pages 263-267.
- JACKSON, K., G. CHRISTENSON, R. BISTLINE, 1969.
IRREPARABLE INJURY PRODUCED BY X-IRRADIATION OF RAT THYMOCYTES IN VITRO
RADIATION RESEARCH, Vol 38, 1969, Pages 560-568.
- JACKSON, K.L., J.P. GERACI, 1986.
PHYSIOLOGICAL MECHANISMS OF ACUTE INTESTINAL RADIATION DEATH.
DNA-TR-86-241.
DEFENSE NUCLEAR AGENCY, WASHINGTON, DC, June 1, 1986.
- JENNINGS, F., A. ARDEN, 1962.
DEVELOPMENT OF RADIATION PNEUMONITIS:
TIME AND DOSE FACTORS.
ARCHIVES OF PATHOLOGY, Vol 74, 1962, Pages 351-360.
- JONES, D., J. KREBS, 1970.
RADIOBIOLOGY OF LARGE ANIMALS.
ANNUAL REPORT, 1970.
STANFORD RESEARCH INSTITUTE, PROJECT PYU-8150, 1970.
- JONES, D., J. KREBS, 1971.
RADIOBIOLOGY OF LARGE ANIMALS.
ANNUAL REPORT, 1971.
STANFORD RESEARCH INSTITUTE, PROJECT PYU-8150, August 1971.
- JONES, D., J. KREBS, 1973.
RADIOBIOLOGY OF LARGE ANIMALS.
ANNUAL REPORT, 1973.
STANFORD RESEARCH INSTITUTE, PROJECT PYU-8150, August 1973.
- JOSLIN, C., N. RAMSEY, J. ANDREWS, 1967.
COMPARISON OF THE LETHAL EFFECT OF RADIATION ON MICE FOR ACUTE AND PROTRACTED RADIATION.
BRITISH JOURNAL OF RADIOLOGY, Vol 40, 1967, Pages 627-630.
- KAL, H., H. SISSINGH, 1974.
EFFECTIVENESS OF CONTINUOUS LOW DOSE RATE GAMMA IRRADIATION ON RAT SKIN.
BRITISH JOURNAL OF RADIOLOGY, Vol 47, 1974, Pages 673-678.
- KALLMAN, R., 1958.
THE EFFECT OF DOSE RATE ON THE KILLING EFFICIENCY AND MODE OF DEATH OF MICE BY WHOLE-BODY IRRADIATION.
RADIATION RESEARCH, Vol 9, 1958, Pages 137.
- KALLMAN, R., 1962.
THE EFFECT OF DOSE RATE ON MODE OF ACUTE RADIATION DEATH OF C57BL AND BALB/C MICE.
RADIATION RESEARCH, Vol 16, 1962, Pages 796-810.
- KALLMAN, R.F., G. SILINI, 1964.
RECUPERATION FROM LETHAL INJURY BY WHOLE-BODY IRRADIATION. I. KINETIC ASPECTS
AND THE RELATIONSHIP WITH CONDITIONING DOSE IN C57BL.
RADIATION RESEARCH, Vol 22, 1964, Pages 662-642.
- KAPLAN, H.S., M.B. BROWN, 1952.
MORTALITY OF MICE AFTER TOTAL-BODY IRRADIATION AS INFLUENCED BY ALTERATIONS IN TOTAL DOSE,
FRACTIONATION, AND PERIODICITY OF TREATMENT
JOURNAL OF THE NATIONAL CANCER INSTITUTE, Vol 12, 1952, Pages 765-775.
- KARAS, J.S., J.B. STANBURY, 1965.
FATAL RADIATION SYNDROMES FROM AN ACCIDENTAL NUCLEAR EXCURSION.
NEW ENGLAND JOURNAL OF MEDICINE, Vol 272, 1965, Pages 755-761.
- KEANE, T., ET AL., 1981.
IDIOPATHIC INTERSTITIAL PNEUMONIA FOLLOWING BONE MARROW TRANSPLANTATION:
THE RELATIONSHIP WITH TOTAL BODY IRRADIATION.
INT. J. OF RADIATION ONCOLOGY, BIOLOGY, AND PHYSICS, Vol 7, 1981, Pages 1365-1370.
- KEREIAKES, J.G., W.H. PARR, A.T. KREBS, 1957.
FRACTIONATED DOSE EFFECTS ON SURVIVAL AND ORGAN WEIGHTS IN X-IRRADIATED MICE
AMERICAN JOURNAL OF PHYSIOLOGY, Vol 191, 1957, Pages 131-134.
- KHAIKOV, R.M., 1971.
IMPAIRMENTS IN OSTEOGENESIS AT REMOTE TIMES AFTER CHRONIC GAMMA IRRADIATION
U.S. ATOMIC ENERGY COMMISSION, DIV. OF TECHNICAL INFORMATION, 1971, Pages 154-157.
- KIGA, M., I. TAZAKI, 1967.
DOSE SURVIVAL CURVES OF FRACTIONATED IRRADIATION IN MICE.
JOURNAL OF RADIATION RESEARCH, Vol 8, 1967, Pages 72-79.
- KIM, H., W. RYBKA, S. LEHNERT, E. PODGORSAK, C. FREEMAN, 1985.
INTERSTITIAL PNEUMONITIS FOLLOWING BONE MARROW TRANSPLANTATION USING TWO DIFFERENT DOSE RATES.
INT. J. OF RADIATION ONCOLOGY, BIOLOGY, AND PHYSICS, Vol 11, 1985, Pages 1285-1291.

- KIMMEL, M., 1980.
CELLULAR POPULATION DYNAMICS.
I. MODEL CONSTRUCTION AND REFORMULATION
MATHEMATICAL BIOSCIENCES, Vol 48, 1980, Pages 211-224.
- KIMMEL, M., 1980.
CELLULAR POPULATION DYNAMICS.
II. INVESTIGATION OF SOLUTIONS
MATHEMATICAL BIOSCIENCES, Vol 48, 1980, Pages 225-239.
- KIMMEL, M., 1981.
GENERAL THEORY OF CELL CYCLE DYNAMICS BASED ON BRANCHING PROCESSES IN VARYING ENVIRONMENT
DEVELOPMENT IN CELL BIOLOGY SERIES: EDITOR: M. ROTENBERG
ELSEVIER NORTH HOLLAND, INC., NEW YORK, 1981, Pages 357-373.
- KIMMEL, M., M. WAZEWSKA-CZYZE, 1982.
STOCHASTIC APPROACH TO THE PROCESS OF RED CELL DESTRUCTION
ZASTOSOWANIA MATEMATYKI (APPLICATIONES MATHEMATICAE), Vol 17, 1982, Pages 217-225.
- KING, G. L., 1988.
CHARACTERIZATION OF RADIATION-INDUCED EMESIS IN THE FERRET.
RADIATION RESEARCH, Vol. 114, 1988, Pages 599-612.
- KIRK, J., W.M. GRAY, E.R. WATSON, 1971.
CUMULATIVE RADIATION EFFECT PART I: FRACTIONATED TREATMENT REGIMES
CLINICAL RADIOLOGY
Vol 22, 1971, Pages 145-155.
- KLENER, V., R. TUSCANY, J. VEJLUPKOVA, J. DVORAK, P. VLUKONIC, 1986.
LONG-TERM FOLLOW-UP AFTER ACCIDENTAL GAMMA IRRADIATION FROM A CO-60 SOURCE.
HEALTH PHYSICS, Vol 51, November 1986, Pages 601-607.
- KNAPP, H.A., 1965.
MAGNITUDE AND DISTRIBUTION OF WEAPON EFFECTS FOR THE DESIGN OF SHELTERS FOR
PROTECTION AGAINST FALLOUT.
INSTITUTE FOR DEFENSE ANALYSIS, ARLINGTON, VA, July 1965, Pages 194.
- KOLB, H., I. RIEDER, U. BODENBERGER, B. NETZEL, E. SCHAFER, S. THIERFELDER, 1979.
DOSE RATE AND DOSE FRACTIONATION STUDIES IN TOTAL BODY IRRADIATION OF DOGS.
PATHOLOGIE BIOLOGIE, Vol 27, 1979, Pages 370-372.
- KONISHI, K., J. HORIUCHI, 1978.
AN EVALUATION OF PROTRACTED LOW DOSE RATE IRRADIATION FROM AN ACUTE DOSE SURVIVAL CURVE.
BRITISH JOURNAL OF CANCER, Vol 42, 1978, Pages 2211-2215.
- KORNFIELD, L., V. GREENMAN, 1967.
EFFECTS OF CONTINUOUS LOW-LEVEL GAMMA IRRADIATION ON CIRCULATING AND PERITONEAL MONONUCLEAR LEUKOCYTES OF MICE.
RADIATION RESEARCH, Vol 31, 1967, Pages 889-895.
- KOZNOVA, L.B., 1972.
QUANTITATIVE ESTIMATION OF RADIATION DAMAGE FOLLOWING PROLONGED IRRADIATION
BIOLOGICAL EFFECTS OF RADIATION FROM EXTERNAL AND INTERNAL SOURCES
1972, Pages 33-42.
- KOZNOVA, L.B., R.M. ZAYTSEVA, L.K. TIKHOMIROVA, 1972.
CHANGES IN TOTAL QUANTITY OF MARROW CELLS AND THEIR MITOTIC INDEX IN RATS, FOLLOWING BRIEF
AND PROLONGED GAMMA IRRADIATION
U.S. ATOMIC ENERGY COMMISSION, DIV. OF TECHNICAL INFORMATION, 1972, Pages 43-49.
- KREBS, J.S., R.W. BRAUER, 1965.
ACCUMULATION OF LETHAL IRRADIATION DOSES BY FRACTIONATED EXPOSURE TO X-RAYS
RADIATION RESEARCH, Vol 25, 1965, Pages 480-488.
- KREBS, J.S., R.W. BRAUER, H. KALBACH, 1959.
THE ESTIMATION OF THE NONRECUPERABLE INJURY CAUSED BY IONIZING RADIATION.
RADIATION RESEARCH, Vol 10, 1959, Pages 80-88.
- KREBS, J.S., D.C.L. JONES, 1972.
THE LD50 AND THE SURVIVAL OF BONE-MARROW COLONY-FORMING CELLS IN MICE; EFFECT OF RATE OF EXPOSURE TO IONIZING RADIATION.
RADIATION RESEARCH, Vol 51, 1972, Pages 374-380.
- KREBS, J.S., D.C.L. JONES, 1975.
RADIOBIOLOGY OF LARGE ANIMALS.
FINAL REPORT. (SEE NTIS-AD-A015187).
STANFORD RESEARCH INSTITUTE, PROJECT PYU-8150, June 1975.
- KREBS, J.S., G. LEONG, 1970.
EFFECT EXPOSURE RATE ON THE GASTROINTESTINAL LD50 OF MICE EXPOSED TO 60CO GAMMA RAYS OR 250 KVP X-RAYS.
RADIATION RESEARCH, Vol 42, 1970, Pages 601-613.
- KRISE, G.M., J.W. AUSTIN, E.W. HUPP, 1968.
LETHAL EFFECTS OF ACUTE AND CONTINUOUS RADIATION IN GOATS. (ABSTRACT)
RADIATION RESEARCH, Vol 35, 1968, Pages 532.

- KUMATORI, T., 1971.
HEMATOLOGICAL EFFECTS ON HEAVILY IRRADIATED JAPANESE FISHERMEN
BIOLOGICAL ASPECTS OF RADIATION PROTECTION
IGAKU SHOIN LTD., TOKYO, JAPAN, 1971, Pages 64-73.
- KUMATORI, T., T. ISHIHARA, K. HIRASHIMA, H. SUGIYAMA, S. ISHII, K. MIYOSHI, 1980.
FOLLOW-UP STUDIES OVER A 25-YEAR PERIOD ON THE JAPANESE FISHERMEN EXPOSED TO RADIOACTIVE FALLOUT IN 1954.
"THE MEDICAL BASIS FOR RADIATION ACCIDENT PREPAREDNESS", K. HUBNER AND S. FRY, EDS.
ELSEVIER NORTH HOLLAND, INC., NEW YORK, 1980, Pages 33-54.
- KUROHARA, S.S., P. RUBIN, L.H. HEMPELMANN, 1961.
CREATINURIA AND FATIGUE IN PATIENTS UNDERGOING RADIATION THERAPY.
RADIOLOGY, Vol 77, 1961, Pages 804-812.
- KURSHACKOV, N.A., (ED.), 1962.
SLUCHAY OSTRAY LUCHE-VOY BOLENZI U CHELOVEKA 'A CASE OF ACUTE RADIATION SICKNESS IN MAN'.
GOSUDARSTVENNOE IZDATEL'STVO MEDITSINSKOY LITERATURY, MOSKVA, 1962, Pages 150.
- LAJTHA, L.G., R. OLIVER, 1961.
SOME RADIOBIOLOGICAL CONSIDERATIONS IN RADIOTHERAPY.
BRITISH JOURNAL OF RADIOLOGY, Vol 14, 1961, Pages 252-257.
- LAJTHA, L.G., R. OLIVER, C.W. GURNEY, 1962.
KINETIC MODEL OF A BONE-MARROW STEM-CELL POPULATION
BRITISH JOURNAL HAEMATOLOGY, Vol 8, 1962, Pages 442-460.
- LAMERTON, L.
EFFECTS OF PROTRACTED IRRADIATION ON THE BLOOD-FORMING ORGANS OF THE RAT.
I. CONTINUOUS EXPOSURE
BRITISH JOURNAL OF RADIOLOGY, Vol 33, Pages 287-301.
- LAMERTON, L., V. COURTENAY, 1968.
THE STEADY STATE UNDER CONTINUOUS IRRADIATION.
DOSE RATE IN MAMMALIAN RADIATION BIOLOGY, A SYMPOSIUM CO-SPONSORED BY
UT-AEC AGRICULTURAL RESEARCH LABORATORY, OAK RIDGE, TN, CONF-680410.
U.S. ATOMIC ENERGY COMMISSION, DIV. OF TECHNICAL INFORMATION, 1968.
- LAMERTON, L.F., 1966.
CELL PROLIFERATION UNDER CONTINUOUS IRRADIATION
RADIATION RESEARCH, Vol 27, 1966, Pages 119-138.
- LANG, I.M., J. MARVIG, 1989.
FUNCTIONAL LOCALIZATION OF SPECIFIC RECEPTORS MEDIATING GASTROINTESTINAL MOTOR CORRELATES OF VOMITING.
AMERICAN JOURNAL OF PHYSIOLOGY, Vol 256, 1989, Pages 692-699.
- LANGE, C.S., C.W. GILBERT, 1968.
STUDIES ON THE CELLULAR BASIS OF RADIATION LETHALITY III.
THE MEASUREMENT OF STEM-CELL REPOPULATION PROBABILITY
INT. J. OF RADIATION BIOLOGY, Vol 14, 1968, Pages 373-388.
- LANGHAM, W., K.T. WOODWARD, S.M. ROTHERMEL, P.S. HARRIS, C.C. LUSHBAUGH, J.B. STONER, 1956.
STUDIES OF THE EFFECT OF RAPIDLY DELIVERED, MASSIVE DOSES OF GAMMA RAYS ON MAMMALS.
RADIATION RESEARCH, Vol 5, 1956, Pages 404-432.
- LANGHAM, W.H., (EDITOR), 1967.
RADIOBIOLOGICAL FACTORS IN MANNED SPACE FLIGHT.
REPORT OF THE SPACE RADIATION STUDY PANEL OF THE LIFE SCIENCES COMMITTEE, PUBLICATION 1487.
NATIONAL ACADEMY OF SCIENCES/NATIONAL RESEARCH COUNCIL, WASHINGTON, DC, 1967.
- LANGHAM, W.M., 1965.
CONSIDERATIONS OF BIOSPHERIC CONTAMINATION BY RADIOACTIVE FALLOUT
RADIOACTIVE FALLOUT, SOILS, PLANTS, FOODS, MAN (EDITOR: ERIC B. FOWLER)
ELSEVIER NORTH HOLLAND, INC., NEW YORK, 1965, Pages 3-18.
- LAUMETS, E., 1965.
TIME HISTORY OF BIOLOGICAL RESPONSE TO IONIZING RADIATION.
USNRDL-TR-905.
NAVAL RADIOLOGICAL DEFENSE LAB, SAN FRANCISCO, CA, 1965.
- LEHNERT, S., 1985.
RESPONSE OF THE LUNG TO INTERMITTENT IRRADIATION:
THE IMPORTANCE OF AVERAGE VERSUS INSTANTANEOUS DOSE RATE.
INT. J. OF RADIATION ONCOLOGY, BIOLOGY, AND PHYSICS, Vol 11, 1985, Pages 2183-2184.
- LEITH, J.T., W.A. SCHILLING, J.T. LYMAN, J. HOWARD, 1975.
COMPARISON OF SKIN RESPONSES OF MICE AFTER SINGLE OR FRACTIONATED EXPOSURE TO
CYCLOTRON-ACCELERATED HELIUM IONS AND 230 KV X-IRRADIATION
RADIATION RESEARCH, Vol 62, 1975, Pages 195-215.
- LEONG, G., W. WISECUP, J. GRISHAM, 1964.
EFFECTS OF DIVIDED DOSES OF X-RAY ON MORTALITY AND HEMATOLOGY OF SMALL AND LARGE DOMESTIC ANIMALS.
ANNALS OF THE NEW YORK ACADEMY OF SCIENCES, Vol 114, 1964, Pages 138-146.
- LESHER, S., 1967.
COMPENSATORY REACTIONS IN INTESTINAL CRYPT CELLS AFTER 300 ROENTGENS OF COBALT-60 GAMMA IRRADIATION.
RADIATION RESEARCH, Vol 32, 1967, Pages 510-519.

- LEVICH, C., L.J. SEIGNEUR, C.L. HANSEN, 1967.
THE EFFECT OF DOSE RATE/PULSE WIDTH ON THE SURVIVAL TIME OF LETHALLY IRRADIATED MONKEYS AND RATS
RADIATION RESEARCH, Vol 31, 1967, Pages 533.
- LEVIN, W.C., M. SCHNEDIER, H.B. GERSTNER, 1959.
INITIAL CLINICAL REACTION TO THERAPEUTIC WHOLE-BODY X-RADIATION - - SOME CIVIL DEFENSE CONSIDERATIONS.
REPORT NO. 60-1.
U.S.A.F. SCHOOL OF AEROSPACE MEDICINE, BROOKS AF BASE, TX, 1959.
- LICHTER, A., D. TRACY, W. LAM, S. ORDER, 1980.
TOTAL BODY IRRADIATION IN BONE MARROW TRANSPLANTATION:
THE INFLUENCE OF FRACTIONATION AND DELAY OF MARROW INFUSION.
INT. J. OF RADIATION ONCOLOGY, BIOLOGY, AND PHYSICS, Vol 6, 1980, Pages 301-309.
- LINDOP, P.J., 1965.
RADIATION AND LIFESPAN
THE SCIENTIFIC BASIS OF MEDICINE ANNUAL REVIEWS
1965, Pages 91-109.
- LINECKI, J., 1971.
EFFECT OF DOSE-RATE UPON YIELD OF DICENTRIC CHROMOSOMES IN PERIPHERAL BLOOD LYMPHOCYTES
IRRADIATED IN VITRO WITH GAMMA-RAYS.
BULLETIN AC. POLISH SCI. SER. SCI. BIOL., Vol 19, 1971, Pages 593-599.
- LINECKI, J., A. BAJERSKA, K. WYSZYNSKA, B. CISOWSKA, 1977.
GAMMA-RADIATION-INDUCED CHROMOSOMAL ABERRATIONS IN HUMAN LYMPHOCYTES:
DOSE-RATE EFFECTS IN STIMULATED AND NON-STIMULATED CELLS.
EXCERPTA MEDICA AMSTERDAM, Vol 43, 1977, Pages 291-304.
- LITTLE, J., 1968.
CELLULAR EFFECTS OF IONIZING RADIATION.
NEW ENGLAND JOURNAL OF MEDICINE
Vol 278, 1968, Pages 308-315.
- LOEFFLER, M., R. STEIN, H.E. WICHMANN, C.S. POTTEN, P. KAUR, S. CHWALINSKI, 1986.
INTESTINAL CELL PROLIFERATION. I. A COMPREHENSIVE MODEL OF STEADY-STATE PROLIFERATION IN THE CRYPT
CELL TISSUE KINET.
Vol 19, 1986, Pages 627-645.
- LOEFFLER, M., H.E. WICHMANN, 1980.
A COMPREHENSIVE MATHEMATICAL MODEL OF STEM CELL PROLIFERATION WHICH REPRODUCES MOST OF THE PUBLISHED
EXPERIMENTAL RESULTS
CELL AND TISSUE KINETICS, Vol 13, 1980, Pages 543-561.
- LOGIE, L., 1960.
ANALYSIS OF THE LD50/30 AS RELATED TO RADIATION INTENSITY.
RADIATION RESEARCH, Vol 12, 1960, Pages 349-356.
- LORD, B., 1965.
HEMOPOIETIC CHANGES IN THE RAT DURING GROWTH AND DURING CONTINUOUS GAMMA IRRADIATION OF THE ADULT ANIMAL.
BRITISH JOURNAL HAEMATOLOGY, Vol 2, 1965, Pages 525-536.
- LORENZ, E., 1950.
SOME BIOLOGIC EFFECTS ON LONG CONTINUED IRRADIATION.
AMERICAN JOURNAL OF ROENTGENOLOGY, Vol 63, 1950, Pages 176-185.
- LORENZ, E., 1954.
EFFECTS OF LONG-CONTINUED TOTAL-BODY GAMMA IRRADIATION ON MICE, GUINEA PIGS, AND RABBITS.
EFFECTS OF LIFE SPAN, WEIGHT, BODY PICTURE, AND CARCINOGENESIS AND THE ROLE OF THE INTENSITY OF RADIATION. NATL. NUCL.
ENERGY SER., DIV IV
Vol 22, 1954, Pages CHAPTER 3.
- LUSHBAUGH, C.C., 1969.
THEORETICAL AND PRACTICAL ASPECTS OF MODELS EXPLAINING "GASTROINTESTINAL DEATH" AND OTHER LETHAL RADIATION SYNDROMES.
COMPARATIVE CELLULAR AND SPECIES RADIOSENSITIVITY, V.P. BOND & T. SUGAHARA (EDITORS)
IGAKU SHOIN LTD., TOKYO, JAPAN, 1969.
- LUSHBAUGH, C.C., 1969.
REFLECTIONS ON SOME RECENT PROGRESS IN HUMAN RADIOBIOLOGY.
IN "ADVANCES IN RADIATION BIOLOGY".
ACADEMIC PRESS, NEW YORK, NY, Vol 3, 1969, Pages 227-315.
- LUSHBAUGH, C.C., 1973.
HUMAN RADIATION TOLERANCE (CHAPTER 10).
BIOASTRONAUTICS DATA BOOK, J. PARKER AND V.R. WEST, EDS.; NASA-S-30006.
NATIONAL AERONAUTICS AND SPACE ADMINISTRATION, WASHINGTON, DC, 1973.
- LUSHBAUGH, C.C., 1974.
HUMAN RADIATION TOLERANCE, CHAPTER 10
SPACE RADIATION BIOLOGY AND RELATED TOPICS (EDITORS: C. TOBIAS, P. TODD), AMER. INSTIT. OF BIOL. SCIENCES & U.S. ATOMIC
ENERGY COMMISSION
1974, Pages 475-522.
- LUSHBAUGH, C.C., 1982.
THE IMPACT OF ESTIMATES OF HUMAN RADIATION TOLERANCE UPON RADIATION EMERGENCY MANAGEMENT.
THE CONTROL OF EXPOSURE OF THE PUBLIC TO IONIZING RADIATION IN THE EVENT OF ACCIDENT OR ATTACK, RESTON, VA, APRIL 1981.
NATIONAL COUNCIL ON RADIATION PROTECTION AND MEASUREMENT, BETHESDA, MD, May 1982, Pages 46-57.

- LUSHBAUGH, C.C., 1989.
PRIVATE COMMUNICATION
ALEXANDRIA, VA
OAK RIDGE ASSOCIATED UNIVERSITIES, OAK RIDGE, TN, May 4, 1989.
- LUSHBAUGH, C.C., F. COMAS, C.L. EDWARDS, G.A. ANDREWS, 1968.
CLINICAL EVIDENCE OF DOSE RATE EFFECTS IN TOTAL BODY IRRADIATION IN MAN.
DOSE RATE IN MAMMALIAN RADIATION BIOLOGY, A SYMPOSIUM CO-SPONSORED
BY UT-AEC AGRICULTURAL RESEARCH LABORATORY, OAK RIDGE, TN; CONF-680410.
U.S. ATOMIC ENERGY COMMISSION, DIV. OF TECHNICAL INFORMATION, July 12, 1968.
- LUSHBAUGH, C.C., F. COMAS, R. HOFSTRA, 1967.
CLINICAL STUDIES OF RADIATION EFFECTS IN MAN: A PRELIMINARY REPORT OF A
RETROSPECTIVE SEARCH FOR DOSE RESPONSE RELATIONSHIPS IN THE PRODROMAL SYNDROME.
RADIATION RESEARCH SUPPLEMENT, Vol 7, 1967, Pages 398-412.
- MAH, K., J. VAN DYK, T. KEANE, P. POON, 1987.
ACUTE RADIATION-INDUCED PULMONARY DAMAGE: A CLINICAL STUDY ON THE RESPONSE TO FRACTIONATED RADIATION THERAPY
INT. J. OF RADIATION ONCOLOGY, BIOLOGY, AND PHYSICS, Vol 13, 1987, Pages 179-188.
- MAISIN, J., J.R. MAISIN, A. DUNJAC, 1971.
THE GASTROINTESTINAL TRACT.
PATHOLOGY OF IRRADIATION, C.C. BERDJIS, ED.
WILLIAMS & WILKINS, BALTIMORE, MD, 1971, Pages 296-344.
- MARKS, J.E., J. WONG, 1985.
THE RISK OF CEREBRAL RADIONECROSIS IN RELATION TO DOSE, TIME AND FRACTIONATION
A FOLLOW-UP STUDY (PROG. EXP. TUMOR RES.)
Vol 29, 1985, Pages 210-218.
- MARTIN, J., 1985.
THE SCIENTIFIC BASIS FOR THE DEVELOPMENT OF GUIDANCE AND OPERATIONAL PROCEDURES FOR LIVING
UNDER RADIOACTIVE FALLOUT CONDITIONS.
PUBLICATION 20/85, SR AND D BRANCH,
BUTTERWORTHS, LONDON, BOSTON, 1985.
- MARTINEZ, G.R., H.G. CASSAB, G.G. GANEM, K.E. GULTAN, L.M. LIEBERNAM, ET AL., 1964.
ACCIDENT FROM RADIATION:
OBSERVATIONS ON THE ACCIDENTAL EXPOSURE OF A FAMILY TO A SOURCE OF COBALT-60.
REV. MED. INST. MEX. SEGRE SOCIAL, SUPPL. 1, Vol 3, 1964, Pages 14-69.
- MASON, K.A., H.R. WITHERS, W.H. MCBRIDE, C.A. FAVIS, J. SMATHERS, 1989.
COMPARISON OF THE GASTROINTESTINAL SYNDROME AFTER TOTAL-BODY OR TOTAL-ABDOMINAL IRRADIATION.
RADIATION RESEARCH, Vol 117, 1989, Pages 480-488.
- MATSUZAWA, T., R. WILSON, 1965.
THE INTESTINAL MUCOSA OF GERM-FREE MICE AFTER WHOLE-BODY X-IRRADIATION WITH 3 KILORENTGENS.
RADIATION RESEARCH, Vol 25, 1965, Pages 15-24.
- MATTSON, J.L., R.E. CORDTS, M.G. YACHMOWITZ, K.A. HANDY, 1984.
PREVENTION OF RADIATION EMESIS IN DOGS BY COMBINATIONS OF DRUGS.
INT. J. OF RADIATION ONCOLOGY, BIOLOGY, AND PHYSICS, Vol 10, 1984, Pages 1067-1072.
- MCCLELLAN, G.E., G.H. ANNO, 1986.
CONUS STRATEGIC POSTATTACK RECOVERY -- RADIOBIOLOGICAL CONSIDERATIONS.
DNA-TR-86-212.
DEFENSE NUCLEAR AGENCY, WASHINGTON, DC, May 30, 1986.
- MCCLELLAN, R.O., 1976.
INFLUENCE OF VARIATIONS IN DOSE AND DOSE RATES ON BIOLOGICAL EFFECTS OF INHALED BETA-EMITTING RADIONUCLIDES
FROM: BIOLOGICAL AND ENVIRONMENTAL EFFECTS OF LOW-LEVEL RADIATION, INTERNATIONAL ATOMIC ENERGY AGENCY
Vol 2, 1976, Pages 4-19.
- MCCLELLAN, R.O., 1982.
HEALTH EFFECTS FROM INTERNALLY DEPOSITED RADIONUCLIDES RELEASED IN NUCLEAR DISASTERS.
THE CONTROL OF EXPOSURE OF THE PUBLIC TO IONIZING RADIATION IN THE EVENT OF ACCIDENT OR ATTACK, RESTON, VA, APRIL 1981.
NATIONAL COUNCIL ON RADIATION PROTECTION AND MEASUREMENT, BETHESDA, MD, May 15, 1982, Pages 28-39.
- MCCLELLAN, R.O., 1986.
INHALATION TOXICOLOGY RESEARCH INSTITUTE ANNUAL REPORT
PREPARED FOR THE OFFICE OF HEALTH AND ENVIRONMENTAL RESEARCH OF THE U.S. DEPT OF ENERGY
December 1986, Pages 1-480.
- MCDERMOTT, C., N. GENGOZIAN, 1980.
THE EFFECT OF LOW EXPOSURE RATE GAMMA IRRADIATION ON T AND B LYMPHOCYTE FUNCTION IN THE MOUSE.
INT. J. OF RADIATION BIOLOGY, Vol 37, 1980, Pages 415-428.
- MEDINGER, F., L. CRAVER, 1942.
TOTAL BODY IRRADIATION (WITH REVIEW OF CASES)
AMERICAN JOURNAL OF ROENTGENOLOGY, Vol 48, 1942, Pages 651-671.
- MELVILLE, G.S., F.P. CONTE, M. SLATER, A.C. UPTON, 1957.
ACUTE LETHALITY OF MICE AS INFLUENCED BY THE PERIODICITY OF PAIRED EXPOSURES TO FAST NEUTRONS OR X-RAYS.
BRITISH JOURNAL OF RADIOLOGY, Vol 30, 1957, Pages 196-199.

- MESSERSCHMIDT, O., 1979.
MEDICAL PROCEDURES IN A NUCLEAR DISASTER.
VERLAG KARL THIEMING, MUNICH, 1979.
- MEWISSEN, D.J., C.L. COMAR, B.F. TRUM, J.H. RUST, 1957.
A FORMULA FOR CHRONIC RADIATION DOSAGE VERSUS SHORTENING OF LIFE SPAN: APPLICATION TO A LARGE MAMMAL
RADIATION RESEARCH, Vol 6, 1957, Pages 450-459.
- MEXICO, 1984.
THE RADIOLOGICAL ACCIDENT OF CIUDAD JUAREZ, CHILUALUA (MEXICO)
COMISION NACIONAL DE SEGURIDAD NUCLEAR Y SALVAGUARDIAS, 1984.
- MEYN, R.E., D.J. GRDINA, S.E. FLETCHER, 1980.
REPAIR OF RADIATION DAMAGE IN VIVO
"RADIATION BIOLOGY IN CANCER RESEARCH", RAYMOND E. MEYN & H. RODNEY WITHERS, EDS.
RAVEN PRESS, NEW YORK, 1980, Pages 95-102.
- MICHAELSON, S.M., L.T. ODLAND, 1962.
RELATIONSHIP BETWEEN METABOLIC RATE AND RECOVERY FROM RADIATION INJURY
RADIATION RESEARCH, Vol 16, 1962, Pages 281-285.
- MICHAELSON, S.M., L.T. ODLAND, J.W. HOWLAND, 1962.
MECHANISMS OF INJURY AND RECOVERY FROM WHOLE AND PARTIAL BODY EXPOSURE TO IONIZING RADIATION
UNIVERSITY OF ROCHESTER, ATOMIC ENERGY PROJECT, MEDICAL DIVISION
1962, Pages 3-27.
- MICHAELSON, S.M., K.T. WOODWARD, L.T. ODLAND, J.W. HOLAND, 19.
RADIATION TIME INTENSITY AND PATHOPHYSIOLOGIC CORRELATIONS IN WHOLE AND PARTIAL BODY X-IRRADIATED BEAGLES.
REPORT NO. UR-49-913. DEPT OF RAD. BIOL. & BIOPHYSICS, UNIV. OF ROCHESTER, SCHOOL OF MED. & DENTISTRY
19, Pages 21 PP.
- MICHAELSON, S.M., K.T. WOODWARD, L.T. ODLAND, J.W. HOWLAND, 1968.
RADIATION TIME-INTENSITY AND PATHOPHYSIOLOGIC CORRELATIONS IN WHOLE BODY X-IRRADIATED BEAGLES.
U.S. ATOMIC ENERGY COMMISSION, DIVISION OF TECHNICAL INFORMATION, CONF.-680410 (TID-4500)
1968, Pages 7.1-7.21.
- MICHALOWSKI, A., 1981.
EFFECTS OF RADIATION ON NORMAL TISSUES:
HYPOTHETICAL MECHANISMS AND LIMITATIONS OF IN SITU ASSAYS OF CLONOGENICITY
RADIATION ENVIRONMENTAL BIOPHYSICS, Vol 19, 1981, Pages 157-172.
- MILLBURN, L.F., L. O'GRADY, F.R. HENDRICKSON, 1968.
RADICAL RADIATION THERAPY AND TOTAL BODY IRRADIATION IN THE TREATMENT OF EWINGS SARCOMA.
CANCER, Vol 22, 1968, Pages 919-925.
- MILLER, L.S., G.H. FLETCHER, H.B. GERSTNER, 1958.
RADIOBIOLOGIC OBSERVATIONS ON CANCER PATIENTS TREATED WITH WHOLE-BODY X-IRRADIATION.
RADIATION RESEARCH, Vol 8, 1958, Pages 150-165.
- MITCHELL, J.B., J.S. BEDFORD, 1977.
DOSE-RATE EFFECTS IN SYNCHRONOUS MAMMALIAN CELLS IN CULTURE.
II. A COMPARISON OF LIFE CYCLE OF HELA CELLS DURING CONTINUOUS IRRADIATION OR MULTIPLE-DOSE FRACTIONATION
RADIATION RESEARCH, Vol 71, 1977, Pages 547-560.
- MITCHELL, J.B., J.S. BEDFORD, S.M. BAILEY, 1979.
DOSE-RATE EFFECTS IN MAMMALIAN CELLS IN CULTURE.
III. COMPARISON OF CELL KILLING AND CELL PROLIFERATION DURING CONTINUOUS IRRADIATION FOR SIX DIFFERENT CELL LINES
RADIATION RESEARCH, Vol 79, 1979, Pages 537-551.
- MITCHELL, J.B., J.S. BEDFORD, S.M. BAILEY, 1979.
DOSE-RATE EFFECTS ON THE CELL CYCLE AND SURVIVAL OF S3 HELA AND V79 CELLS
RADIATION RESEARCH, Vol 79, 1979, Pages 520-536.
- MITCHELL, J.B., J.S. BEDFORD, S.M. BAILEY, 1979.
DOSE-RATE EFFECTS IN PLATEAU-PHASE CULTURES OF S3 HELA AND V79 CELLS
RADIATION RESEARCH, Vol 79, 1979, Pages 552-567.
- MOBLEY, T.S., 1974.
EFFECTS OF VARIOUS DOSE RATES OF MIXED NEUTRON-GAMMA RADIATIONS ON THE LD50(60) RESPONSE OF SHEEP
NATIONAL TECHNICAL INFORMATION SERVICE, U.S. DEPARTMENT OF COMMERCE (PREPARED FOR DEFENSE NUCLEAR AGENCY)
September 1974, Pages 1-24.
- MOLE, R.H., 1955.
ON WASTED RADIATION AND THE INTERPRETATION OF EXPERIMENTS WITH CHRONIC IRRADIATION.
JOURNAL OF NATIONAL CANCER INSTITUTE
Vol 15, 1955, Pages 907-914.
- MOLE, R.H., 1955.
ON WASTED RADIATION AND THE INTERPRETATION OF EXPERIMENTS WITH
CHRONIC IRRADIATION.
JOURNAL OF THE NATIONAL CANCER INSTITUTE, Vol 15, 1955, Pages 907-913.
- MOLE, R.H., 1959.
PATTERNS OF RESPONSE TO WHOLE-BODY IRRADIATION:
THE EFFECT OF DOSE INTENSITY AND EXPOSURE TIME ON DURATION OF LIFE AND TUMOUR PRODUCTION.
BRITISH JOURNAL OF RADIOLOGY, Vol 32, August 1959, Pages 497-501.

- MOLE, R.H., A.M. THOMAS, 1961.
LIFE-SHORTENING IN FEMALE CBA MICE EXPOSED TO DAILY IRRADIATION FOR LIMITED PERIODS OF TIME.
INT. J. OF RADIATION BIOLOGY, Vol 3, 1961, Pages 493-508.
- MORLEY, A., E.A. KING-SMITH, F., JR. STOHLMAN, 1970.
THE OSCILLATORY NATURE OF HEMOPOIESIS.
"HEMOPOIETIC CELLULAR PROLIFERATION", F. STOHLMAN JR., ED.
GRUNE & STRATTON, NEW YORK, NY, 1970, Pages 3-14.
- MORRISON, R., 1981.
LOW VS. HIGH DOSE RATE EFFECTS ON THE ACUTE REACTION OF PIG SKIN TO COBALT-60 GAMMA RAYS.
INT. J. OF RADIATION ONCOLOGY, BIOLOGY, AND PHYSICS, Vol 7, 1981, Pages 359-364.
- NACHTWAY, D.S., E.J. AINSWORTH, G.R. LEONG, 1967.
RECOVERY FROM RADIATION INJURY IN SWINE AS EVALUATED BY THE SPLIT-DOSE TECHNIQUE.
RADIATION RESEARCH, Vol 31, 1967, Pages 353-367.
- NATO, 1973.
NATO HANDBOOK ON THE MEDICAL ASPECTS OF NBC DEFENSIVE OPERATIONS.
REPORT AMED P-6.
U.S. DEPARTMENTS OF THE ARMY, NAVY, AND AIR FORCE, WASHINGTON, DC, August 1973.
- NCRP, 1974.
RADIOLOGICAL FACTORS AFFECTING DECISION-MAKING IN A NUCLEAR ATTACK.
REPORT 42.
NATIONAL COUNCIL ON RADIATION PROTECTION AND MEASUREMENT, BETHESDA, MD, November 15, 1974.
- NEAL, F., 1960.
VARIATION IN ACUTE MORTALITY WITH DOSE-RATE IN MICE EXPOSED TO SINGLE LARGE DOSES OF WHOLE BODY X-RADIATION.
INT. J. OF RADIATION BIOLOGY, Vol 2, 1960, Pages 295-300.
- NICKSON, J., 1945.
BLOOD CHANGES IN HUMAN BEINGS FOLLOWING TOTAL-BODY IRRADIATION.
AMERICAN JOURNAL OF ROENTGOLOGY, RADIUM THERAPY AND NUCLEAR MEDICINE, 1945, Pages 308-337.
- NORRIS, W.P., T.E. FRITZ, 1972.
INTERACTIONS OF TOTAL DOSE AND DOSE RATE IN DETERMINING TISSUE RESPONSES TO IONIZING RADIATIONS
RADIOBIOLOGY OF PLUTONIUM, (EDITORS: B.J. STOVER, W.W. JEE)
J.W. PRESS, SALT LAKE CITY, 1972, Pages 243-260.
- NORRIS, W.P., T.E. FRITZ, C.M. POOLE, F.S. WILLIAMSON, C.E. REHFELD, 1966.
THE RESPONSE OF BEAGLE DOGS TO CONTINUOUS EXPOSURE TO CO60 GAMMA RAYS
BIOLOGICAL AND MEDICAL RESEARCH DIVISION ANNUAL REPORT 1966, ARGONNE NATIONAL LABORATORY
December 1966, Pages 102-106.
- NORRIS, W.P., S.A. TYLER, G.A. SACHER, 1966.
AN INTERSPECIES COMPARISON OF RESPONSES OF MICE AND DOGS TO CONTINUOUS 60COY IRRADIATION
U.S. ENERGY RESEARCH AND DEVELOPMENT ADMINISTRATION
1966, Pages 147-156.
- OUGHTERSON, A.W., S. WARREN, 1956.
MEDICAL EFFECTS OF THE ATOMIC BOMB IN JAPAN.
MCGRAW-HILL, NEW YORK, NY, 1956.
- PAGE, N.P., 1968.
THE EFFECT OF DOSE PROTRACTION ON RADIATION LETHALITY OF LARGE ANIMALS.
DOSE RATE IN MAMMALIAN RADIATION BIOLOGY, A SYMPOSIUM CO-SPONSORED
BY UT-AEC AGRICULTURAL RESEARCH LABORATORY, OAK RIDGE, TN; CONF-680410.
U.S. ATOMIC ENERGY COMMISSION, DIV. OF TECHNICAL INFORMATION, July 12, 1968.
- PAGE, N.P., E.J. AINSWORTH, G.F. LEONG, 1968.
THE RELATIONSHIP OF EXPOSURE RATE AND EXPOSURE TIME TO RADIATION INJURY IN SHEEP.
RADIATION RESEARCH, Vol 33, 1968, Pages 94-106.
- PAGE, N.P., E.J. AINSWORTH, E. TAYLOR, G.F. LEONG, 1971.
RECOVERY OF SHEEP AFTER WHOLE BODY IRRADIATION:
A COMPARISON OF CHANGES IN RADIOSENSITIVITY AFTER EITHER ACUTE OR PROTRACTED SUBLETHAL EXPOSURES.
RADIATION RESEARCH, Vol 46, 1971, Pages 301-316.
- PAGE, N.P., D.S. NACHTWEY, G.F. LEONG, E.J. AINSWORTH, E.L. ALPEN, 1965.
RECOVERY FROM RADIATION INJURY IN SHEEP, SWINE AND DOGS AS EVALUATED BY THE SPLIT-DOSE TECHNIQUE.
RADIATION RESEARCH, Vol 25, 1965, Pages 224.
- PATRICK, G.
THE EFFECTS OF RADIATION ON CELL MEMBRANES
MAMMALIAN CELL MEMBRANES, VOL. 5: RESPONSES OF PLASMA MEMBRANES, G.A. JAMIESON AND D.M. ROBINSON, EDS.
BUTTERWORTHS, LONDON, BOSTON, Pages 72-104.
- PATTERSON, E., 1954.
FACTORS INFLUENCING RECOVERY AFTER WHOLE-BODY RADIATION.
JOURNAL OF THE FACULTY OF RADIOLOGY, Vol 5, 1954, Pages 189-199.
- PATTERSON, E., C.W. GILBERT, M.V. HAIGH, 1956.
EFFECTS OF PAIRED DOSES OF WHOLE BODY IRRADIATION IN THE RHESUS MONKEY
BRITISH JOURNAL OF RADIOLOGY, Vol 29, 1956, Pages 218-226.

- PATTERSON, E., C.W. GILBERT, J. MATHEWS, 1947.
TIME INTENSITY FACTORS AND WHOLE BODY IRRADIATION
BRITISH JOURNAL OF RADIOLOGY, Vol 25, 1947.
- PEEL, D.M., J.W. HOPEWELL, R.H. SIMMONDS, P. DODD, M.L. MEISTRICH, 1984.
SPLIT-DOSE RECOVERY IN EPITHELIAL AND VASCULAR-CONNECTIVE TISSUE OF PIG SKIN
RADIOTHERAPY AND ONCOLOGY, Vol 2, 1984, Pages 151-157.
- PERNICK, A., I. LEVANON, 1987.
AN EVALUATION OF THE U.S. ARMY FALLOUT PREDICTION MODEL
HEALTH PHYSICS, Vol 52, 1987, Pages 739-751.
- PETERS, L., H.R. WITHERS, J.H. CURDIFF, K.A. DICKE, 1979.
RADIOBIOLOGICAL CONSIDERATIONS IN USE OF TOTAL-BODY IRRADIATION FOR BONE-MARROW TRANSPLANTATION.
RADIOLOGY, Vol 131, 1979, Pages 243-247.
- PORTER, E., 1964.
DOSE-RATE AND SURVIVAL CURVES.
BRITISH JOURNAL OF RADIOLOGY, Vol 38, 1964, Pages 607-612.
- POTTEN, C.S., J.H. HENDRY, 1975.
DIFFERENTIAL REGENERATION OF INTESTINAL PROLIFERATIVE CELLS AND CYTOGENIC CELLS AFTER IRRADIATION.
INT. J. OF RADIATION BIOLOGY, Vol 27, 1975, Pages 413-424.
- POTTEN, C.S., J.H. HENDRY, EDS., 1983.
CYTOTOXIC INSULT TO TISSUE:
EFFECTS ON CELL LINEAGES.
CHURCHILL LIVINGSTON, EDINBURGH, 1983.
- PRESS, W.H., B.P. FLANNERY, S.A. TEUKOLUSKY, W.T. VETTERLING, 1986.
NUMERICAL RECIPES
CAMBRIDGE UNIVERSITY PRESS, CAMBRIDGE, MA, 1986.
- PURRATT, R., E. REEDER, 1976.
THE EFFECT OF CHANGES IN DOSE RATE ON THE YIELD OF CHROMOSOME ABERRATIONS IN HUMAN LYMPHOCYTES
EXPOSED TO GAMMA RADIATION.
MUTATION RESEARCH, Vol 35, 1976, Pages 437-444.
- PURRATT, R., E. REEDER, 1976.
CHROMOSOME ABBERRATION YIELDS IN HUMAN LYMPHOCYTES INDUCED BY FRACTIONATED DOSES OF X-RADIATION.
MUTATION RESEARCH, Vol 34, 1976, Pages 437-446.
- QUAIFE, M.A., J. DEBOER, R.K. JONES, A.T. ICHIKI, W.R. GODDEN, H. DAVIS, 1963.
COMPARISON OF CLINICAL AND LABORATORY RESPONSES IN SHEEP AND DOGS FOLLOWING WHOLE BODY EXPOSURES
TO 250-KVP X-RAYS AND FISSION SPECTRUM NEUT.
BIOL. EFF. NEUTRON AND PROTON IRRADIATION PROC. SYMP.
Vol 2, 1963, Pages 73-91.
- QUASTLER, H., 1959.
CELL RENEWAL AND ACUTE RADIATION DAMAGE.
RADIOLOGY, Vol 73, 1959, Pages 161.
- QUASTLER, H., J.P.M. BENSTED, L.F. LAMBERTON, S.M. SIMPSON, 1959.
ADAPTATION TO CONTINUOUS IRRADIATION:
OBSERVATIONS ON THE RAT INTESTINE.
BRITISH JOURNAL OF RADIOLOGY, Vol 32, 1959, Pages 501.
- REDPATH, J.L., R.M. DAVID, L. COHEN, 1978.
DOSE-FRACTIONATION STUDIES ON MOUSE GUT AND MARROW:
AN INTEERCOMPARISON OF 6-MEV PHOTONS AND FAST NEUTRONS 9E=24 MEV)
RADIATION RESEARCH, Vol 75, 1978, Pages 642-648.
- REDPATH, J.L., D.M. PEEL, P. DODD, R.H. SIMMONDS, J.W. HOPEWELL, 1985.
REPOPULATION IN IRRADIATED PIG SKIN:
LATE VERSUS EARLY EFFECTS
RADIOTHERAPY AND ONCOLOGY, Vol 3, 1985, Pages 173-176.
- RICKS, R.C., C.C. LUSHBAUGH, E. MCDOW, E. FROME, 1972.
PULMONARY-IMPEDANCE POWER SPECTRAL ANALYSIS: A FACILE MEANS OF DETECTING RADIATION-INDUCED
GI DISTRESS AND PERFORMANCE DECREMENT IN MAN.
NATIONAL SYMPOSIUM ON NATURAL AND MANMADE RADIATION IN SPACE, LAS VEGAS, NV, E.A. WARMAN, ED.; NASA TM X-2440.
NATIONAL AERONAUTICS AND SPACE ADMINISTRATION, WASHINGTON, DC, 1972, Pages 238-248.
- RIDER, W.D., R. HASSELBACK, 1968.
THE SYMPTOMATIC AND HEMATOLOGICAL DISTURBANCE FOLLOWING TOTAL BODY RADIATION AT 300-RAD GAMMA-RAY IRRADIATION.
GUIDELINES TO RADIOLOGICAL HEALTH, ENVIRONMENTAL HEALTH SERIES; PUBLICATION NO. 999-RH-33.
U.S. PUBLIC HEALTH SERVICE, 1968, Pages 138-144.
- RINGDEN, O., ET AL., 1983.
INCREASED MORTALITY BY SEPTICEMIA, INTERSTITIAL PNEUMONITIS AND PULMONARY FIBROSIS AMONG
BONE MARROW TRANSPLANT RECIPIENTS RECEIVING AN INCREASED MEAN DOSE OF TOTAL IRRADIATION.
ACTA RADIOLOGICA ONCOLOGY, Vol 22, 1983, Pages 423-428.
- ROBINSON, C., 1968.
RELATIONSHIP BETWEEN ANIMAL AND STEM CELL DOSE-SURVIVAL CURVES.
RADIATION RESEARCH, Vol 35, 1968, Pages 318-344.

- RUBIN, P., G.W. CASARETT, 1968.
CLINICAL RADIATION PATHOLOGY.
W. B. SAUNDERS CO., PHILADELPHIA, PA, 1968.
- RUST, J.H., B.F. TRUM, J. HEGLIN, E. MCCULLOCH, T.J. HALEY, 1954.
EFFECT OF 200 ROENTGENS FRACTIONAL WHOLE BODY IRRADIATION IN THE BURRO
PROC. SOC. EXP. BIOL. MED
Vol 85, 1954, Pages 258-261.
- RUST, J.H., B.F. TRUM, J.J. LANE, U.S.G. KUHN, 1955.
EFFECTS OF 50 ROENTGENS AND 25 ROENTGENS FRACTIONAL DAILY TOTAL BODY GAMMA IRRADIATION IN THE BURRO
RADIATION RESEARCH, Vol 2, 1955, Pages 475-482.
- RUST, J.H., B.F. TRUM, E. MCCULLOCH, T.J. HALEY, 1954.
EFFECT OF 200 ROENTGENS FRACTIONAL WHOLE BODY IRRADIATION IN THE BURRO
PROC. SOC. EXPTL. BIOL. MED.
Vol 85, 1954, Pages 216-258.
- SACHER, G.A., 1956.
SURVIVAL OF MICE UNDER DURATION OF LIFE EXPOSURE TO X RAYS AT VARIOUS RATES.
BIOLOGICAL EFFECTS OF EXTERNAL X AND GAMMA RADIATION, PART 2, R. ZIRKLE, ED.
U.S. ATOMIC ENERGY COMM., TECH. INFORM. SERVICE EXTENSION, OAK RIDGE, TN, 1956.
- SACHER, G.A., 1956.
APPROACHES TO THE QUANTITATIVE ESTIMATION OF RADIATION INJURY AND LETHALITY
THE SHORTER-TERM BIOLOGICAL HAZARDS OF A FALLOUT FIELD, EDITORS: G. DUNNING, J. HILCKEN, U.S. ATOMIC ENERGY COMMISSION
December 12, 1956, Pages 101-112.
- SACHER, G.A., 1958.
REPAIRABLE AND IRREPAIRABLE INJURY: A JURY OF THE POSITION IN EXPERIMENT AND THEORY
RADIATION BIOLOGY AND MEDICINE, EDITED BY: W.D. CLAUS
1958, Pages 283-313.
- SACHER, G.A., 1968.
MATHEMATICAL ANALYSIS OF THE DIVISION DELAY PRODUCED BY IONIZING RADIATIONS
RADIATION RESEARCH, Vol 33, 1968, Pages 644-658.
- SACHER, G.A., 1976.
DOSE, DOSE RATE, RADIATION QUALITY, AND HOST FACTORS FOR RADIATION-INDUCED LIFE SHORTENING
AGING, CARCINOGENESIS AND RADIATION BIOLOGY, THE RULE OF NUCLEAR ACID ADDITION REACTIONS, (EDITOR: K.C. SMITH)
PLENUM PRESS, NEW YORK & LONDON, 1976, Pages 493-517.
- SACHER, G.A., D. GRAHN, S. LESHER, 1958.
DEPENDENCE OF ACUTE AND SUBACUTE RADIOSENSITIVITY ON AGE IN THE LAF MOUSE
BIOLOGICAL AND MEDICAL RESEARCH DIVISION SEMIANNUAL REPORT, ARGONNE NATIONAL LABORATORY
1958, Pages 84-86.
- SACHER, G.A., E. TRUCCO, 1966.
THEORY OF RADIATION INJURY AND RECOVERY IN SELF-RENEWING CELL POPULATIONS
RADIATION RESEARCH, Vol 29, 1966, Pages 236-256.
- SAENGER, E.L., 1963.
MEDICAL ASPECTS OF RADIATION ACCIDENTS.
AVAILABLE FROM NATIONAL TECHNICAL INFORMATION SERVICE, SPRINGFIELD, VA.
U.S. ATOMIC ENERGY COMMISSION, WASHINGTON, DC, 1963.
- SAENGER, E.L., 1982.
PRIVATE COMMUNICATION.
CLINICAL DATA PRESENTED AT THE DNA INTERMEDIATE DOSE PROGRAM MEDICAL/RADIOBIOLOGICAL MEETING,
BETHESDA, MD, 27-28 MAY 1982.
UNIVERSITY OF CINCINNATI MEDICAL SCHOOL, CINCINNATI, OH, May 27, 1982.
- SAENGER, E.L., ET AL., 1973.
WHOLE BODY AND PARTIAL BODY RADIOTHERAPY OF ADVANCED CANCER.
AMERICAN JOURNAL OF ROENTGOLOGY, RADIUM THERAPY AND NUCLEAR MEDICINE, Vol 117, 1973, Pages 670-684.
- SALAZAR, O.M., P. RUBIN, B. KELLER, C. SCARANTINO, 1978.
SYSTEMIC (HALF-BODY) RADIATION THERAPY:
RESPONSE AND TOXICITY.
INT. J. OF RADIATION ONCOLOGY, BIOLOGY, AND PHYSICS, Vol 4, 1978, Pages 937-950.
- SCHMIDT, L.A., 1981.
A STUDY OF TWENTY-FOUR NATIONWIDE FALLOUT PATTERNS FROM TWELVE WINDS.
PAPER 1604.
INSTITUTE FOR DEFENSE ANALYSES, WASHINGTON, DC, September 1981.
- SCOTT, B.R., 1977.
MECHANISTIC STATE VECTOR MODEL FOR CELL KILLING BY IONIZING RADIATION
RAD. AND ENVIRONMENTAL BIOPHYSICS
Vol 14, 1977, Pages 195-211.
- SCOTT, B.R., 1980.
A MODEL FOR EARLY DEATH CAUSED BY RADIATION PNEUMONITIS AND PULMONARY FIBROSIS AFTER
INHALING INSOLUBLE RADIOACTIVE PARTICLES
BULLETIN OF MATHEMATICAL BIOLOGY
Vol 42, 1980, Pages 447-459.

- SCOTT, B.R., 1982.
METHOD OF ANALYSIS OF MONOTONE DOSE-RESPONSE PROBABILITIES AFTER LONG-TERM EXPOSURE TO A TOXICANTUBLE RADIOACTIVE PARTICLES
HEALTH PHYSICS, Vol 42, 1982, Pages 305-315.
- SCOTT, B.R., 1987.
RESPONSE-SURFACE MODEL FOR ORGAN DYSFUNCTION AFTER PROTRACTED IRRADIATION
PROCEEDINGS OF THE SIXTH INTERNATIONAL CONFERENCE ON MATHEMATICAL MODELING
INHALATION TOXICOLOGY RESEARCH INSTITUTE, 1987.
- SCOTT, B.R., E.J. AINSWORTH, 1980.
STATE-VECTOR MODEL FOR LIFE SHORTENING IN MICE AFTER BRIEF EXPOSURES TO LOW DOSES OF IONIZING RADIATION
MATHEMATICAL BIOSCIENCES
Vol 49, 1980, Pages 185-205.
- SCOTT, B.R., F.F. HAHN, R.G. CUDDIHY, B.B. BOECKER, F.A. SEILER, 1984.
HAZARD-FUNCTION MODELING OF EARLY EFFECTS MORTALITY RISKS ASSOCIATED WITH LIGHT WATER NUCLEAR REACTOR ACCIDENTS
PROCEEDINGS OF THE 1984 STATISTICAL SYMPOSIUM ON NATIONAL ENERGY
INHALATION TOXICOLOGY RESEARCH INSTITUTE, 1984.
- SCOTT, B.R., F.F. HAHN, R.O. MCCLELLAN, F.A. SEILER
RISK ESTIMATORS FOR RADIATION-INDUCED BONE MARROW SYNDROME
RISK ANALYSIS IN PRESS
Pages 1-24.
- SCOTT, B.R., F.F. HAHN, G.J. NEWTON, M.B. SNIPES, E.G. DAMON, J.L. MAUDERLY, 1987.
EXPERIMENTAL STUDIES OF THE EARLY EFFECTS OF INHALED BETA-EMITTING RADIONUCLIDES FOR NUCLEAR ACCIDENT RISK ASSESSMENT.
PHASE II REPORT
PREPARED FOR U.S. NUCLEAR REGULATORY COMMISSION
1987, Pages 100 PGS.
- SEED, T.M., T.E. FRITZ, D.V. TOLLE, C.M. POOLE, L. LOMBARD, D. DOYLE, 1984.
SURVIVAL PATTERNS AND HEMOPATHOLOGICAL RESPONSES OF DOGS UNDER CONTINUOUS GAMMA IRRADIATION.
"RESPONSE OF DIFFERENT SPECIES TO TOTAL BODY IRRADIATION", J.J. BROERSE & T.J. MACVITTIE, EDS.
MARTINUS NIGHOFF PUBLISHERS, DORDRECHT, THE NETHERLANDS, 1984.
- SEED, T.M., D.V. TOLLE, T.E. FRITZ, S.M. CULLEN, L.V. KASPAR, C.M. POOLE, 1978.
HAEMOPATHOLOGICAL CONSEQUENCES OF PROTRACTED GAMMA IRRADIATION IN THE BEAGLE
LATE BIOLOGICAL EFFECTS OF IONIZING RADIATION
INTERNATIONAL ATOMIC ENERGY AGENCY, VIENNA, Vol 1, 1978, Pages 531-545.
- SELTZER, V.K., N.V. LOSEVA, 1971.
COMPENSATORY POSSIBILITIES OF THE CARDIOVASCULAR SYSTEM OF RABBITS DURING FIVE YEARS OF CONTINUOUS IRRADIATION
U.S. ATOMIC ENERGY COMMISSION, DIV. OF TECHNICAL INFORMATION, 1971, Pages 119-125.
- SONG, C., ET AL., 1981.
RADIOBIOLOGICAL BASIS OF TOTAL BODY IRRADIATION WITH DIFFERENT DOSE RATE AND FRACTIONATION:
REPAIR CAPACITY OF HEMOPOIETIC CELLS.
INT. J. OF RADIATION ONCOLOGY, BIOLOGY, AND PHYSICS, Vol 7, 1981, Pages 1695-1701.
- SPALDING, J., L. HOLLAND, J. PRINE, P. LA BAUVE, J. LONDON, 1973.
COMPARATIVE EFFECTS OF DOSE PROTRACTION AND RESIDUAL INJURY IN DOGS AND MONKEYS
RADIATION RESEARCH, Vol 54, 1973, Pages 453-462.
- SPALDING, J.E., O.S. JOHNSON, P.C. MCWILLIAMS, 1967.
DOSE RATE/EM TOTAL DOSE EFFECT FROM SINGLE SHORT DURATION GAMMA RAY EXPOSURE ON SURVIVAL TIME IN MICE.
MUTATION RESEARCH, Vol 32, 1967, Pages 21-26.
- SPALDING, J.F., L.M. HOLLAND, 1979.
NEAR-TERM AND LATE BIOLOGICAL EFFECTS OF ACUTE AND LOW-DOSE-RATE CONTINUOUS GAMMA-RAY EXPOSURE IN DOGS AND MONKEYS
1979, Pages 1-9.
- SPALDING, J.F., L.M. HOLLAND, J.R. PRINE, 1972.
THE EFFECTS OF DOSE PROTRACTION ON HEMATOPOIESIS IN THE PRIMATE AND DOG
LIFE SCIENCES AND SPACE RESEARCH X, COSPAR, (EDITOR: W. VISHNIAC)
AKADEMIE-VERLAG, BERLIN, 1972, Pages 155-164.
- SPALDING, J.F., T.T. TRUJILLO, LESTROUGEON, 1961.
DEPENDENCE OF RATE OF RECOVERY FROM ACUTE GAMMA-RAY EXPOSURE ON SIZE OF THE CONDITIONING DOSE.
RADIATION RESEARCH, Vol 15, 1961, Pages 378-389.
- SPARGO, B., J.R. BLOOMFIELD, D.J. GLOTZER, G. LEITER, W. NICHOLS, 1951.
HISTOLOGICAL EFFECTS OF LONG-CONTINUED WHOLE BODY GAMMA IRRADIATION OF MICE.
JOURNAL OF NATIONAL CANCER INSTITUTE
Vol 12, 1951, Pages 615-655.
- STANBRIDGE, E.J., 1990.
IDENTIFYING TUMOR SUPPRESSOR GENES IN HUMAN COLORECTAL CANCER
SCIENCE, Vol 247, 1990, Pages 12-13.
- STEARNER, S.P., 1951.
EFFECT OF VARIATION IN DOSAGE RATE OF ROENTGEN RAYS ON SURVIVAL IN YOUNG BIRDS.
AMERICAN JOURNAL OF ROENTGENOLOGY, Vol 65, 1951, Pages 265-271.
- STEARNER, S.P., S.A. TYLER, 1957.
AN ANALYSIS OF THE ROLE OF DOSE AND DOSAGE RATE IN THE EARLY RADIATION MORTALITY OF THE CHICK.
RADIATION RESEARCH, Vol 7, 1957, Pages 253-266.

- STERNER, S.P., S.A. TYLER, 1963.
RADIATION MORTALITY IN THE MOUSE:
MODEL OF THE KINETICS OF INJURY ACCUMULATION. - I. PROTRACTED DOSES IN THE 30-DAY LETHAL RANGE.
RADIATION RESEARCH, Vol 20, 1963, Pages 619-630.
- STEEL, G., J. DOWN, J. PEACOCK, T. STEPHENS, 1986.
DOSE-RATE EFFECTS AND THE REPAIR OF RADIATION DAMAGE.
RADIOTHERAPY AND ONCOLOGY, Vol 5, 1986, Pages 321-331.
- STEINBACH, K.H., H. RAFFLER, G. PABST, T.M. FLIEDNER, 1980.
A MATHEMATICAL MODEL OF CANINE GRANULOCYTOPOIESIS
JOURNAL OF MATHEMATICAL BIOLOGY, Vol 10, 1980, Pages 1-12.
- STERNER, S.P., S.A. TYLER, 1963.
RADIATION MORTALITY IN THE MOUSE:
MODEL OF KINETICS OF INJURY ACCUMULATION I. PROTRACTED DOSES IN THE 30-DAY LETHAL RANGE.
RADIATION RESEARCH, Vol 20, 1963, Pages 619-630.
- STILL, E., ET AL., 1969.
MORTALITY OF SHEEP SUBJECTED TO ACUTE AND SUBSEQUENT PROTRACTED IRRADIATION.
NRDL-TR-69-32
NAVAL RADIOLOGICAL DEFENSE LAB, SAN FRANCISCO, CA, June 9, 1969.
- STILL, E., N.P. PAGE, J.F. TAYLOR, W.G. WISECUP, E.J. AINSWORTH, G.F. LEONG, 1969.
ACUTE MORTALITY AND RECOVERY STUDIES IN BURROS IRRADIATED WITH 1 MVP X-RAYS.
RADIATION RESEARCH, Vol 39, 1969, Pages 580-593.
- STILL, E., S. TAKETA, E. AINSWORTH, G. LEONG, J. TAYLOR, 1969.
HEMATOLOGICAL RESPONSE IN SHEEP GIVEN PROTRACTED EXPOSURES TO 60 CO GAMMA RADIATION.
NRDL-TR-69-6
NAVAL RADIOLOGICAL DEFENSE LAB, SAN FRANCISCO, CA, January 28, 1969.
- STORER, J.B., 1956.
RATE OF REPAIR OF RADIATION DAMAGE IN MICE
THE SHORTER-TERM BIOLOGICAL HAZARDS OF A FALLOUT FIELD, (EDITORS: GORDON M. DUNNING, JOHN A. HILCKEN)
U.S. DEPARTMENT OF DEFENSE, ATOMIC ENERGY COMMISSION, 1956, Pages 93-99.
- STORER, J.B., 1961.
EFFECT OF DOSE SIZE ON RATE OF RECOVERY FROM RADIATION DAMAGE IN MICE
RADIATION RESEARCH, Vol 14, 1961, Pages 206-212.
- STORER, J.B., 1965.
RADIATION RESISTANCE WITH AGE IN NORMAL AND IRRADIATED POPULATIONS OF MICE
RADIATION RESEARCH, Vol 25, 1965, Pages 435-459.
- STORER, J.B., L.J. SERRANO, E.B. DARDEN, M.C. JERNIGAN, R.L. ULLRICH, 1979.
LIFE SHORTENING IN RFM AND BALB/C MICE AS A FUNCTION OF RADIATION QUALITY, DOSE AND DOSE RATE.
RADIATION RESEARCH, Vol 78, 1979, Pages 122-161.
- STOVER, R., W. HALL, 1958.
THE DEPRESSANT EFFECT OF CONTINUOUS COBALT-60 RADIATION ON THE SECONDARY TETANUS ANTITOXIN IN MICE.
RADIATION RESEARCH, Vol 8, 1958, Pages 438-448.
- STRANDQVIST, M., 1944.
STUDIEN UBER DIE KUMULATIVE WIRKUNG DER RONTGENSTRAHLEN BEI FRAKTIONIERUNG:
ERFAHRUNGEN AUS DEM RADIUMHEMMET AN 280 HAUT UND LIPPENKARZINOMEN.
ACTA RADIOLOGICA SUPPLEMENT, Vol 55, 1944, Pages 1-300.
- SUNDARESHAN, M.K., R. FUNDAKOWSKI, 1984.
ON THE EQUIVALENCE OF MATHEMATICAL MODELS FOR CELL PROLIFERATION KINETICS
CELL AND TISSUE KINETICS, Vol 17, 1984, Pages 609-618.
- SVETINA, S., 1977.
AN EXTENDED TRANSITION PROBABILITY MODEL OF THE VARIABILITY OF CELL GENERATION TIMES
CELL AND TISSUE KINETICS, Vol 10, 1977, Pages 575-581.
- SWIFT, M.N., S.T. TAKETA, V.P. BOND, 1954.
REGIONALLY FRACTIONED X-IRRADIATION EQUIVALENT IN DOSE TO TOTAL BODY EXPOSURE
RADIATION RESEARCH, 1954, Pages 241-252.
- SZABUNIEWICZ, M., W.E. HUPP, R.H. DAVIS, S.O. BROWN, 1964.
CLINICAL SIGNS AND PHYSIOLOGICAL OBSERVATIONS IN THE BOAT FOLLOWING FRACTIONATED GAMMA RADIATION
SOUTHWESTERN VETERINARIAN
Vol 17, 1964, Pages 305-314.
- TAYLOR, J., E.J. AINSWORTH, N.P. PAGE, G.F. LEONG, 1969.
THE INFLUENCES OF EXPOSURE ASPECT ON RADIATION LETHALITY IN SHEEP.
NRDL-TR-69-15.
NAVAL RADIOLOGICAL DEFENSE LAB, SAN FRANCISCO, CA, March 24, 1969.
- TAYLOR, J., E. STILL, N. PAGE, G. LEONG, E. AINSWORTH, 1971.
ACUTE LETHALITY AND RECOVERY OF GOATS AFTER 1 MVP X-IRRADIATION.
RADIATION RESEARCH, Vol 45, 1971, Pages 110-126.

- TAYLOR, J.M.G., H.R. WITHERS, 1988.
A COMPARISON OF MATHEMATICAL MODELS FOR REGENERATION IN ACUTELY RESPONDING TISSUES.
UCLA MEDICAL CENTER, LOS ANGELES, CA, 1988.
- THAMES, H.D., 1985.
"INCOMPLETE REPAIR" MODEL FOR SURVIVAL AFTER FRACTIONATED AND CONTINUOUS IRRADIATIONS.
INT. J. OF RADIATION BIOLOGY, Vol 47, 1985, Pages 319-339.
- THAMES, H.D., J.H. HENDRY, 1987.
FRACTIONATION IN RADIOTHERAPY
TAYLOR & FRANCIS LTD., LONDON-NEW YORK-PHILADELPHIA, 1987.
- THAMES, H.D., H.R. WITHERS, K.A. MASON, B.O. REID, 1981.
DOSE-SURVIVAL CHARACTERISTICS OF MOUSE JEJUNAL CRYPT CELLS
INT. J. OF RADIATION ONCOLOGY, BIOLOGY, AND PHYSICS, Vol 7, November 1981, Pages 1591-1597.
- THAMES, H.D., H.R. WITHERS, L.J. PETERS, 1984.
TISSUE REPAIR CAPACITY AND REPAIR KINETICS DEDUCED FROM MULTIFRACTIONATED OR CONTINUOUS IRRADIATION REGIMENS WITH INCOMPLETE REPAIR
BRITISH JOURNAL OF CANCER, Vol 49, 1984, Pages 263-269.
- THAMES, H.D., H.R. WITHERS, L.J. PETERS, G.H. LETCHER, 1982.
CHANGES IN EARLY AND LATE RADIATION RESPONSES WITH ALTERED DOSE FRACTIONATION: IMPLICATIONS FOR DOSE SURVIVAL RELATIONSHIPS.
INT. J. OF RADIATION ONCOLOGY, BIOLOGY, AND PHYSICS, Vol 8, 1982, Pages 219-226.
- THOMA, G.E., JR., N. WALD, 1959.
THE DIAGNOSIS AND MANAGEMENT OF ACCIDENTAL RADIATION INJURY.
JOURNAL OF OCCUPATIONAL MEDICINE, Vol 1, August 1959, Pages 421-447.
- THOMAS, E.P., ET AL., 1971.
ALLOGENIC MARROW GRAFTING FOR HEMATOLOGIC MALIGNANCY USING HL-A MATCHED DONOR-RECIPIENT SIBLING PAIRS.
BLOOD, Vol 38, 1971, Pages 267-287.
- THOMSON, J., W. TOURTELLOTT, 1953.
THE EFFECT OF DOSE RATE ON THE LD50 OF MICE EXPOSED TO GAMMA RADIATION FROM COBALT-60 SOURCES.
AMERICAN JOURNAL OF ROENTGENOLOGY, Vol 69, 1953, Pages 826-829.
- THOMSON, J.F., W.W. TOURTELLOTT, M.S. CARTTAR, R.S. COX, J.E. WILSON, 1953.
STUDIES ON THE EFFECTS OF CONTINUOUS EXPOSURE OF ANIMALS TO GAMMA RADIATION FROM COBALT 60 PLANE SOURCES
AMERICAN JOURNAL OF ROENTGENOLOGY, RADIUM THERAPY AND NUCLEAR MEDICINE, Vol 69, 1953, Pages 830-838.
- THOMSON, J.F., W. WALLACE, M. TOURTELLOTT, R. CORTLAR, J. COX, J. WILSON, 1953.
STUDIES ON THE EFFECTS OF CONTINUOUS EXPOSURE OF ANIMALS TO GAMMA RADIATION FROM COBALT 60 PLANE SOURCES.
AMERICAN JOURNAL OF ROENTGENOLOGY, Vol 69, 1953, Pages 830-838.
- THOMSON, J.F., F.S. WILLIAMSON, D. GRAHN, E.J. AINSWORTH, 1981.
LIFE SHORTENING IN MICE EXPOSED TO FISSION NEUTRONS AND γ RAYS
II. DURATION-OF-LIFE AND LONG-TERM FRACTIONATED EXPOSURES
RADIATION RESEARCH, Vol 86, 1981, Pages 573-579.
- TICHELLI, A., A. GRATWOHL, B. SPECK, B. OSTERWALDER, C. NISSEN, A. LORI, 1986.
NEBENWIRKUNGEN DER GANZKORPERBESTRAHLUNG IM RAHMEN DER KNOCHENMARK TRANSPLANTATION: PROPHYLAXE UND THERAPIE.
SCHWEIZ. MED. WCHSCHR.
Vol 116, 1986, Pages 1560-1566.
- TICHELLI, A., E. WALTHER, A. GRATWOHL, B. OSTERWALDER, B. SPECK, 1987.
SIDE EFFECTS OF TOTAL BODY IRRADIATION BEFORE BONE MARROW TRANSPLANTATION.
BASEL EXPERIENCE JULY 1979 TO MARCH 1986. STRAHLENTHERAPIE UND ONKOLOGIE
STRAHLENTHERAPIE UND ONKOLOGIE, Vol 163, 1987, Pages 245-246.
- TOBIAS, C.A., A. BLAKELY, F.Q. NGO, T.C. YANG, 1980.
THE REPAIR-MISREPAIR MODEL OF CELL SURVIVAL
"RADIATION BIOLOGY IN CANCER RESEARCH", RAYMOND E. MEYN & H. RODNEY WITHERS, EDS.
RAVEN PRESS, NEW YORK, 1980, Pages 195-230.
- TOTAFURNO, J., M. BJERKNES, H. CHENG
THE CRYPT CYCLE
CRYPTS AND VILLUS PRODUCTION IN THE ADULT INTESTINAL EPITHELIUM
- TRAVIS, E., 1980.
RADIATION PNEUMONITIS AND FIBROSIS IN MOUSE LUNG ASSAYED BY RESPIRATORY FREQUENCY AND HISTOLOGY.
RADIATION RESEARCH, Vol 84, 1980, Pages 133-143.
- TRAVIS, E., 1983.
REPAIR IN MOUSE LUNG BETWEEN MULTIPLE SMALL DOSES OF X-RAYS.
RADIATION RESEARCH, Vol 94, 1983, Pages 326.
- TRAVIS, E., J. DOWN, 1981.
REPAIR IN MOUSE LUNG AFTER SPLIT DOSES OF X-RAYS.
RADIATION RESEARCH, Vol 87, 1981, Pages 166.
- TRAVIS, E., ET AL., 1983.
IS THERE A LOSS OF REPAIR CAPACITY IN MOUSE LUNGS WITH INCREASING NUMBERS OF DOSE FRACTIONS.
INT. J. OF RADIATION ONCOLOGY, BIOLOGY, AND PHYSICS, Vol 9, 1983, Pages 691.

- TRAVIS, E.L., L.J. PETERS, J. MCNEILL, H.D., JR. THAMES, C. KAROKS, 1985.
EFFECT OF DOSE-RATE ON TOTAL BODY IRRADIATION:
LETHALITY AND PATHOLOGIC FINDINGS.
RADIOTHERAPY AND ONCOLOGY, Vol 4, 1985, Pages 341-351.
- TRAYNOR, E., 1967.
THE EFFECT OF DOSE RATE ON THE LD50/30 OF MICE EXPOSED TO COBALT-60.
RADIATION RESEARCH, Vol 31, 1967, Pages 535.
- TRUM, B.F., 1955.
EXTERNAL RADIATION STUDIES WITH LARGE ANIMALS.
AEC AGRICULTURAL RESEARCH PROJECT, SEMI-ANNUAL PROGRESS REPORT ORO-145.
UNIVERSITY OF TENNESSEE, June 30, 1955.
- TRUM, B.F., T.J. HALEY, M. BASSIN, J. HEGLIN, J.H. RUST, 1953.
EFFECT OF 400 R FRACTIONAL WHOLE BODY GAMMA IRRADIATION IN THE BURRO
AMERICAN JOURNAL OF PHYSIOLOGY, Vol 174, 1953, Pages 57-60.
- TRUM, B.F., J. SHIVELY, U. KUHN, W. CARLL, 1959.
RADIATION INJURY AND RECOVERY IN SWINE.
RADIATION RESEARCH, Vol 11, 1959, Pages 324-326.
- TURESSON, I., G. NOTTER, 1974.
SKIN REACTIONS AFTER DIFFERENT FRACTIONATION SCHEDULES GIVING THE SAME CUMULATIVE RADIATION EFFECT
ACTA RADIOLOGICAL
Vol 14, 1974, Pages 475-484.
- TWENTYMAU, P., N. BLACKETT, 1970.
RED CELL PRODUCTION IN THE CONTINUOUSLY IRRADIATED MOUSE.
BRITISH JOURNAL OF RADIOLOGY, Vol 43, 1970, Pages 898-902.
- TYAZHELOVA, V.G., I.G. AKOEY, 1975.
EQUIVALENT CONDITIONS OF IRRADIATION OF MAMMALS.
RADIOBIOLOGY
Vol 15, 1975, Pages 103-107.
- UPTON, A.C., 1968.
EFFECTS OF RADIATION ON MAN
ANNUAL REVIEW OF NUCLEAR SCIENCE, Vol 18, 1968, Pages 495-528.
- VATISTAS, S., A. HERDAN, R. ELLIS, 1968.
THE ROLE OF THE INTESTINE IN ACUTE POSTIRRADIATION MORTALITY OF MICE.
REPORT OF A SYMPOSIUM HELD AT RICHLAND, WASH. U.S.A., SEPT. 25-28, 1966
1968.
- VOIDOPICK, H., G.A. ANDREWS, 1980.
THE UNIVERSITY OF TENNESSEE COMPARATIVE ANIMAL RESEARCH LABORATORY ACCIDENT IN 1971.
THE MEDICAL BASIS FOR RADIATION ACCIDENT PREPAREDNESS, K.F. HUBNER AND S.A. FRY, EDS.
ELSEVIER NORTH HOLLAND, INC., NEW YORK, 1980.
- VOGEL, H.H., 1956.
FRACTIONATION AND PROTRACTION OF CO60 GAMMA RADIATION:
STUDY OF ACUTE LETHALITY IN MICE.
RADIATION RESEARCH, Vol 5, 1956, Pages 601.
- VOGEL, H.H., J.W. CLARK, D.L. JORDAN, 1957.
COMPARATIVE MORTALITY AFTER 24-HOUR WHOLE BODY, EXPOSURES OF MICE TO FISSION NEUTRONS AND COBALT-60 GAMMA RAYS
RADIATION RESEARCH, Vol 6, 1957, Pages 460-468.
- VOGEL, H.H., ET AL., 1957.
COMPARATIVE FATALITIES AFTER 24-H WHOLE BODY EXPOSURE OF MICE TO FISSION NEUTRONS AND COBALT-60 GAMMA RAYS.
RADIATION RESEARCH, Vol 6, 1957, Pages 640-668.
- VOGEL, H.H., D.L. JORDAN, 1958.
THE EFFECT UPON MOUSE LONGEVITY OF FRACTIONATION OF A DOSE OF FISSION NEUTRONS
BIOLOGICAL AND MEDICAL RESEARCH DIVISION SEMI-ANNUAL REPORT
1958, Pages 95-96.
- VOGEL, H.H., D.L. JORDAN, 1964.
FRACTIONATED, LOW-DOSE RATE IRRADIATION OF MICE WITH FISSION NEUTRONS AND 60 CO GAMMA RAYS.
ANNALS OF THE NEW YORK ACADEMY OF SCIENCES, Vol 114, 1964, Pages 185-188.
- VOGEL, H.H., P. STEARNER, 1955.
THE EFFECTS OF DOSE RATE VARIATION OF FISSION NEUTRONS AND OF CO 60 GAMMA-RAYS ON SURVIVAL OF YOUNG CHICKS.
RADIATION RESEARCH, Vol 2, 1955, Pages 513-521.
- VOSS, O., 1972.
STEM CELL REMOVAL IN SPLEEN AND BONE MARROW OF MICE AFTER REPEATED TOTAL-BODY IRRADIATIONS.
INT. J. OF RADIATION BIOLOGY, Vol 22, 1972, Pages 41-50.
- VRIJSEN-DORP, H.M., D.W. VAN BEKKUM, 1984.
SUSCEPTIBILITY TO TOTAL BODY IRRADIATION.
"RESPONSE OF DIFFERENT SPECIES TO TOTAL BODY IRRADIATION", J.J. BROERSE & T.J. MACVITTIE, EDS.
MARTINUS NIGHOFF PUBLISHERS, DORDRECHT, THE NETHERLANDS, 1984, Pages 43-57.

- VRIESENDROP, H.M., D.W. VAN BEKKUM, 1980.
ROLE OF TOTAL BODY IRRADIATION IN CONDITIONING FOR BONE MARROW TRANSPLANTATION.
IMMUNOBIOLOGY OF BONE MARROW TRANSPLANTATION SUPPLEMENT TO "BLUNT", SPRINGER VERLAG BERLIN, HEIDELBERG
1980, Pages 349-363.
- WALD, N., G.E. THOMA, 1961.
RADIATION ACCIDENTS: MEDICAL ASPECTS OF NEUTRON AND GAMMA-RAY EXPOSURES.
OAK RIDGE NATIONAL LABORATORY REPORT ONRL-2748, PART B.
U.S. DEPT. OF ENERGY TECHNICAL INFOR. CENTER, OAK RIDGE, TN, 1961.
- WAMBERSIE, A., M. STIENON-SMOES, M. OCTAVE-PRIGNOT, J. DUTREIX, 1979.
EFFECT OF DOSE RATE ON INTESTINAL TOLERANCE IN MICE, IMPLICATIONS IN RADIOTHERAPY
BRITISH JOURNAL OF RADIOLOGY, Vol 52, 1979, Pages 153-155.
- WANKERSIE, A., 1979.
EFFECT OF DOSE RATE ON INTESTINAL TOLERANCE IN MICE. IMPLICATION IN RADIOTHERAPY.
BRITISH JOURNAL OF RADIOLOGY, Vol 52, 1979, Pages 153-155.
- WARA, W., T. PHILLIPS, L. MARGOLIS, 1973.
RADIATION PNEUMONITIS. A NEW APPROACH TO THE DERIVATION OF TIME-DOSE FACTOR .
BRITISH JOURNAL OF CANCER, Vol 32, 1973, Pages 547.
- WARREN, S., D. GRAHN, 1973.
IONIZING RADIATION (CHAPTER 9).
BIOASTRONAUTICS DATA BOOK, J. PARKER JR. AND V.R. WEST EDS.; NASA SP-3006.
NATIONAL AERONAUTICS AND SPACE ADMINISTRATION, WASHINGTON, DC, 1973.
- WEST, J.E., F.A. MITCHELL, S.R. JONES, J. WITZ, 1973.
BONE MARROW RESPONSE OF BEAGLES TO FRACTIONATED DOSES OF MIXED GAMMA-NEUTRON RADIATION
AFRRI SCIENTIFIC REPORT
1973, Pages 19 PGS.
- WESTBROOK, J.G., A. BARRETT, 1987.
VOMITING ASSOCIATED WITH WHOLE BODY IRRADIATION.
CLINICAL RADIOLOGY, Vol 38, 1987, Pages 263-266.
- WHELDON, T.E., 1975.
MATHEMATICAL MODELS OF OSCILLATORY BLOOD CELL PRODUCTION
MATHEMATICAL BIOSCIENCES, Vol 24, 1975, Pages 289-305.
- WHELDON, T.E., A.S. MICHALOWSKI, J. KIRK, 1982.
THE EFFECT OF IRRADIATION ON FUNCTION IN SELF-RENEWING NORMAL TISSUES WITH DIFFERING PROLIFERATIVE ORGANISATION
BRITISH JOURNAL OF RADIOLOGY, Vol 55, 1982, Pages 759-766.
- WICHMANN, H.E., M.D. GERHARDTS, H. SPECHTMEYER, R. GROSS, 1979.
A MATHEMATICAL MODEL OF THROMBOPOIESIS IN RATS
CELL AND TISSUE KINETICS, Vol 12, 1979, Pages 551-567.
- WICHMANN, H.E., M. LOEFFLER, 1982.
A SOLUTION TO THE CONTROVERSY ON STEM CELL REGULATION
BLOOD CELLS
Vol 8, 1982, Pages 461-465.
- WICHMANN, H.E., M. LOEFFLER, EDS., 1985.
MATHEMATICAL MODELING OF CELL PROLIFERATION:
STEM CELL REGULATION IN HEMOPOIESIS, VOLS. I & II.
CRC PRESS, INC., BOCA RATON, FLORIDA, 1985.
- WITHERS, H.R., 1967.
RECOVERY AND REPOPULATION IN VIVO BY MOUSE SKIN EPITHELIAL CELL DURING FRACTIONATED IRRADIATION.
RADIATION RESEARCH, Vol 32, 1967, Pages 227-239.
- WITHERS, H.R., 1969.
CAPACITY FOR REPAIR IN CELLS OF NORMAL AND MALIGNANT TISSUES
TIME AND DOSE RELATIONSHIPS IN RADIATION BIOLOGY AS APPLIED TO RADIOTHERAPY
1969, Pages 54-69.
- WITHERS, H.R., 1971.
REGENERATION OF INTESTINAL MUCOSA AFTER IRRADIATION
CANCER, Vol 28, July 1, 1971, Pages 75-81.
- WITHERS, H.R., 1972.
CELL REMOVAL SYSTEM CONCEPTS AND THE RADIATION RESPONSE.
FRONTIERS OF RADIATION THERAPY AND ONCOLOGY, J.M. VAETH, ED.
S. KARGER, BASEL, Vol 6, 1972, Pages 93-107.
- WITHERS, H.R., 1989.
PRIVATE COMMUNICATION.
DEPARTMENT OF RADIATION ONCOLOGY.
UCLA MEDICAL CENTER, LOS ANGELES, CA, March 1989.
- WITHERS, H.R., A.M. CHU, B.O. REID, D.H. HUSSEY, 1975.
RESPONSE OF MOUSE JEJUNUM TO MULTIFRACTION RADIATION.
INT. J. OF RADIATION ONCOLOGY, BIOLOGY, AND PHYSICS, Vol 1, 1975, Pages 41-52.

- WITHERS, H.R., M.M. ELKIND, 1968.
DOSE-SURVIVAL CHARACTERISTICS OF EPITHELIAL CELLS OF MOUSE INTESTINAL MUCOSA.
RADIOLOGY, Vol 91, 1968, Pages 998-1000.
- WITHERS, H.R., M.M. ELKIND, 1969.
RADIOSENSITIVITY AND FRACTIONATION RESPONSE OF CRYPT CELLS OF MOUSE JEJUNUM
RADIATION RESEARCH, Vol 38, 1969, Pages 598-613.
- WITHERS, H.R., M.M. ELKIND, 1970.
MICROCOLONY SURVIVAL ASSAY FOR CELLS OF MOUSE INTESTINAL MUCOSA EXPOSED TO RADIATION
INT. J. OF RADIATION BIOLOGY, Vol 17, January 2, 1970, Pages 261-267.
- WITHERS, H.R., K. MASON, B.O. REID, N. DUBRAVSKY, H.T. BARKLEY, ET AL., 1974.
RESPONSE OF MOUSE INTESTINE TO NEUTRONS AND GAMMA RAYS IN RELATION TO DOSE
CANCER, Vol 34, July 1974, Pages 39-47.
- WITHERS, H.R., G., JR. OLIVER, D. GLENN, 1971.
RESPONSE OF MOUSE JEPUNAL CRYPT CELLS TO LOW DOSE RATE IRRADIATION WITH CALIFORNIUM NEUTRONS OR RADIUM GAMMA-RAYS
RADIATION RESEARCH, Vol 48, 1971, Pages 484-494.
- WITHERS, H.R., H.D. THAMES, L.J. PETERS, 1983.
A NEW ISOEFFECT CURVE FOR CHANGE IN DOSE PER FRACTION.
RADIOTHERAPY AND ONCOLOGY, Vol 1, 1983, Pages 187-191.
- WOODWARD, K., S. MICHAELSON, T. NOONAN, J. HOWLAND, 1967.
THE EFFECT OF DOSE-RATE ON THE ACUTE LETHAL RESPONSE OF DOGS.
INT. J. OF RADIATION BIOLOGY, Vol 12, 1967, Pages 265-276.
- XU, C.X., J.H. HENDRY, N.G. TESTA, 1983.
THE RESPONSE OF STROMAL PROGENITOR CELLS IN MOUSE MARROW TO GRADED REPEATED DOSES OF X RAYS OR NEUTRONS
RADIATION RESEARCH, Vol 96, 1983, Pages 82-89.
- YOCHMOWITZ, M., R. PATRICK, R. JAEGER, D. BARNES, 1977.
PROTRACTED RADIATION-STRESSED PRIMATE PERFORMANCE
AVIATION, SPACE AND ENVIRONMENTAL MEDICINE
July 1977, Pages 598-606.
- YOUNG, J.D., Z.A. COHN, 1988.
HOW KILLER CELLS KILL
SCIENTIFIC AMERICAN, Vol 258, January 1988, Pages 38-44.
- YOUNG, R.W., 1986.
ACUTE RADIATION SYNDROME.
MECHANISMS AND TREATMENT OF RADIATION-INDUCED NAUSEA AND VOMITING, C.J. DAVIS, G.V. LAKE-BAKAAR,
AND D.G. GRAHAME-SMITH, EDS.
SPRINGER-VERLAG, BERLIN, HEIDELBERG, 1986, Pages 94-109.
- YOUNG, R.W., D.L. AUTON, S.G. LEVIN, 1990.
THE EFFECT OF TOTAL BODY IRRADIATION ON THE PERFORMANCE OF COMBAT CREW PERSONNEL.
IN PRESS.
DEFENSE NUCLEAR AGENCY, WASHINGTON, DC, 1990.
- ZAPOL'SKAYA, N.A., A.V. FEDOROVA, Y.D. PAVLITSKAYA, L.N. LAVRENTYEV, N.G. YAKOVLEVA, 1971.
BIOLOGICAL EFFECTS AT REMOTE TIMES INDUCES BY COMBINED EXTERNAL IRRADIATION AND IRRADIATION
FROM ISOTOPES INCORPORATED IN THE BODY
U.S. ATOMIC ENERGY COMMISSION, DIV. OF TECHNICAL INFORMATION, 1971, Pages 523-531.
- ZELLMER, R.W., 1961.
HUMAN ABILITY TO PERFORM AFTER ACUTE SUBLETHAL RADIATION.
MILITARY MEDICINE, Vol 126, 1961, Pages 681-687.
- ZELLMER, R.W., J. PICKERING, 1960.
BIOLOGIC EFFECTS OF NUCLEAR RADIATION IN PRIMATES
SCHOOL OF AVIATION MEDICINE REPORT
August 1960.
- ZEMAN, E.M., J.S. BEDFORD, 1984.
CHANGES IN EARLY AND LATE EFFECTS WITH DOSE-PER-FRACTION:
ALPHA, BETA, REDISTRIBUTION AND REPAIR
INT. J. OF RADIATION ONCOLOGY, BIOLOGY, AND PHYSICS, Vol 10, 1984, Pages 1039-1047.
- ZOOK, B.C., E.W. BRADLEY, G.W. CASARETT, M.P. FISHER, C.C. ROGERS, 1981.
THE EFFECTS OF FRACTIONATED DOSES OF FAST NEUTRONS OR PHOTONS ON THE CANINE CEEERVICAL SPINAL CORD
RADIATION RESEARCH, Vol 88, 1981, Pages 165-179.
- ZOOK, B.C., E.W. BRADLEY, G.W. CASARETT, C.C. ROGERS, 1981.
PATHOLOGIC CHANGES IN THE HEARTS OF BEAGLES IRRADIATED WITH FRACTIONATED FAST NEUTRONS OR PHOTONS
RADIATION RESEARCH, Vol 88, 1981, Pages 607-618.

APPENDIX A **UGIDM EQUATIONS FOR ACUTE AND CONSTANT DOSE RATE EXPOSURES**

This appendix derives solutions of the UGIDM equations for two specific cases of radiation exposure: acute (or prompt) and constant dose rate. The model variables and parameters are:

Variables

C = depletable reservoir (target tissue) level, Gy
P = potential toxin, Gy
A = active toxin, Gy
R = dose rate, Gy/h⁻¹
D = dose, Gy

Parameters

α = potential toxin conversion rate/active toxin production rate, h⁻¹
 β = active toxin clearing rate, h⁻¹
 μ = depletable reservoir reconstitution rate, h⁻¹
C₀ = initial reservoir level, Gy
D₀ = characteristic target tissue dose (=C₀), Gy
A_{0.5} = half-maximum value of A, Gy
 γ = severity response slope

A.1 ACUTE EXPOSURE.

The UGIDM differential equations for acute exposure are,

$$\text{depletable reservoir: } \frac{dC}{dt} = \mu(C_0 - C) \quad (\text{A.1})$$

$$\text{potential toxin: } \frac{dP}{dt} = -\alpha P \quad (\text{A.2})$$

$$\text{active toxin: } \frac{dA}{dt} = \alpha P - \beta A \quad (\text{A.3})$$

Following an acute exposure, the initial amount of potential toxin derives from the depletable reservoir in the UGIDM. This can be determined by taking the appropriate limits of the solution to the differential equation for the depletable reservoir at a constant dose rate, R , given by,

$$\frac{dC}{dt} = - \left(\frac{R}{D_o} \right) C + \mu (C_o - C) , \quad (A.4)$$

or
$$\frac{dC}{dt} + KC = \mu C_o , \quad K = R/D_o + \mu$$

and then,
$$\frac{d}{dt} (C e^{Kt}) = \mu C_o e^{Kt} .$$

Integrating,
$$\int_{C_o}^{C e^{Kt}} d(C e^{Kt}) = \mu C_o \int_0^t e^{Kt} dt ,$$

and solving for $C(t)$ gives,

$$C(t) = \frac{\mu C_o}{K} (1 - e^{-Kt}) + C_o e^{-Kt} \quad (A.5)$$

Taking limits of the dose rate (R) and time (t) along the fixed relationship, $D = Rt$ (where $R/D_o \gg \mu$),

$$\lim_{\substack{R \rightarrow \infty \\ t \rightarrow 0}} C(t) = C_o e^{-D/D_o} .$$

The initial amount of potential toxin P_o is then,

$$P_o = C_o - C_o e^{-D/D_o} . \quad (A.6)$$

The solution to Eq (A.2) is,

$$P(t) = P_o e^{-\alpha t} . \quad (A.7)$$

For the active toxin, Eq.(A.3) is,

$$\frac{dA}{dt} + \beta A = \alpha P ,$$

and,
$$\frac{d}{dt} (Ae^{\beta t}) = \alpha P_o e^{-\alpha t} \cdot e^{\beta t} ,$$

where $e^{\beta t}$ is the integrating factor.

Integrating,
$$\int_{A_o}^{Ae^{\beta t}} d(Ae^{\beta t}) = \alpha P_o \int_0^t e^{(\beta-\alpha)t} dt ,$$

and solving for $A(t)$ gives,

$$A(t) = \frac{\alpha P_o}{\beta - \alpha} \left(e^{-\alpha t} - e^{-\beta t} \right) , \quad (A.8)$$

where $A_o = 0$.

The maximum UG severity level following an acute exposure is obtained by maximizing $A(t)$. That is, for $dA/dt = 0$, the time that A is a maximum following acute exposure is obtained as,

$$t_{\max} = \left(\ln \frac{\beta}{\alpha} \right) / (\beta - \alpha) . \quad (A.9)$$

Then the maximum UG severity is,

$$S_{\max} = 1 + 4 \left\{ 1 - \exp \left[- \left[A(t_{\max}) / A_{0.5} \right]^\gamma \right] \right\} \quad (A.10)$$

A.2 CONSTANT DOSE RATE EXPOSURE.

The UGIDM differential equations for constant dose rate exposure are,

$$\text{depletable reservoir: } \frac{dC}{dt} = \left(\frac{R}{D_o} \right) C + \mu (C_o - C) \quad (\text{A.11})$$

$$\text{potential toxin: } \frac{dP}{dt} = \left(\frac{R}{D_o} \right) C - \alpha P \quad (\text{A.12})$$

$$\text{active toxin: } \frac{dA}{dt} = \alpha P - \beta A \quad (\text{A.13})$$

The solution to Eq. (A.11) is given by Eq. (A.5) above. Multiplying by the integrating factor $e^{\alpha t}$, Eq. (A.12) may be given by,

$$\frac{d}{dt} (P e^{\alpha t}) = \frac{R_o}{D_o} \left[\frac{\alpha C_o}{K} (1 - e^{-Kt}) + C_o e^{-Kt} \right] e^{\alpha t} .$$

Integrating,

$$\int_{P_o}^{P e^{\alpha t}} d(P e^{\alpha t}) = \frac{R_o}{D_o} \int_0^t \left[\frac{\mu C_o}{K} (1 - e^{-Kt}) + C_o e^{-Kt} \right] e^{\alpha t} dt ,$$

and solving for $P(t)$ gives,

$$P(t) = \frac{RC_o}{KD_o} \left[\frac{\mu}{\alpha} (1 - e^{-\alpha t}) - \left(\frac{K-\mu}{\alpha-\mu} \right) (e^{-Kt} - e^{-\alpha t}) \right] + P_o e^{-\alpha t} . \quad (\text{A.14})$$

Multiplying by the integrating factor $e^{\beta t}$, Eq (A.13) may be given by,

$$\frac{d}{dt} (A e^{\beta t}) = \left\{ \frac{\alpha RC_o}{KD_o} \left[\frac{\mu}{\alpha} (1 - e^{-\alpha t}) - \left(\frac{K-\mu}{\alpha-\mu} \right) (e^{-Kt} - e^{-\alpha t}) \right] + \alpha P_o e^{-\alpha t} \right\} e^{\beta t} .$$

Integrating,

$$\int_{A_0}^{Ae^{\beta t}} (Ae^{\beta t}) = \alpha P_0 \int_0^t e^{(\beta-\alpha)t} dt$$

$$+ \frac{RC_0}{KD_0} \int_0^t \left\{ \mu [e^{\beta t} - e^{(\beta-\mu)t}] - \alpha \left(\frac{K-\mu}{\alpha-\mu} \right) [e^{(\beta-K)t} - e^{(\beta-\alpha)t}] \right\} dt ,$$

and solving for $A(t)$ gives,

$$A(t) = \frac{RC_0}{KD_0} \left[\frac{\mu}{\beta} (1 - e^{-\beta t}) + \frac{1}{\beta-\alpha} \left(\mu - \frac{K-\mu}{\alpha-\mu} \right) (e^{-\beta t} - e^{-\alpha t}) \right.$$

$$\left. - \frac{\alpha}{\beta-K} \left(\frac{K-\mu}{\alpha-\mu} \right) (e^{-Kt} - e^{-\beta t}) \right] + \frac{\alpha P_0}{\beta-\alpha} (e^{-\alpha t} - e^{-\beta t}) + A_0 e^{-\beta t} \quad (A.15)$$

Eq. (A.15) gives the active toxin value as a function of exposure time. When $P_0, A_0 \neq 0$, they would be residual values from previous exposure(s) referenced from $t=0$ at the beginning of the current constant dose rate exposure; otherwise, $P_0, A_0 = 0$ and the last two terms are zero. For this condition, the time that A is a maximum during irradiation (which may the time irradiation ceases) can be determined for $dA(t)/dt = 0$; then when $P_0, A_0 = 0$, a transcendental relationship results which must be solved for $t = t_{\max}$ numerically, i.e., of the form below,

$$e^{-(K-\beta)t} + Ae^{-(\alpha-\beta)t} = B ,$$

where, the A, B , and K are constants that depend on the dose rate R and model parameters.

The active toxin $A(t')$ after irradiation ceases is,

$$A(t') = \frac{\alpha P'_0}{\beta-\alpha} (e^{-\alpha t'} - e^{-\beta t'}) + A'_0 e^{-\beta t'} \quad (A.16)$$

where, t' is the time measured after irradiation ceases, starting from zero at that point, and P'_0 and A'_0 are the existing values then for P and A ; they are given by Eqs. (A.14) and (A.15), respectively, for P_0 , $A_0 = 0$. The time $A(t')$ is a maximum after irradiation ceases is determined for, $dA(t')/dt' = 0$, given by,

$$t'_{\max} = (\beta - \alpha)^{-1} \ln \left[1 - \frac{A'_0}{P'_0} \left(\frac{\beta - \alpha}{\alpha} \right) \right] \quad (\text{A.17})$$

The maximum severity level of UG distress is then given by $S(t'_{\max})$ according to Eq. (A.10).

APPENDIX B
INCIDENCE OF NAUSEA AND VOMITING WITHIN 24 HOURS
IN NUCLEAR ACCIDENT EXPOSURES

A log likelihood analysis was performed based on 40 different cases of accidental acute exposure of humans to nuclear radiation. Five different models including the normal, lognormal, Weibull, logistic, and loglogistic forms were applied to fit nausea and vomiting response data for the first 24-h postexposure. Two sets of calculations were performed based on somewhat different internal whole-body dose estimates for 13 of the 40 cases. Most of the accidents involved mixed neutron and gamma radiation exposure, and an RBE = 1 was assumed for analyzing the nausea and vomiting responses.

ED₅₀ estimates range from 148 to 177 cGy for nausea and 160 to 190 cGy for vomiting when all five models and both data sets are considered. All of the models fit the data reasonably well; the lowest χ^2 values were obtained for the lognormal, Weibull, and loglogistic models. Based on data set I and the lognormal model, ED₅₀ values of 157 (± 58) cGy were obtained for nausea and 170 (± 60) cGy for vomiting. The ED₅₀ values for the alternative data set are essentially the same, differing by about 9 cGy.

Calculations were performed to estimate the incidence of nausea and vomiting for acute radiation exposure in order to establish an acute (or high dose rate) basis relevant to our study of protracted radiation exposure. The population we chose to analyze for this purpose consists of 40 nuclear accident cases documented in the literature where total body radiation exposures were all delivered in the order of minutes or less at rates exceeding ~ 2000 cGy h⁻¹. Much of the large body of clinical information for total body irradiation (TBI) of patients with various malignant diseases also involves acute radiation exposure rates. However, the prodromal response is altered to varying degrees due to chemotherapy often administered prior to TBI, premedication (antiemetics, sedatives, analgesics, and steroids) as well as the health condition and well-being of the patients.

Accordingly, we avoided the use of clinical TBI data because of these limitations.

B.1 DATA.

Nuclear accident data used for this analysis of the incidence are given in Table 31. The data covering a variety of incidents are adapted from the literature. Each of the 40 cases are for an individual accidentally exposed to acute ionizing radiation and are labeled (column 1) designating geographical location and specific clinical case (see Table 31 footnote); in some instances, more than one individual was exposed during a given incident. Specifically for the regression analysis, we utilized the dose values given in column 4 and the response data in columns 5 and 6 where "X" indicates a positive quantal response.

Most of the case data in Table 31 were originally compiled by Thoma and Wald [1959]. However, based on subsequent dosimetric analysis, some of the originally reported dose values were revised downward to reflect internal dose estimates to the midline of the body or the mean bone marrow dose. Table 31 includes the revised dose values as well as the doses for additional accident cases given in the other references [Lushbaugh, 1969; Hübner and Fry, 1980; Klener et al., 1986; and Fanger and Lushbaugh, 1967] listed in Table 31. More recently, Baverstock and Ash [1983] also performed additional dosimetric analysis of the Oak Ridge (OR) and Yugoslavian (Y) accidents. They estimated somewhat lower dose values for 13 of the 40 accident cases, as given by the values in parenthesis in Table 31. Our analysis considered both sets of dose data.

A large majority (about 80%) of the accident cases shown in Table 31 involve substantially varying proportions of mixed neutron and gamma radiation (column 3) due to nuclear criticality incidents. Data are lacking, however, to assign any neutron RBE effect to the nausea and vomiting response in humans. Accordingly, we have tacitly assumed an RBE of unity for those prodromal responses, and the neutron and gamma doses (in gray units) are utilized additively.

Table 31. Nuclear accident cases--nausea and vomiting within 24 hours.

Case ^a	Reference ^b	Dosimetry		Prodromal Response	
		n/y Ratio	Internal Dose (cGy) ^c	Nausea	Vomiting
LA2	1,2	80	8.1	--	--
LA10	1,2	3.5	9.0	--	--
A4	1	0.08	10.8	--	--
LA9	1,2	3.0	12.0	--	--
LA8	1,2	3.0	16.0	--	--
OR8(H)	1,2,3	0.36	22.8	--	--
LA7	1,2	3.7	42.0	--	--
A3	1	0.1	60.5	--	--
LA6	1,2	4.6	62.0	--	--
OR6(F)	1,2,3,4	0.36	68.5(66.5) ^d	--	--
OR7(G)	1,2,3,4	0.36	68.5(66.5)	--	--
P(A)	2	0.0	100.0	--	--
A2	3	0.083	125.6	--	--
C	5	0.0	140.0	--	--
Y6(B)	1,2,4,6	0.28	145.0(127.0)	X	--
A1	1	0.098	159.2	X	X
UT/CARL	2	0.0	165.0 ^e	--	X
LA4	1,2	6.4	192.0	X	X
NJ(2)	2	0.0	200.0	X	X
Y5(H)	1,2,4,6	0.26	226.0(201.0)	X	X
OR5(E)	1,2,3,4	0.36	236.0(225.0)	X	--
OR4(B)	1,2,3,4	0.36	270.0(265.0)	X	X
Y4(G)	1,2,4,6	0.28	290.0(216.0)	X	X
Y2(D)	1,2,4,6	0.28	293.0(217.0)	X	X
Y3(M)	1,2,4,6	0.27	298.0(267.0)	X	X
R2	1	?	300.0	X	X
P(B)	2	0.0	300.0	X	X
Y1(V)	1,2,4,6	0.26	305.0(273.0)	X	X
LA1	1,2	0.55	310.0	X	X
OR3(D)	1,2,3,4	0.36	327.0(315.0)	X	X
OR2(C)	1,2,3,4	0.36	339.0(330.0)	--	--
OR1(A)	1,2,3,4	0.36	365.0(350.0)	X	X
NJ(1)	2	0.0	410.0	X	X
R1	1	?	450.0	X	X
B	2	0.1	550.0	X	X
P(C)	2	0.0	600.0	X	X
LA3	1,2	8.8	1114.0	X	X
I	2	0.0	1200.0	X	X
LA11(K)	7	0.25	4500.0	X	X
RI(P)	7	0.33	8800.0	X	X

^aCase nomenclature relates to that reported in the literature; numbers and/or letters that may be parenthetical following the geographical location keys given below, designate specific individuals.

LA: Los Alamos A: Argonne RI: Rhode Island P: Pittsburgh
 NJ: New Jersey R: Russia UT: U. of Tennessee OR: Oak Ridge
 B: Belgium I: Italy C: Czechoslovakia Y: Yugoslavia

^bKey to References:

1. Thoma and Wald, 1959.
2. Hübner and Fry, 1980.
3. Andrews et al., 1959.
4. Braverstock and Ash, 1983.
5. Klener et al., 1986.
6. Lushbaugh, 1969.
7. Fanger and Lushbaugh, 1967.

^cMidline body or mean bone marrow dose neutron (RBE = 1).

^dDose estimates in parenthesis from Braverstock and Ash, 1983.

^eAverage dose to stomach and intestines.

B.2 ANALYSIS.

The data in Table 31 were assumed to result from a cumulative distribution, $\theta(D; \alpha, \beta)$, that represents the fraction of individuals with symptoms or signs after an acute dose, D . The two adjustable parameters, α and β , were determined by the maximum likelihood technique [Cox, 1983], which uses the data in binary form. We were then able to avoid the disadvantages of having to divide the data into arbitrary groups, as required for a standard regression analysis.

For each of the 40 data points from Table 31, the fractional incidence, y_i , for the i th point is unity if the symptom occurred (X), or zero if not (--). If the corresponding dose is D_i , then the likelihood function has a factor $\theta(D_i)$ whenever $y_i = 1$, and a factor of $1 - \theta(D_i)$ otherwise, i.e.,

$$L = \prod \theta(D_i)^{y_i} \cdot (1 - \theta(D_i))^{(1 - y_i)}, \quad (\text{B.1})$$

where the product extends over the 40 points. The best fit to the distribution $\theta(D)$ then results from minimizing the negative log of this function, i.e., we find the parameters of the distribution models which minimize

$$-\ln L = - \sum (y_i \ln \theta(D_i) + (1 - y_i) \ln(1 - \theta(D_i))) . \quad (\text{B.2})$$

Values for the two adjustable parameters, α and β , were determined for each of the five distributions considered, using a simplex algorithm [Press et al., 1986]. Table 32 gives the values for the α and β parameters. The log likelihood function was then used to develop and calculate the variance-covariance matrix for the optimized values of α and β . The resulting parameter standard deviations (σ_α and σ_β) and covariances ($\text{cov}(\alpha, \beta)$) are also included in Table 32, as are the functional forms for statistical models, $\theta(D; \alpha, \beta)$.

Table 32. Regression Models and Parameters

	Model ^a	α	σ_{α}	β	σ_{β}	cov(α, β)
Set I Nausea	Normal	-2.196	0.6798	0.01243	0.003220	-0.001946
	Log-normal	-11.944	4.0604	2.362	0.7654	-3.097
	Weibull	-11.369	3.6275	2.158	0.6584	-2.380
	Logistic	-4.055	1.4077	0.02391	0.007621	-0.009753
	Log-logit	-22.473	8.6452	4.452	1.661	-14.32
Set I Vomiting	Normal	-2.289	0.7089	0.01207	0.003206	-0.002053
	Log-normal	-12.024	4.1769	2.342	0.7788	-3.243
	Weibull	-11.989	3.9672	2.243	0.7166	-2.835
	Logistic	-4.013	1.3610	0.02180	0.006751	-0.008375
	Log-logit	-21.596	8.1033	4.214	1.534	-12.40
Set II Nausea	Normal	-2.097	0.6575	0.01258	0.003326	-0.001946
	Log-normal	-11.363	3.8822	2.274	0.7407	-2.865
	Weibull	-10.671	3.4010	2.048	0.6256	-2.120
	Logistic	-3.988	1.4194	0.02487	0.008059	-0.01051
	Log-logit	-21.352	8.2970	4.276	1.607	-13.30
Set II Vomiting	Normal	-2.236	0.7013	0.01248	0.00339	-0.002153
	Log-normal	-12.050	4.2532	2.369	0.8016	-3.400
	Weibull	-11.498	3.7530	2.175	0.6864	-2.568
	Logistic	-4.071	1.4277	0.02359	0.007621	-0.01006
	Log-logit	-22.210	8.6266	4.374	1.651	-14.21

^aModels:

Normal	$\theta(D) = \Phi(\alpha + \beta D)$
Log-normal	$\theta(\ln D) = \Phi(\alpha + \beta \ln D)$
Weibull	$\theta(\ln D) = 1 - \exp \{-e^{\alpha + \beta \ln D}\}$
Logistic	$\theta(D) = 1/(1 + \exp [-(\alpha + \beta D)])$
Log-logistic	$\theta(\ln D) = 1/(1 + \exp [-(\alpha + \beta \ln D)])$

B.3 RESULTS.

Using the regression relationship, dose response calculations were performed based on the dual data sets (data sets I and II). Data set II differs from set I only for the dose values in parentheses in Table 31, reflecting the estimates of Baverstock and Ash [1983]. Dose response probability for nausea and vomiting are expressed in Tables 33 and 34.

Table 33 summarizes the effective 10, 50, and 90 percentile doses based on data set I for the incidence of nausea and vomiting for each of the five statistical models. Also included are the 90 percent confidence limits for each value. Table 34 gives analogous information for data set II. Based on the χ^2 goodness-of-fit statistic, the normal and logistic distribution models seem to provide the least best fits of the data which is not surprising since those models do not predict zero incidence at zero dose. Actually, all the models fit both sets of data reasonably well, and which one that is chosen to represent the response becomes a matter of preference.

Nausea and vomiting response curves are plotted in Figs. 92 and 93 based on the analysis of data set I using the log-normal distribution model (graphic results for data set II are not plotted due to the similarity with data set I). Doses in Fig. 92 are midline tissue (MLT) absorbed dose values, and in Fig. 93 they are free-in-air (FIA) exposure values. For convenience, dual plots are shown: the top row are plots of incidence with linear probability (vertical) scales, while the bottom row has nonlinear (probability) scales that produce straight line plots for incidence; in both cases, the abscissas are log dose. The 90 percent confidence bounds (dashed lines) are also indicated in the plots.

The question of neutron RBE still remains an open one, and it is unlikely that it will be resolved empirically for humans short of possibly future clinical experience utilizing neutron radiation therapy. With regard to laboratory work with monkeys, Young [1986] has suggested that neutrons are more effective than gamma radiation in producing emesis. On the other hand, based on reactor irradiation studies with dogs, Cordts et al. [1985] found neutrons less effective

Table 33. Effective Doses (ED) and 95% Confidence Intervals for 10, 50, and 90 percent Nausea and Vomiting Probabilities Within 24 Hours Postexposure
Basis: Data Set I (N = 40, $\nu = 38$ dgf.)

Model	Nausea			χ^2	α
	ED10	ED50	ED90		
Normal	73.6 \pm 76	177 \pm 49	280 \pm 68	53.3	0.051
Log-normal	91.3 \pm 39 + 69	157 \pm 43 + 58	270 \pm 79 +111	34.7	0.62
Weibull	68.4 \pm 38 + 84	164 \pm 49 + 70	285 \pm 71 + 94	35.1	0.61
Logistic	77.7 \pm 74	170 \pm 48	261 \pm 76	64.9	0.005
Log-logistic	95.0 \pm 40 + 68	156 \pm 40 + 53	255 \pm 80 +117	38.5	0.45

Model	Vomiting			χ^2	α
	ED10	ED50	ED90		
Normal	83.5 \pm 78	190 \pm 50	296 \pm 70	37.7	0.48
Log-normal	98.3 \pm 42 + 75	170 \pm 45 + 60	294 \pm 86 +122	27.9	0.89
Weibull	76.8 \pm 42 + 91	178 \pm 50 + 70	304 \pm 75 +100	28.3	0.87
Logistic	83.3 \pm 79	184 \pm 50	285 \pm 79	40.1	0.38
Log-logistic	99.8 \pm 42 + 73	168 \pm 43 + 57	283 \pm 91 +133	29.4	0.85

Table 34. Effective Doses (ED) and 95% Confidence Intervals for 10, 50, and 90 percent Nausea and Vomiting Probabilities Within 24 Hours Postexposure
Basis: Data Set II (N = 40, $\nu = 38$ dgf.)

Model	Nausea			χ^2	α
	ED10	ED50	ED90		
Normal	64.5 \pm 74	166 \pm 47	268 \pm 67	59.0	0.02
Log-normal	84.2 \pm 37 + 66	148 \pm 40 + 55	260 \pm 78 +111	36.4	0.54
Weibull	61.1 \pm 34 + 79	153 \pm 46 + 67	275 \pm 72 + 97	36.1	0.56
Logistic	72.0 \pm 72	160 \pm 44	249 \pm 40	76.4	<0.001
Log-logistic	88.2 \pm 38 + 67	148 \pm 38 + 51	247 \pm 78 +114	39.0	0.43

Model	Vomiting			χ^2	α
	ED10	ED50	ED90		
Normal	76.4 \pm 75	179 \pm 47	282 \pm 69	43.5	0.25
Log-normal	94.3 \pm 40 + 71	162 \pm 42 + 56	278 \pm 82 +115	30.7	0.79
Weibull	70.3 \pm 38 + 84	167 \pm 47 + 66	290 \pm 74 +100	30.3	0.80
Logistic	79.4 \pm 75	173 \pm 45	266 \pm 74	51.7	0.07
Log-logistic	97.1 \pm 40 + 69	160 \pm 39 + 52	265 \pm 83 +121	33.6	0.67

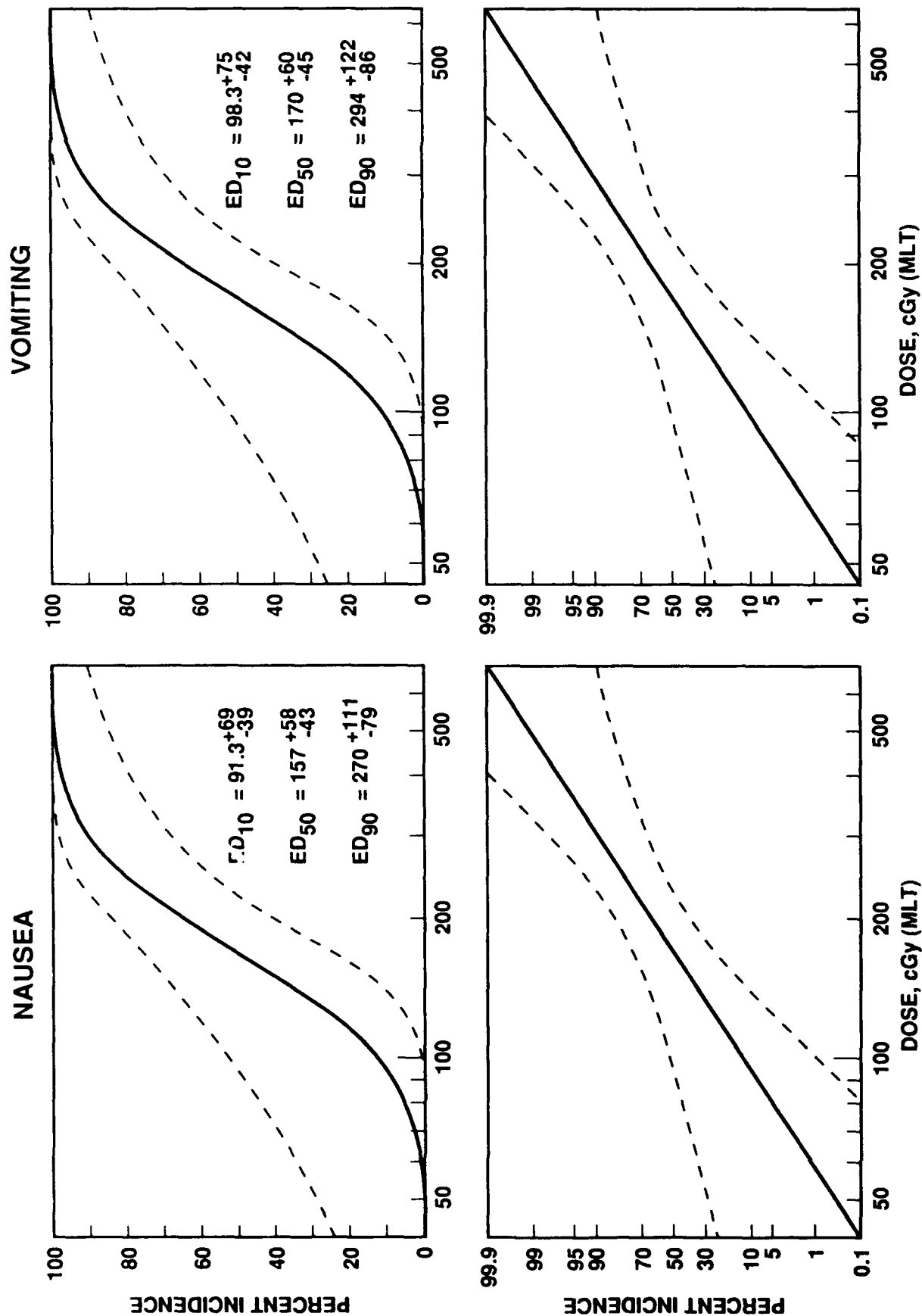


Figure 92. Incidence of nausea and vomiting within 24 hours (data set I, lognormal model).

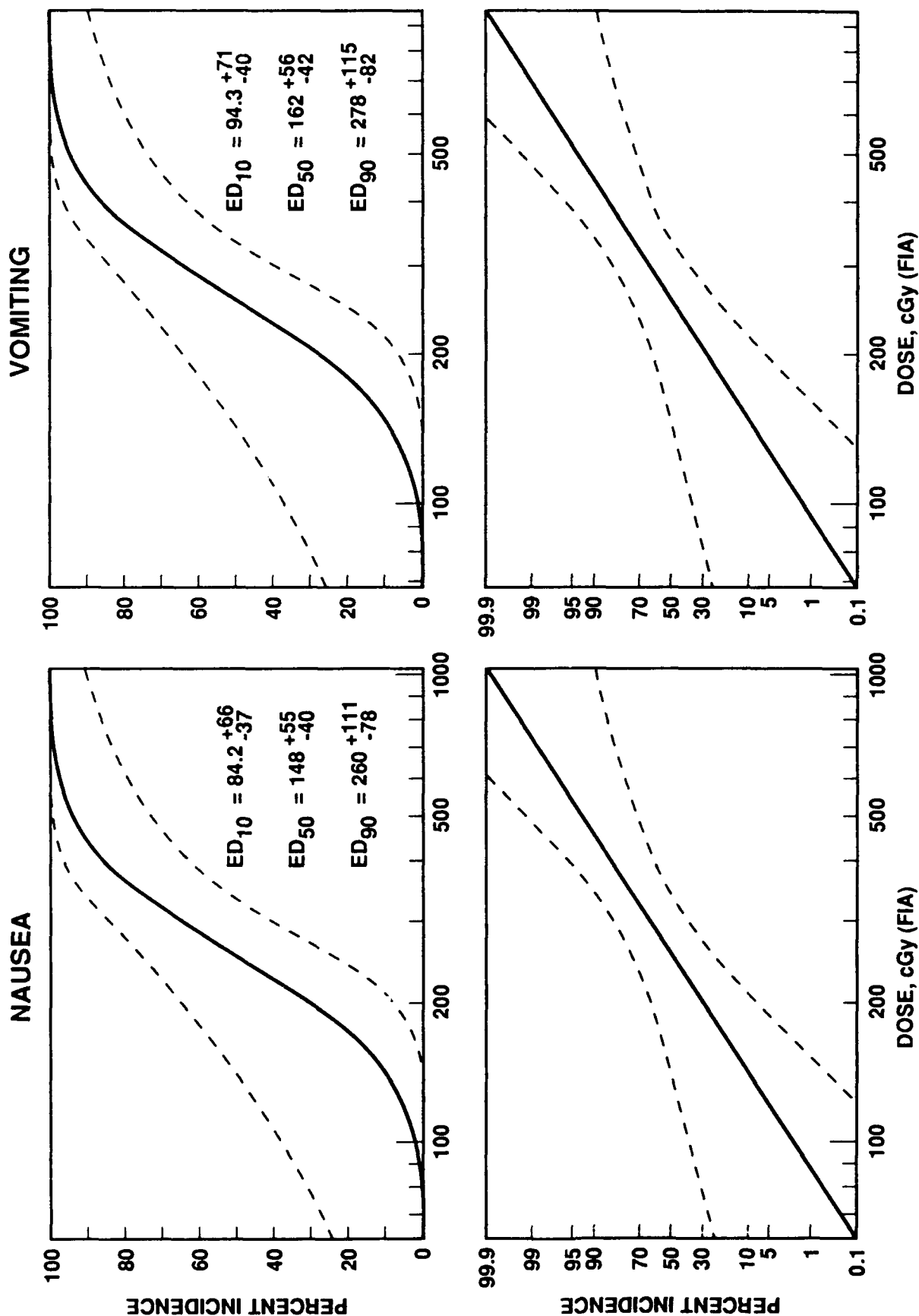


Figure 93. Incidence of nausea and vomiting within 24 hours (data set I, lognormal model).

(RBE = 0.48) in producing emesis. Before a more definitive application of RBE can be specified for emesis in humans, further animal experimentation will be required together with a more thorough delineation of the radiation-induced mechanisms.

As an exercise to illustrate the effect of neutron RBE, we performed some additional likelihood calculations utilizing a lognormal model to analyze the accident data (data set I). Based on the n/γ ratios given in column 3 of Table 31, we assumed various values for the neutron RBE ranging from 0.5 to 2.0 and reanalyzed the vomiting response for those conditions. The calculated neutron RBE effect obtained is shown in Fig. 94 for the ED₅₀ emesis endpoint both in terms of MLT and FIA dose; it amounts to about a 33 percent increase in the ED₅₀ for a factor of four decrease in RBE.

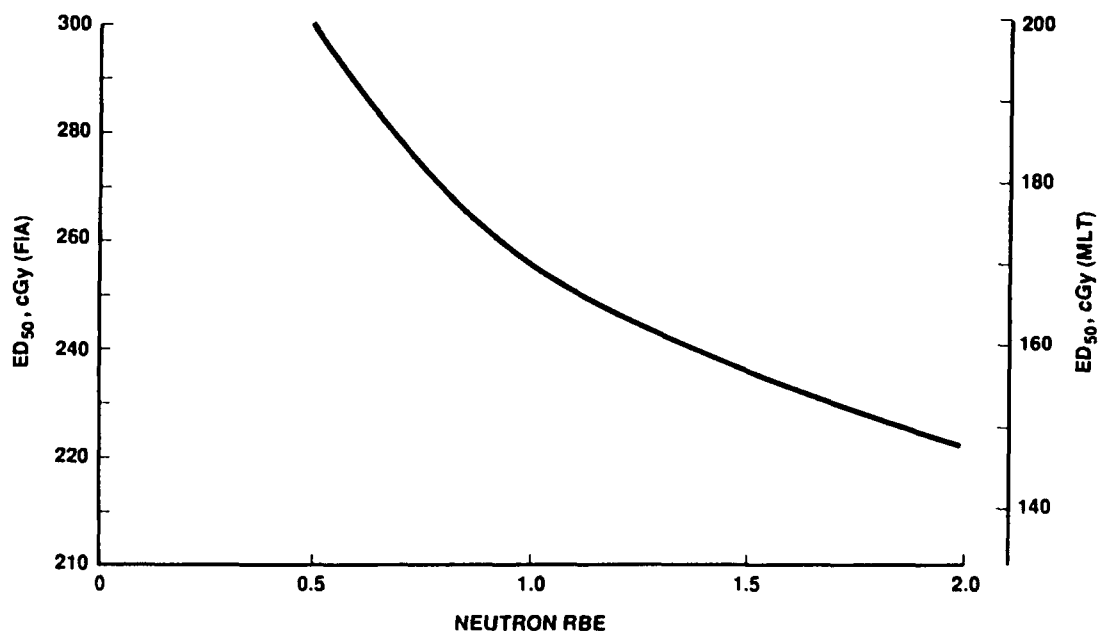


Figure 94. ED₅₀ for emesis versus neutron RBE (basis: data set I; lognormal model).

APPENDIX C

EQUATIONS OF THE GUT INJURY MODEL

This appendix presents the equations for the gut injury model (GIM). The physiological and anatomical basis for the model and the structure of the model are discussed in Sec. 5 of this report.

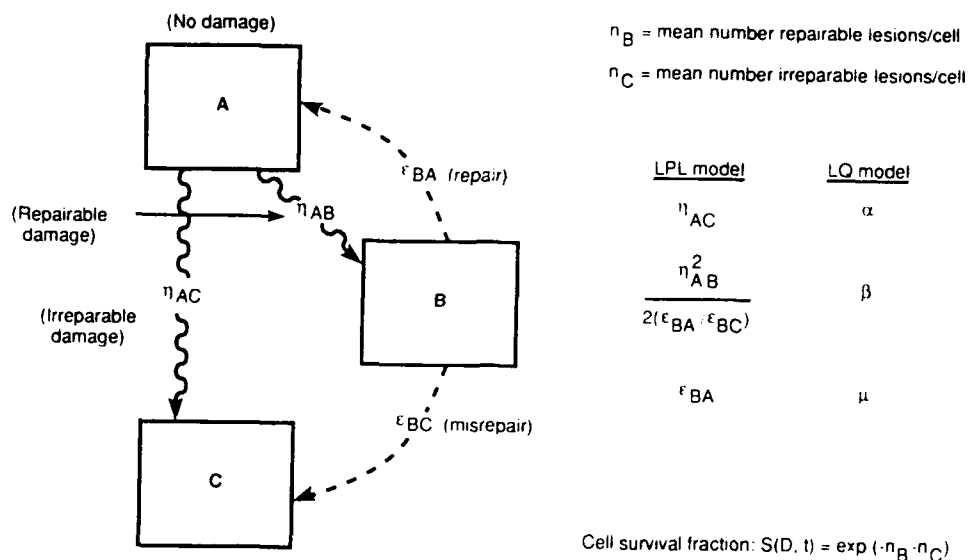
The foundation for the radiation response of the GIM is the lethal potentially lethal (LPL) model. Curtis [1986] has published a full discussion of the LPL model and its application to a wide range of radiobiological response data. That model includes two types of radiation-induced chromosome lesions, lethal lesions, and potentially lethal lesions. The lethal lesions, having an average number of n_C per cell, are irreparable and prevent mitosis. A cell may have more than one lethal lesion, but any one is sufficient to cause reproductive death of the cell. The potentially lethal (PL) lesions, having an average number of n_B per cell, are repairable by a process based on linear kinetics. All PL lesions can be repaired in time; however, a cell that enters mitosis with an unrepaired PL lesion will fail to divide and be reproductively dead. The LPL model also includes a misrepair term that generates lethal (irreparable) lesions from PL lesions at a rate that is quadratic in the concentration of PL lesions. This nonlinear term produces a shoulder on the cell survival curve and provides a link to the linear-quadratic (LQ), or alpha/beta, model frequently used to analyze cell survival data.

The equations for the LPL model are:

$$\dot{n}_B = \eta_{AB} R - \epsilon_{BA} n_B - \epsilon_{BC} n_B^2, \quad (1)$$

$$\dot{n}_C = \eta_{AC} R + \epsilon_{BC} n_B^2, \quad (2)$$

where R is the dose rate. Both types of lesions are produced at a rate proportional to R . Figure 95 provides a diagrammatic definition of the rate coefficients and variables in these equations and shows



Source: Thames (1985), based on Tobias et al. (1980), and Curtis (1982).

Figure 95. Cell radiation response based on the lethal, potentially lethal (LPL) cell lesions model.

the correspondence with the parameters customarily used in the LQ model.

In the LPL model, the distribution of each type of lesion among a group of cells is assumed to follow a Poisson distribution since the lesions are produced at random by radiation exposure. This assumption leads to the exponential expression for cell survival shown in Fig. 95. The expression is simply the probability that a given cell has no lesions of either kind at the time it enters mitosis.

We had to address a major problem crucial to applying the LPL model to a proliferating tissue. Previously, the LPL model had been applied only to data where the exposure and repair times were short compared to the cell cycle. The difficulty for longer times arises from the fact that proliferation disrupts the Poisson distribution of lesions. Successful cell division occurs in cells with no lesions, lowering the average number of lesions per cell but not in a random manner. Likewise, the death of a cell entering into mitosis due to the presence of one or more lesions removes any or all lesions present. We therefore had to develop equations that would track both lesion number and cell number over long periods of time given any

exposure history. In addition, we needed to replace the simple cell survival formula shown in Fig. 95 with a formulation based on these same principles.

Probably the most straightforward analytic approach to this problem would be a Monte Carlo procedure for tracking a large number of cells. The distribution of lesions would then evolve into a non-Poisson form as it must do so in reality. To avoid the extensive calculation requirements of a Monte Carlo model, we derived an approximate solution based on continuous time differential equations. We refer to our formulation as the proliferation and intracellular repair (PAIR) model.

The key to this approximate solution was to divide the proliferating cells into three classes, labeled A, B, and C, in a manner similar to Curtis's classes of lesions. However, it is important to point out that in the PAIR model, the classes refer to cells and not to lesions. The number of cells in each class and the definitions of the classes are as follows:

- N_A = number of cells with no lesions of either kind (uninjured cells),
- N_B = number of cells with one or more PL lesions, but no lethal lesion (injured cells), and
- N_C = number of cells with at least one lethal lesion (mitotically dead cells).

Proliferation increases the number of cells in class A in the normal manner but does not occur in class C since those cells are mitotically dead. Proliferation (attempted division) of class B results in cell death and moves them to class C since we assume, following Curtis, that any cell entering mitosis with a PL lesion suffers mitotic death.

It is not necessary to track the number of lesions in class C cells since they are mitotically dead. However, we track the number of C cells because they are still present in the tissue. We assume that their presence affects homeostasis and that they differentiate to form mature, functional cells. These assumptions seem to fit the

dynamics of the intestinal epithelium but may not be appropriate for every type of tissue.

The only lesion number that must be tracked in the PAIR model is that of the class B cells, where:

n_B = mean number of PL lesions in class B cells.

Note that by the definition of class B cells, n_B is always greater than or equal to one. Therefore, n_B is not the average number of PL lesions as defined in the LPL model since that number goes to zero in the absence of radiation exposure. For convenience, we define a different number that does correspond to the LPL model:

n_{PL} = mean number of PL lesions in a hypothetical pool of cells with a Poisson distribution of PL lesions and for which the number of cells with one or more PL lesions and no lethal lesions is N_B .

In other words, we approximate the actual distribution of lesions in the B class of cells by assuming that it is a truncated Poisson distribution from this hypothetical pool of cells. The accuracy of this assumption remains to be investigated. The advantage of the assumption is that proliferation of class A cells can occur without upsetting the statistical distribution of lesions in class B cells. Furthermore, in the limit of no proliferation, the mathematical results match those of the LPL model.

The value of n_B in terms of n_{PL} is given by:

$$n_B = \frac{n_{PL}}{1 - e^{-n_{PL}}} \quad (3)$$

The rate equations for the average number of PL lesions per cell in the injured compartment is:

$$\begin{aligned} \dot{n}_{PL} = & \eta_{AB} RE - (n_B - 1) \left(\frac{N_A}{N_B} \right) \eta_{AB} RE \\ & \text{Exposure} \qquad \qquad \text{Dilution} \\ & - \epsilon_{BA} n_{PL} - \epsilon_{BC} n_{PL} n_B [2 - (n_B - n_{PL})] E, \\ & \text{Repair} \qquad \qquad \text{Misrepair} \end{aligned} \quad (4)$$

where R is the radiation exposure rate (Gy/h),

$$\begin{aligned} E = & \left(\frac{n_{PL}}{n_B} \right) \frac{1}{1 - (n_B - n_{PL})}, \\ \text{and } \lim_{n_{PL} \rightarrow 0} E = & \lim_{n_B \rightarrow 1} \frac{1}{n_B (n_B - 1/2)} = 2. \end{aligned} \quad (5)$$

The rate equation for the number of uninjured cells N_A is:

$$\begin{aligned} \dot{N}_A = & \lambda N_A - (\eta_{AB} + \eta_{AC}) R N_A \\ & \text{Proliferation} \qquad \text{Exposure Losses} \\ & + \epsilon_{BA} (n_B - n_{PL}) N_B - \theta N_A \\ & \text{Repair of Injured Cells} \qquad \text{To Pipeline} \end{aligned} \quad (6)$$

The coefficient θ which determines the rate at which clonogens feed the "pipeline" to the transit compartment is defined below, as is the clonogen division rate λ .

The rate equation for the number of injured cells N_B (potentially lethal injury only) is:

$$\begin{aligned}
\dot{N}_B = & - \lambda N_B + \eta_{AB}^R N_A - \eta_{AC}^R N_B \\
& \text{Mitotic Death} \quad \text{Exposure of Uninjured Cells} \quad \text{Exposure Causing Lethal Injury} \\
& - \epsilon_{BA} (n_B - n_{PL}) N_B - \epsilon_{BC} n_{PL} n_B N_B - \theta N_B \\
& \text{Repair} \quad \text{Misrepair} \quad \text{Pipeline}
\end{aligned} \tag{7}$$

The rate equation for the number of killed cells N_C (lethally injured or mitotically dead, but still functional) is:

$$\begin{aligned}
\dot{N}_C = & \eta_{AC}^R (N_A + N_B) + \epsilon_{BC} n_{PL} n_B N_B + \lambda N_B - \theta N_C \\
& \text{Exposure} \quad \text{Misrepair} \quad \text{Mitotic Death of Injured Cells} \quad \text{Pipeline}
\end{aligned} \tag{8}$$

The instantaneous clonogen division rate λ is affected by both homeostasis and mitotic delay as given by:

$$\lambda = HM\gamma \tag{9}$$

where,

H = homeostasis factor (dimensionless)

M = mitotic delay factor (dimensionless)

γ = normal division rate to balance attrition (h^{-1}).

Normal conditions give $H = M = 1$ and $\lambda = \gamma$. The maximum value of λ is λ_m , determined by H . The minimum value of λ is 0, determined by M .

Radiation exposure slows down cell division through a mitotic delay process. For the GIM, we have modeled this process based on a saturable enzyme repair concept where a hypothetical damage level Q is reduced by the action of a finite pool of repair enzymes. Assuming cell cycling proceeds normally when the repair enzymes are not activated, and slows down when they are activated, we employed a

Michaelis-Menten form to describe activated enzyme saturation. This results in our rate equation to express cellular damage given by:

$$\dot{Q} = \underset{\text{Damage Production}}{R} - \left(\frac{\lambda_m}{\delta} \right) \underset{\text{Damage Repair}}{\frac{Q}{A+Q}} \quad (10)$$

Q = cellular damage (Gy)

λ_m = freely growing (maximum) cell division rate (h^{-1})

δ = acute dose mitotic delay constant (Gy^{-1})

A = threshold for saturation of repair = 0.1 Gy

R = dose rate (Gy/h)

The mitotic delay factor M in Eq. (9) above is then given by:

$$M = [1 - \tanh(Q/A)] \quad (11)$$

When the damage level Q is low, M approaches one and cell division proceeds normally. When the damage level increases beyond the characteristic value A , M rapidly approaches zero according to the hyperbolic tangent function, effectively halting the progression of cell cycling.

An H-tissue such as the intestinal epithelium must have communication mechanisms between compartments in order to maintain homeostatic equilibrium. Figure 81 in Sec. 5 illustrates the control mechanisms that govern the GIM model. Many links are possible, and the nature and number of links have not yet been established experimentally. We have attempted to choose the simplest and minimum number of (feedback) control links that will both maintain equilibrium in the three GIM compartments and provide a correct qualitative response to radiation insult.

The primary homeostasis loop is the control of clonogen proliferation through the division rate λ . When the tissue is in

equilibrium with N_0 clonogenic cells, the normal division rate is γ expressed in units of divisions per hour per cell. Compensatory proliferation is accomplished through the homeostatic control factor H . In equilibrium, both factors M and H are equal to 1, and the production rate of new clonogens is N_0 , just balancing the attrition rate from the villi to the intestinal lumen.

The mathematical form of the homeostasis factor H is presented in Fig. 96. The primary purpose of H in the GIM is to increase the cell division rate to its maximum value λ_m when the population of the transit compartment drops to zero. At first, we used a linear dependence on N_T , but found that the delayed recognition of damage was not properly represented. This phenomenon shows up in both fractionated [Withers and Elkind, 1969] and constant dose rate [Withers, 1972] studies. In spite of cell depletion, it is found that rapid proliferation is delayed for at least two days. We introduce this behavior by using a small value for the exponent $a = 0.21$, to moderate the increase in cell division rate as N_T decreases. A final factor $f(N/N_0)$, shown in Fig. 96, is used to limit the growth of the clonogenic compartment to twice its normal value. As explained later, N_T is not allowed to go above its equilibrium value N_{T0} , so that the

$$H = 1 + \frac{\lambda_m - \gamma}{\gamma} \left[1 - \left(\frac{N_T}{N_{T0}} \right)^a \right] f \left(\frac{N}{N_0} \right)$$

N_T equilibrium Limit
on N

f = population limiting factor

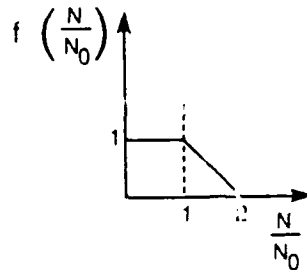
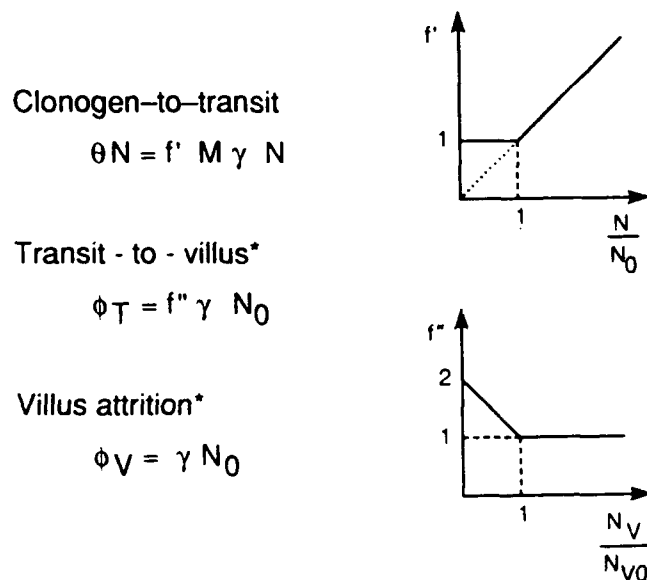


Figure 96. Clonogen homeostasis factor, H .

factor H will not drop below 1. This restriction ensures a supply of cells to balance the normal attrition rate unless overridden by mitotic delay.

The GIM model uses the transit population N_T rather than the villi population N_V to control compensatory proliferation mainly on the grounds of physical proximity. We do not have experimental data to support this choice. In fact, it might be useful to include N_V in the equation for H as an attempt to improve the description of delayed recognition of damage.

The remaining control mechanisms shown in Fig. 81 of Sec. 5 involve the fluxes of cells in and out of the three compartments. Figure 97 shows the mathematical expressions for the fluxes. The attrition rate from the villus has the simplest mathematical form. It is held fixed at the normal level γN_0 when the villus population is between 0 and its equilibrium value N_{V0} . When the population is zero, the villus output is set equal to its input if the input is less than γN_0 and is equal to γN_0 otherwise. The assumption is that the villus has atrophied completely and will not grow until the supply of cells from the transit compartment exceeds the normal attrition rate. When



* Both transit and villus compartments have output equal to input when compartment population is at 0 or at the equilibrium value

Figure 97. Cell fluxes between compartments in the GIM model; note that ϕ is subscripted, but θ is not in the equations.

the population reaches its full value N_{V0} , any input level that exceeds γN_0 is passed on through in order to limit the villi to their normal size.

The flux of cells from the transit compartment to the villus is increased linearly from its normal value γN_0 to twice that value as the villus level drops from normal to zero. Like the villus, the transit compartment is assumed to shrink to zero size when it is empty so that output is equal to the input if the input is less than the output demanded by the villus based on the function $f''(N_V/N_{V0})$. Also, when the transit compartment reaches full size, it passes excessive inputs on through in order to limit its size to N_{T0} .

The output from the clonogen compartment is more complex. Like the others, it is designed to provide a flux equal to the attrition rate γN_0 at equilibrium. The flux θN shown in Fig. 81 of Sec. 5 is defined in Fig. 97. The mitotic delay factor M appears in the output flux θN as well as in the division rate λ . The assumption is that if mitotic delay turns off cell division, it will also turn off cell differentiation that moves cells from the clonogen compartment to the transit compartment. Otherwise, mitotic delay in the model causes an anomalous depletion of the clonogen compartment that is not consistent with experimental data.

DISTRIBUTION LIST

DNA-TR-90-157

DEPARTMENT OF DEFENSE

ARMED FORCES RADIOBIOLOGY RSCH INST
ATTN: AFFRI-DEPT OF RAD BIOCHEMISTRY
ATTN: BHS
ATTN: DIRECTOR
ATTN: EXH
ATTN: MRA
ATTN: PHY
ATTN: RSD
ATTN: SCIENTIFIC DIRECTOR
ATTN: TECHNICAL LIBRARY

ASSISTANT SEC OF DEF (C3I)
ATTN: DIR S&TNFC3

ASSISTANT SECRETARY OF DEFENSE
INTERNATIONAL SECURITY POLICY
ATTN: NUC FORCES & ARMS CONTROL PLCY

ASSISTANT TO THE SECRETARY OF DEFENSE
ATTN: EXECUTIVE ASSISTANT
ATTN: MIL APPL
ATTN: MIL APPL C FIELD

DEFENSE INTELLIGENCE AGENCY
ATTN: DB
5 CYS ATTN: DB-4 RSCH RESOURCES DIV
ATTN: DB-5C
ATTN: DB-6
ATTN: DB-6B
ATTN: DIA/VPA-2
ATTN: DN
ATTN: DT
ATTN: OS

DEFENSE INTELLIGENCE COLLEGE
ATTN: DIC/RTS-2
ATTN: DIC/2C

DEFENSE NUCLEAR AGENCY
ATTN: CID
ATTN: DFRA
ATTN: NANF
ATTN: NASF
ATTN: OPNA
ATTN: OPNS
20 CYS ATTN: RARP
2 CYS ATTN: TITL

DEFENSE TECHNICAL INFORMATION CENTER
2 CYS ATTN: DTIC/FDAB

FIELD COMMAND DEFENSE NUCLEAR AGENCY
ATTN: FCPR

FIELD COMMAND DEFENSE NUCLEAR AGENCY
ATTN: FCNM
2 CYS ATTN: FCTT W SUMMA

INTELLIGENCE CENTER, PACIFIC
ATTN: COMIPAC

INTERSERVICE NUCLEAR WEAPONS SCHOOL
ATTN: TTV
2 CYS ATTN: TTV 3416TH TTSQ

NATIONAL DEFENSE UNIVERSITY
ATTN: ICAF TECH LIB
ATTN: NWCLB-CR
ATTN: LIBRARY

NET ASSESSMENT
ATTN: DOCUMENT CONTROL

OFC OF MILITARY PER ASSESSMENT TECHNOLOGY
ATTN: F HEGGE

PROGRAM ANALYSIS & EVALUATION
ATTN: NAVAL FORCES
ATTN: STRATEGIC PROGRAMS & TNF

STRATEGIC AND THEATER NUCLEAR FORCES
ATTN: DR E SEVIN
ATTN: DR SCHNEITER

THE JOINT STAFF
ATTN: JKAC
ATTN: JKC ATTN DNA REP
ATTN: JLT
ATTN: JPEP

THE JOINT STAFF
ATTN: ED30
ATTN: J-3 SPECIAL OPERATIONS
ATTN: J-8
ATTN: JAD/SFD
ATTN: JSOA

UNDER SEC OF DEFENSE FOR POLICY
ATTN: DUSP/P
ATTN: USD/P

DEPARTMENT OF THE ARMY

DEP CH OF STAFF FOR OPS & PLANS
ATTN: DAMO-FDQ
ATTN: DAMO-SWN
ATTN: DAMO-ZXA

HARRY DIAMOND LABORATORIES
ATTN: SLCIS-IM-TL

JOINT SPECIAL OPERATIONS COMMAND
ATTN: J-2
ATTN: J-5

U S ARMY AIR DEFENSE ARTILLERY SCHOOL
ATTN: COMMANDANT

U S ARMY ARMOR SCHOOL
ATTN: ATSB-CTD
ATTN: TECH LIBRARY

U S ARMY BALLISTIC RESEARCH LAB
ATTN: SLCBR-DD-T
ATTN: SLCBR-VL-I DR KLOPCIC

DNA-TR-90-157 (DL CONTINUED)

U S ARMY COMD & GENERAL STAFF COLLEGE
ATTN: ATZL-SWJ-CA
ATTN: ATZL-SWT-A

U S ARMY CONCEPTS ANALYSIS AGENCY
ATTN: TECHNICAL LIBRARY

U S ARMY FIELD ARTILLERY SCHOOL
ATTN: ATSF-CD

U S ARMY FOREIGN SCIENCE & TECH CTR
ATTN: C WARD

U S ARMY INFANTRY CENTER
ATTN: ATSH-CD-CSO

U S ARMY ITAC
ATTN: IAX-Z

U S ARMY LABORATORY COMMAND
ATTN: DIRECTOR
ATTN: DR D HODGE

U S ARMY MATERIAL COMMAND
ATTN: DRCDE-D

U S ARMY NUCLEAR & CHEMICAL AGENCY
ATTN: MONA-NU

U S ARMY TEST & EVALUATION COMMAND
ATTN: STECS-NE

U S ARMY WAR COLLEGE
ATTN: LIBRARY
ATTN: STRATEGIC STUDIES INSTITUTE

U S MILITARY ACADEMY
ATTN: DEPT OF BEHAV SCI & LEADERSHIP
ATTN: COL J G CAMPBELL

US ARMY MATERIEL SYS ANALYSIS ACTVY
ATTN: DRXS-DS

USA SURVIVABILITY MANAGMENT OFFICE
ATTN: SLCSM-SE J BRAND

USACACDA
ATTN: ATZL-CAD-N

DEPARTMENT OF THE NAVY

MARINE CORPS
ATTN: CODE PPO
ATTN: PSI G/RASP

NAVAL AIR SYSTEMS COMMAND
ATTN: PMS-423
ATTN: SEA-06GN

NAVAL OCEAN SYSTEMS CENTER
ATTN: CODE 9642-B

NAVAL PERSONNEL RES & DEV CENTER
ATTN: CODE P302

NAVAL POSTGRADUATE SCHOOL
ATTN: CODE 1424

NAVAL RESEARCH LABORATORY
ATTN: CODE 1240
ATTN: CODE 2627

NAVAL SURFACE WARFARE CENTER
ATTN: CODE F-31
ATTN: G RIEL

NAVAL TECHNICAL INTELLIGENCE CTR
ATTN: NTIC-DA30

NAVAL WAR COLLEGE
ATTN: CODE E-11
ATTN: CTR FOR NAV WARFARE STUDIES
ATTN: DOCUMENT CONTROL
ATTN: LIBRARY
ATTN: STRATEGY DEPT

NAVAL WEAPONS EVALUATION FACILITY
ATTN: CLASSIFIED LIBRARY

NUCLEAR WEAPONS TNG GROUP, ATLANTIC
ATTN: CODE 222
ATTN: DOCUMENT CONTROL

NUCLEAR WEAPONS TNG GROUP, PACIFIC
ATTN: CODE 32

OFFICE OF CHIEF OF NAVAL OPERATIONS
ATTN: NOP 50
ATTN: OP 654
ATTN: PMS/PMA-423

OPERATIONAL TEST & EVALUATION FORCE
ATTN: COMMANDER

PLANS, POLICY & OPERATIONS
ATTN: CODE-P
ATTN: CODE-POC-30

TACTICAL TRAINING GROUP, PACIFIC
ATTN: COMMANDER

DEPARTMENT OF THE AIR FORCE

ACADEMY LIBRARY DFSELD
ATTN: LIBRARY

AFIS/INT
ATTN: INT

AIR UNIVERSITY
ATTN: STRATEGIC STUDIES

AIR UNIVERSITY LIBRARY
ATTN: AUL-LSE
ATTN: LIBRARY

ASSISTANT CHIEF OF STAFF
2 CYS ATTN: AF/SAMI

ASSISTANT CHIEF OF THE AIR FORCE
ATTN: SAF/ALR

DEPUTY CHIEF OF STAFF/XOX
ATTN: AFXOOSS

FOREIGN TECHNOLOGY DIVISION
ATTN: CCN
ATTN: SDA

PHILLIPS LABORATORY
ATTN: NTCA

STRATEGIC AIR COMMAND/SPD
ATTN: SPD

STRATEGIC AIR COMMAND/STIC
ATTN: 544 SIW/DI

STRATEGIC AIR COMMAND/XOXO
ATTN: XOXO

STRATEGIC AIR COMMAND/XPX
ATTN: XPZ

STRATEGIC AIR COMMAND/XRFS
ATTN: XRFS

TACTICAL AIR COMMAND/XPSC
ATTN: TAC/DOA

USAF SCHOOL OF AEROSPACE MEDICINE
ATTN: RADIATION SCIENCES DIV

DEPARTMENT OF ENERGY

LAWRENCE LIVERMORE NATIONAL LAB
ATTN: Z DIVISION LIBRARY

LOS ALAMOS NATIONAL LABORATORY
ATTN: D STROTTMAN
ATTN: REPORT LIBRARY

MARTIN MARIETTA ENERGY SYSTEMS INC
ATTN: B SANTORO
ATTN: G KERR
ATTN: W RHOADES

SANDIA NATIONAL LABORATORIES
ATTN: TECH LIB 3141

OTHER GOVERNMENT

CENTRAL INTELLIGENCE AGENCY
ATTN: MEDICAL SERVICES
ATTN: NIO-T
ATTN: N10 - STRATEGIC SYS
ATTN: R & D SUBCOMMITTEE

FEDERAL BUREAU OF INVEST ACADEMY
ATTN: BEHAVIORAL RSCH UNIT
ATTN: LIBRARY

FEDERAL EMERGENCY MANAGEMENT AGENCY
ATTN: ASST ASSOC DIR FOR RSCH
ATTN: CIVIL SECURITY DIVISION
ATTN: G ORRELL NP-CP
ATTN: OFC OF CIVIL DEFENSE J F JACOBS

U S DEPARTMENT OF STATE
ATTN: PM/STM

U S NUCLEAR REGULATORY COMMISSION
ATTN: DIR DIV OF SAFEGUARDS
ATTN: S YANIV

DEPARTMENT OF DEFENSE CONTRACTORS

ARES CORP
ATTN: A DEVERILL

HORIZONS TECHNOLOGY, INC
ATTN: F GREY

HORIZONS TECHNOLOGY, INC
ATTN: J MARSHALL-MISE

KAMAN SCIENCES CORP
ATTN: DASAC

KAMAN SCIENCES CORPORATION
ATTN: R STOHLER

KAMAN SCIENCES CORPORATION
ATTN: DASAC

LOGICON R & D ASSOCIATES
ATTN: S WOODFORD

MICRO ANALYSIS AND DESIGN
ATTN: R LAUGHERY

PACIFIC-SIERRA RESEARCH CORP
2 CYS ATTN: G ANNO
2 CYS ATTN: G MCCLELLAN
2 CYS ATTN: M DORE
2 CYS ATTN: S BAUM

PACIFIC-SIERRA RESEARCH CORP
ATTN: D GORMLEY
2 CYS ATTN: G MCCLELLAN

SCIENCE APPLICATIONS INTL CORP
ATTN: D KAUL
ATTN: DOCUMENT CONTROL
ATTN: W WOOLSON

SCIENCE APPLICATIONS INTL CORP
ATTN: D BAREIS
ATTN: DOCUMENT CONTROL
ATTN: J MCGAHAN
ATTN: J PETERS

SCIENCE APPLICATIONS INTL CORP
ATTN: R CRAVER

SCIENCE APPLICATIONS INTL CORP
ATTN: JOHN A SHANNON

TECHNICO SOUTHWEST INC
ATTN: S LEVIN

UNIVERSITY OF CINCINNATI MEDICAL CENTER
ATTN: E SILBERSTEIN